Development of ^{18}F-labelled radioligands for molecular imaging of the dopamine D_4 receptor

Fabian Kügler

JÜLICH
FORSCHUNGSZENTRUM

Mitglied der Helmholtz-Gemeinschaft

Schriften des Forschungszentrums Jülich
Reihe Gesundheit / Health Band / Volume 43

Forschungszentrum Jülich GmbH
Institute of Neuroscience and Medicine (INM)
Nuclear Chemistry (INM-5)

Development of ^{18}F-labelled radioligands for molecular imaging of the dopamine D_4 receptor

Fabian Kügler

Schriften des Forschungszentrums Jülich
Reihe Gesundheit / Health

Band / Volume 43

ISSN 1866-1785

ISBN 978-3-89336-738-2

Bibliographic information published by the Deutsche Nationalbibliothek.
The Deutsche Nationalbibliothek lists this publication in the Deutsche Nationalbibliografie; detailed bibliographic data are available in the Internet at http://dnb.d-nb.de.

Publisher and Distributor:	Forschungszentrum Jülich GmbH Zentralbibliothek 52425 Jülich Phone +49 (0) 24 61 61-53 68 · Fax +49 (0) 24 61 61-61 03 e-mail: zb-publikation@fz-juelich.de Internet: http://www.fz-juelich.de/zb
Cover Design:	Grafische Medien, Forschungszentrum Jülich GmbH
Source cover image:	© fotolia.com
Printer:	Grafische Medien, Forschungszentrum Jülich GmbH
Copyright:	Forschungszentrum Jülich 2011

Schriften des Forschungszentrums Jülich
Reihe Gesundheit / Health Band / Volume 43

D 38 (Diss., Köln, Univ., 2011)

ISSN 1866-1785
ISBN 978-3-89336-738-2

The complete volume is freely available on the Internet on the Jülicher Open Access Server (JUWEL) at http://www.fz-juelich.de/zb/juwel

Berichterstatter:	Prof. Dr. H. H. Coenen
	Prof. Dr. A. Griesbeck
Tag der mündlichen Prüfung:	04. April 2011

Die Arbeit wurde in der Zeit von März 2008 bis Februar 2011 am Institut für Neurowissenschaften und Medizin, INM-5: Nuklearchemie, der Forschungszentrum Jülich GmbH unter der Anleitung von Herrn Prof. Dr. H. H. Coenen (Lehrstuhl für Nuklearchemie der Universität zu Köln) durchgeführt.

…Neuroscience goes directly to work on the brain - and the mind follows…

Leon Kass

"If the human brain were so simple that we could understand it,
we would be so simple that we couldn´t."

Emerson M. Pugh

Abstract

The five subtypes of the dopamine receptor play an important role in the human brain. The dopamine D_4 receptor is involved in processes of behaviour control and is assumed to be responsible for the emergence of the attention deficit hyperactivity disorder (ADHD) as well as psychotic diseases like schizophrenia. While most of the other dopamine receptors are well known there is a lack of suitable radioligands for the examination of the D_4 receptor by functional neuroimaging via positron emission tomography (PET). This is due to the extremely low distribution density of D_4 in the central nervous system. In this work the radiosynthesis of such D_4 ligands was developed and pharmacologically evaluated. Therefore, selected pharmaceutical lead structures were labelled via nucleophilic substitution with no-carrier-added (n.c.a.) [^{18}F]fluoride at an aromatic ring and subsequently coupled in a 1-2 step build-up reaction to the desired ligands.

As first approach, an efficient radiosynthesis of the highly selective [^{18}F]FAUC 316 ligand ([^{18}F]**1**) was developed. Starting from ^{18}F-labelling of the symmetric iodonium salts bis(4-bromophenyl)iodonium triflate and bis(4-iodophenyl)iodonium triflate the corresponding 4-[^{18}F]fluorohalobenzenes were obtained in radiochemical yields (RCY) of up to 60 %. Pd-catalyzed cross-coupling of the labelling products and piperazine with $Pd_2(dba)_3$ or $Pd(OAc)_2$ led to 4-[^{18}F]fluorophenylpiperazine in a RCY of up to 42 %. During the synthesis of standard and precursors 5-Cyanoindol-2-carbaldehyd was synthesized in four reaction steps with an overall yield of 15 % and coupled to [^{18}F]FAUC 316. The overall-RCY after high performance liquid chromatography (HPLC) separation was 10 %.

[^{18}F]FAUC 316 was not suitable for further evaluation steps *in vivo* due to the very high non-specific binding content determined by *in vitro* autoradiography. Alternatively, the radioligands 6-(4-[4-[^{18}F]fluorobenzyl]piperazine-1-yl)benzodioxine ([^{18}F]**33a**), 6-(4-[4-[^{18}F]fluoro-(3-methoxy-benzyl)]piperazine-1-yl)benzodioxine ([^{18}F]**33b**), 6-(4-[4-[^{18}F]fluoro-(3-hydroxybenzyl)]piperazine-1-yl)benzodioxine ([^{18}F]**33d**) und 6-(4-[6-[^{18}F]fluoropyridine-3-yl]piperazine-1-yl)benzodioxine ([^{18}F]**33e**) were synthesized as benzodioxine derivatives with decreasing lipophilicity. For this 1-(1,4-benzodioxine-6-yl)piperazine (**30**) was coupled with the corresponding aldehyde derivatives by a reductive amination reaction in overall-RCY of 35 %, 20 %, 9 % and 15 %, respectively.

In vitro autoradiography on rat brain slices confirmed the correlation between non-specific binding and lipophilicity and lend [^{18}F]**33d** and [^{18}F]**33e** as putative radiotracers. Since [^{18}F]**33e** showed better D_4 selectivity, *ex vivo* organ uptake, metabolization rate and brain distribution were determined.

Examinations showed a principle qualification of [^{18}F]**33e** for the visualization of the D_4 receptors, but due to a lack of experiences a clear relation of D_4 to the ligand was not possible up to now. Further examinations *in vivo* are required to verify the ability of mapping D_4 receptors by this new radioligand.

Kurzzusammenfassung

Die fünf Subtypen des Dopaminrezeptors spielen eine entscheidende Rolle im menschlichen Hirn. Der Dopamin-D_4 Rezeptor ist dabei maßgeblich an Steuerungsprozessen des Verhaltens und deren Pathologien beteiligt und wird für die Ausbildung des Aufmerksamkeitsdefizit Syndroms (ADHS) sowie weiterer psychotischer Krankheitsbilder verantwortlich gemacht. Während die meisten Dopaminrezeptoren gut untersucht sind, fehlt es jedoch beim D_4 Rezeptor aufgrund seiner enorm geringen Hirnverteilungsdichte an Radioliganden für ein funktionelles Neuroimaging mittels der Positronen-Emissions-Tomographie (PET). In dieser Arbeit wurde die Radiosynthese potentieller D_4 Liganden entwickelt und diese anschließend pharmakologisch evaluiert. Dazu wurden ausgewählte Leitstrukturen über eine nukleophile Substitutionsreaktion mit trägerarmen (n.c.a.) [^{18}F]Fluorid am aromatischen Ring markiert und in einer 1-2 stufigen Aufbaureaktion zu den gewünschten Zielmolekülen umgesetzt.

Zunächst wurde eine effiziente Radiosynthese des hochselektiven [^{18}F]FAUC 316 ([^{18}F]**1**) entwickelt. Ausgehend von der ^{18}F-Fluorierung der symmetrischen Iodonium-Salze Bis(4-bromphenyl)iodonium triflat und Bis(4-iodphenyl)iodonium triflat zu den entsprechenden 4-[^{18}F]Fluorhalogenbenzolen in radiochemischen Ausbeuten (RCA) bis zu 60 % wurde durch Pd-katalysierte Kreuzkupplung der Markierungsprodukte und Piperazin mit $Pd_2(dba)_3$ oder $Pd(OAc)_2$ 4-[^{18}F]Fluorphenylpiperazin in RCA bis 42 % dargestellt. Parallel wurde neben der Standard- und Vorläufersynthese 5-Cyanoindol-2-carbaldehyd in vier Reaktionsschritten und einer Gesamtausbeute von 15 % synthetisiert und mittels einer reduktiven Aminierung zum [^{18}F]FAUC 316 gekoppelt. Die Gesamt-RCA nach erfolgreicher Hochdruckflüssigchromatographie (HPLC)-Separation belief sich auf 10 %.

Aufgrund des sich aus einer *in vitro* Autoradiographie ergebenen hohen nicht-spezifischen Bindungsanteils des [^{18}F]FAUC 316 war dieses für weiter reichende Untersuchungen *in vivo* nicht geeignet. Stattdessen wurden die Radioliganden 6-(4-[4-[^{18}F]Fluorbenzyl]piperazin-1-yl)benzodioxin ([^{18}F]**33a**), 6-(4-[4-[^{18}F]Fluor-(3-methoxybenzyl)]piperazin-1-yl)benzodioxin ([^{18}F]**33b**), 6-(4-[4-[^{18}F]Fluor-(3-hydroxybenzyl)]piperazin-1-yl)benzodioxin ([^{18}F]**33d**) und 6-(4-[6-[^{18}F]Fluor-pyridin-3-yl]piperazin-1-yl)benzodioxin ([^{18}F]**33e**) als Benzodioxin-Derivate mit abnehmender Lipophilie dargestellt. Dazu wurde die Vorstufe 1-(1,4-Benzodioxin-6-yl)piperazin mit den entsprechenden Aldehyden in einer gesamt-RCA von 35 %, 20 %, 9 % und 15 % gekoppelt.

Die Autoradiographie an Rattenhirnschnitten bestätigte den Zusammenhang zwischen nicht-spezifischer Bindung und Lipophilie und zeigte die potentielle Eignung von [^{18}F]**33d** und [^{18}F]**33e** als Radioligand. Aufgrund seiner günstigeren Affinität wurde von [^{18}F]**33e** *ex vivo* die Organaufnahme, Hirnverteilung sowie Metabolisierungsraten bestimmt.

Die Untersuchungen zeigten eine prinzipielle Eignung von [^{18}F]**33e** zur Darstellung der D_4 Rezeptoren, aufgrund mangelnder Erfahrungswerte ist eine eindeutige Zuordnung bislang jedoch nicht möglich. Weitere Untersuchungen *in vivo* sind erforderlich, um die Darstellbarkeit der D_4 Rezeptoren mittels [^{18}F]**33e** zu verifizieren.

Danksagung - Acknowledgement

Meinem Doktorvater Herrn Prof. Dr. Heinz H. Coenen möchte ich für die sehr spannende Themenstellung danken. Dabei nahm er besondere Rücksicht auf meine Interessen und setzte sich stets dafür ein, dass ich meine Ergebnisse auf diversen Konferenzen präsentieren durfte. Auch für die exzellenten Arbeitsbedingungen, wie sie nur selten in Forschungsbetrieben zu finden sind, möchte ich ihm danken.

Ein besonderer Dank gilt Herrn PD Dr. Johannes Ermert, welcher immer mehr war als bloßer Betreuer. Er war der ständige Begleiter, den man sich wünschen kann, mit stets offenem Ohr auch für mein Gejammer, wenn die Ergebnisse wieder mal nicht meinen Wunschvorstellungen entsprachen. Immer baute er mich wieder auf. Dabei hatte ich das große Glück von seinen umfangreichen Erfahrungen lernen zu können, nicht zuletzt während tausender Autobahnkilometer, nur unterbrochen vom einen oder anderen Schlagloch.

Herrn Dr. Dirk Bier und Herrn Dr. Markus Holschbach, welche doch meist vergesellschaftet auftreten (HoBi) möchte ich hier dennoch einzeln danken, da ihr Anteil so groß war:

Dirk, er nahm sich immer so viel Zeit für alle meine Anliegen, dass ich manchmal schon ein schlechtes Gewissen hatte. Mein Interesse an pharmakologischen Fragestellungen befriedigte er vollauf. Sicher wäre diese Arbeit ohne ihn ganz anders verlaufen.

Markus, sein schon als legendär geltender Fundus an organisch-chemischem Wissen war stets ein Segen. Kaum eine Frage, die er nicht sogleich aus eigener Erfahrung beantworten konnte.

Auch von Frau Dr. Wiebke Sihver lernte ich eine Menge über das Durchführen und Auswerten der biologischen Experimente. Nicht nur wegen der Arbeit, sondern auch wegen ihrer Gesellschaft freute ich mich stets auf jede neue pharmakologische

Evaluierung. Für ihre neue Stelle am Forschungszentrum Rossendorf wünsche ich ihr ganz viel Spaß und viele nette Kollegen.

Herrn Walter Wutz danke ich für die Durchführung der Tierversuche. Ich bin doch froh, dass er mir diese unangenehme und kniffelige Aufgabe abnahm.

Auch Frau Anette Schulze unterstützte mich immer geduldig.

Mein besonderer Dank gilt auch Herrn Peter Kaufholz, Kumpel, Mitarbeiter, Laborant, Bachelor und vieles mehr. Seine Unterstützung gab mir stets Kraft und um seine Routine bei der Arbeit beneideten mich meine Kollegen. Durch seine halbe Stelle teilte sich die Woche immer in die schönen und die normalen Tage.

Meinen Bürokollegen und Mitdoktoranden Herrn Andreas Helfer und Herrn Jens Cardinale danke ich für die angenehme Gesellschaft und die vielen fruchtbaren Gespräche, in denen wir demonstrierten wie wichtig der wissenschaftliche Austausch ist.

Andy, langjähriger Studienkollege, ihm muss ich wohl zunächst dafür danken, dass ich überhaupt in der Nuklearchemie gelandet bin. Von seiner entspannten Haltung auch bei Problemen und Unannehmlichkeiten konnte nicht nur ich viel lernen.

Jens, Meister des hypervalenten Iods, er war immer eine große Hilfe. Mit ihm teilte ich viele Laborprobleme und konnte mich wunderbar gemeinsam aufregen, sei es über ungenügende Literaturvorschriften oder das unverschämte Syntheseglück bestimmter Personen.

Allen beiden wünsche ich viel Erfolg und Spaß für ihre weitere Arbeit.

También con el señor Johnny Castillo Maleán, el “Cocinero Eterno” o el “Rey de Incas”, se pudo charlar sobre cada el problema de síntesis. ¡Hey pana!, su alegría siempre fue apasionante y sólo se la nubló a causa de los problemas realmentes decisivos de la vida: “¡Comida es importante – no la es diverción!”

Frau Silke Grafmüller, Herrn Sascha Rehbein, Frau Erika Wabbels und der Zyclotroncrew bestehend aus Herrn Klaus Adrian und Herrn Manfred Holzgreve danke ich für das zur Verfügung stellen des [^{18}F]Fluorids. Ihre kompetente Arbeit stellte die Grundlage, ohne die meine Arbeit gar nicht möglich gewesen wäre. Nicht zu vergessen sind auch die gefühlten 100.000 Batterien für Maus und Tastatur. Danke auch dafür, Klaus und Manni.

Herrn Ingo Montag danke ich für die Unterstützung bei den IT Fragen. Durch seine Hilfe löste sich viel Kopfzerbrechen in Wohlgefallen auf.

Herrn Karl-Heinz Riedel danke ich für seine Unterstützung und Kompetenz bei allen mechanischen Problemen.

Darüber hinaus gilt mein Dank allen Mitarbeitern des Instituts für Nuklearchemie am Forschungszentrum Jülich GmbH deren Wirken und Gesellschaft diese Arbeit möglich machten und sie stets bereicherten.

Ein besonderer Dank gilt meinen lieben Eltern, die mir das Studium ermöglicht haben und stets eine sehr wichtige Stütze gewesen sind. Sie und meine Geschwister waren immer für mich da.

Mit meiner Freundin Alexandra teilte ich schöne und anstrengende Momente. Sie hat mich stets bestärkt, wenn ich an mir gezweifelt habe.

Index

List of Important Symbols and Abbreviations

5-HT$_X$	subtypes of serotonin (5-hydroxy*t*ryptamine) receptors
Å	Ångström; 1 Å = 10^{-10}m
A	activity of radiation (*Bq* or *Ci*)
$A_{M;\,S}$	molar (M) and specific (S) activity
ADME	adsorption, distribution, metabolism, and elimination
ArC	microdomain of aromatic amino acids
Asp	asparagine (amino acid)
b	broad signal (NMR)
BBB	blood brain barrier
Bn	benzyl group
Boc	*tert.*-butyloxycarbamate (amine protection group)
Bq	Becquerel (1 Bq = 1 decay per second [s^{-1}] = 2.7 10^{-11} Ci)
BuLi	butyl lithium
c	concentration
C18	octadecyl chains on solid phase silica particles
c.a.	carrier added
CA	cornu ammonis (part of hippocampus)
cAMP	cyclic adenosine monophosphate
c.f.	carrier free
cLog P	calculated logarithmic distribution coefficient of lipophilicity (referred to one species)
CNS	central nervous system
CoMFA	comparative molecular field analysis
CT	computer x-ray tomography
d	deuterium
$D_{1\text{-}5}$	subtypes 1-5 of dopamine receptors
D_{2long}	long haplotype of dopamine D_2 receptor (443 amino acids)
D_{2short}	short haplotype of dopamine D_2 receptor (414 amino acids)
$D_{4.x}$	different haplotypes of dopamine D_4
DCM	methylene chloride

DEA	diethylamine
DMAA	*N,N*-dimethylacetamide
DMF	*N,N*-dimethylformamide
DMSO	dimethylsulfoxide
e^+	positron
e^-	electron
E	extracellular loop
EA	ethylacetate
EC	electron capture
EOS	end of synthesis
eV	electron volts
$G_{i;\,s;\,o}$	guanine nucleotides (i = inhibating; s = stimulating; o = other)
GD	gyrus dentatus
h	Stunde
h, m, p (receptor)	human, mourine, porcine receptor
HBC	Hartwig-Buchwald coupling
HPLC	high performance liquid chromatography
Ht	hematocrit
I	intracellular loop
ID	injected Dose
IC_{50}	half maximal inhibitory concentration
IUPAC	international union of pure and applied chemistry
K_i	inhibition constant
K_D	dissociation constant
k_{off}	reaction constant from bound to unbound state
k_{on}	reaction constant from unbound to bound state
Leu	leucine (amino acid)
Log $D_{7.4}$	partition coefficient of *all* species of *one* compound in solution at pH 7.4
Log $P_{7.4}$	partition coefficient of *one* species of *one* compound in solution at pH 7.4
m	multiplett

MeCN	acetonitrile
min	minute
MS	mass spectroscopy
n	neutron
N	number of moles
n.c.a.	no carrier added
nM	nano molar
NMR	nuclear magnetic resonance (spectroscopy or tomography)
NMRI	naval medical research institute
OECD	organisation for economic co-operation and development
OAc	acetate
OMe	methoxy
OTf	triflate
OTs	tosylate
p	proton
P450	cytochrome P450 (CYP) enzyme group
	(often related to monooxygenase reaction)
PET	positron emission tomography
Pd	palladium
PGP	permeability glycoprotein
p.i.	post injection
pH	negative logarithm of proton concentration in solution
Ph	phenyl group
Phe	phenylalanine (amino acid)
ppm	parts per million
r	recovery
RCY	radiochemical Yield
Rh	rhodium
rt	room temperature
s	second
SAR	structure activity relationship

SD	standard deviation
Ser	serotonine
S_N2	bimolecular nucleophilic substitution
SPECT	single photon emission computer tomography
t	triplett
$T_{1/2}$	half life
THF	tetrahydrofurane
TLC	thin layer chromatography
Tf	triflyl
TM	transmembrane helix
Trp	tryptophane (amino acid)
Ts	tosyl
Tyr	tyrosine (amino acid)
UTR	untranslated region
UV	ultraviolet spectra
VNTR	variation number of tandem repeat (polymorphism)

α	alpha decay (particle)
α_1	alpha-1 adrenergic receptor
β^+	positron decay
γ	gamma radiation (photon)
δ	chemical shift
ν_e	electron neutrino
∏	aromatic system

1. Introduction

"Cogito ergo sum" – Man is presumed to be the only animal able to reflect its thinking. This designates our existence. Since the realization that the brain is the location of cognitive abilities, its function engrosses generations of scientists and still fascinates mankind.

Hippocrates of Kos described already in the "Corpus Hippocratum" the brain and mentioned epilepsy as a functional brain disease[1], but it was a long way until the awareness of a chemical signal transmission by Dale and Loewi (NP 1936) and its pathological aberrances. Nevertheless, the next step was now set to the corresponding neuroreceptors as the main interests.

In vivo neuroreceptor imaging was conceivable for the first time in the mid of the 1970s with the emergence of autoradiographic methods using radiotracers[2]. The possibility of a clinical application with new tomographic methods enabled the young field of neuroscience to determine functional correlations of neuroreceptor / neurotransmitter systems in the human brain. Nowadays, despite the development of a series of alternative non-radioactive brain imaging techniques, autoradiography still represents an integral part in functional brain mapping. Typical examples for neuroreceptor imaging with radiopharmaceuticals include: (1) normal physiology[3], (2) pathophysiology[4], for example, the interaction of receptors in psychiatric diseases or differentiation between state and trait, (3) disease monitoring[4] for observation of progression or recession of a disease or a treatment, and (4) drug design and development including mechanisms and dosing[5]. The targets for some of the first successful radioligands for the central nervous system (CNS) were the in high density expressed receptors of dopamine D_2[6] and serotonin 5-HT_{2A}[7] but meanwhile more than 150 PET radioligands, labelled with ^{11}C or ^{18}F, for circa 20 neuroreceptor subtypes (from about 80 known and about 600 assumed[8]) were developed, including other dopamine[9] and serotonin subtypes[10,11] , dopamine and serotonin transporters[12-14] , adrenergic[15],

nicotinic cholinergic[16], muscarinic cholinergic[17], GABAergic[18,19] , histamine[20], and others.

2. Basics and Methods

2.1 Imaging of neurofunctions with positron emission tomography (PET)

Positron emission tomography (PET) represents a modern nuclear medicine imaging technique which is mainly used for diagnostics and research in oncology[21-23], cardiology[24-27], neurology[28-31], and psychiatry[32-34].

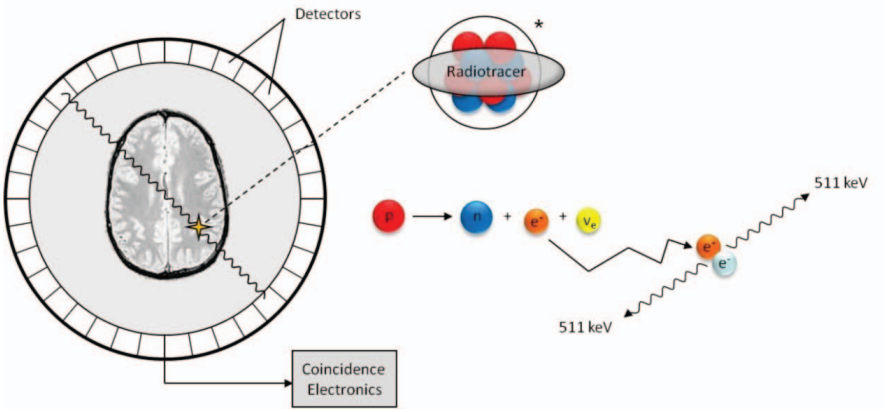

Figure 2.1: Coincidence measurement of a normal PET scan setup. In the radionuclide of the tracer a proton converts into a neutron which results in the emission of a positron and an electron neutrino. After thermalisation the positron subsequently annihilates with an electron to γ-rays. For imaging only coincedently detected signals cause a count. p = proton, n = neutron, e^+ = positron, e^- = electron, ν_e = electron neutrino.

Basic principle of PET is the recombination of a positron and an electron. Positrons represent the anti matter of electrons and vice versa. The recombination and subsequent annihilation results in axial symmetrically emitted γ-quantums of 511 keV, respectively, which can be detected easily. The positron sources consist of neutron deficient nuclides (e.g. ^{11}C, ^{13}N, ^{18}F, etc.) which are stabilized by conversion of a proton to a neutron and

simultaneous emission of a positron and an electron neutrino. While the cross section for interaction with matter of the electron neutrino is extremely low, the positron is captured "real in time and space" by its anti matter (Fig. 2.1). After thermalisation the positron forms an exotic atom, the para-positronium, in a singulet state (S = 0) which decays by annihilation. Since only small kinetic energy of the positron is left this results in a generally negligible linear momentum during annihilation. Comparatively the unsymmetrical annihilation of the ortho positronium (triplet state, S = 1) is very rare[35] with 0.4 % in water and not perturbing. Thus, the collision of the positron with an electron causes in over 99.6 % of the cases the above mentioned coincedently and antipodal emitted γ-quantums. The γ-quantums are registered outside of the body by the circular arranged detectors of the PET scanner. The position of annihilation is located through a simultaneous detection of 511 keV incidents on the interception of the virtual lines (lines of response = LOR) between two detectors, respectively. The resolution of this method is mainly limited by the starting kinetic energy of the emitted positron which defines the local average range until thermalisation and annihilation.

The application of a pharmaceutical labelled with a positron emitting nuclide allows an *in vivo* high-resoluting monitoring of the radiopharmaceutical non-invasively with a comparatively small radioactivity of tracers. Due to the generally small amounts of pharmaceuticals which are applied, physiological equilibriums remain unaffected[36]. The particular characteristic of this method is the possibility of an actual molecular imaging of biochemical processes in contrast to alternative tomographic methods like (X-ray) computer tomography (CT), nuclear magnetic resonance (NMR) and single photon emission computer tomography (SPECT). Since the coincidence measurement of the β^+-decay enables an exact correction for absorption and scattering of photons along the LORs, in contrast to SPECT radioactivity can be measured quantitatively by PET[37]. Assumed that the metabolism of the radiotracer is generally known bio-mathematical models allow for a quantification of these processes[38-40].

2.2 Steps of radioligand development

As illustrated in Figure 2.2, the development of a PET radioligand is a complex and multidisciplinary process. Starting from the identification of the biological target or ligand up to human studies or even approval, often plenty of years are needed and thousands of disappointments have to be got over. Due to that fact and the comparable small number of radiochemical working groups, statistically only every 15 years a new radiotracer comes to approval[41].

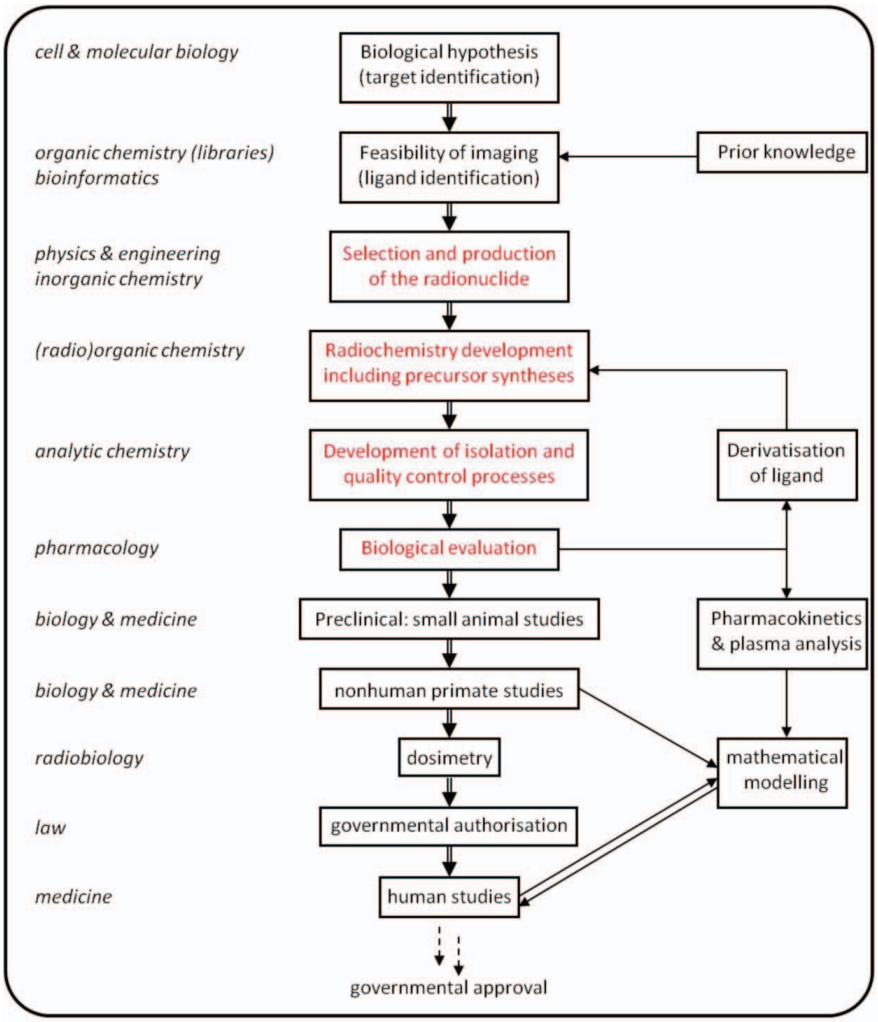

Figure 2.2: Simplified scheme of PET neuroreceptor radiopharmaceutical development (adapted with changes from[5]). Despite very strong interdisciplinary cooperation, core tasks of radiochemistry are shown in red.

Following descriptions especially shall enlighten the steps of development directly regarded to the radiochemist in developing a CNS radioligand.

2.2.1 Preceding considerations

The identification of the biological target which is the first and particularly for commercial drug development most important step is not discussed here in detail. Reasons are that the interests of this work lay in the reverse questioning of the relevance of a neuroreceptor of the central nervous system as such an appropriate target. Therefore, first considerations focus on the selection of a suitable ligand for labelling. Although the success of a radiopharmaceutical is mostly based on empiricism and serendipity a number of criteria will increase the chances: (1) the affinity of the ligand for the target receptor has to be high enough in compliance with its selectivity and target density. Because not all of the about 600 assumed different subreceptors can be tested or are known at all, it has to be balanced which are of critical interest. Determination of the binding profile has to be conducted to obtain affinities which is part of biological evaluation and is described in chapter 2.2.4. (2) The physico-chemical parameters of the potential tracers such as lipophilicity have to be in an adequate range for solubility, uptake and binding conditions. Consequences of lipophilicity are explicitly specified in chapter 2.5. (3) A radionuclide for PET or alternatively SPECT has to be selected before a basic labelling concept can be developed. While large molecules about 1000 u can be linked with a radiometal carrying marker, smaller ones need to be labelled by one of their atoms by a radionuclide (authentic tracer) or a radionuclide carrying substitute with similar physico-chemical properties (analogue tracer). (4) The limited prediction of success let it seem meaningful to keep option open for an easy derivatisation of the chosen ligand for a rapid readjustment of physikochemical parameters without decisive alteration of the chosen radiolabelling process and as far as possible of its pharmacological affinities.

2.2.2 Selection and production of short-lived positron emitting radionuclides especially fluorine-18

As described above radionuclides for PET applications involve organic elements and metals (Tab. 2.1). Irrespective of the nature of the element a suitable PET nuclide has to fulfill a few basic demands. The physical half life should be in a range which is preferably short for a low exposure of patients and repeatability of experiments but nevertheless long enough to permit a few synthetic steps. The half life of some relevant organic nuclides like ^{13}N ($T_{1/2}$ = 9.96 min) or ^{15}O ($T_{1/2}$ = 2.03 min) is so short that integration in larger molecules is impossible in most cases but they can be converted on-line to small tracers like [^{13}N]NH_3 or [^{15}O]OH_2. Furthermore, the maximum decay energy and thus kinetic energy of the emitted positrons should be as low as possible because it limits the resolution of this imaging method. Beside this, electron capture (EC) as a competing decay mode exists for most positron emitters and is not desired in high percentage.

Tab. 2.1: Nuclear data of important radionuclides for positron-emission tomography and their production routes [from[42-45]].

Nuclide	*Half life*	*Percentage of β^+-Decay*	*Maximum β^+-Energy [MeV]*	*Production Route*
^{11}C	20.4 min	β^+ (99.8 %)	0.96	$^{14}N(p,\alpha)^{11}C$
^{13}N	10.0 min	β^+ (100 %)	1.19	$^{12}C(d,n)^{13}N$ $^{16}O(p,\alpha)^{13}N$
^{15}O	2.0 min	β^+ (99.9 %)	1.72	$^{14}N(d,n)^{15}O$ $^{15}N(p,n)^{15}O$
^{18}F	109.7 min	β^+ (97 %)	**0.64**	$^{18}O(p,n)^{18}F$ $^{20}Ne(d,\alpha)^{18}F$
^{73}Se	7.1 h	β^+ (65 %)	1.30	$^{75}As(p,3n)^{73}Se$
^{82}Rb	1.3 min	β^+ (96 %)	3.35	generator $^{82}Sr(T_{1/2}$ = 25d)
^{120}I	1.4 h	β^+ (64 %)	4.1	$^{122}Te(p,3n)^{120}I$

Due to its low positron energy of 650 keV (mean tissue/water range of 0.3 mm) and its balanced half life of 109.7 min, fluorine-18 is a nearly ideal nuclide for PET and is the most often used radionuclide for diagnostics with PET although it is rarely an original part of a natural biomolecule. In favour its half life permits imaging protocols long enough for investigation of even slow tracer kinetics of up to about 6 h[23]. Radiometals can only be used as part of complex systems why application is more limited. However, the fact that many of them can be obtained as daughter nuclides from a generator is an unquestionable advantage and enables clinical utilization far away from a cyclotron unit. Since they are neutron deficient nuclides, positron emitters can generally not directly be produced by neutron bombardment in a reactor or by spallation sources. Major source of PET nuclides is therefore the bombardment with charged particles like protons or deuterons in a cyclotron. These projectiles are accelerated by an electric field circulated by a magnetic field and deflected by a capacitor to hit the target. Targets are special designed for its application as liquid or gas targets but always intensively cooled. In Figure 2.3 a cross-section scetch of a water target for the production of [^{18}F]fluoride is presented. After radiation of enriched [^{18}O]OH_2 with a 17 MeV proton beam the aqueous [^{18}F]fluoride solution is directly transfered by a shielded capillary system into a hot cell.

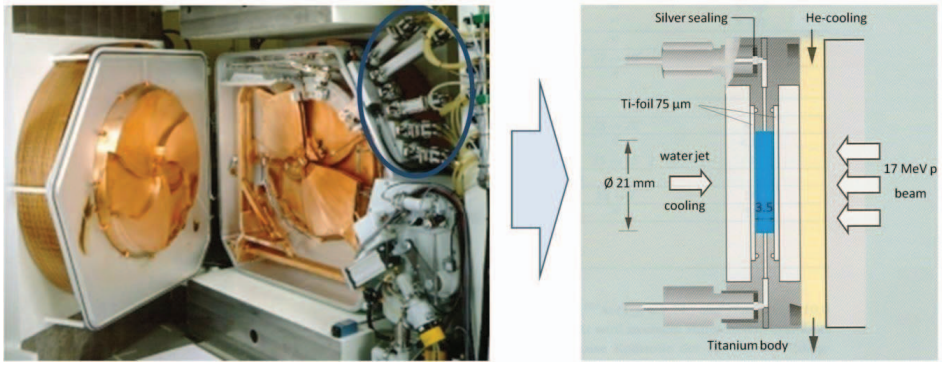

Figure 2.3: Interior of a cyclotron (GE PETtrace) for the production of PET-relevant nuclides (left)[46]. Position of targets is indicated by a blue circle. As an example the scheme of a middle pressure water target for production of [^{18}F]F^- over the ^{18}O(p,n)reaction is displayed (right)[42]. The interior space of 3.5 mm thickness ingests a volume of 1.3 ml.

For electrophilic [^{18}F]F_2 production a Ne or [^{18}O]O_2 gas target is used. Due to the low mass of produced [^{18}F]fluorine an amount of inactive fluorine has to be added followed by a second short irradiation to override chemical adsorption[47]. Problems of the presence of such a carrier are discussed in the next chapter.

2.2.3 Development of labelling methods with fluorine-18

Radiosyntheses of organic molecules are very different from conventional organic chemistry. Thereby three alternatives are to differentiate depending on the amount of inactive tracer or rather isotope, called carrier. The chemistry of carrier-added (c.a.) reactions is more similar to those which are performed non-radioactive. Though, for most applications such as neuroreceptor imaging, a high amount of carrier is inappropriate due to its pharmacological influence. Therefore, in most cases a carrier free (c.f.) situation is aspired. Due to the fact that this is only possible for nuclides without natural abundance (or extremely little such as technetium or astate) the normal situation involves a small amount of carrier (no-carrier-added = n.c.a.). This is displayed in the molar activity (A_M) or specific activity (A_S)[48]:

$$A_M = \frac{A}{N} \ \frac{Bq}{mol} \ . \tag{2.1}$$

$$A_S = \frac{A}{M} \ \frac{Bq}{kg} \ . \tag{2.2}$$

For low specific / molar activity material are inactive reaction partners in an extreme excess. Thus, the reaction kinetics of labelling processes with reactants of high A_S (A_M) is pseudo first order. Besides the short half-life, non-equimolarity and nanomolare range make n.c.a. reactions difficult and necessitate special synthetic techniques. Because of the difficulty to determine the specific activity of n.c.a. [^{18}F]fluoride direct after production, reproducibility is often more problematic than in the same but non-radioactive and therefore equimolecular reactions. Nevertheless, selecting fluorine-18 as the radionuclide of choice the next step has to be a feasible radiosynthesis strategy. In most cases especially in authentic labelling the fluorine carrying moiety is aromatic. It is preferred due to the normally higher *in vivo* stability of aromatic fluoro compounds. This leads to two conceivable options from the general concepts of fluoro-organic chemistry: electrophilic and nucleophilic substitution.

A problem that should not be underestimated is the identification and separation of the obtained products which can only identified indirectly by chromatographic methods using a standard compound due to the extremely low masses under n.c.a. conditions. Thus, accidental consistency can appear and losses of activity due to adsorption often cause bad comparability of yields when working under n.c.a. conditions.

Apart from the few times when simple solid phase extraction can be used, separation of products requires generally high performance (pressure) liquid chromatography (HPLC). Besides alluded losses of n.c.a. compounds HPLC separation involves other problems:

- When the number or concentration of reactants is high it can overlay the active product fraction. Efficient prepurification sometimes including a derivatisation step can help but has to be in balance with time and accessory product loss.
- Similar substituents can be challenging. In some cases even the substitution of nitro by fluorine leads to such compounds which cannot be separated acceptably by HPLC. Reduction of nitro to amine after fluorination results in viable separation but presents an undesired time consuming secondary reaction step.

Electrophilic fluorination

The electrophilic fluorination with elemental F_2 is a suitable method in organic chemistry although its toxicity, reactivity and gaseous state makes it difficult to handle. Furthermore, handling a radioactive species causes even higher problems. The main problem, however, in using $[^{18}F]F_2$ is, that it cannot be obtained without a considerable amount of inactive fluorine. Thus, reactions are always carrier-added ($[^{18}F]F^- < 3.7 \cdot 10^{15}$ Bq/mmol; $[^{18}F]F_2 < 3.7 \cdot 10^{11}$ Bq/mmol)[49]. Electrophilic fluorination is therefore only suitable to generate radiotracers when a pharmacologically and metabolically relevant amount can be tolerated, *e.g.* aromatic amino acids like 2-[^{18}F]fluoro-L-tyrosine[50] or 6-[^{18}F]fluoro-L–DOPA[51,52]. For these and other aromatic compounds many different electrophilic fluorination methods are described using $[^{18}F]F_2$ or AcOO[^{18}F]F[53], Xe[^{18}F]F_2[54] often in combination with demetallation reactions with silicon, germanium, stannyl and mercury. Over the years several reviews about electrophilic fluorination were published describing these methods in detail[55-57].

Nucleophilic fluorination

In principle [^{18}F]fluoride can be obtained almost free of inactive fluoride (only very small amounts of fluorine-19 from surroundings). Therefore, no-carrier-added nucleophilic fluorination methods play a more decisive role and are the only possibility for the ^{18}F-fluorination of neuroligands with high A_S. One problem is, that n.c.a. [^{18}F]fluoride is obtained in form of an aqueous solution from the target. Here, the fluoride is highly solvatisated ($\Delta_{hydrate}$ = 506 kJ/mol) and therefore not nucleophilic. Before a ^{18}F-substitution can be conducted, the [^{18}F]fluoride solution has to be dried generally by azeotropic distillation with acetonitrile. Then the dry [^{18}F]fluoride is resolubilized by a polar and aprotic solvent, *e.g*. dimethyl sulfoxide (DMSO), *N,N*-dimethyl formamide (DMF), *N,N*-dimethyl acetamide (DMAA) or acetonitrile (MeCN). To avoid a loss of radioactivity during distillation, as well as wall adsorption, carbonates or oxalates are added as non-nucleofugic base and non-isotopic carrier. The binding strength of the counter cation (mostly potassium or cesium) to the dried [^{18}F]F^- affects its chemical reactivity. Voluminous complexes of the cation with crown ethers or aminopolyethers such as Kryptofix®2.2.2, create a nearly “naked” fluoride in dipolar aprotic solvents and increase its nucleophilicity and hence its reactivity dramatically but unfortunately also its basicity[58-60].

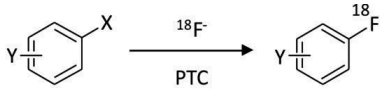

Y = NO_2, CN, CHO, RCO, COOR
X = F, NO_2, $^+N(CH_3)_3$, Cl, Br, I
PTC = $[K2.2.2]^+_2CO_3^{2-}$; $[K2.2.2]^+_2CO_3^{2-}$/ $C_2O_4^{2-}$; R_4N^+; Cs^+: Rb^+

Figure 2.4: Nucleophilic aromatic ^{18}F-fluorination of activated arenes.[60,61]

A limitation of an aromatic nucleophilic fluorination is the required electron deficiency of the aromatic ring. Nucleophilic substitution can be achieved through the presence of an activating group. Favourable are electron withdrawing substituents in *ortho* or *para* position to a leaving group. For activating eminently suitable are nitro, cyano or carbonyl groups because they feature good π-acceptors with high Hammett σ-constants[62]. Further reaction steps can contain the cleavage of these groups as well as cleavage or

transformation of contingently required protection groups.

For the underlying $S_N(Ar)$ mechanism in arenes, fluorine itself is one of the best leaving group but cannot be used for n.c.a. syntheses. It is followed by the nitro group and the trimethylammonium cation. The latter often results in higher yields but in case of poorly activating substituents and of sterical hindrance [^{18}F]fluoromethane is obtained as main product[63,64]. Other halogens can also be used especially for $S_N(Ar)$ reaction in pyridines[65].

2.2.4 Special methods in n.c.a. ^{18}F-fluorination

The above described methods display the basic methods of direct labelling with fluorine-18. Due to their limitation many applications demand progressive methodical developments, including special precursors, substrates, reaction parameters or pathways. Following labelling methods used in this work are considered in detail.

2.2.4.1 Secondary labelling compounds

As mentioned in chapter 2.2.3 it is desirable to introduce fluorine-18 at the latest possible reaction step, due to the short half life of 109.7 min. Therefore, direct nucleophilic fluorination represents the preferred labelling method. Further eligible ^{18}F-labelling reactions consist of maximum two steps: the actual ^{18}F-fluorination and, if necessary, cleavage of protection groups. Nevertheless, some aromatic molecules do not admit direct labelling due to a lack of electron withdrawing activation. Other disadvantages of direct fluorination are the relatively harsh conditions needed. Decomposition or racemisation can occur with sensitive compounds. In these cases build-up syntheses are necessary starting from small molecules. An assortment of these small aromatic molecules which are meanwhile established as labelling synthons are listed in Figure 2.5. Some of these synthons have to be build in some reaction steps themselves. N.c.a. 4-[^{18}F]fluorophenol for example cannot be obtained by direct labelling (Fig. 2.5; **A**). For build-up of ^{18}F-fluorinated arylethers the synthon has to be generated by labelling the ketone and its transformation by Bayer-Villiger oxidation and subsequent saponification of the ester[66]. Other build-up syntheses include oxidation, reduction or hydrolysation of a strongly activating aryl-substituent which lead to a variation of secondary compounds. Typical starting agents are ketones (Fig. 2.5; **B**[67], **C**[68,69]), aldehydes (Fig. 2.5; **D**[70], **E**[71,72]) or sulfonyles (Fig. 2.5; **F**[73,74]) and pyridines (Fig. 2.5; **G**[75,76]). As substituents with extremely

high Hammet constants the nitro (Fig. 2.5; **H**[77]) and nitrile (Fig. 2.5; **I**[78,79]) group are of special interest and can be easily converted to amines. It is tried to avoid longer pathways but in some cases yields and reaction time reach the level of direct labelling. For the synthons a further advantage consists in an increased possibility of generating trimethylammonium triflates as precursors. More complex biomolecules mostly contain methylation sensitive moieties like basic amines.

Nevertheless, the most common used secondary labelling compounds are not aromatic. 2-[^{18}F]fluoroethyl tosylate[80] and [^{18}F]fluoromethyl bromide[81] are mostly used to substitute the methyl of a methoxy group but can commonly not used in authentic labelling.

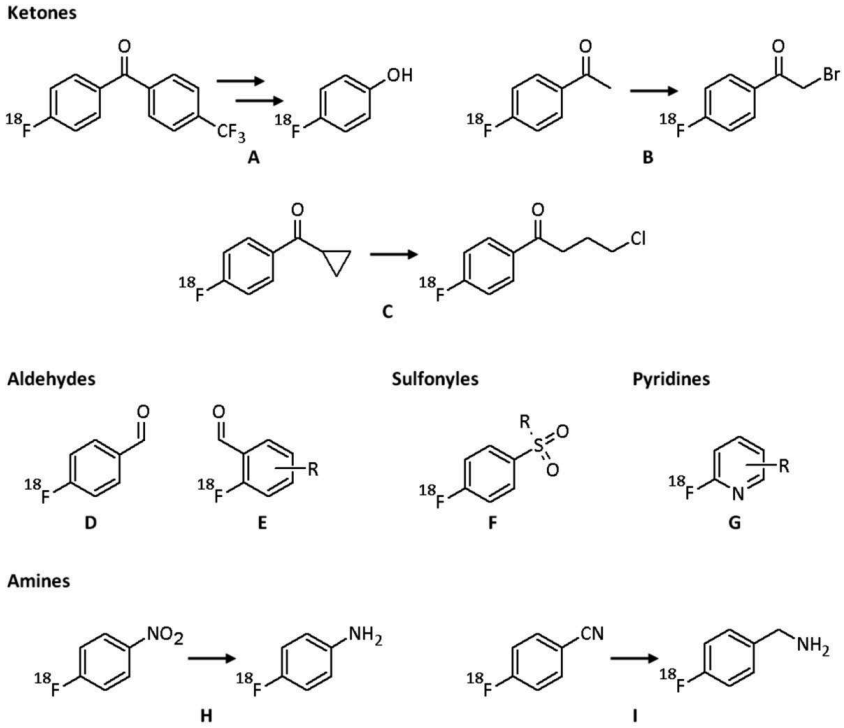

Figure 2.5: List of important aromatic synthons for build-up syntheses.

In aromatic ^{18}F-chemistry [^{18}F]fluorobenzaldehyde and its derivatives are the most versatile building blocks. The highly activating carbonyl group leads to high radiochemical yields with a vast amount of derivatives in short reaction times, especially when trimethylammonium triflate is used as leaving group[57]. Subsequently the aldehyde group

can be transferred to the carboacid, to the benzyl alcohol and benzyl halide and others as displayed in Figure 2.6. [^{18}F]Fluorobenzylethers and –amines can hereby easily be generated.

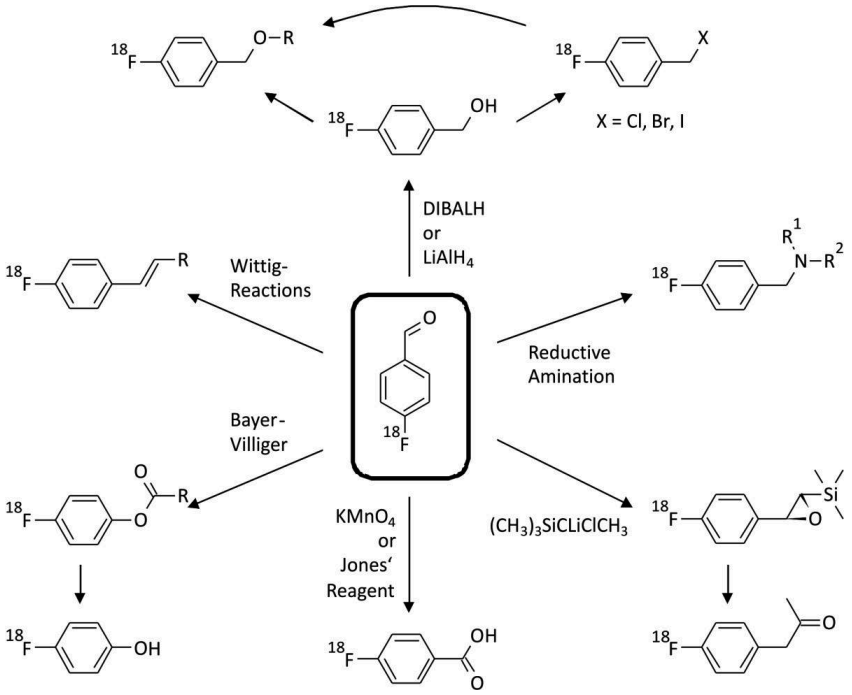

Figure 2.6: Sample of important build-up syntheses starting from 4-[^{18}F]fluorobenzaldehyde (adapted with changes from[82]).

2.2.4.2 Iodonium salts in fluorine-18 chemistry

Diaryl iodonium salts have recently proven excellent precursors for aromatic radiofluorination. They consist of a iodo(III) species covalently bound to two aryl groups and carrying a positive charge. The corresponding anion mostly is a halide, triflate or tosylate. Since their first application in fluorine chemistry[85] they proved as highly potent precursors especially to introduce [^{18}F]fluoride in electron rich aryls which is otherwise not possible. Despite its high relevance, the mechanism of this fluorination is not totally understood. Three different processes are involved and controversially discussed. First consideration is an analogous mechanism to standard $S_N(Ar)$ fluorination. Here, the iodo(III) moiety acts as activating and leaving group concurrently. In a first step the nucleophile ([^{18}F]F$^-$) attacks the onium iodine to bind covalently. Due to the two lone

electron pairs (phantom ligands) a trigonal bipyramidal intermediate state is composed as displayed in Figure 2.8 (A).

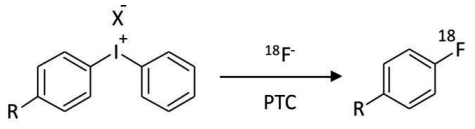

X = $^-$OTf, $^-$OTs, Cl^-, Br^-, I^-
R = Me, C_4H_9, OMe, OBn, I, Br, Cl
PTC = $[K2.2.2]^+_2CO_3^{2-}$; $[K2.2.2]^+_2CO_3^{2-}$ / $C_2O_4^{2-}$; R_4N^+; Cs^+: Rb^+

Figure 2.7: Nucleophilic fluorination of an unsymmetrical iodonium salt.

Subsequently the complex undergoes intramolecular aromatic nucleophilic substitution. In this model a bulkier aryl group would occupy the less encumbered equatorial position with two near and two far neighbours. Thus, the bulkier ligand is closer to the attacking nucleophile when "collapsing". Such an *ortho*-effect in fact is observed[84-86] also in corresponding radiofluorination reactions *via* diaryliodonium salts[87,88]. It is an explanation why normally desactivating methyl groups in *ortho*-position lead to higher yields. Nevertheless, this model cannot explain the influence of the counter anion and the fact that the *ortho*-effect even with four methyl-substitutes is comparatively small. Furthermore, studies with phosphorous pentahydride showed that apical-equatorial interactions in a trigonal bipyramidal structure are symmetry forbidden[89]. By Berry pseudo rotation tetragonal pyramidal constitutions can be reached in which an interaction between the nucleophile and an aryl ligand would be symmetry allowed[90]. A resulting reductive elimination, similar to a metal catalyzed coupling, would be effected by the counter anion. Here the two aryls now are equidistant to the nucleophile (B).

The *ortho*-effect needs to be explained with kinetic effects during elimination, since elimination of the bulkier ligand leads to a faster decrease of tension. Otherwise the extreme softness of iodine could possibly reduce the grade of forbiddance.

So far, an influence of radical reactions can also be discussed. On the one hand a radical mechanism cannot stand on its own because above described influences, *e.g.* the *ortho*-effect would not be explainable. On the other hand the use of radical scavengers like 2,2,6,6-tetramethylpiperidinoxyl (TEMPO) improve radiochemical yields or reproducability[91,92]. Furthermore, side products which can only be explained with

radicals, like biaryls are observed. Therefore, it is probably that a radical mechanism only takes place in decomposition of the iodonium salt in absence of a nucleophile.

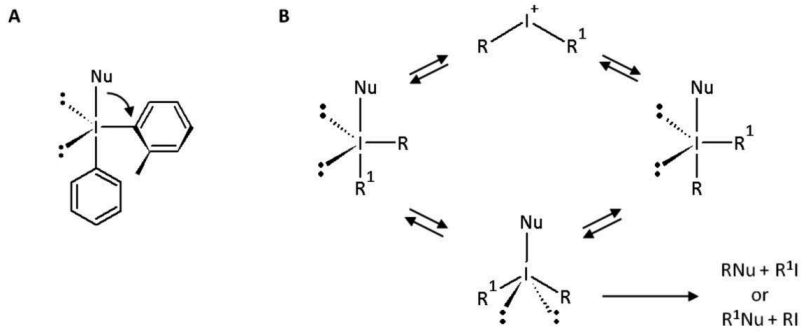

Figure 2.8: Comparison of the two assumed mechanisms of nucleophilic reaction on iodonium salts[93].

A further characteristic of iodonium reactions is the bad use of DMSO as solvent[94-96]. The semipolar character of the S=O "lance" of DMSO leads to S^{+}-O^{-} which strongly solvates cations[97]. Solvation of the iodine(III) moiety would reduce its activity. Otherwise, use of DMSO sometimes is described when phase transfer catalysts other than Kryptofix are used[98]. All other standard solvents can be used but without a clear preference.

Up to now the ^{18}F-labelled product of a iodonium precursor is generally used as a synthon for build up syntheses. The reason is that in the case of more complex molecules past studies led to very low RCY or failed completely or the iodonium salts were not achievable.

2.2.4.3 Palladium-mediated cross-coupling reactions in ^{18}F-radiosyntheses

The role of transition metals in radiochemistry especially with fluorine-18 has increased in recent years. One of the most upcoming reactions is the copper-mediated [3+2] cycloaddition from Huisgen et. al[99], often called click-chemistry[100,101]. It is mainly used to introduce ^{18}F-labelled linkers in large molecules like peptides and proteins but meanwhile also in smaller ones[102]. Furthermore, Pd- and Rh-mediated decarbonylation is sometimes used for removing aldehyde groups.

Cross-coupling reactions using Pd(0) complexes and specific designed ligands to form

carbon-carbon or carbon-heteroatom bonds, starting from the corresponding arylhalids have distinctly enhanced organic chemistry syntheses in recent years by gaining access to challenging structures in single-step routes with high yields[103,104]. This is confirmed by awarding Richard F. Heck, Ei-ichi Negishi, and Akira Suzuki the Nobel Prize in 2010. Advantages like high reaction rates and yields and a comparable easy handling make it very interesting for syntheses with short-lived positron emitters. Nevertheless, only some applications of palladium in fluorine-18 chemistry were released until now. Several problems can cause this fact. On the one hand slight or different solubility of reactants can complicate an automated synthesis. Furthermore, the high number of reactands together with the standard usage of unpolar solvents complicates isolation and separation procedures of n.c.a. products. On the other hand for the most palladium catalysed syntheses with aromatics, arylhalides are required. [^{18}F]Fluoroarylhalides can only conveniently be obtained suitable from iodonium precursors. Former reaction routs, starting from a trimethylammonium salt precursor resulted in poor radiochemical yields[105]. This nihilates advantages of following reaction steps. But often also iodonium precursors result in low reproducability of radiochemical yields.

Tab. 2.2: Previous applications of Pd-mediated cross-coupling reactions with fluorine-18 labelled synthons (Ph = C_6H_5).

Type	*Entry*	*^{18}F-coupling synthon*	*RCY*	*Lit.*
Stille	Ph-$SnBu_3$	[^{18}F]F-Ph-Br	70-90 %	106
Stille	H_2C=CH- $SnBu_3$	[^{18}F]F-Ph-I	56-53 %	107
Stille	CHR^{I}=CR^{II}-$SnBu_3$	[^{18}F]F-Ph-Br	56-74 %	108
Stille	Nucleoside-$SnBu_3$	[^{18}F]F-Ph-I	50-70 %	109
Sonogashira	HO-CR_2CCH	[^{18}F]F-Ph-I	34-88 %	110
Hartwig-Buchwald	R_2NH	[^{18}F]F-Ph-Br	~60 %	111
Hartwig-Buchwald	Indole-NH	[^{18}F]F-Ph-I	36-70 %	112
Suzuki	Ph-$B(OH)_2$	[^{18}F]F-Ph-I	~90 %	113

Nevertheless, described cross-coupling reactions generally resulted in high yield (Tab. 2.2). This underlines the potential of these reaction types for fluorine-18 chemistry. The Pd-catalyzed cross-coupling amination (Hartwig-Buchwald) directly leads to arylamines[114,115]. These structures exhibit a central structural motif in many drugs and other biologically active compounds such as neuroligands. The reaction mechanism is very similar to those of other cross-coupling reactions and displayed in Figure 2.9.

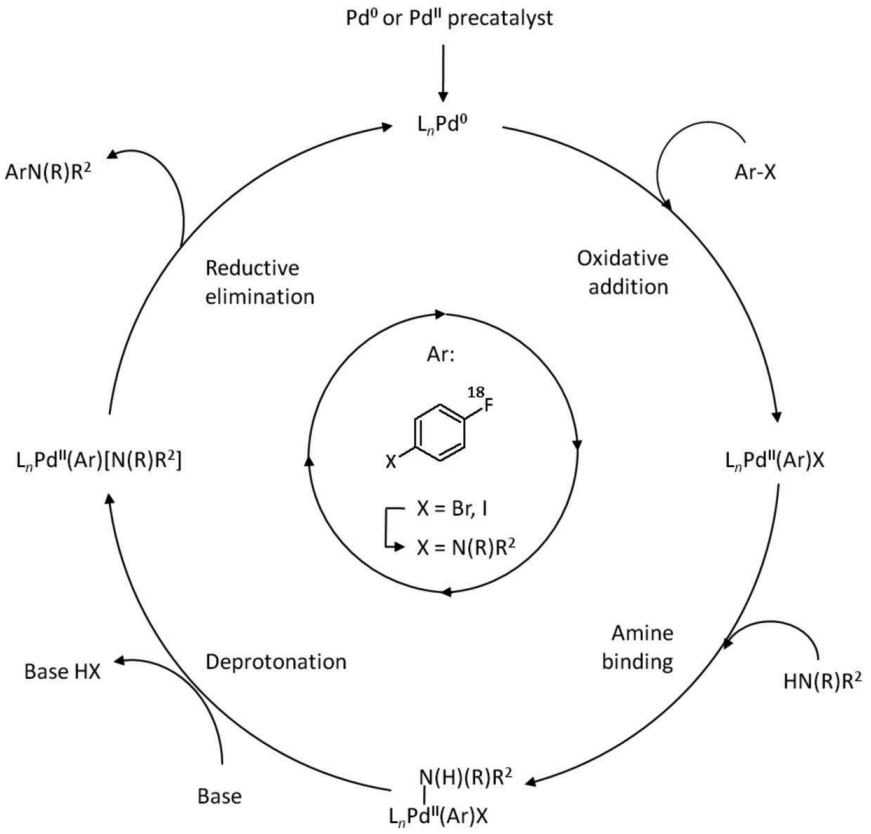

Figure 2.9: Mechanism of the Hartwig-Buchwald *N*-arylation with 4-[^{18}F]fluorohalobenzene as example for a palladium-mediated cross-coupling reaction circle (adapted with changes from[204]).

In order to find the optimal parameters for the chosen entries there are many possibilities for variation. As precatalysts, $Pd_2(dba)_3$ and $Pd(OAc)_2$ are the most common ones but many other exist. The selection of the Pd source impacts the efficient formation

of the active catalyst species. For instance, using a Pd(II) source means that before the first circle step, reduction has to take place which can take a significant amount of time. If no reduction agent is added sometimes a further equivalent of amine or phosphine ligand is need. These ligands, all biphenyl phosphines, are special developments for application in the Buchwald-Hartwig *N*-arylation. Its choice depends distinctly on substrate combination.

As seen in Figure 2.9, for Hartwig-Buchwald coupling (HBC) in contrast to some other cross-coupling reactions a base has to be added due to necessary deprotonation. Strong (NaO*t*-Bu, LHMDS) or weak (Cs_2CO_3, K_2CO_3, K_3PO_4) bases can be chosen to influence the reaction rate, functional group tolerance and side-product formation. Furthermore, the solubility of the base as well as other substances can be low dependent on the selected solvent. The most commonly employed solvent is toluene, but it causes problems in solving polar reactants. The usage of THF, 1,4-dioxane, DMF, DMA, DMSO and even water was also successful in recent studies but its practicability strongly depends on all other parameters[205].

2.2.5 Pharmacological evaluation of radioligands for the central nervous system

An essential part of the pharmacological evaluation of a radioligand is the study of binding affinities. Normally this is done before or during the selection of ligands for labelling with the inactive standard compounds but should also be conducted with the n.c.a. labelled ligands.

The basic principel of all binding studies is the equilibrium between free ligands and free receptors and the binding complexes of both.

$$[R] + [L] \underset{k_{off}}{\overset{k_{on}}{\rightleftharpoons}} [RL] \tag{2.3}$$

The dissociation constant (K_D) characterises therefore the affinity of a ligand [L] to a receptor [R], or in more detail the equilibrium between bound [RL] and unbound state. A low K_D value thus represents a high affinity.

$$K_D = \frac{k_{off}}{k_{on}} = \frac{R \cdot [L]}{[RL]} \quad \frac{mol}{L} \tag{2.4}$$

With the *radioligand* the dissociation constant (K_D) and the number of receptors (B_{max}) can directly be measured. Cells exposing the specific receptor (preferently overexpressed) are treated with different concentrations of the radioligand, washed and subsequently measured. The expected graph obtained by plotting bound radioactive ligand (RL or B) versus the concentration of free ligand (cf. Fig. 2.10) should come to saturation when all receptors are occupied, resulting $[RL]_{max} = [R]_{total} = B_{max}$ (saturation experiment). Due to (2.5) and (2.6) the K_D value can be determined directly.

$$RL \triangleq B = \frac{B_{max} \cdot [L]}{K_D + [L]} \tag{2.5}$$

$$B = \frac{B_{max}}{2} \Leftrightarrow L = K_D \tag{2.6}$$

However, the obtained total binding always contains a non- and unspecific binding fraction (s. chapter 2.4) due to all other bindings of the radioligand apart from the desired one. These binding parts ideally lead to a linear growth after saturation of the specific binding. Non- and unspecific binding can be determined and subtracted subsequently by a further measurement at high concentrations of the radioligand. Since unspecific binding often results in a deviation from linear growth normally a second experiment is conducted instead with involve concurrent receptor saturation with an excess of a different highly affine ligand. The inactive standard compound cannot be used because it would also saturate unspecific binding.

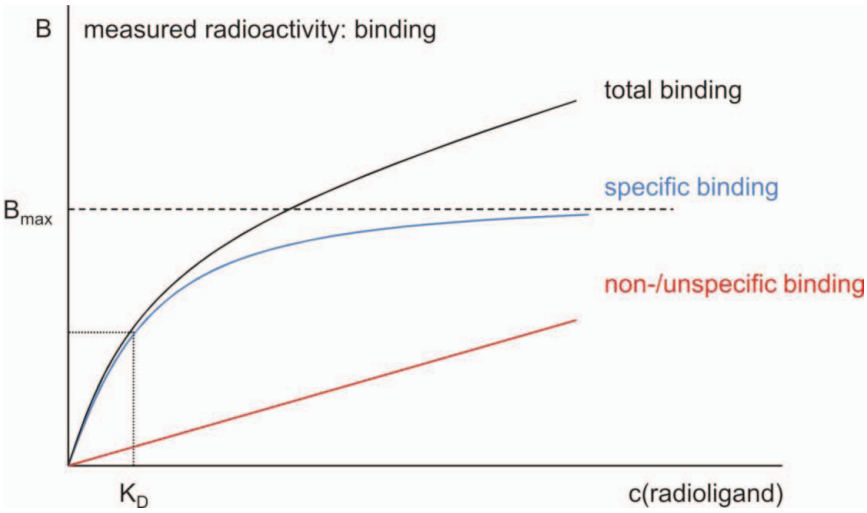

Figure 2.10: Generalized example of a saturation experiment to determine the dissociation constant (K_D) of a radioligand. The specific binding curve (blue) is obtained by subtracting the measured non/unspecific binding (red) from the total binding (black). Measured bound radioactivity (B) of radioligand to the receptors [RL] is plotted against its concentration (c).

Are *inactive ligands* available only, it is possible to determine binding affinities indirectly. For this purpose a radioligand (mostly tritiated) with known K_D for the specific receptor is applied in a fixed concentration and mixed with different concentrations of the determining inactive ligand (competition study) similar to the above described experiment. At low concentrations a plateau shows the total binding until beginning of competition. The curve ends in a second plateau which displays the nonspecific binding content. The inflexion point of the curve marks the concentration where half of the receptor is ocuppied (IC_{50}) which is correlated with the ligand-receptor affinity. Dependent on the K_D of the used radioligand and its concentration Cheng and Prusoff established the following correlation[116]:

$$K_I = \frac{IC_{50}}{1 + \frac{c\ (radioligand)}{K_D\ (radioligand}} \tag{2.7}$$

This equation results from enzyme kinetics. For an enzyme [E] and its substrate [S] transformation to the product [P] is determined by its reaction constants k.

$$[E] + [S] \underset{k_{-1}}{\overset{k_1}{\rightleftharpoons}} [ES] \xrightarrow{k_2} [E] + [P] \tag{2.8}$$

For this the Michaelis-Menten kinetics (2.9) is applied:

$$v_0 = \frac{v_{max} \cdot [S]}{K_M + [S]} \tag{2.9}$$

With $v_{max} = k_2[E]_{total}$ and K_M = Michaelis-Menten constant. In presence of an inhibitor [I] as displayed in (2.10)

$$[EI] \underset{k_{-3}}{\overset{k_3}{\rightleftharpoons}} [I] + [E] + [S] \underset{k_{-1}}{\overset{k_1}{\rightleftharpoons}} [ES] \xrightarrow{k_2} [E] + [P] \tag{2.10}$$

equation 2.9 changes to

$$v_I = \frac{v_{max} \cdot [S]}{K_M \cdot \left(1 + \frac{[I]}{K_I}\right) + [S]} \tag{2.11}$$

with $K_i = k_{-3}/k_3$ due to (2.12-2.14).

$$v_{max} = ([E] + [ES] + [EI]) \cdot k_2 \tag{2.12}$$

$$[EI] = \frac{k_3 \cdot [I] \cdot K_M \cdot [EI]}{k_3 \cdot [S]} \tag{2.13}$$

$$[EI] = \frac{K_M \cdot [ES]}{[S]} \tag{2.14}$$

The concentration of [I], when half of the enzyme is inhibited is defined as IC_{50}. Thus

$$v_0 = 2 \cdot v_I \tag{2.15}$$

when

$$[I] = IC_{50} \tag{2.16}$$

Replacing v_I and [I] in equation 2.11 results in

$$IC_{50} = K_I \cdot \left(1 + \frac{[S]}{K_M}\right) \Leftrightarrow K_I = \frac{IC_{50}}{1 + \frac{[S]}{K_M}} \tag{2.17}$$

With $K_M = K_D$ for a receptor instead of an enzyme and the concentration of the

radioligand instead of [S] this is the Cheng-Prusoff equation (2.7).

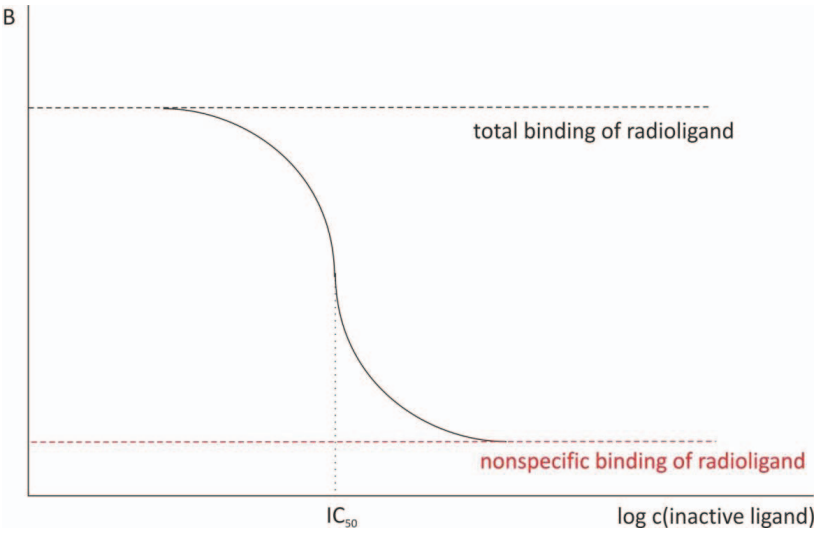

Figure 2.11: Generalized example of a competition experiment to determine the affinity of an inactive ligand by substituting an active one. Measured bound radioactivity (B) of radioligand to the receptors [RL*] is plotted against the logarithmic concentration of the inactive ligand.

Theoretically, the inhibitory constant (K_i) should be identical with the dissociation constant (K_D) from saturation experiments but it is generally higher due to the fact that the nonspecific (but not unspecific) binding fraction can be measured by this method. Unspecific binding of the radioligand is also occupied by the cold ligand but in an unpredictable way because of different and unknown nature and affinity of the involved binding sites from different receptors.

Binding affinities, although of particular interest, are not the only criterion of suitability of ligands. Further criteria can only be determined with the n.c.a. labelled product. *In vitro* autoradiography studies are conducted with brain slices of small animals containing the relevant parts of the brain where the receptor of interest is expressed. By blocking with an excess of inactive standard compounds nonspecific binding in brain tissue can be estimated. Very high values above 70 % mark a “knock-out” criterion for most radioligands. Is the distribution of the determined receptor significant and its density

high, a higher non-specific binding content can be tolerated. If nonspecific binding is low enough, the obtained autoradiographic images should represent regions of high receptor concentration and can be compared with references. In case of a non-existence of such a reference receptor localisation has to be determined or narrowed down by laborious genetic methods. Results from such methods like RNA hybridisation studies or special antigenes can be used for comparison but often give unsure conclusions.

If the tracer show low non-specific binding and an expected brain distribution *in vitro*, *ex vivo* studies lead to biodistribution and pharmacokinetics. For CNS radiotracers especially brain uptake and metabolites in this organ are of special interest. For identification of observed metabolites standard compounds of assumed metabolic products have to be synthesized. For a future modelling and therefore quantification knowledge about pharmacokinetics is necessary for subsequent preclinical studies with small animal PET scanners.

It has to be considered that the behaviour of tracers in small animal tissue can decisively differ to that in humans. On the one hand this can lead to a failure in later (at least clinical) steps but more problematic is the reverse case when a radioligand suitable for human application fails in animal experiments.

2.3 Dopamine receptors and ligands

2.3.1 Subtypes of dopamine receptors – the D_4 receptor

All fife known subreceptors of the dopaminergic system are G-protein coupled ones. That means after binding of a ligand the induced signal from the activated receptor is transmitted inside the cell by a second messenger cascade starting with coupling of receptor parts to a guanine nucleotide (G-protein), the effector. For further signal transduction subunits of the G-protein affect either adenylate cyclase (G_s, G_i) or phospholipase C (G_q). Dopamine receptors affect the adenylate cyclase and therefore the production of cyclic AMP[117].

At first two different types of dopamine receptors could be differentiated. The one activates the adenylate cyclase (D_1), the other inhibits it (D_2). These two receptors account for nearly the whole contingent of dopamine receptors in the brain and were

therefore considered as the only ones for a long time[118]. Not until the late 80th further subtypes were identified with a significantly lower occurrence. They could be allocated by their pharmacologic behaviour to one of the two types[119], or now families. On the one hand the D_5 receptor[120] (or D_{1B} in mice and rats) which belongs to the D_1 family and on the other hand the D_3[121] and D_4[122] receptors which belong to the D_2 family. That they all are different is directly represented by the fact that although they all represent dopamine receptors their affinity to dopamine is different. Dopamine affinity follows the order $D_3 > D_5 > D_2 > D_4 > D_1$[123].

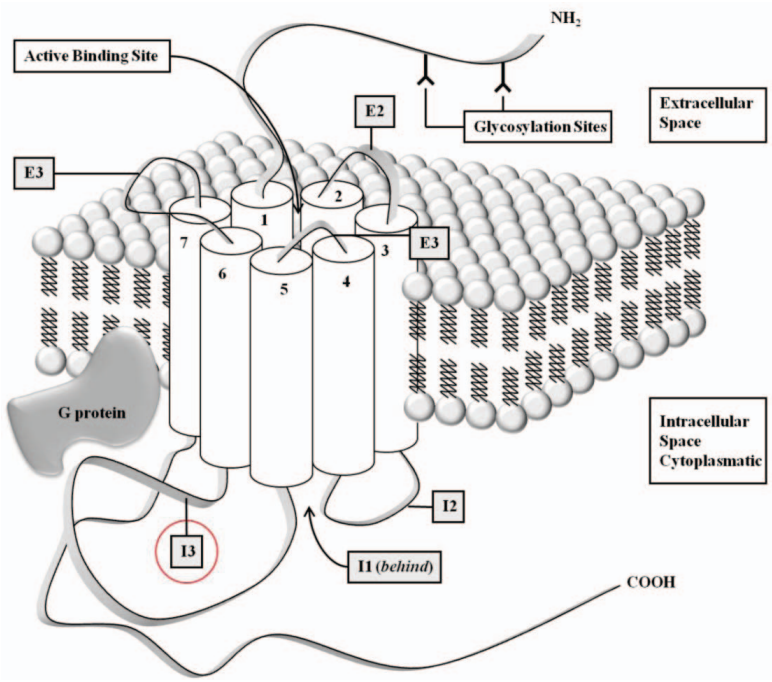

Figure 2.12: Sketch of the structure of a dopamine receptor as a typical G protein coupled receptor (GPCR). The membrane spanning helices (1-7) are displayed as tubes. D_2-like receptors (D_2, D_3, D_4) have a shorter C-terminus and a longer third intracellular loop (red circle). They also defer from the D_2-like receptors in a different number of glycosylation sites at the N-terminus. E = Extracellular loop; I = Intracellular loop

Like all G protein coupled receptors thouse for dopamine consist of seven transmembrane helices (TM), connected with three intracellular and three extracellular

loops (Fig. 2.12). The similarity of the helices within the family of D_1-like receptors is about 80 %. In contrast the D_2 receptor shares 75 % of homology with the D_3 receptor and only 53 % with D_4[124-126]. Meanwhile for all subtypes a various number of polymorphisms is known, mostly represented by single nucleotide polymorphisms or located in uncoding regions of the corresponding gene (UTR). From the D_2 receptor two phenotypes (D_{2short} and D_{2long}) exist with a different length of the third intracellular loop (I3). The importance of this loop is based on its function to bind to the G protein effector upon receptor activation. A characteristic of the D_4 receptor is its hypervariability of this region by a high number (2-11) of tandem repeat (VNTR). Therefore, this receptor is normally written as $D_{4.x}$, where x is the number of repeats. Data of the dopamine receptor subtypes are summerized in Table 2.5.

Table 2.5: Some molecular characteristics of the dopamine receptors.[127,238]

Family	***D_1-like***		***D_2-like***		
Subreceptor	***D_1***	***D_5***	***D_2***	***D_3***	**D_4**
Chromosomal location	5q35.1	4p16.1	11q23	3q13.3	*11p15.5*
Amino acids	446	477	414-443	400	*387-515*
Polymorphisms	12	17	18	8	*over 30*
Splice variants			D_{2s}; D_{2L}		*10 (VNTR)*
G protein	G_s (stimulatory)		G_i (inhibitory)		*G_o (other)*
Effect	activates cAMP		inhibits cAMP		
Main localisation in human brain	Nucleus acumbens, Basal ganglia	Limpic system	Corpus striatum	Cerebellum, Nucleus acumbens	*Prefrontal cortex, Limbic system,*

The D_4 receptor is attributed to an extremely low density in brain[128,129]. Therefore, there is still ambiguity about physiological and pathophysiological functions as well as exact local density of this subtype[130,131], although the dopamine D_4 receptor was already first cloned in 1991[132]. Immunohistochemistry and *in vitro* hybridization led to contradicting findings and differences between species, but revealed an expected higher

expression of D_4 in the prefrontal cortex and the limbic system and also in the temporal cortex, parts of tectum and cerebellum[130,131,133-135].

The D_4 receptor became of more interest since it had emerged that the atypical neuroleptic clozapine showed a tenfold higher affinity for D_4 than for D_2 receptor[132]. Therefore, the higher efficacy of clozapine to non-responders as well as to therapy of negative symptomatology was discussed as a consequence of D_4 binding. The fact that further studies did not reproducibly evidence a direct relation between schizophrenia and the D_4 receptor density[136,137], which could also be a result of a lack of true D_4 antagonists, its role in psychiatric diseases remains unclear.

It is assumed that differences in haplotypes of the D_4 receptor (tandem repeats) which are described above, are responsible for libido dysfunctions as well as for other neurobehavioural disorders like attention deficit hyperactivity disorder[138,139], novelty seeking[140,141] and substance abuse[142].

2.3.2 Dopamine D_4 receptor subtype-selective ligands

Due to the low brain density of D_4 receptors requirements of affinity and selectivity for new subtype-selective radioligands are high. Up to now various selective ligands were developed for the D_4 receptor[143-145]. It attracts attention that they all share definite structure similarities. The basic structure consists of a nitrogen containing backbone flanked with two aromatic rings, one of them being an aryl amine (s. Fig. 2.13). From one of the first selective D_4 agonist PD-168077, developed by Glase[146] in 1997, up to the more novel developments, such as the benzoimidazole A-381393[147], these molecule parts are fix components. The most important is the arylamine moiety. It is necessary for a suitable selectivity for the D_2 receptor. As main representative D_2 has statistically the highest binding probability within its family. Pharmacologically similar but underrepresented receptors D_3 and D_4 are therefore definitely discriminated. Simpson et al.[148] could show that one side of the binding crevice is more hindered in D_2 than in D_4. From the transmembrane helices (TM) 2, 3 and 7 of the D_2 receptor bulky aromatic amino acids extend into the crevice. In contrast, at the D_4 receptor they are replaced by small aliphatic ones (valine and leucine). The arylamine moiety of a ligand should retard D_2 binding due to its bulky character. *N*-aryls are in a planar and not tetrahedral orientation like other amines, since the free electron pair of the nitrogen overlaps with the ∏-system.

Therefore, the aromatic moiety cannot avoid the clash with bulky amino acids in the D_2 receptor. Replacing nitrogen against carbon decreases the selectivity significantly. In this case the aryl moiety of the ligand can be oriented away by rotating.

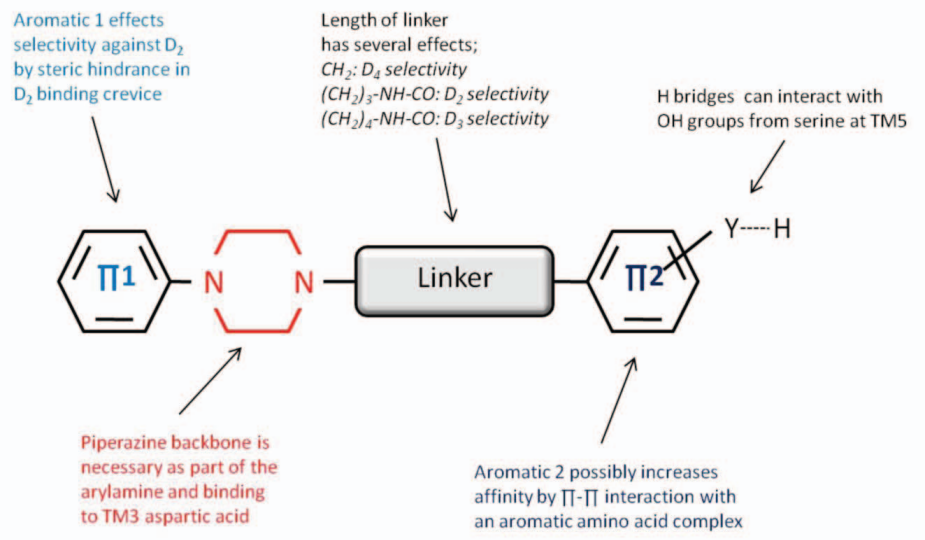

Figure 2.13: Basic components of a D_4 selective ligand influencing its affinity and selectivity.

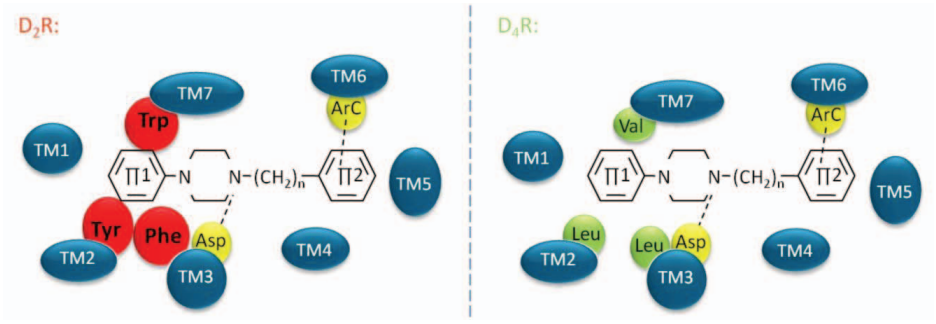

Figure 2.14: Simplified model of a D_4 selective ligand in a D_2 (left) and D_4 (right) binding crevice. Bulky aromatic amino acids in D_2 (red) hinder binding of sterically demanding ligand moieties at this part of the crevice. In D_4 the same space of the helices is occupied by amino acids with small residues (green). Here the ligand fits. Also shown is the interaction with the basic amine and with the second aromatic ring. Serine(TM5)-hydrogen bridge interaction is not displayed. TM = Transmembrane helix; Trp = Tryptophane; Tyr = Tyrosine; Phe = Phenylalanine; Val = Valine; Leu = Leucine; Asp = Aspartic acid; ArC = Microdomain of aromatic amino acids.

The influence and necessity of other parts of a selective D_4 ligand is discussed more controversially. Although most D_4 ligands consist of a piperazine, substitution by piperidine seems to be sufficient as long as the above described *N*-aryl remains untouched. While the basicity of the *N*-aryl is decreased it suffices for interaction with aspartic acid at TM3 (Asp114). The carbon linker in D_4 ligands mostly consists of a CH_2 group but some exceptions are known as well. CoMFA (comparative molecular field analysis) studies show that the ideal distance between the two aromatic moieties lies within 8 Å. Longer linkers often decrease D_4 selectivity but can lead to other selectivities. Introduction of an *N*-butylcarboxamide chain as linker can cause D_3 selectivity as observed at azaindoles[149-151]. It is not proven that the second aromatic moiety is essential but probably facilitates affinity to G protein coupled receptors by interacting with several aromatic amino acids at TM6 (Trp386, Phe389, Phe390). Groups on this aromatic ring which can form hydrogen bridges (N, NH, OH), as it is known for dopamine itself, can also assist binding by interacting with serine residues at TM5 (Ser193, Ser194, Ser197).

Since all this assumptions are collected with statistical, computanal and cloning studies using known selective ligands, one can consider ligand development from this point.

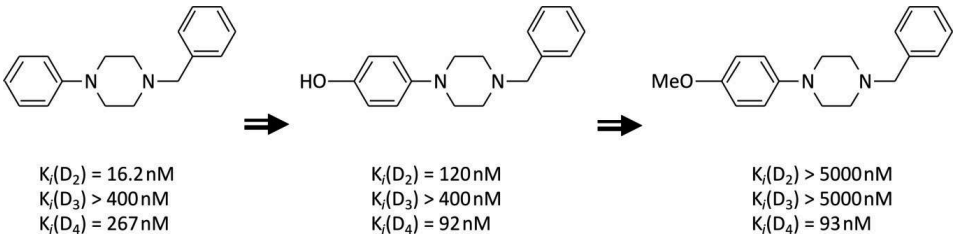

Figure 2.15: Change of D_4 affinity and selectivity by substituation of the basic 1-phenyl-4-benzylpiperazine backbone[151].

The easiest structure which fulfils minimal requirements of the above mentioned points is 1-phenyl-4-benzylpiperazine. The fact that this structure is very unselective and even more affine for D_2 shows the differences between known theory and reality. A problem of aryl-aryl interaction is the balance between steric hindrance on the one hand and ∏-∏ interaction on the other hand. The latter can possibly lead to a higher D_2 binding of this ligand. But a hydroxyl substitution in 4-position of the *N*-aryl moiety lowers D_2 and increases D_4 affinity. Further substitution by a methoxy group at this position leads to a

compound with shows the same moderate D_4 affinity but now is inactive at the D_2 and D_3 receptor[152].

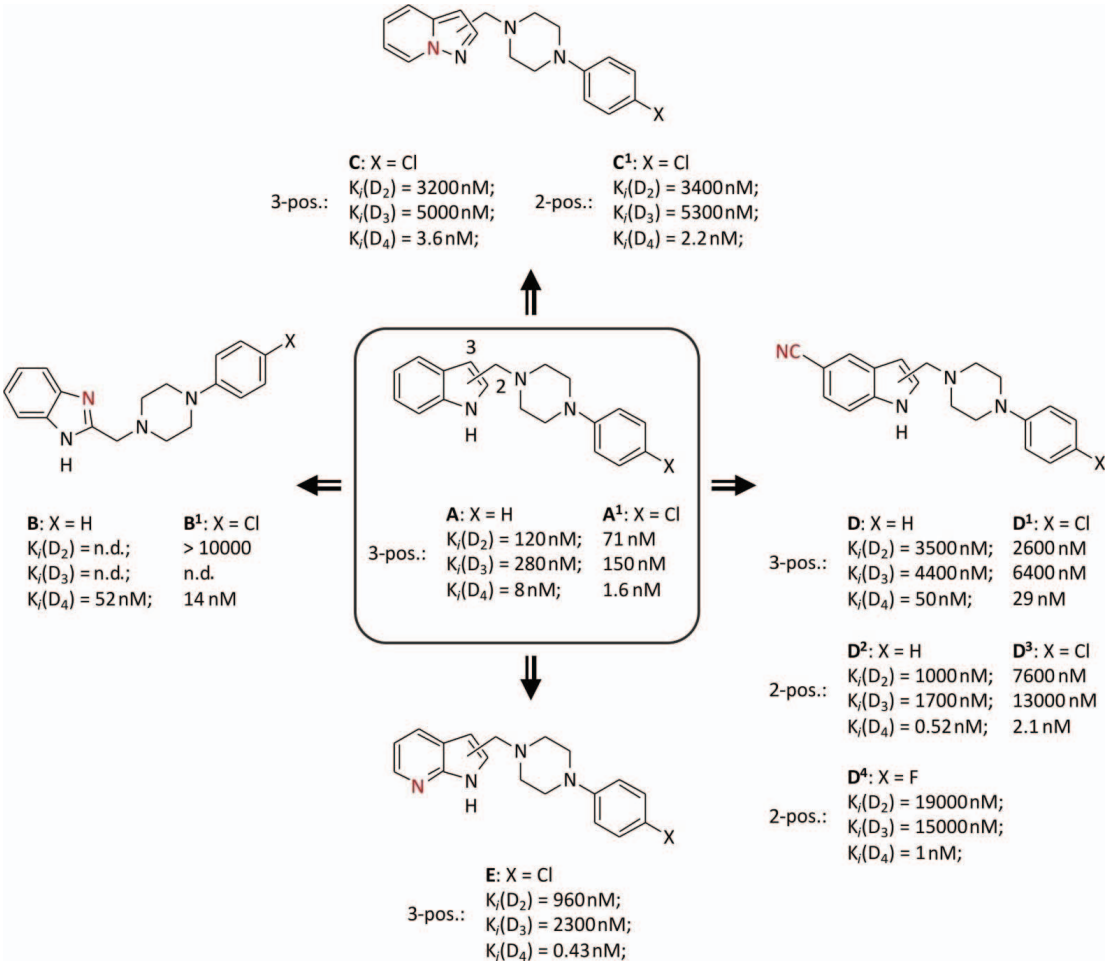

Figure 2.16: A high promising class of D_4 selective ligands starts from 2- or 3-substituted indole. Different variations lead to ligands with high D_4 affinity and high selectivity within the D_2 family[152-155].

It can be expected that further developments would extend substitution at the *N*-aryl. Nevertheless, most of the selective D_4 ligands developed until now contain only a small *N*-aryl moiety with less variation (*e.g.* OMe, F, Cl, I). Instead, the main variation part presents the other aromatic side beyond the spacer carbon. A wide group of subtype-

selective D_4 ligands exhibit *N*-heteroaromatics of indene with a spacer linkage in 2- or 3-position. Starting from the unsubstituted indole linked in 3-position (Fig. 2.16; **A**) it shows good affinity but moderate selectivity. A 4-chloro substitution of the *N*-aryl ring increases all measured affinities without clear priority but results in a 3-fold higher selectivity for D_4. The insertion of a second nitrogen in the aromatic system increases selectivity dramatically. It leads to a higher activity at D_4 with exception of the benzoimidazoles (Fig. 2.16; **B** and **B**[1]) in all cases[153-156]. Thereby also a higher affinity of the 4-chloro derivatives can be observed as described for indole. Instead of a second heteroatom, the introduction of a strong electron-withdrawing group like nitrile can also be successful. Here the best values for both affinity and selectivity are obtained with the fluorine derivative[157].

The above mentioned expansion of the *N*-aryl moiety is strived by Hodgetts et al.[158], who enlarged the *N*-aryl side by adding a heterocyclic moiety. As a continuation of the promising methoxy substituent they used oxygen as heteroatoms. On the other hand the linked aromatic side was derivatised by methoxy or halo substituents. Using benzodioxine as *N*-aryl moiety resulted in very high selectivities and affinities for the D_4 receptor for nearly all determined structures. Most of them represent antagonists of D_4 which are clearly underrepresented in the total pool of D_4 ligands. Ligands with a true D_4 antagonism are useful in determining the D_4 hypothesis of schizophrenia as mentioned in chapter 2.4.1.

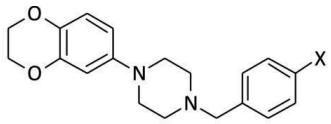

X = H	X = OMe	X = Cl	X = F
$K_i(D_2)$ > 5000 nM;	1424 nM;	526 nM;	5000 nM
$K_i(D_3)$ > 5000 nM;	1293 nM;	1396 nM;	5000 nM
$K_i(D_4)$ = 47 nM;	5 nM;	2 nM;	4 nM

Figure 2.17: Different D_4 agonists from the class of benzodioxinpiperazines[158].

The fact that the residues used for variation are mostly methoxy or halo groups is obliged for radiochemical development. Therefore, fluorine or iodine are more often components of a promising ligand than usual. Furthermore, besides the authentic

labelling of methoxy with ^{11}C, this group could also be displaced by a [^{18}F]fluoroethoxy moiety. Thus for radiochemists possibilities exist to choose from the pool of known and characterized ligands such compounds, which can be labelled without strong pharmacological alterations.

2.4 Lipophilicity – A key property for radioligands

The International Union of Pure and Applied Chemistry (IUPAC) defines lipophilicity as the affinity of a molecule or moiety for a non-polar environment[159,160]. Besides the dipole characteristics of compound parts the lipophilicity of a molecule is influenced by molecular size and weight, hydrogen binding capacity, resonance contributions and 3-D structure. As a physicochemical property it can be assessed theoretically or measured experimentally by different methods. The most common experimental measurement is partitioning of a compound between an octanol and an aqueous buffer. This is also referred to as “shake flask” method. The ratio of the compound concentration in the two layers is defined as the measure for lipophilicity. It is measured by HPLC or in case of a radiotracer by determination of the radioactivity distribution. Octanol is mostly used to mimic the bilipid layer of a cell membrane but it is not agreed as best choice[161-163]. Other used organic solvents include hexane, decane and several branched alcohols[164,165]. As an advantage the measured value contains the lipophilicity of all species in solution (Log *D*)[166]. Another method is the liquid / solid partitioning on a HPLC column with a buffered solvent. In this case the obtained retention times can be compared with standard compounds where the Log *P* values are well known[167-169]. It is a very fast method but only one species in solution is measured (Log *P*) and unforeseen interactions with mobile and stationary phase can create a variance from actual distribution coefficients. The buffers commonly used are adjusted at pH 7.4, since this represents the physiological pH value of blood serum. With computational methods electronic and resonance contributions of the whole molecule are difficult to calculate adequately. This leads often to higher values than obtained by experimental methods.

For drug development of radioactive and as well non-radioactive pharmaceuticals, lipophilicity exhibits a pivotal role, since it is important for all four essential parameters in pharmacokinetics: adsorption, distribution, metabolism, and elimination (ADME). In the

following some of these effects are discussed in more detail.

Plasma protein binding

In most cases an administered pharmaceutical does not exist in a free form but is bound reversibly to proteins in plasma[170]. An equilibrium between bound and unbound condition exists, similar to that described for a receptor and a ligand. The higher the lipophilicity of a compound, the more is bound. Albumin is the first plasma protein to mention for this interaction, especially for acidic drugs like aspirin or diazepam[171,172]. Several other proteins like α_1-glycoprotein for basic molecules like propranolol or quinidine are also relevant. In the majority of therapeutic drugs the bound allotment is nearly steady and displays a reservoir. The large protein-drug complex can neither reach its pharmacological target nor be eliminated. Due to the very rapid equilibration, removed free molecules are delivered directly from bound ones. The distinct lower concentration of radiotracers can lead to a total absorption of high lipophilic pharmaceuticals due to protein binding. This is one reason why radiotracer concentration beyond cell membranes like the blood brain barrier (BBB) decreases with high tracer lipophilicity.

Permeation of blood-brain barrier (BBB)

The BBB consists of a layer of endothelial cells which protects the sensitive organ from harmful polar substances[173,174]. Its endothelic cells lay closer than in other tissue. Besides the tight junctions the presence of efflux pumps and specific enzymes within the endothelic cells efficiently isolate the brain from the periphery. The barrier is impermeable for all hydrophilic molecules bigger than urea (M = 60 g/mol; Ø ≈ 0.2 nm). To facilitate passage of essential hydrophilic molecules like amino acids and glucose there are different carriers[175,176]. Some pharmaceuticals can use those carriers to penetrate without regard of their lipophilicity. Otherwise pharmaceuticals can also be affine to efflux pumps (for instance p-glycoprotein (PGP)) or functional metabolic enzymes[177,178]. For all other molecules a higher lipophilicity should lead to a higher permeation rate and result in a linear connection. In reality high lipophilic compounds show a distinct lower brain uptake. A higher non-specific binding to efflux pumps and enzymes can be a reason[179,180]. Together with a higher affinity also to metabolic enzymes in the periphery

such as P450[181], an increased liver and spleen uptake and a higher lung deposition will cause that nothing of the pharmaceutical will reach the brain. For very lipophilic molecules these mechanisms, as well as the above described plasma protein binding become dominant, especially for n.c.a. radiotracers. Otherwise for the latter the rival hypothesis exists, due to which non-specifically bound drugs can also enter the brain by approach of the plasma proteins to the cell membrane[182]. This could be an explanation why some radiotracers with an extremely high plasma protein binding over 90 % still present an adequate penetration of blood-brain barrier. Nevertheless, in total the relationship between drug lipophilicity and brain uptake is most often a negative parabola. The "window" of expedient lipophilicity lies between a Log *P* or Log *D* of around 2, provided that no specific affinity for membrane proteins (PGP or other) can be expected[183,184].

The problem of non-specific binding

Besides an adequate brain uptake for neurotracer imaging studies another extremely important aspect associated with lipophilicity is the subsequent non-specific binding in the brain. While the former is very much considered during drug development, the latter is often ignored. Therefore, non-specific binding of radioligands, both *in vitro* and *in vivo*, is poorly understood. For radiopharmaceutical development this is an essential problem, since many promising radiotracers for PET or SPECT which target the CNS fail due to an inappropriate non-specific binding to the brain tissue[185].

Lipophilic radiotracers generally exhibit high non-specific binding in lipid-rich tissues like the brain. About 60 % of the human brain consist of lipids, especially myelin-rich parts which are therefore named white matter. Due to this fact radiotracers with higher Log *P* or Log *D* values than 3 are often characterized by high non-specific membrane binding which hence displays a limiting factor for central nervous system imaging tracers. Nevertheless, many molecules within the optimal range of lipophilicity exhibit high non-specific binding or such with very high lipophilicity do not. Non-specific binding therefore displays a major confounding factor in the development of new radioligands for receptor imaging.

When dealing with protein binding three kinds of "specificity" are to differentiate. Specific binding generally describes the desired or expected protein binding of a ligand,

unspecific binding its interaction with active binding-sites of other proteins. Both kinds are of the same type (only differentiated by the meaning of the experimentalist) and therefore reversible and saturable. In contrast, non-specific binding is unknown but different. Nevertheless, terms of un- and non-specific binding are often not strictly distinguished and used synonymously.

The most widely used operational definition for non-specific binding describes a binding that is not displaceable by an excess of unlabelled ligand and therefore unsaturable[186]. Although this model seems to be useful for many studies there are some findings known for long time which contest this definition. Many working groups found a displaceable binding situation of labelled molecules and membranes devoid of receptors[187-190]. It could also be shown that the relationship between non-specific binding and free ligand concentration is not linear at high ligand concentrations[191]. In some cases very high free ligand concentrations led to a distinct displaceability. Instead of an irreversible binding, non-specific binding can therefore be seen as reversible binding to low affine binding sites of very high concentration. Recent studies give advice that small molecules affect the spacing between adjacent membrane bilayers to produce its own binding sites as shown with spiperone and haloperidol[192]. The ability of this process (the rate of catalysis) would be structure dependent, the pre-condition (membrane interaction) lipophilicity dependent. This could be an explanation why the non-specific binding behaviour of two pharmacologically different molecules cannot be compared in general.

3. Aims and Scope

The knowledge about functional interactions in the human brain is significantly limited by the understanding of the function of our neuroreceptors which is still fragmentary. Receptor subtype selective radioligands may help to close gaps of understanding. This becomes more and more difficult, if only a low density of the investigated receptors is prevalent, since every binding apart from the specific one may be exceeded. A faintly represented but important neuroreceptor is the dopamine D_4 receptor which shows an extremely low distribution density in the central nervous system. Although many neurological effects are attributed to this receptor subtype so far there is no possibility of its measurement *in vivo* by positron emission tomography due to the absence of a suitable radioligand.

This work should make a contribution to alter this situation. So far the only concrete indication for a selection of a suitable candidate to be radiolabelled is the D_4-affinity of known ligands as well as their selectivity over similar receptor types. Thus, the aim of this work was to label recently published ligands with such binding profiles with cyclotron produced no-carrier-added [^{18}F]fluoride. The compound FAUC 316 was selected due to its excellent affinity and selectivity for D_4 receptors. Furthermore, as an alternative the likewise highly selective 6-(4-[4-fluorobenzyl]piperazine-1-yl)benzodioxine exhibited a convenient modifiability.

The first objective was the development of an effective strategy for the radiosynthesis and the preparation of according precursors and reference compounds. In the case of FAUC 316 a concept for the basic 2-substituted cyanoindole structure was to develop by chosing a suitable indole synthesis for 5-cyanoindole-2-carbaldehyde. The key step of the radiosynthesis of [^{18}F]FAUC 316 was the preparation of the 4-[^{18}F]fluorophenylpiperazine moiety. For this purpose, special interest laid in the application of a palladium catalyzed cross-coupling reaction which should be examined for an n.c.a. ^{18}F-labelling procedure. Previously, n.c.a. 4-[^{18}F]fluorohalobenzenes had directly be obtained from ^{18}F-labelling by

nucleophilic substitution (S_NAr) on adequate iodonium salts. Beside comparing the 4-[^{18}F]fluorohalobenzenes for their suitability as coupling partners for a Hartwig-Buchwald coupling (HBC), the focus of optimization studies on this coupling reaction was particularly on the solvent system, precursor concentration, and reaction temperature.

In order to prepare n.c.a. 6-(4-[4-[^{18}F]fluorobenzyl]piperazine-1-yl)benzodioxine different synthetic strategies like direct nucleophilic substitution of an aromatic compound (S_NAr) as well as a multi-step synthesis using a reductive amination reaction on corresponding n.c.a. [^{18}F]fluorobenzaldehydes appears attractive to investigate. For this, different precursors and reference compounds for identification of n.c.a. products of each radioactive reaction step has to be synthesized as well. Special emphasis should be laid on every single reaction step regarding of reaction conditions in order to compare their efficiency. The best labelling strategy should be used to generate n.c.a. ^{18}F-labelled derivatives of 6-(4-[4-[^{18}F]fluorobenzyl]piperazine-1-yl)benzodioxine with different pharmacological properties. This required modification of precursors, reference compounds, radiochemistry and separation. With regard to the known lipophilicity and expected high non-specific binding of the benzodioxine ligand new planned derivatives of 6-(4-[4-[^{18}F]fluorobenzyl]piperazine-1-yl)benzodioxine should be more hydrophilic. Considering a narrow frame of variation due to the necessity of sufficient membrane penetration and therefore brain uptake, such a modification must then be examined with regard to avoid the loss of specificity for D_4 receptors.

For identification and determination of the radiochemical yield and purity of the labelled compounds a suitable radio HPLC and in some cases radio TLC systems had to be developed. In addition, a major concern was the development of suitable separation and purification methods especially using solid phase extraction and radio HPLC in order to enable an evaluation of the compounds pharmacologically. A major aim of this work should be the determination of the actual binding behaviour in the tissue of the central nervous system with special regard to non-specific membrane binding. This property presents the major “knock-out” criteria for putative D_4 ligands when applied as radiolabelled ligands *in vivo*.

Finally, the most promising radioligand should be further evaluated in *ex vivo* animal experiments for its qualification as an *in vivo* imaging tracer. For this, all n.c.a. ^{18}F-labelled derivatives are to examine in order to obtain first preclinical data.

4. Synthesis and ^{18}F-labelling of FAUC 316

In order to create a suitable radioligand for the D_4 receptor the cyanoindole FAUC 316 (**1**) was elected since it exhibits excellent values for affinity ($K_i(D_4)$ = 1 nM) and selectivity against a lot of dopamine receptors and subreceptors known as pharmacologically similar, especially D_2.

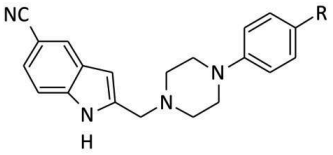

	R = F FAUC 316 (**1**)	R = OEtF
$D_{4.4}$	**= 1.0 ± 0.057 nM**	**= 9.9 ± 0.4 nM**
D_1	= 8 600± 2 400 nM	= 38 000± 5000 nM
D_{2long}	= 28 000 ± 6 500 nM	= 4 200 ± 330 nM
D_{2short}	= 19 000 ± 4 000 nM	= 4 100 ± 830 nM
D_3	= 15 000± 2 000 nM	= 2 500 ± 690 nM

Figure 4.1: K_i-values of the highly affine and selective D_4 ligand FAUC 316 (**1**) and its fluoroethyl derivative which can be used as tracer analogue but shows a distinct inferior binding profile[156].

Displacement of the fluorine substituent with fluorine-18 should leave the excellent binding profile untouched. On the other hand the nature of the molecule does not admit an easy nucleophilic n.c.a. ^{18}F-fluorination procedure. A common alternative is the use of a [^{18}F]fluoroethyl or -ethoxy group instead of authentic aromatic fluorine-18. The resulted aliphatic fluourination is much easier but decreases affinity and selectivity of the ligand dramatically by a factor of 45 to 70 (Fig. 4.1). Due to the lack of D_4 radioligands and therefore its high requirements it makes sense to go for an authentic labelling, even if this is more difficult to achieve. Difficulties lay in the fluorine carrying aromatic moiety which is directly bound to the amine. An adequate activation for nucleophilic fluorination is therefore only possible by insertion of a formyl group in *ortho*-position. However, the subsequent cleavage of this group has to take place with one of the heterogenous catalysts tris(triphenylphosphine)rhodium(I)chloride under harsh conditions[193] or palladium on charcoal with estimated low yields[194]. All alternatives include radiochemical built-up of the basic structure. [^{18}F]Fluoroaniline as intermediate can be used for a Prelog ring closure. However, the amine has to be synthesised itself by two previous steps and

results of the ring closure reaction in radiochemistry are described as very poor[195].

Since the radiosynthesis of [^{18}F]fluorohalobenzenes by labelling of iodonium precursors is an established method, the transition metal catalyzed coupling of amine and halobenzene displays an adequate option to achieve *N,N*-dialkyl[^{18}F]fluoroanilines. With three radioactive reaction steps the Hartwig-Buchwald coupling (HBC; Fig. 4.2, B) is comparable with direct labelling of an *ortho*-aldehyde (Fig. 4.2, C) and also includes the same disadvantage in using totally or partly heterogenous compounds. HBC is chosen due to the easier synthesis of according inactive compounds and more extensive possibilities in varying the reaction conditions.

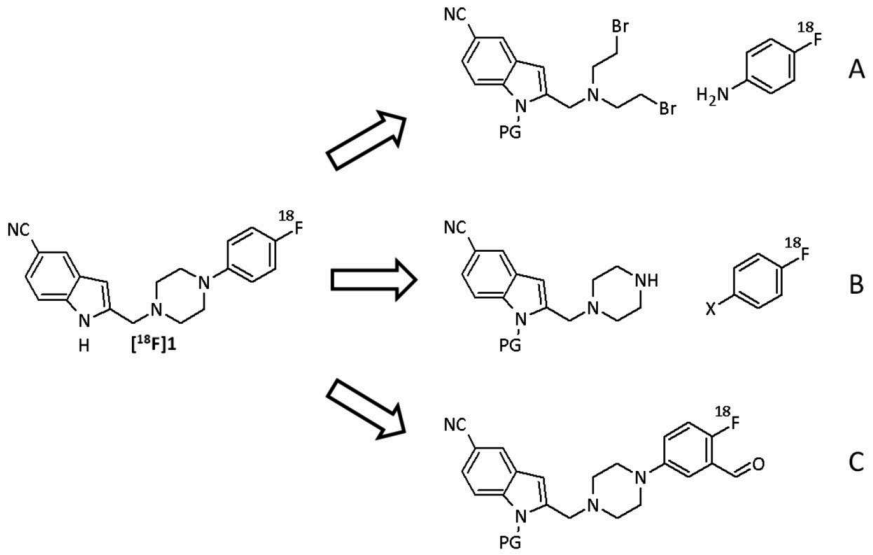

Figure 4.2: Three main possibilities of retrosyntheses for the radiosynthesis of [^{18}F]FAUC 316 ([^{18}F]**1**).

4.1 Syntheses of standard and precursor compounds

All syntheses of FAUC 316 and its analogues described in the literature for distribution of the binding profile started from 2-(hydroxymethyl)indole-5-carbonitrile (**7**) which synthesis was not described. For the synthesis of 2-substituted indole derivatives it is not possible to start reactions from the heterocycle, conducting a substitution or addition procedure. In contrast to pyrrol, furan, and benzofuran, the 3-position of indole is

distinctly more activated then the 2-position. A direct aminomethylation of indoles, analogue to a Mannich reaction using formaldehyde, leads to an indole-3-aldehyde as well as does an electrophilic substitution by Vilsmeier-Haack with DMF and $POCl_3$. It is therefore necessary to build-up the indole-heterocycle. From sigmatropic rearrangements like the Fischer synthesis over radical mechanisms up to more complex reactions using alkines, arynes or azirines, a lot of different indole syntheses exist[196].

4.1.1 Formation of 2-carboxylic indole *via* palladium mediated intramolecular coupling

An elegant method to obtain 2-substituted indolecarbonyles in only one reaction step is provided by a palladium catalyzed coupling starting from *ortho*-iodoaniline described by Chen et al.[197] It is very similar to the better known Larock[198] synthesis but using ketones instead of alkines.

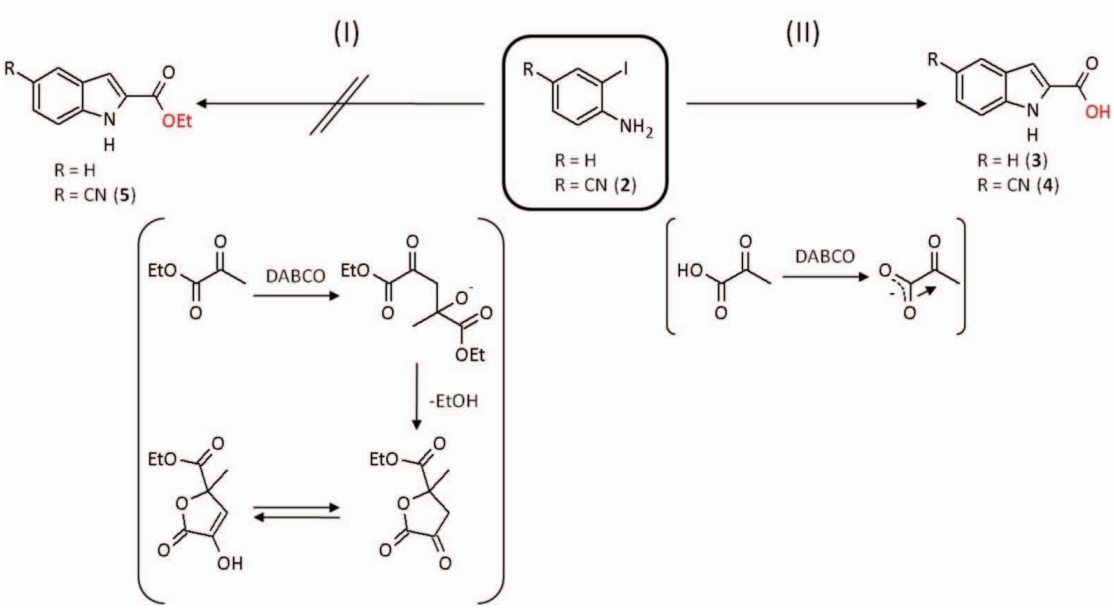

Figure 4.3: Palladium mediated indole coupling which is possible with the acid but not with its corresponding ester due to a self-condensation under basic conditions (left side). In case of the acid, electronic condition of the unprotonated state prevents from aldolic reactions (right side). Reaction conditions: $Pd(OAc)_2$, DABCO, DMF, 100 °C, 4h.

The reaction proceeds by formation of an enamine and subsequent intramolecular annulation by Heck-coupling of the en- and the aryliodide-moiety. In order to achieve the primary alcohol (**7**) the most obvious procedure was the reaction of ethyle pyruvate with 5-cyano-3-iodoaniline leading to the ethylester as intermediate product. Unfortunately, this is not possible in general, presumable due to a rapid self-condensation of the ethyl pyruvate under basic conditions. This way it is described for similar reaction conditions and substances[199]. With free pyruvic acid this decomposition is not observed although an aldol-addition is also conceivable in this case. An explanation includes the preceeding deprotonation of the more acidic carboacid moiety which leads to an excellent electron-donating group directly adjacent to the carbonyl. As a result, the acidity of the β-carbon-hydrogen bond is lowered. This explanation is in accordance with the finding that an excess of minimum four equivalents of diazabicyclo[2.2.2]octane (DABCO) as amine base was essential for achieving the synthesis.

A further disadvantage is the presence of the nitrile group. As a good electron-withdrawing substituent nitrile lowers basicity of the aniline lone-pair for an enamine building as well as coordination of the aromatic during the Heck-coupling. Thus, the yields decrease distinctly from 60 % to 40 % when changing to the nitrile derivative (Tab. 4.1).

Table 4.1: Influence of the cyano group of indole-2-carboxylic acids with cyclization on yield, stability and solubility.

Molecule	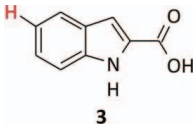 **3**	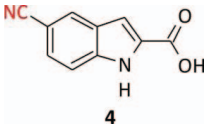 **4**
Yield	60 %	40 %
Melting Point	202-206 °C	331 °C (decomposition)
Solubility	CH_2Cl_2, $CHCl_3$, DMF, DMSO, ethylacetate, diethylether (slightly), tetrahydrofurane	DMSO

Due to this electronic situation of 5-cyanoindole-2-carboxylic acid (**4**) and its low solubility in most common reaction solvents, its reactivity for further reaction steps is low. Thus, it was not successful to esterify the molecule with methanol, ethanol and even

methyliodide. While the unsubstituted indolecarboxylic acid (**3**) can be easily transferred to the acid chloride by oxalyle chloride in methylene chloride, this is only possible with **3** by using very harsh conditions or reactands like PCl_5. A subsequent direct reduction to the alcohol showed no reaction with mild reduction agents like $NaBH_3$ and led to decomposition with $LiAlH_4$. Otherwise the conversion of the acid chloride to the amide was conducted in high yields independent of the nitrile, but which could not be reduced to the amine in any way. In conclusion this procedure proved not practicable for generating **7**.

4.1.2 Formation of 2-carboxylic indole by intramolecular reductive amination

An alternative which should lead to the ester ethyl-5-cyano-*1H*-indole-2-carboxylate (**5**) in two steps is the classic indole synthesis by Reissert et al.[200] Starting from an *o*-nitrotoluene, ethoxy condensation takes place with ethyl oxalate and a strong ethanolate base to form an *o*-nitrophenylpyruvate (**6**). Due to the harsh basic conditions electronic influences of further substituents like the nitrile group are nearly negligible.

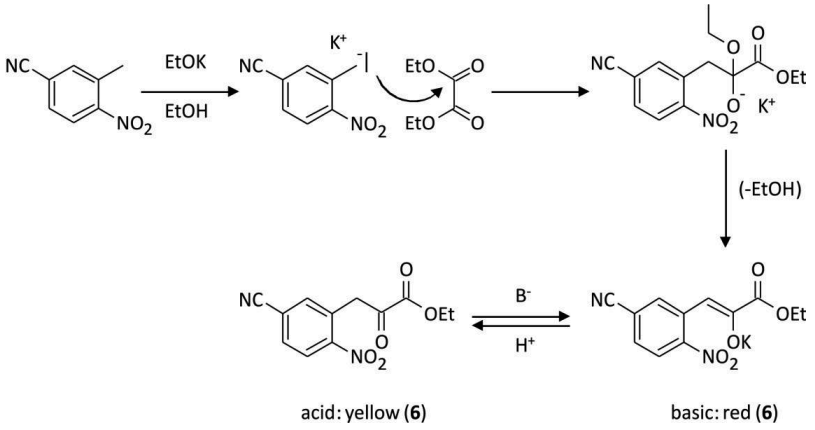

Figure 4.4: Mechanism of the first step of the Reissert indole synthesis to generate *o*-nitrophenylpyruvate (**6**).

With **6** a subsequent reductive amination cyclisation results in the ester **5**. For this procedure powder of elemental zinc in glacial acetic acid is typically used. Usually high yields are obtained with these substrates but with the disadvantage of poor

reproducibility. Therefore palladium on charcoal as reduction agent was used with decaborane ($B_{10}H_{14}$) as H-donor. The use of cyclohexene instead of decaborane showed no results.

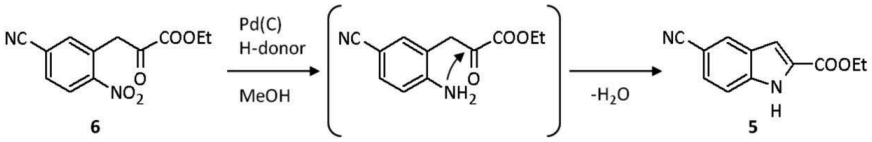

Figure 4.5: Intramolecular reductive coupling of the 5-cyano-o-nitrophenylpyruvate to the corresponding indole ester.

4.1.3 Reduction of 5-cyano-2-carboxyindole ester

The ester was then reduced to the primary alcohol **7**, which is a key intermediate compound. Although reduction sensibility of esters is described as high, no conversion could be obtained with the borohydride reduction agents $NaBH_3$, $LiBH_3$ and $Ca(BH_3)_2$ which were used as commercially available as well as produced in situ. The nitrile substituent as a further reduction sensitive group complicates the application of stronger reduction agents. Nevertheless, the ester group can be totally reduced to the alcohol in presence of the cyano group with $LiAlH_4$ in diethylether at very low temperatures (-78 °C) and subsequent cautious thawing. Replacing diethylether by tetrahydrofuran leads to a decomposition of the starting material under identical reaction conditions.

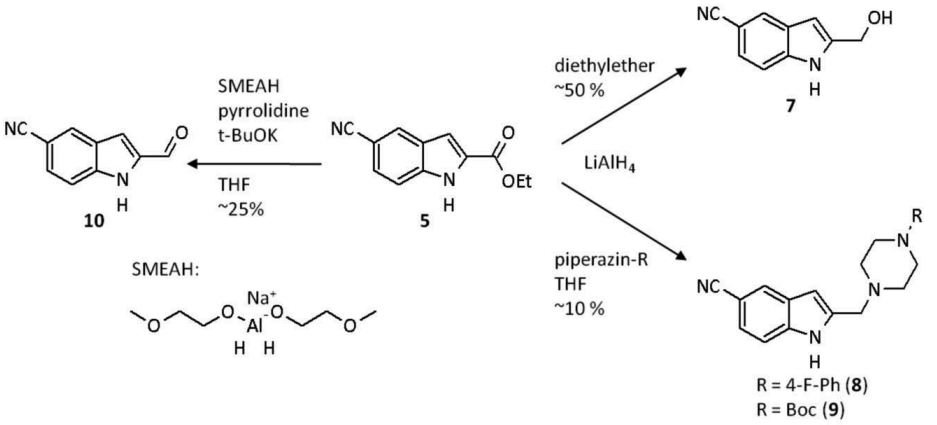

Figure 4.6: Different reductive procedures of the cyanoindole ester.

On the other hand, the use of THF is possible for a direct reductive amination reaction of the ester to the methylenepiperazines **8** and **9**. Saving reaction steps in this case, however, is bought by very poor yields. Higher yields of reductive amination are obtained in the classical way starting from the aldehyde (**10**) as it is displayed in Figure 4.7. The nearly quantitatively selective oxidation of the alcohol with Dess-Martin periodinane results in the most suitable route *via* the alcohol **7**. A direct selective reduction from the ester to the aldehyde with sodium bis(2-methoxyethoxy)aluminiumhydride (SMEAH) and pyrrolidine is possible but with a yield of about 25 % it can also not compete with the two step route.

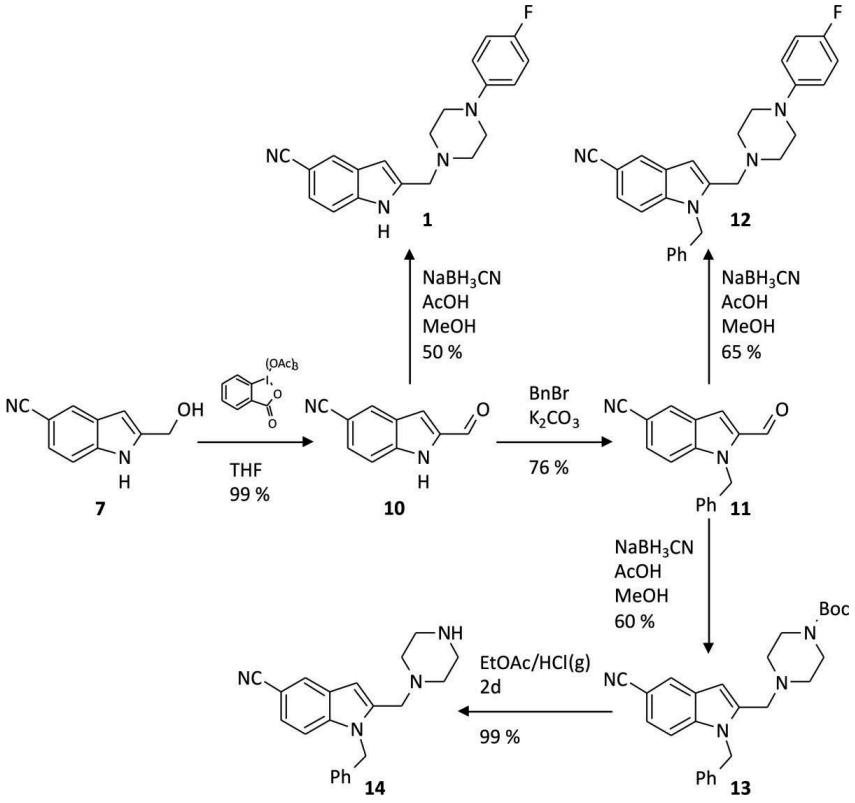

Figure 4.7: Reaction paths starting from 5-cyanoindole-2-methanol to the standards **1** and **12** and the precursor **14**.

All further reaction steps which led to the precursor **14** and the reference compounds **1** and **12** display standard reactions and resulted in yields from 50 to 99 %. The selective cleavage of the Boc protection group in presence of the benzyl protection group was

conducted on the basis of an investigation of F. Cavelier and C. Enjalbal[201]. It was taken advantage of the small difference in the acid sensitivity of the both groups. Dry HCl gas was dissolved in ethyl acetate and used as agent for cleavage. After 48 h a nearly quantitative and selective conversation was observed. A longer reaction time led to an additional cleavage of the benzyloxy moiety.

4.1.4 Syntheses of iodonium precursors

For the radiosynthesis of [^{18}F]fluorobromobenzene and [^{18}F]fluoroiodobenzene the labelling procedure by iodonium salts was chosen as most reasonable. Symmetric iodonium precursors were of special interest due to estimated higher yields and a decreased number of different side products (chapter 2.2.4.2).

The synthesis of bis(4-bromophenyl)iodonium trifluoromethansulfonate (**16**) was conducted by the common method developed by McKillop et al.[202] For this at first iodide was oxidised in presence of glacial acetic acid to iodine(III). A subsequent ligand replacement led to an overall yield of 56 %. Due to the easy oxidability of iodine (iodide) in contrast to bromine (bromide) the second substituent remained untouched during the whole reaction as well as no autooxidation processes were estimated. This was in contrast to the diiodo species bis(4-iodophenyl)iodonium trifluoromethansulfonate (**20**) which is displayed in Figure 4.9. Therefore, it was necessary to produce a reactive intermediate. 2-(Hydroxy(tosyloxy)iodotoluene (**18**) was formed by oxidation and ligand replacement. Such iodine(III) compounds with a hydroxy and a tosylate ligand are named "Koser's reagents"[203].

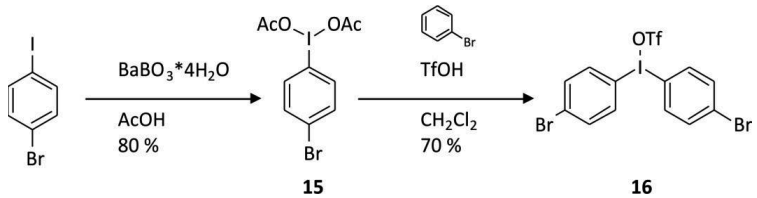

Figure 4.8: Two-step synthesis of the symmetric iodonium precursor bis(4-bromophenyl)iodonium trifluoromethansulfonate (**16**).

The critical step was the oxidative substitution reaction with o-diiodobenzene which resulted in poor yields. Due to the fact that both product and educt have the possibility for oxidation and replacement, the existence of an equilibrium was conceivable. This

postulate would explain the low yield. However an explanation for the higher stability of 2-(hydroxy(tosyloxy)iodotoluene (**18**) was owing up to now.

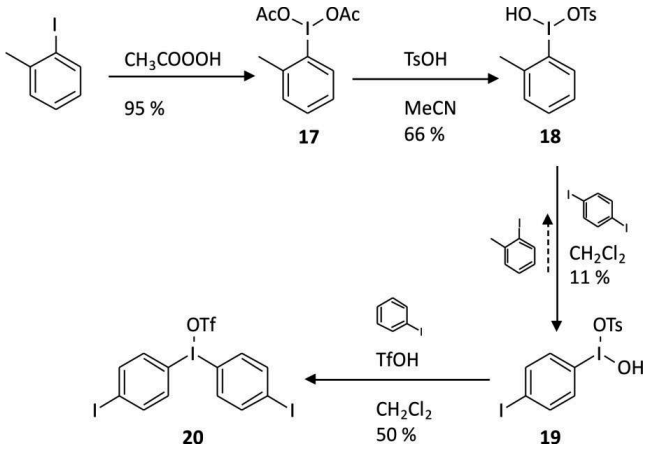

Figure 4.9: Four-step synthesis of the symmetric iodonium precursor bis(4-iodophenyl)iodonium trifluoromethansulfonate (**20**).

In a last step a ligand replacement similar to the bromo analogue led to the desired precursor with an overall yield of 3.5 %. It has to be noted that in principle an oxidative substitution analogue to the previous reaction step is conceivable as competing reaction. In fact this seems to proceed mainly when the reaction velocity is low as it is in the case when weaker acids than trifluoromethanesulfonic acid are used.

4.2 Radiosynthesis of [^{18}F]FAUC 316

4.2.1 Synthesis of 4-[^{18}F]fluorobromobenzene and 4-[^{18}F]fluoroiodobenzene

The synthesis of both [^{18}F]fluorohalobenzenes as secondary labelling agents was conducted in DMF at high temperatures of 130 °C. The well known aminopolyether Kryptofix 2.2.2 and potassium carbonate were used as base system for radiofluorination. Due to the popularity of the iodonium precursors no comprehensive process optimization was done here. Thus by thermical decomposition of 30 µmol of the iodonium precursors

16 and **20** in presence of n.c.a. [^{18}F]fluoride, radiochemical yields of 50 ± 5 % of 4-[^{18}F]fluorobromobenzene ([^{18}F]**21**) and 60 ± 9 % of 4-[^{18}F]fluoroiodobenzene ([^{18}F]**22**) were obtained. Lower precursor concentrations led to a dramatically decrease of yield. Half of the concentration (15 µmol in 0.8 mL DMF) results in radiochemical yields of only about 20 %. The necessity of abnormal high precursor concentration is a general phenomenon of iodonium salts and presumably this is due to their rapid degradation which includes radical procedures. A scavenger like 2,2,6,6-tetramethylpiperidine-*N*-oxyl (TEMPO) is sometimes added for prevention[92,93]. Due to the high number of different reagents in subsequent reaction steps and the high number of unavoidable side products this was not considered as an option in this work.

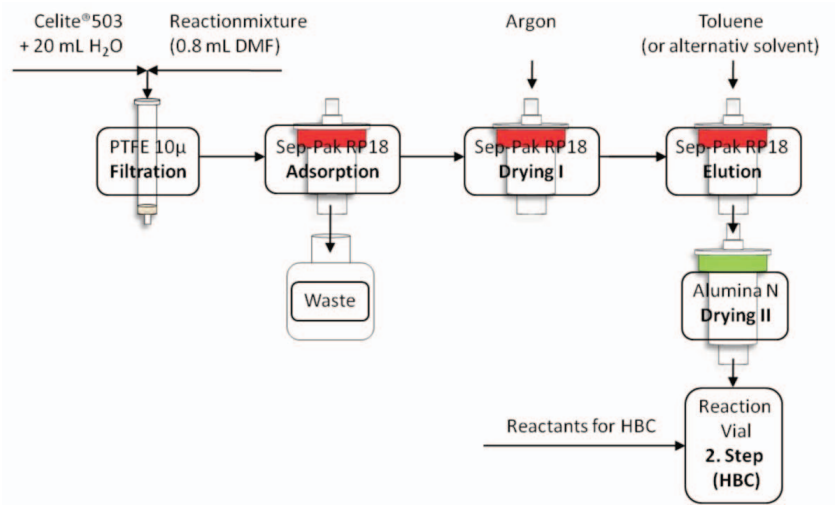

Figure 4.10: Scheme of solid phase extraction (SPE) route for the separation of 4-[^{18}F]fluoroiodobenzene ([^{18}F]**22**).

The latter mentioned side products as well as a free choice of solvent for the subsequent cross-coupling reaction necessitate a solid phase extraction procedure for which the moderately unpolar silica phase Sep-Pak RP18 was chosen. The procedure was unproblematic using bis(4-bromophenyl)iodonium trifluoromethansulfonate **16**, but decomposition products of bis(4-iodophenyl)iodonium trifluoromethansulfonate **20** produced a colloidal precipitate with water which obstructed cartridges and passed filter frits (3µ). An adequate filtration can be reached by previous addition of 100 mL of the

diatomaceous earth Celite®503 to water and filtration through a 10µ PTFE filter. The obtained slightly milky solution passed every cartridge without objection. Due to the fact that a palladium mediated cross-coupling reaction should be free of moisture an elaborate drying had to follow. The whole procedure is graphically displayed in Figure 4.10 and resulted in a product loss of up to 15 %.

4.2.2 Piperidine and 1-methylpiperazine as model compounds for a radioactive palladium-catalyzed Buchwald-Hartwig cross-coupling

Test syntheses with small cyclic amines were performed as a proof of principle of the Hartwig-Buchwald coupling under the present n.c.a. conditions. Due to the high number of different combinations of parameters (catalyst, ligand, base and solvent) as well as the fact that no evidence for process optimization existed[204] parameters were initially carried over from the only existing reference in radiochemistry[205]. As test systems piperidine as simplest and 1-methylpiperazine as more similar to the target structure **1** were used and coupled with 4-[^{18}F]fluorobromobenzene ([^{18}F]**21**) and 4-[^{18}F]fluoroiodobenzene ([^{18}F]**22**) using $Pd_2(dba)_3$, 2-dicyclohexylphosphino-2'-(*N,N*-dimethylamino)biphenyl (DavePhos) and NaO*t*Bu in toluene at 100 °C. Coupling results are displayed for two reaction times in Figure 4.11.

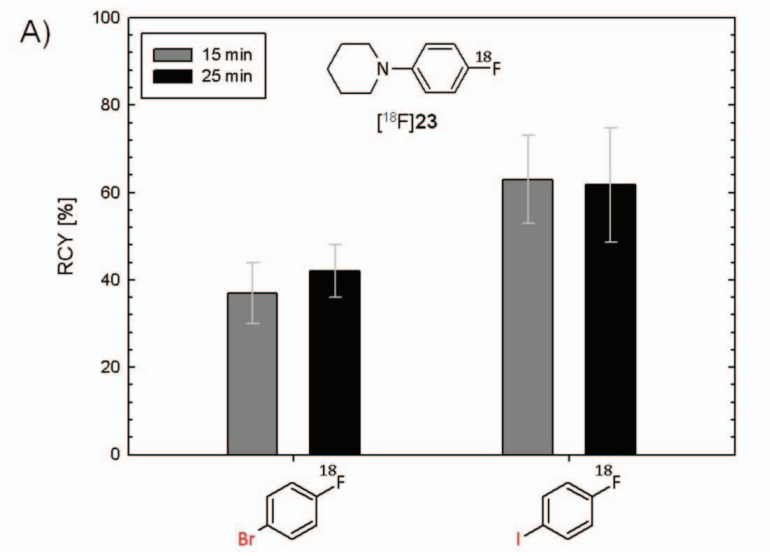

Figure 4.11 A: Radiochemical yield (RCY) of the Hartwig-Buchald coupling (HBC) of 4-[^{18}F]fluorobromobenzene ([^{18}F]**21**) and 4-[^{18}F]fluoroiodobenzene ([^{18}F]**22**) with piperidine.

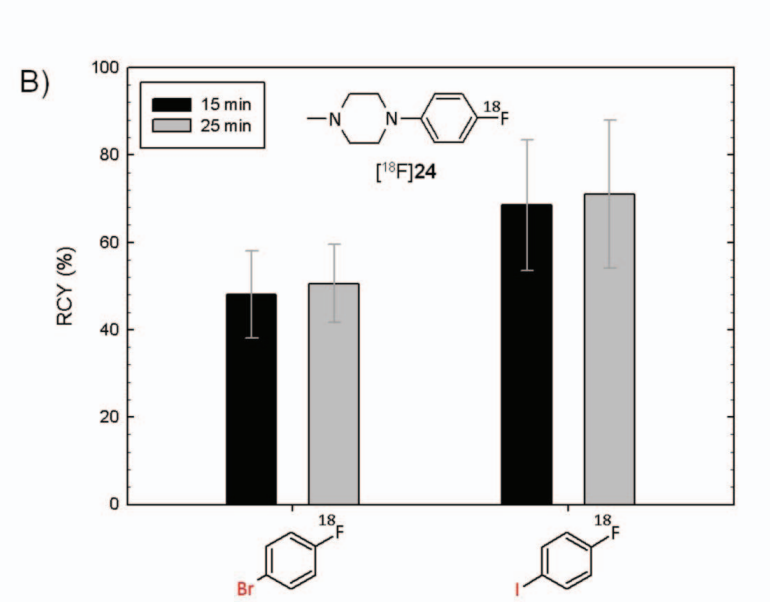

Figure 4.11 B: Radiochemical yield (RCY) of the Hartwig-Buchald coupling (HBC) of 4-[^{18}F]fluorobromobenzene ([^{18}F]**21**) and 4-[^{18}F]fluoroiodobenzene ([^{18}F]**22**) with 1-methylpiperazine.

It is obvious that iodobenzene is more suitable offering higher yields, which is a confirmation of a known fact for inactive organic compounds[206-208]. Direct comparison of both test systems did not show distinct differences. Thus, introduction of further tertiary amines were not supposed to exert an influence on the reaction.

Solvent dependence

While the alteration of the used HB-reactants (especially catalyst and ligand) would "only" influence the conversion rate which is already high, the choice of solvent has more expansive consequences. Therefore, the yield of conversion of 4-[^{18}F]fluoroiodobenzene ([^{18}F]**22**) with 1-methylpiperazine was compared in three different solvents. Beside m-xylene, toluene is the most used solvent for HBC with high yields but with a few disadvantages. It is not mixable with water due to its unpolarity. This is a problem for an easy, rapid and preferably lossless solid phase extraction subsequently to the coupling reaction. It is therefore suitable to use a water-soluble solvent from which separation and purification is assuaged. Moreover, the dipolar, aprotic *N,N*-dimethylformamide (DMF)

would provide the opportunity of a one-pot synthesis without an intermediate separation step. In addition to the simplified procedure, especially for the iodo-derivative, and the time savings this would minimize losses due to adsorption processes and incomplete fixation and elution. A further advantage is the relatively high boiling point of 150 °C of DMF which allows a wide range of temperature variation. Otherwise its physicochemical parameters are very different to toluene and xylene. Therefore, 1,4-dioxane was used as an alternative which is also dipolar and aprotic but should behave more like toluene due to a very similar dipole moment and dielectric constant (Tab. 4.2).

Tab. 4.2: Solvent dependence of the radiochemical yield of HBC[209] related to [^{18}F]**22**.

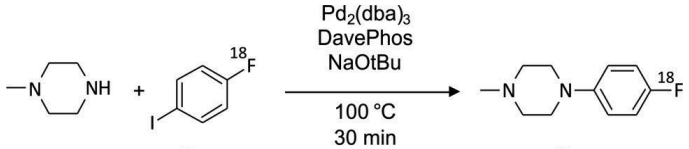

[^{18}F]**22** [^{18}F]**24**

solvent	*dipole moment μ*	*dielctricity constant ε*	*RCY*
toluene	1.23 10^{-30} Cm	2.4	70 %
1,4-dioxane	1.5 10^{-30} Cm	2.2	40 %
DMF	13.1 10^{-30} Cm	37.8	0 %
DMF/toluene	-	-	0 %

In order to guarantee the comparability of solvent influences the HBC was carried out at constant reaction parameters and analysed by radio-HPLC and if possible radio-TLC. Thereby no conversion to the desired arylamine product was observed in DMF. Instead of the side product could be identified as the dehalogenated product [^{18}F]fluorobenzene. Identification and especially quantitation of this product was difficult due to its high volatility. A mixture of DMF and toluene proved also unsuitable and led to the same results as the use of pure DMF. Thus, a subsequent addition of toluene after the labelling step for HBC proved not an alternative.

The HBC in 1,4-dioxane results in moderate yields of 40 % but with a high amount of different radioactive side products which were not identified in detail. Toluene was maintained as solvent of choice due to the distinct better yield. In addition in toluene no radioactive side products were observed and this solvent showed a more complete

elution of 4-[^{18}]fluoroiodobenzene ([^{18}F]**22**) from the solid phase cartridge than 1,4-dioxane and DMF.

Reasons for the failure of a cross-coupling in DMF can be attributed to a complexation of DMF by palladium. A steric hinderance leads to a preference of the β-hydrid elimination which results in the dehalogenated product and an imine[210]. This is in accordance to Beletskaya et al.[211] who showed that the reduction of the arylhalide is favoured when the deprotonation of the amine is slow.

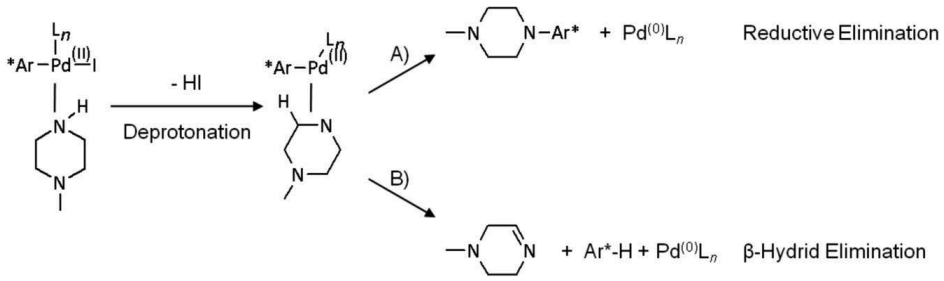

Figure 4.12: Part of the cross-coupling cycle of the Hartwig-Buchwald reaction. When deprotonation is quick the typical reductive elimination procedure is occur (A), if it is slow, due to a steric hinderance, β-hydrid elimination becomes predominant (B).

4.2.3 Direct Buchwald-Hartwig coupling with 1-benzyl-2-(piperazine-1-yl-methyl)-*1H*-indole-5-carbonitrile

The cross-coupling to the benzyl-protected ligand Bn[^{18}F]FAUC 316 ([^{18}F]**12**) was the next step. As a consequence of the preliminary determinations in the previous chapter the reaction was also conducted in toluene at 100 °C with 4-[^{18}F]fluoroiodobenzene ([^{18}F]**22**), $Pd_2(dba)_3$, 2-dicyclohexylphosphino-2'-(*N,N*-dimethylamino)biphenyl (DavePhos) and NaO*t*Bu. No conversion could be observed, even after a reaction time of one hour. A possible explanation for the failure of the radiosynthetic cross-coupling with **14** is the presence of the cyano-group which is known as well-coordinating, possibly better than the amine group, to build strong complexes. Furthermore, the extent of the bigger coupling partner potentially causes a restriction of complexation and decreases the reaction velocity.

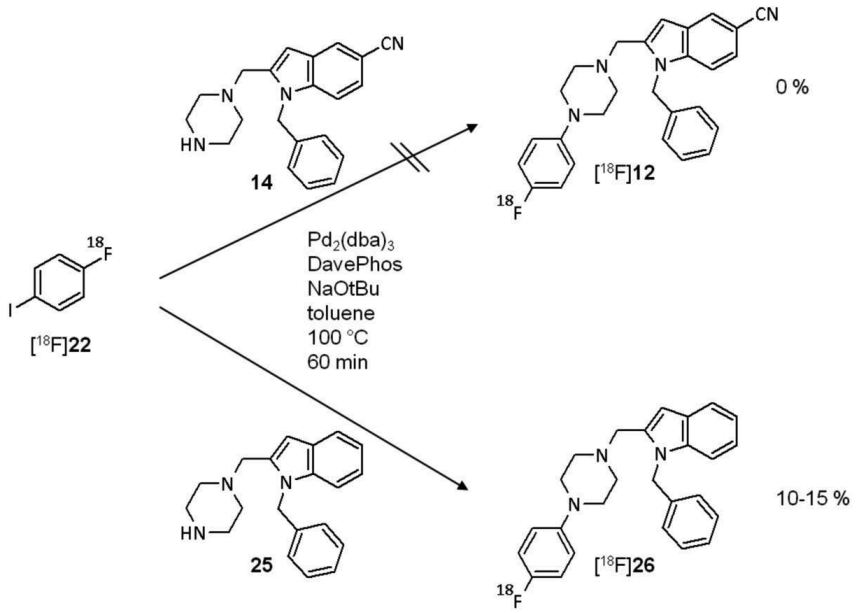

Figure 4.13: Direct cross-coupling of 4-[^{18}F]fluoroiodobenzene ([^{18}F]**22**) with the benzylprotected indolepiperazine with (**14**) and without (**25**) a cyano-substituent. The presence of the cyano group seems to hamper coupling reaction under the chosen conditions as obvious from radiochemical yields.

The former assumption is supported by the fact that in absence of the cyano-group a conversion proceeds. On the other hand the dehalogenation product [^{18}F]fluorobenzene was not found as major by-product. The low yields of 10-15 % obtained with the unsubstituted but benzylprotected 1-benzyl-2-(piperazine-1-ylmethyl)-*1H*-indole (**25**) confirm the thesis of an influence of the bulky character of the amine substituent. Due to the high distant between the two moieties, electronic influences of the cyano group should be excluded in this process.

4.2.4 Synthesis of [^{18}F]FAUC 316 *via* 4-[^{18}F]fluorophenylpiperazine

The failure of a direct coupling of 4-[^{18}F]fluoroiodobenzene ([^{18}F]**22**) with piperazine-1-ylmethyl-1-*H*-indoles necessitated an alternative procedure. In chapter 4.2.2 preexaminatins showed a high yield conversation of small cyclic amines. Therefore, the synthesis of 4-[^{18}F]fluorophenylpiperazine as intermediate product was attempted. In accordance with the inactive syntheses a subsequent reductive amination with 5-

cyanoindole-2-aldehyde (**10**) should follow. Due to the unsensitivity of the reductive amination procedure the indole must not be protected.

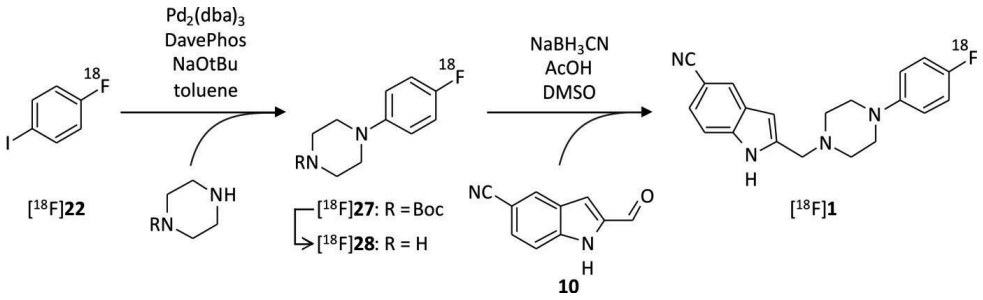

Figure 4.14: Successful reaction pathway to [^{18}F]FAUC 316 [^{18}F]**1** starting from 4-[^{18}F]fluoroiodobenzene [^{18}F]**22**. Protection of one piperazine side and therefore a later cleavage of the Boc-group is not necessary for the HB coupling reaction.

First examinations started from coupling of *tert*-butyl-piperazine-1-carboxylate and subsequent cleavage of the Boc-group as a typical reaction path due to literature procedures. The cross-coupling yielded about 70 % radiochemical yield (RCY) after 25 min. Although the carbamat moiety of the Boc-group showed similarities to DMF, RCY of the successful Hartwig-Buchwad coupling to tert-butyl-4-(4-[^{18}F]fluorophenyl)piperazine-1-carboxylate ([^{18}F]**27**) was in the same range like to 1-(4-[^{18}F]fluorophenyl)piperidine ([^{18}F]**23**) and to 1-(4-[^{18}F]fluorophenyl)-4-methylpiperazine ([^{18}F]**24**). The subsequent cleavage of the Boc-group was finished with concentrated HCl after 15 min and with trifluoroacetic acid after 5 min. The coupling reaction was also performed with the unprotected piperazine due to the problems using strong acids during radiosyntheses and in condiseration of saving one reaction step. Inactive preexaminations showed that even with an excess of the aryl componend double *N*-arylation is disfavoured. Furthermore, Christensen et al.[210] could show that the arylpiperazine is less reactive for a cross-coupling than piperazine. In the radiosynthesis 4-[^{18}F]fluoroiodobenzene is the substoichiometric partner but reactions with inactive haloaryl side products from the iodonium decomposition are conceivable.

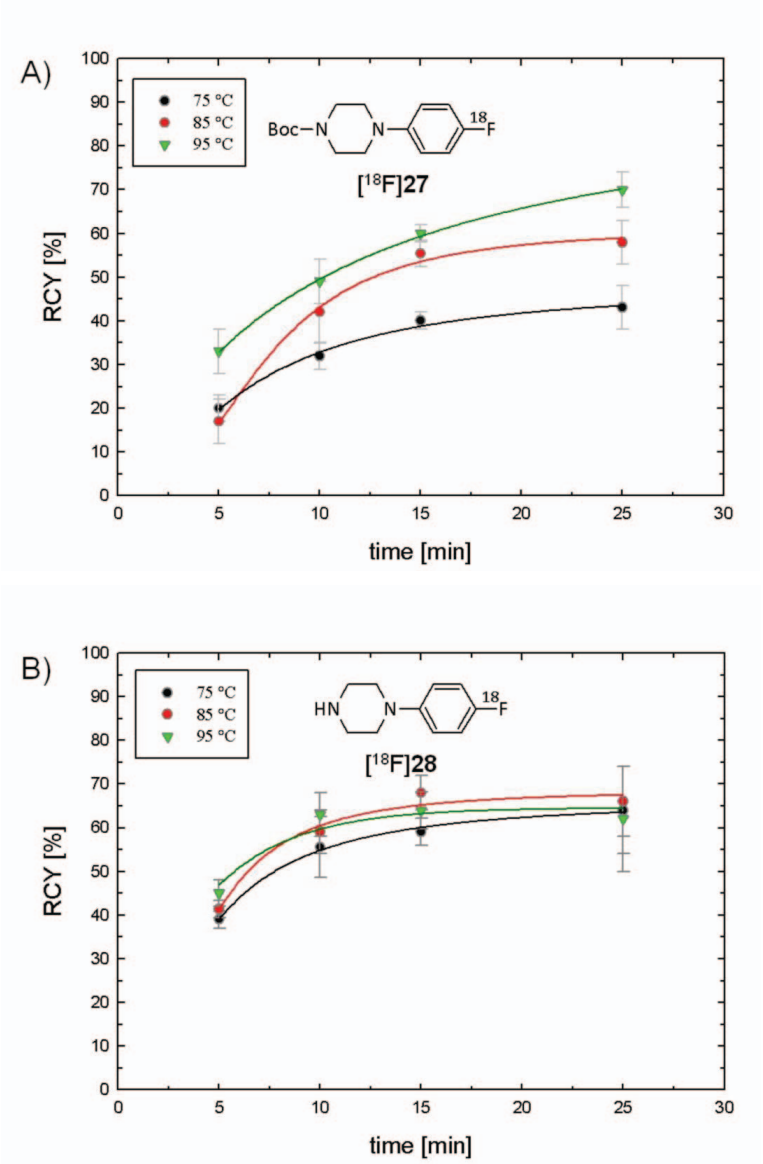

Figure 4.15: Temperature dependence of the radiochemical yield (RCY) of the HBC to [^{18}F]**27** (A) and [^{18}F]**27** (B). In case of the free piperazine temperature sensitivity of the reaction is lower than when using the *N*-Boc precursor.

It is shown that the maximum yields of both reactions did not differ distinctly, thus, the use of the unprotected piperazine is favoured. In fact, direct comparison of the temperature dependence displays a lower sensibility to temperature fluctuations of the

piperazine coupling which maintain its yield even with a temperature decrease of 20 °C. The latter reaction seems to run faster reacting saturation already after about 15 min, which is probably due to the two reaction centers. Otherwise, in accordance to the equimolar examinations, a multiple aryl-coupling of piperazine could be ruled out by using inactive standards. Thus, after prepurification of 4-[^{18}F]fluorophenylpiperazine ([^{18}F]**28**) and reductive amination the overall sum of steps do not differ from the original pathway. The elaborated extraction procedure of the arylpiperazine intermediate is described in detail in the next chapter.

Tab. 4.3: Different catalyst systems for radio-HBC in toluene and DMF at 100 °C.

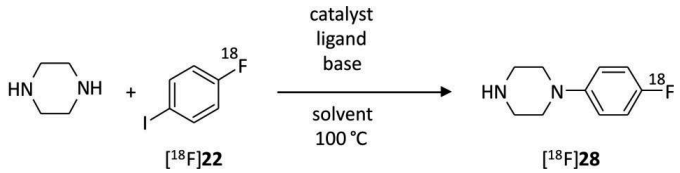

[^{18}F]**22** [^{18}F]**28**

catalyst	*ligand*	*base*	*solvent*	*time (min)*	*RCY*
Pd-cinnamyl	BrettPhos	NaO*t*Bu	toluene	30	25 %
$Pd_2(dba)_3$	RuPhos	NaO*t*Bu	toluene	30	73 %
$Pd_2(dba)_3$	DavePhos	NaO*t*Bu	toluene	20	70 %
$[P(t\text{-}Bu)_3PdBr]_2$	-	K_2CO_3	DMF	30	0 %
$[P(t\text{-}Bu)_3PdBr]_2$	-	K_3PO_4	DMF	30	0 %
$Pd(OAc)_2$	RuPhos	NaO*t*Bu	toluene	5	60 %
$Pd(OAc)_2$	RuPhos	NaO*t*Bu	toluene	10	74 %
$Pd(OAc)_2$	RuPhos	NaO*t*Bu	DMF	30	0 %

Due to the high number of elaborate purification steps often with substantial loss of radioactivity, under the chosen conditions and reactands other coupling systems were tested with piperazine in order to use other solvents than toluene (chapter 4.2.2) or even to get higher yields. With some examples the use of polar, aprotic solvents such as DMSO, DMF and DMAA has been described for the inactive Hartwig-Buchwald syntheses[212-215] and in some cases even an aqueous solution has been used[216,217]. Thus, solvent

dependence seems to be associated with the Pd-source and ligand system. Catalysts like the Pd(I)-dimer $[P(t\text{-}Bu)_3PdBr]_2$, the polar $PdOAc_2$ as well as the $Pd_2(dba)_3$/2-(dicyclohexylphosphino)3,6-dimethoxy-2',4',6'-triisopropyl-1,1'-biphenyl (BrettPhos)/KOH system were used for which general good yields in polar solvents are described. 2-Dicyclohexylphosphino-2',6'-diisopropoxybiphenyl (RuPhos) was also tested in this context due to its known high potency in conversation of secondary amines[203]. All tested systems are listed in Table 4.3. Nevertheless, none of these showed any sign of conversion to the desired 4-[^{18}F]fluorophenylpiperazine ([^{18}F]**28**) when DMF was used as solvent and [^{18}F]fluorobenzene as main side product did not appear generally. Otherwise a very rapid reaction rate was observed using $PdOAc_2$/RuPhos/NaOtBu in toluene which resulted in a considerable saving of reaction time.

The subsequent reductive amination with 5-cyanoindole-2-aldehyde (**10**) was performed with $NaBH_3CN$ in DMSO and toluene and previously tested with the commercially available indole-2-aldehyde. No distinct differences were observed between both reactants so that the substituent does not seem to influence this reaction.

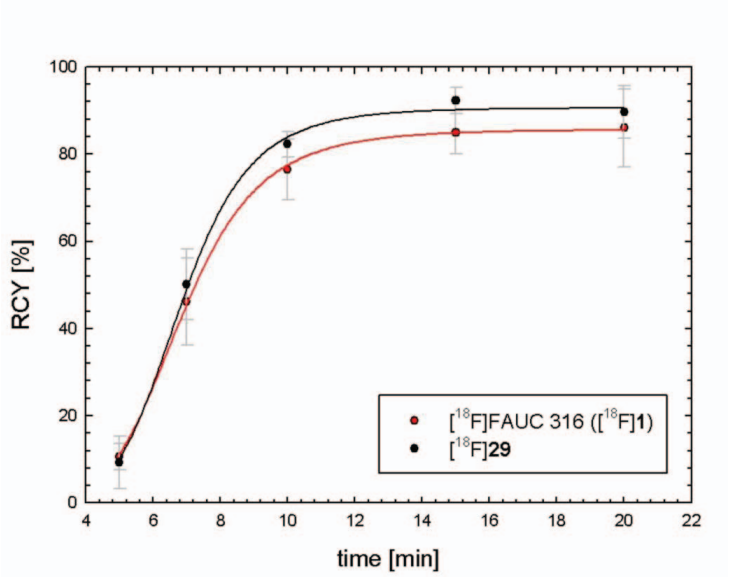

Figure 4.16: Time dependence of the radiochemical yield of the reductive amination reaction of 4-[^{18}F]flourophenylpiperazine with 5-cyanoindole-2-aldehyde (**10**) to FAUC 316 ([^{18}F]**1**) (red) and with indole-2-aldehyde to 2-((4-(4-[^{18}F]fluorophenyl)piperazine-1-yl)methyl-*1H*-indole ([^{18}F]**29**) (black).

4.2.5 Purification and isolation of [^{18}F]FAUC 316

The good radiochemical yields (measured by radio-HPLC) of every single reaction step show good practicability of the HBC in radiosyntheses with n.c.a. ^{18}F-labelled compounds. Otherwise the overall radiochemical yield at the end of synthesis is with about 10 % relatively low and the total reaction time of about 120 min represents more than one half life of fluorine-18. Limitations of total yield and reaction time are dependent on the intricate purification methods following every reaction step. Purification of the arylhalide by solid phase extraction after the labelling procedure depends on the iodonium salt used as precursor and is described there in detail (chapter 4.2.1).

4.2.5.1 Prepurification of 4-[^{18}F]fluorophenylpiperazine ([^{18}F]28)

The influences of reactants and byproducts on the following reaction steps are not sure due to the large amount of impurities which are present after the cross-coupling reaction in the reaction mixture. A preliminary purification of the product is therefore essential following the Buchwald-Hartwig coupling. Furthermore, the free amine of the piperazine moiety allows a unique purification by acid extraction at this point of the reaction sequence. Two options appear attractive: liquid-liquid extraction as well as solid-liquid extraction.

The liquid-liquid extraction of the coupled product [^{18}F]**28** with hydrochloric acid (2 mol/L) allowed a selective separation of the reaction mixture containing amines as well as water soluble substances. The development of progress extraction could be traced very well by the distribution of radioactivity between the two phases. After repeated extraction of the toluene reaction mixture with hydrochloric acid, the aqueous phase was made basic with sodium hydroxide for conversion of the product into the water-insoluble amine form. Subsequent adsorption of the organic ingredients on a Sep Pack C18 solid phase cartridge allows a change of solvent and removed all water-soluble compounds. For the elution of the amine from the cartridge the appropriate solvent of the following reaction may be used (here DMSO); in the case of 4-[^{18}F]fluorophenylpiperazine ([^{18}F]**28**) a suitable solvent for the semi-preparative HPLC separation. Acetonitrile was used for the elution before application to HPLC. HPL chromatographic analysis showed a significant purification of the substance by liquid-liquid extraction and allowed the isolation by a

semi-preparative HPLC separation. The liquid-liquid extraction was almost quantitative without substantial losses of [^{18}F]**28**.

For solid phase extraction Strata X-CW were used as cation exchanger cartridges. The reaction mixture was diluted with methanol and applied directly to the ion exchanger previously conditioned with methanol and water. Subsequently, the cartridge was washed with an ammonium formate buffer (pH 6.3) and methanol and the product was eluted with methanolic sodiumacetoborhydrid solution from the cartridge. The HPLC analysis showed, as in case of the liquid-liqid extraction, a clear purification of [^{18}F]**28**. The process procedure provides a product yield of [^{18}F]**28** of 20 ± 4% which is distinctly lower than from the former method. Otherwise the solid phase extraction allows an easier practicability.

*Pharmacoceutical relevance of 4-[^{18}F]fluorophenylpiperazine ([^{18}F]**28**)*

4-Fluorophenylpiperazine (4-FPP, **28**) or "fluoperazin" is a not yet listed (2010) psychoactive substance that is used as a substitute for amphetamines (NMDA, ecstasy, etc.) like a few other phenylpiperazines, due to their better commercial availability. Their effect is usually attributed to their 5-HT agonism (K_i(5-HT_{1A}) = 302 nM; K_i(5-HT_{1B}) = 794 nM; K_i(5-HT_{2A}) = 3236 nM; K_i(α1) = 776 nM; K_i(D_2/H_1/mAch) > 100.000nM)[218], at least with 4-FPP its euphoric and stimulating effect can not be explained sufficiently this way. Thus an effect as SRI and NARI is suspected. An effect on the norepinephrine receptor (agonistic) may be causative; an analogous mechanism to the amphetamines as an indirect sympathomimetic is also conceivable due to the only moderate affinity. This is confirmed by the advisement that an euphoric effect (dopamine) may not be triggered directly. As an indirect sympathomimetic it would release norepinephrine non-exocytotic from the axoplasm and simulate this way the effect of NA agonists. For this purpose there are two requirements: First, penetration of the BBB is necessary for a CNS effect. The existence of a carrier is likely due to the low lipophilicity of 4-FPP. Furthermore, 4-FPP has to be able to use the corresponding transmitter-carrier (with cotransport of Na^+) in Axolemn (intake inhibition by competition) and the inclusion of the transmitter in the synaptic vesicles and/or prevent its degradation by monoamine oxidases (MAO). 4-FPP has no corresponding structural similarity to such compounds (phenylethylamine), but there are also similar compounds which show these effects, *e.g.* Amezinium.

4.2.5.2 HPLC purification of final products

For a final purification semipreparative radio-HPLC had to be used in order to arrange pharmacological evaluations. This regards not only the final product [^{18}F]FAUC 316 ([^{18}F]**12**), since a HPLC-purification of the intermediate 4-[^{18}F]fluorophenylpiperazine ([^{18}F]**28**) was aspired as well for future applications due to its pharmaceutical relevance.

Large quantities of iodobenzene were acieved by decomposition of the iodonium salt during the production of the secondary labelling precursor (Chapter 4.2.1) beside the desired 4-[^{18}F]fluoroiodobenzene [^{18}F]**22**. The inactive iodobenzene is implemented in the Hartwig Buchwald coupling analogous to [^{18}F]**22** to produce N-arylpiperazine which pass all following extraction steps and reacts in the reductive amination reaction as well. The compounds only differ by a fluorine atom, which represents a very similar molecule also for most chromatographic columns. This places special requirements on the used HPLC system.

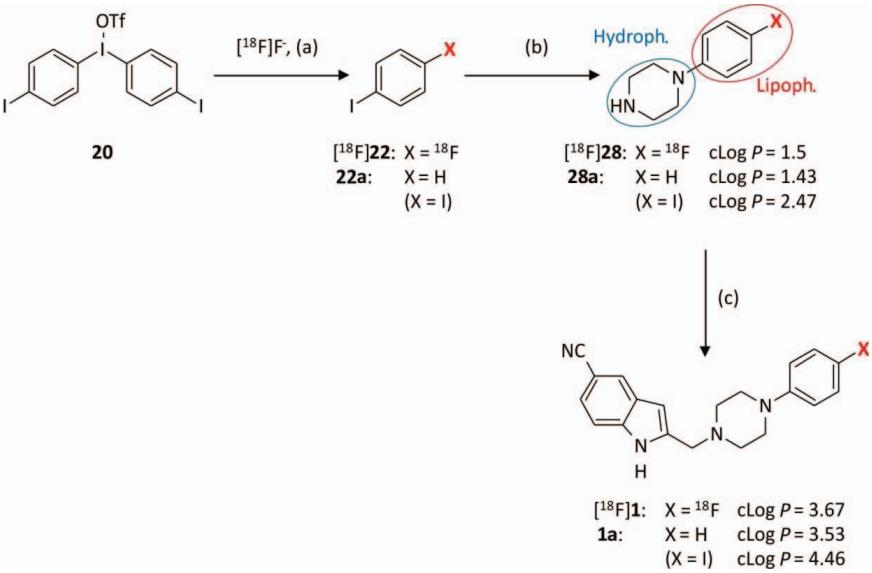

Figure 4.17: Generating of the unsubstituted derivates (**22a**, **28a**, **1a**) during all reaction steps with very similar properties. The amphiphilicity of the phenylpiperazines (**28**, **28a**) is marked by a blue circle for a hydrophilic and a red circle for a lipophilic area. Generation of the iodo derivatives is also conceivable but without strong impact due to its very different Log *P* and therefore retention time. All cLog *P* values were calculated by Marvin Sketch 5.1.4.[239]

Reaction conditions: (a) K2.2.2, Na_2CO_3, DMF; (b) $Pd_2(dba)_3$, DavePhos, NaOtBu, toluene, 100 °C (c) **10**, $NaBH_3CN$, AcOH, DMSO

There is a further problem for the chromatographic purification of the 4-[^{18}F]fluorophenylpiperazine due to its nearly amphiphilic character. This effects that the orientation of the molecule between stationary and mobile phase can depend on the polarity of the eluent. In Figure 4.18 this phenomenon is shown using a MultoHigh 100 RP18 HPLC column for the separation 4-fluorophenylpiperazine and 1-phenylpiperazine.

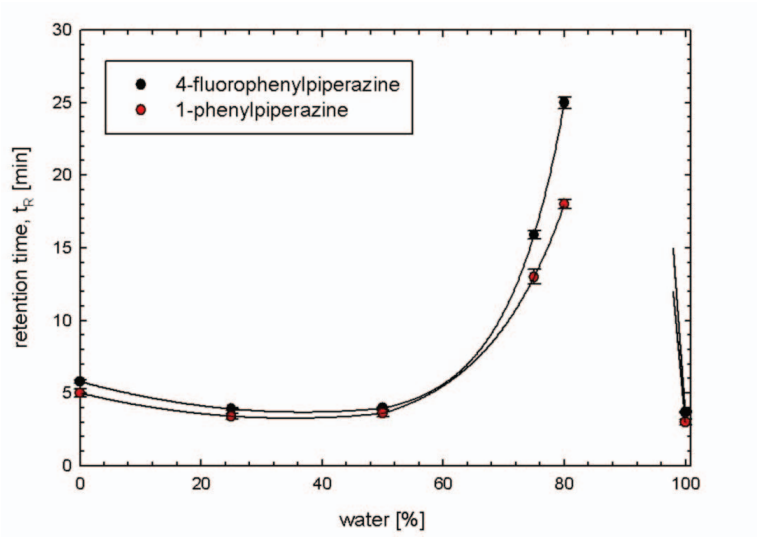

Figure 4.18: Characteristic of the retention time of 4-FPP (**28**) and 1-phenylpiperazine (**28a**) on the water/acetonitrile proportion of the HPLC solvent. Column: CS Service, Multo High 100 RP18 5µ, 250×4.6 mm.

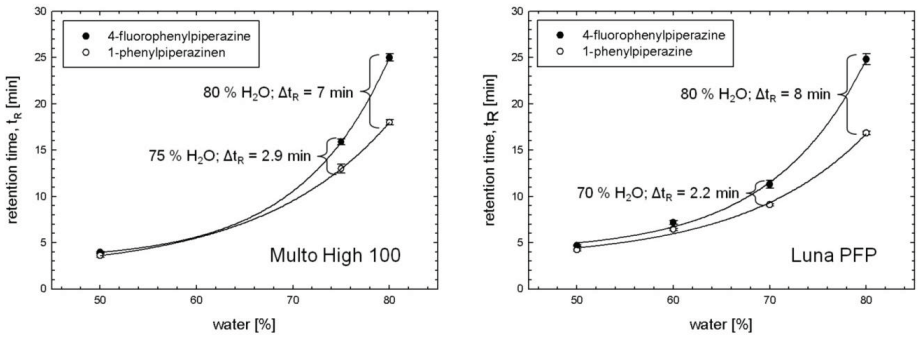

Figure 4.19: Dependence of the retention time of 4-FPP (**28**) and 1-phenylpiperazine (**28a**) on the water/acetonitrile proportion of the HPLC solvent. Δt_R of the phenylpiperazines are compared between the column Multo High 5 µm 100 RP18 250×4.6 mm (left) from Cs Service and the column Luna 5 µm PFP(2) 100 Å 250×4.6 mm (right) from Phenomenex. Solvent: MeCN/H_2O (v/v), 1 mL/min.

The retention time (t_R) is plottet as a function of the water/acetonitril proportion. With high fractions of organic solvent the in general lipophilic compounds (Log *P*(4-fluorophenylpiperazine) = 1.5; Log *P*(1-phenylpiperazine) = 1.43)[239] show low to moderate retention times on the RP phase. Their lipophilic aryl moiety seems mostly orientated to the mobile phase. Interaction variation of eluent composition only causes very little effects. Molecule orientation changes at higher water contents. Now unpolar groups show a strong interaction and the molecule acts like a normal lipophilic compound. Only now a clear separation is possible. That the retention time dramatically decreases at very high proportions of water is possible due to an effect of the stationary phase material. It is known from a few C18-phases (*e.g.* Prontosil®) that a high amount of water causes a reversible retraction of the C18-chains so that unpolar interaction is inhibited.

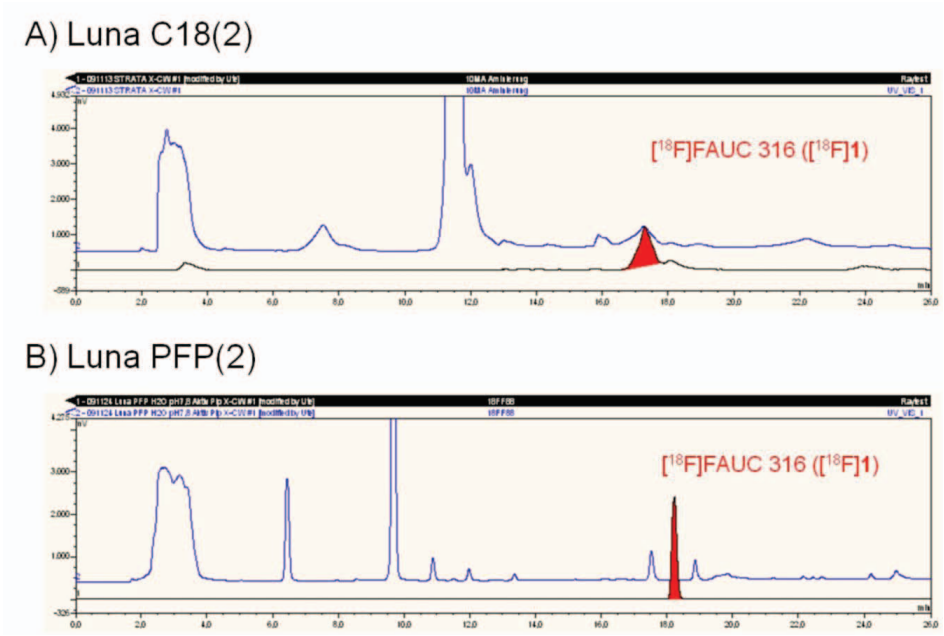

Figure 4.20: Comparison of semipreparative HPLC separation of [^{18}F]FAUC 316 ([^{18}F]**1**) with a "normal" C18 phase (A) and a pentafluorophenylphase (B). Solvent: (A) MeCN/H_2O/TEA 60/40/0.03 (v/v/v) pH 9; (B) MeCN/H_2O/TEA 50/50/0.01 (v/v/v) pH 7.8. HPLC column: (A) Phenomenex Luna 5 µm C18(2) 100 Å 250×10 mm, 4 mL/min; (B) Phenomenex Luna 5 µm PFP(2) 100 Å 250×10 mm, 4 mL/min.

As shown in Fig. 4.18/19 a high amount of water is necessary for a significant separation of the two compounds which limits the available HPLC columns especially as semipreparative ones. Some RP materials are sensitive for high amounts of water or cause an improper counter-pressure due to the higher viscosity of water ($\eta^{20\ °C}$(MeCN) = 0.39 mPa s; $\eta^{20\ °C}$(H_2O) = 0.95 mPa s)[219]. While normal phases or NH phases show now separation, a column material which is optimized for the present separation problem (slightly different halogenated aromatics) is the pentafluorophenyl phase. In Figure 4.19 differences are displayed as moderate but distinct. This phase was used for the final purification of [^{18}F]FAUC 316. In this case a better separation is due to a higher time resolution as shown in Figure 4.20 while this is not that definite with the free amine.

The obtained molar activity (A_M) of about 90 GBq/µmol is very high and allows in general for a specific accumulation as radioligand in pharmacological evaluations.

4.3 Pharmacological evaluation of [^{18}F]FAUC 316

For evaluation of the pharmacological qualification of the high affine D_4 radioligand [^{18}F]FAUC 316 for later *in vivo* applications its accumulation behaviour on rat brain slices was examined by *in vitro* autoradiography in close cooperation with the radiopharmaceutical working group of the INM-5. Thereby the binding of the radioligand was competed with different inactive ligands.

Beside the inactive FAUC 316, competing was done with the unselective but high affine dopaminergic ligand spiperone due to the fact that no applicable gold standard for D_4 exists. Thereby no considerable competition was achieved in any brain area (Tab. 4.3). At a later date experiments were repeated by competing with three of the ligands described in chapter 5. With these substances also no significant blocking of [^{18}F]FAUC 316 was observed.

Reasons are due to the comparatively high lipophilicity of FAUC 316. It causes an extremely high non-specific membrane bindig which is unlike more intensive than specific D_4 binding sites, especially due to the low distribution of D_4 receptors in brain. In spite of the excellent affinity and selectivity of the inactive ligand [^{18}F]FAUC 316, appears therefore not suited for *in vivo* applications.

Table 4.3: Percentage of non-specific binding content in cortex (Cx) and cerebellum (Cbl) of [^{18}F]FAUC 316 ([^{18}F]**1**) on rat brain slices by competing with different substances. No distinct competing was observed in any case.

		Non-specific binding [%]				
	Global binding	***10 µM FAUC 316***	***10 µM Spiperone***	***6 µM 33a***	***6 µM 33d***	***10 µM 33e***
	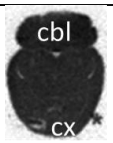					
Cx	/	95	82	96	91	93
Cbl	/	97	79	87	92	88

4.4 Interim summary

Application of the Hartwig-Buchwald *N*-arylation in radiochemistry is an adequate method to generate n.c.a. [^{18}F]fluoroarylamines and therefore a possibility for the production of D_4 selective structures of this which are ^{18}F-labelled at the arylamine moiety. Nevertheless, the procedure is intricate, especially due to its many time- and yield-consuming purification steps. Due to the fact that the replacable moiety indole-2-aldehyde is introduced by an unproblematic reductive amination step, further optimization will refer to the synthesis of 4-[^{18}F]fluorophenylpiperazine ([^{18}F]**28**), a definit compound.

However, [^{18}F]FAUC 316 is unsuitable for *in vivo* imaging methods due to its very high non-specific binding. The logical next step for optimizing of a D_4-radioligand of this class of compounds needs a derivatization of the structure in order to alter properties especially the lipophilicity. But this seems not feasible in this case without worsening its improve binding behaviour. Every derivatization of FAUC 316 would impair its excellent affinity and selectivity values with high probability. Then the complex radiosynthetic procedure would not be worthwhile any longer and it would be better to chose alternative structures with simplier radiosynthetic pathways. Furthermore, a loss complex synthetic procedure is desireable with regard to a possible future implementation in an

automated synthesis device.

5. Synthesis, ^{18}F-labelling and preclinical evaluation of benzodioxine derivatives

Since the results of pharmaceutical evaluation with the highly promising [^{18}F]FAUC 316 ligand demonstrated its uselessness for *in vivo* imaging, the strategies for a development of a D_4 selective radioligand had to be changed. Although the D_4 affinity and the selectivity against the receptors is still an important feature, it became obvious for the choice of prospective lead structures that they had to fulfil further prerequisites. As important property the lipophilicity of FAUC 316 should be regarded as upper limit for further developments. Nevertheless, since the structural backbone of a D_4 ligand is nearly always the same (chapter 2.3) the range of lipohilicity for these ligands is in general small and therefore rarely much different from FAUC 316. Furthermore, the non-specific binding behaviour of a new lead structure cannot be foreseen. It is therefore important to have comparative simple possibilities of functionalization without strong influences on labelling processes.

The benzodioxine 1-(2,3-dihydrobenzo[*b*][1,4]dioxin-6-yl)-4-(4-fluorobenzyl)piperazine (**33a**) seemed to comply with these requirements. It was developed and patented by Hodgetts and Thurkauf[158] for selective blocking of D_4 receptors as a prospective antipsychotic for the treatment of schizophrenia. Published values for affinity and selectivity are excellent but so far only and roughly determined within the D_2 family ($K_i(D_4)$ = 4 nM, $K_i(D_3)$ = >5000 nM, $K_i(D_2)$ = >5000 nM). Affinity values to receptors with known pharmacological similar behaviour like α_1 and 5-HT_{1A} remain unknown as well as no differentiation in haplotypes of the D_2 and the D_4 receptor was examined. It was therefore necessary to determine thoese properties just like for every new derivative (chapter 5.2). The calculated lipophilicity of this new lead structure with a cLog *P* value of 3.35 lay already beneath that of FAUC 316 (cLog *P* = 3.70). Due to the 4-fluorobenzyl group of **33a** many different labelling strategies appeared suitable including possibilities

for direct labelling. This moiety also offered a derivatisation which is discussed in more detail together with the lipophilicity properties of all considered ligands in chapter 5.4.1.

5.1 Synthesis of benzodioxine standard and precursor compounds for ^{18}F-labelling

The synthesis of the non-radioactive standard compounds of derivatives of **32** and **33** was performed for the *in vitro* determination of affinity values (K_i) and *in vivo* evaluation studies on rodents as well as of appropriate analytical conditions for the identification of n.c.a. radiolabelled compounds. The intermediate product 1-(1,4-benzodioxine-6-yl)piperazine (**30**) was synthesized by a Prelog-cyclisation[220,221] of the commercially available aminodioxine 2,3-dihydrobenzo[*b*][1,4]dioxin-6-amine with bis(2-chloroethyl)amine hydrochloride in diethylene glycol or diethylene glycol monomethyl ether analogously to the description of Liu et al.[222]. Thereby higher yields were found while also saving one reaction step when compared to the palladium catalyzed coupling as described by Hodgetts et al.[158] The Prelog annulations displays the easiest method to generate arylpiperazines when suitable anilines are available. This includes not only yield and reaction time, but also the purchase and costs of compounds as well as product purification.

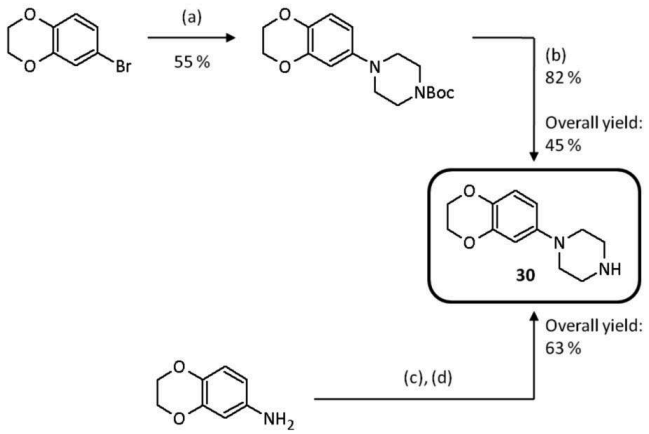

Figure 5.1: Comparison of synthesis routes for the preparation of the important intermediate **30**. Reaction conditions: (a) $Pd_2(dba)_3$, P(*o*-tolyl)$_3$, NaOtBu, 1-boc-piperazine, toluene, 100 °C; (b) TFA, CH_2Cl_2, rt; (c) C_4H_9NCl HCl, $C_2H_6O_2$, 150 °C, 12 h; (d) Na_2CO_3

The intermediate product **30**, obtained by both ways, was the common lead structure for all radioactive and inactive analogues of the lead structures **32** and **33**; with exception of those for direct labelling syntheses. Isolating the hydrochloride product by precipitating the salt from methanol and liberation of the free base with Na_2CO_3 resulted in a pure white solid, directly useful for further synthetic steps. Alternatively the product **30** was obtained from the supernatant by flash chromatography yielding a light yellowish solid which showed no differences neither in analytical properties nor in its reaction behaviour.

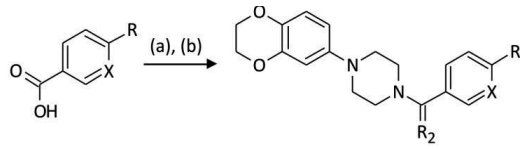

31a: X = CH; R = F
31b: X = CH; R = NO_2
31c: X = N; R = F

32a: X = CH; R = F; R_2 = O
32b: X = CH; R = NO_2; R_2 = O
32c: X = N; R = F; R_2 = O
33e: X = N; R = F; R_2 = H_2

Figure 5.2: Synthesis of the precursor for direct radiolabelling **32b** and its reference compound **32a** and alternative synthesis of title compound **33e** *via* **32c**.

Reaction conditions: (a) $C_2O_2Cl_2$, DMF, CH_2Cl_2, 50 °C, 2h; (b) **30**, CH_3Cl, $(CH_3)_3N$ o. C_5H_5N, rt, 3-24 h; (c) BH_3THF, C_4H_8O, reflux, 24 h.

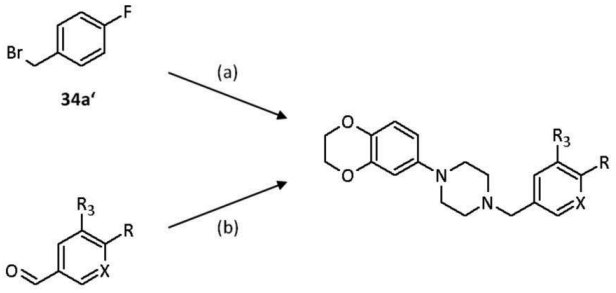

34a: X = CH, R = F; R_3 = H
34b: X = CH, R = F; R_3 = OMe
34c: X = CH, R = F; R_3 = OBn
34d: X = CH, R = F; R_3 = OH
34e: X = N, R = F; R_3 = H
34e': X = N, R = Cl; R_3 = H
34f: X = N, R = H; R_3 = H

33a: X = CH, R = F; R_3 = H
33b: X = CH, R = F; R_3 = OMe
33c: X = CH, R = F; R_3 = OBn
33d: X = CH, R = F; R_3 = OH
33e: X = N, R = F; R_3 = H
33e': X = N, R = Cl; R_3 = H
33f: X = N, R = H; R_3 = H

Scheme 5.3: General synthesis schemes of title structures and reference compounds.

Reaction conditions: (a) **30**, K_2CO_3, KI, CH_3CN, reflux, 18 h; (b) **30**, CH_3OH, CH_3COOH, $NaBH_3CN$, 60 °C, 24 h

The nitro-benzylamid **32b** and its corresponding fluorine-analogue **32a**, as used standard were synthesized from the carboxylic acids by formation of acid chlorides as displayed in Figure 5.2. Due to the high yields of about 70 % of those coupling reactions the fluoropyridine-analogue (4-(2,3-dihydrobenzo[b][1,4]dioxin-6-yl)piperazin-1-yl)(6-fluoropyridin-3-yl)-methanone was also synthesized that way with the intention of subsequent reduction and therefore easy production of the pyridine standard compound **33e**. Problems of reduction, however, occurred as are described below.

The coupling reaction of the starting intermediate **30** to the benzylamines **33a-f** could be performed with corresponding benzylhalides, which led in case of 4-fluorobenzylbromide to good yields of up to 55 % of **33a**. Reductive amination with the appropriate aldehydes **32a-f**, however, was selected as the preferred method, because due to better reproducibility and also easier synthesis of the aldehydes (cf. Scheme 5.3). Thus, a series of new 3-substituted 6-(4-[4-fluorobenzyl]piperazine-1-yl)benzodioxine derivatives were obtained in 20-85 % yield. They all represent standard reference compounds with exception of the pyridine compound **33e'** which is the precursor for direct labelling to [^{18}F]**33e**.

For the preparation of the pyridine reference compounds **33e** and **33e'** 2-fluoronicotinic acid or 2-chloronicotinic acid were used as starting material, respectively. While the chloro compound was commercially available, the fluoro-analogue was obtained by oxidation of 2-fluoro-5-methylpyridine to 2-fluoronicotinic acid which was converted to the nicotinic acid chloride, coupled to the amide, and subsequently reduced to the amine (cf. Fig. 5.2 and 5.4). Alternatively, the acid chloride was reduced to the alcohol, oxidized with Dess-Martin periodinane to the corresponding aldehyde (cf. Fig. 5.4) and coupled by reductive amination as described above. The latter method resulted in higher yields because the conversion of the pyridineamide **32c** to the corresponding amine by reduction with BH_3THF or $LiAlH_4$ proceeded very poorly.

The precursors for direct radiofluorination by nucleophilic substitution with n.c.a. [^{18}F]fluoride, the aldehydes (4-formyl-phenyl)-trimethylammonium triflate (**40a**) and (4-formyl-3-methoxyphenyl)trimethylammonium triflate (**40b**), were synthesized by the well known amination of the corresponding fluorine compounds (commercially available) with dimethylamine hydrochloride and subsequent quaternization with methyltrifluoro-methane sulfonate[223,224].

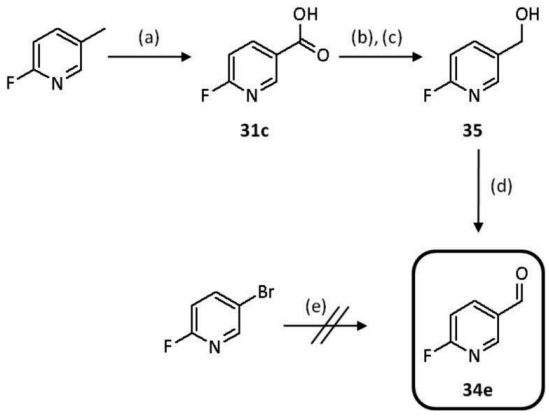

Figure 5.4: Synthesis of 5-nicotinic aldehyde (**34e**) as standard for labelling as well as intermediate to title compound **33e**.

Reaction conditions: (a) $KMnO_4$, H_2O, 100 °C; (b) $C_2O_2Cl_2$, DMF, DCM, rt; (c) $NaBH_3$, THF, 60 °C; (d) Dess-Martin periodinane, DCM, rt; (e) 1. sec-BuLi, $C_4H_{10}O$, -78 °C, 45 min; 2. DMF, rt

The benzyl protected precursor (3-benzyloxy-4-formylphenyl)trimethylammonium triflate (**40c**) was synthesized by a 6-step reaction procedure starting from 4-bromo-*N,N*-dimethylaniline (Fig. 5.5). The key step was the formation of the aldehyde group from the bromo compound with DMF and *sec*-butyllithium. The nitro precursors **40a'** and **40b'** were commercially available while **40c'** was synthesized by a benzylation of 4-nitro-3-hydroxybenzaldehyde at a temperature of 110 °C following a procedure described by Langer et al.[225]. All aldehyde precursors (**40a-e**) are listed in Figure 5.9 (see below Chapt. 5.3.2). A 4-step route starting from 4-fluoro-3-methoxybenzaldehyde by a Lewis acid assisted cleavage of the methyl group was utilized to prepare the corresponding hydroxy and benzyloxy reference compounds (**33c, 33d**) of the according radiolabelled compounds. Thus, the obtained series of compounds included the reference compounds of the desired radiolabelled analogs (**33a**, **33b**, **33d** and **33e**), the precursors for aromatic ^{18}F-for-Cl or ^{18}F-for-NO_2 substitution (**33f** and **32b**), and the precursor compounds **40a-e** suitable for a two-step radiosynthesis of [^{18}F]**33a-e** by reductive amination with intermediate **30**.

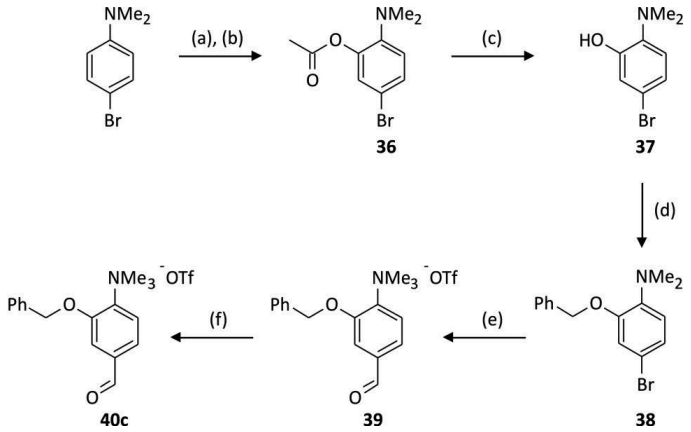

Figure 5.5: Scheme of the 6-step reaction route to the precursor compound (3-benzyloxy-4-formylphenyl)-trimethylammonium triflate **40c**.

Reaction conditions: (a) H_2O_2 (30 %), $C_4H_6O_3$, -78 °C, 2 h (b) $C_4H_6O_3$, 0 °C, 2 h (c) KOH, MeOH, 70 °C, 2 h; (d) C_7H_7Br, K_2CO_3, acetone, reflux, 3 h; (e) 1. sec-BuLi, $C_4H_{10}O$, -78 °C, 45 min; 2. DMF, rt, 1 h; (f) $CF_3SO_3CH_3$, CH_2Cl_2, 40 °C, 7 h

5.2 Receptor binding and intrinsic affinities

The 3-position of the 4-fluorobenzyl moiety was selected as derivatisation place to avoid the distress of problems with the molecule adjustment in the binding crevice. As shown in chapter 2.3.2 three OH-groups from different serines can interact with ligand moieties which are able to undergo hydrogen bridges.

All receptor binding assays were performed in the institute of pharmaceutical chemistry of the Friedrich-Alexander Universität Erlangen-Nürnberg (direction of Prof. Dr. P. Gmeiner) by Dr. H. Hübner. The results are discussed in this work, because the values found are basic facts for modelling of new ligands and evaluation of the radiotracers. Due to the necessity of this cooperationship binding affinities could only be determined with the inactive standard compounds which results in inhibitory constant (K_i) values as explained in chapter 2.2.5. Then main reason for determination of affinities is the obvious problem of an unpredictable alteration of affinity and selectivity of the original lead structure **33a** due to derivatization. Therefore, the lead compound **33a** and its derivatives **33b**, **33d** and **33e** were subjected to receptor binding studies for testing their ability to displace [^{3}H]spiperone from the cloned human dopamine receptors D_{2long}, D_{2short},[226] D_3,[227]

and the most common D_4 polymorphism $D_{4.4}$,[228] being stably expressed in Chinese hamster ovary (CHO) cells.[229] **33a** was tested itself because different displacement studies often show differences.

Additionally, the metabotropic receptors 5-HT_{1A}, 5-HT_{2A} and α_1, from which it is known that they could reveal competing binding affinity for putative D_4 ligands, were measured utilizing porcine cortical membranes and the selective radioligands [^{3}H]WAY600135, [^{3}H]ketanserin and [^{3}H]prazosin, respectively.[230] The in human brain highly expressed but structurally and functionally different dopaminergic receptor D_1 was measured using porcine striatal membranes and the radioligand [^{3}H]SCH23990. The results of the receptor binding studies are presented in Table 5.1.

Table 5.1: Binding affinities of the derivatives **33a, 33b, 33d** and **33e** to the human dopamine receptor subtypes D_{2long}, D_{2short}, D_3, and $D_{4.4}$, the porcine D_1 receptor, as well as the porcine 5-HT_{1A}, 5-HT_2, and α_1 receptors

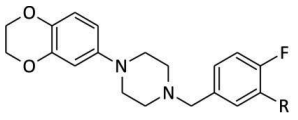

33a, 33b, 33d

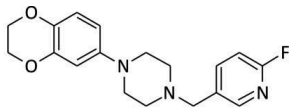

33e

compound		***K_i values ± SD [nM]***[a]							
	R	***$hD2_{long}$***[t]	***hD_{2short}***[b]	***hD_3***[b]	***$hD_{4.4}$***[b]	***pD_1***[c]	***p5-HT_{1A}***[d]	***p5-HT_2***[e]	***pα_1***[f]
33a	*H*	7600 ± 570	5700 ± 1300	3900 ± 71	1.1 ± 0.56	19000 ± 11000	5200 ± 2200	7000 ± 5700	4000 ± 780
33b	*OMe*	17000 ± 1400	16000 ± 2100	5900 ± 640	4.2 ± 0.071	23000 ± 4200	5600 ± 2100	4200 ± 2100	3300 ± 350
33d	*OH*	9000 ± 1100	6100 ± 71	4200 ± 1300	7.3 ± 2.6	15000 ± 3600	6200 ± 710	2300 ± 640	3000 ± 210
33e	-	29000 ± 20000	45000 ± 710	17000 ± 710	15 ± 0.71	35000 ± 4200	21000 ± 2100	5800 ± 2100	11000 ± 710

[a] K_i-Values [nm] are mean values of two independent experiments each done in triplicate. [b] [^{3}H]spiperone. [c] [^{3}H]SCH 23990. [d] [^{3}H]WAY600135. [e] [^{3}H]ketanserin. [f] [^{3}H]prazosin.

All ligands showed a good affinity to the D_4 receptor in the low nanomolar range and weak affinities to all other tested receptors (Tab. 5.1). Among the series of compounds, the lead compound **33a** showed the highest affinity to the D_4 receptor combined with an exceptional D_4 subtype selectivity (Tab. 5.2). Higher values were found here when compared with the earlier measured affinities within the D_2-familiy described by Hodgetts at al.[158] Nevertheless, the introduction of a methoxy or hydroxy group into the fluorophenyl moiety (see **33b**, **33d**) led to a minor decrease in D_4 affinity of these compounds. This is astonishing due to an estimated increase of affinities with insertion of moieties with the ability to form hydrogen bridges. The displacement of the fluorophenyl group by the fluoropyridinyl substituent (**33e**) induced a decrease in D_4 affinity by a factor of about 10. However, the D_4 subtype selectivity of >1000 (D_4/D_3) and >2000 (D_4/D_2) for **33e** appears still adequate for *in vivo* imaging.

In general, the subtype selectivity was high for all derivatives (Tab. 5.2), but highest for **33a**, followed by **33b**, **33e** and **33d**. Remarkably, selectivities of **33a** measured in this study displayed a K_i ratio of more than 5000 for D_2 (D_4/D_2) and 3500 for D_3 (D_4/D_3), which is one of the highest selectivities for D_4 over D_3 reported up to now.

Table 5.2: D_4 subtype selectivity within the family of D_2-like receptors

compound	***$hD_{4.4}$***	***ratio of $K_i(D_2$ or $D_3)$ / $K_i(D_{4.4})$***		
	K_i [nM]	***hD_{2long} / $hD_{4.4}$***	***hD_{2short} / $hD_{4.4}$***	***hD_3 / $hD_{4.4}$***
33a	1.1	6666	5000	3571
33b	4.2	4000	3846	1408
33d	7.3	1250	833	588
33e	15	2000	3030	1136

The original lead structure **33a** is described as an antagonist at the D_4 receptor. Data on receptor affinities were extended by functional data using a previously described mitogenesis assay to confirm this data and to determine the intrinsic activity of the other derivatives [231]. The agonist activation of dopamine receptors is known to increase mitogenesis in heterologously transfected cell lines, measuring the rate of proliferation in

growing cells[232]. Full and partial agonist ligands preferentially bind to the active GPCR conformation (high-affinity state), inverse agonists favour binding to the inactive receptor, and antagonists have equal affinity for the active and inactive state. Since in general the inactive GPCR conformation is predominant, differences in binding kinetics are estimated for agonists and antagonists. It is important to determine the intrinsic activity for a putative radioligand helping to interpret these differences in the in vivo behaviour of radioligands. The intrinsic activity of the series of title compounds was investigated by measuring the [^{3}H]thymidine incorporation into growing CHO cells stably expressing the dopamine D_4 receptor[233]. As shown in Figure 5.6, a neutral antagonism was determined for all title compounds under investigation when compared to the reference quinpirole.

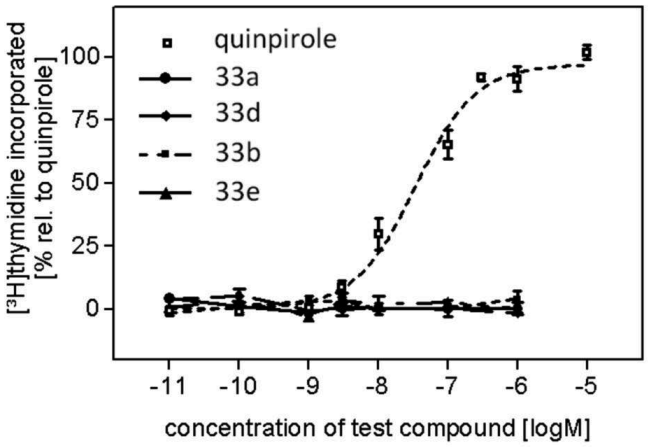

Figure 5.6: Measurement of [^{3}H]thymidine incorporation in D_4 expressing cells as an assay for functional activity; dose-dependent increase of incorporation of radioactivity as a matter of activation of the human dopamine $D_{4.4}$ receptor stably transfected in CHO cells compared to the effect of the full agonist quinpirole (= 100 %).

In summary, the radiosyntheses of the corresponding ^{18}F-labelled antagonistic radioligands **33a**, **33b**, **33d** and **33e** was aspired due to their promising high D_4 receptor affinity and distinct D_4 receptor subtype-selectivity.

5.3 Radiosynthesis of benzodioxine derivatives

5.3.1 Direct n.c.a. ^{18}F-labelling of benzodioxine derivatives

For direct labelling with n.c.a. [^{18}F]fluoride by nucleophilic substitution on arenes the presence of an electron withdrawing group is necessary as previously described in chapter 2.2.3. Therefore, the synthesis of n.c.a. 4-[^{18}F]fluorophenylpiperazines is only suitably practicable by labelling of the corresponding amides and subsequent reduction as described for inactive compounds above. The nitro group was selected as the best adaptable leaving group for the S_NAr reaction. Trimethylammonium triflat cannot be generated in these compounds due to the rivalry of the two tertiary arylamines (dimethyl- and arylpiperazine-group) with very similar pK_a values. Kryptofix 2.2.2 was used as anion activator and DMSO and DMF as solvents. In DMSO substitution of the nitro group resulted in radiochemical yields of up to 50 % after 15 min. As a typical character of direct labelling adequate yields are only obtained with very high reaction temperatures of at least 160 °C. Therefore, DMF cannot be used due to its lower boiling point although it displays considerably higher radiochemical yields at equal temperatures (Fig. 5.8). However, a reproducibility of radiochemical yields cannot be guaranteed using DMF at higher temperatures than 140 °C.

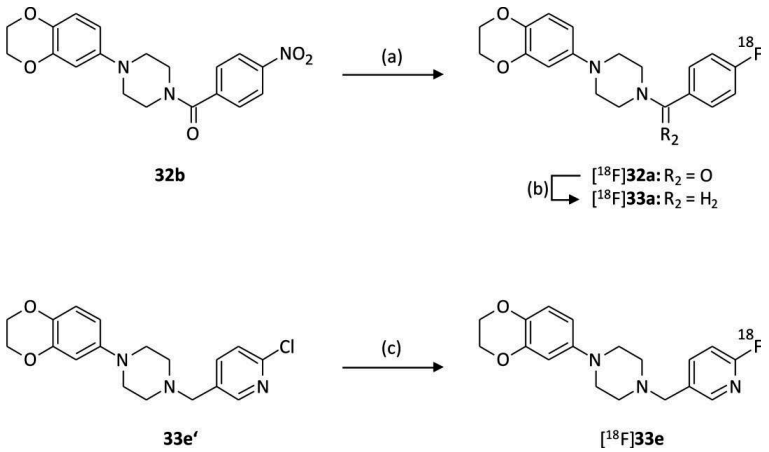

Figure 5.7: Radiosynthesis of [^{18}F]**33a** and [^{18}F]**33e** by direct nucleophilic substitution.
Reaction conditions: (a) [^{18}F]F^-, K⊂ 2.2.2, K_2CO_3, DMSO, 160 °C, 15 min; (b) BH_3THF, THF, 65 °C, 15 min; (c) [^{18}F]F^-, K⊂ 2.2.2, K_2CO_3, DMSO, 160 °C, 20 min

The reduction of the amide [^{18}F]**32a** was at first conducted with the strong reduction system $LiAlH_4/AlCl_3$ in diethylether or THF due to the absence of further substituents for sensitive reduction. Nevertheless, yields of the reduction with $LiAlH_4$ switched from 100 % to zero after 5 min reaction time and no reproducibility could be reached. Furthermore, rapid hydrogen evolution hampers the working conditions. Using the BH_3/THF complex as reducing agent led to a conversion of 42 ± 4 %, but requires 65 °C and 15 min reaction time. Despite a theoretical overall yield of about 20 %, after separation with a semi-preparative HPLC column (Gemini C18, Phenomenex 250×10 mm) the radiochemical yields of [^{18}F]**33a** were only marginally above 1 % at the end of synthesis (EOS). The reason for this is the high number of solid phase extraction steps (3), where each time a loss of yield can be observed as well as losses during subsequent HPLC separation. These poor yields initiated renunciation of direct labelling to build-up radiosynthesis methods which are described in the next chapter.

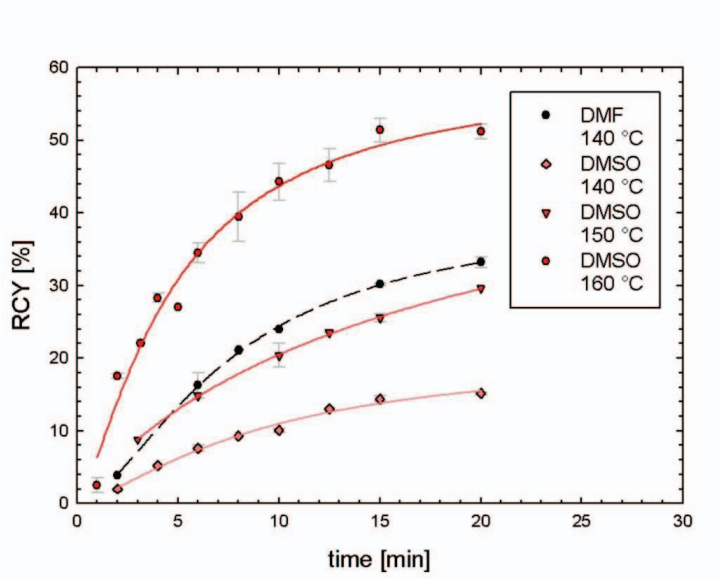

Figure 5.8: Time dependence of radiochemical yield (RCY) of [^{18}F]**32a** at different reaction temperatures in DMSO (red) and DMF (black) by direct ^{18}F-substitution on **32b**.

Reaction conditions: n.c.a. [^{18}F]F^-, [**32b**] = 40 mmol/L, [K⊂2.2.2] = 40 mmol/L, [K_2CO_3] = 20 mmol/L, solvent = 0.5 mL

The situation is different with the pyridine derivative **33e** due to the fact that pyridines itself led, however, to an aromatic activation for nucleophilic substitution in *ortho*- and *para*-position. Only poor radiochemical yields up to 5 % of [^{18}F]**33e** were obtained at 160 °C in DMSO after 30 min despite this fact and high radiochemical yields of 2-[^{18}F]fluoropyridine described in literature[77].

5.3.2 Build-up synthesis of benzodioxine derivatives by reductive amination

Since the first utilization of reductive amination of ^{18}F-labelled aldehydes by Wilson et al.[223], the method has proven convenient to produce corresponding no-carrier-added benzylamines with fluorine-18 in aryl position. The labelling conditions comprise a temperature range of about 130-150 °C, DMSO as solvent and (K⊂2.2.2)/carbonate as anion activator[234]. The normal procedure includs the separation of the labelled aldehyde by solid phase extraction or the HPLC purification and performing the amination reaction in a mixture of MeOH and CH_3CO_2H and temperatures of about 60 °C. As a variation of the Leuckart-Wallach reaction[235,236] sodium cyanoborohydride is commonly chosen as reducing agent instead of an excess of formic acid. Hai-Bin et al. showed that reductive amination reactions can also be performed in the presence of DMSO and Kryptofix 2.2.2[237]. Thus, labelling and reductive amination could be performed as a one-pot reaction using DMSO at the same temperature of 110° C.

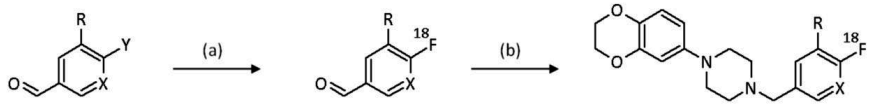

40a: X = CH, R = H; Y = $^{+}NMe_3^{-}OTf$
40a': X = CH, R = H; Y = NO_2
40b: X = CH, R = OMe; Y = $^{+}NMe_3^{-}OTf$
40b': X = CH, R = OMe; Y = NO_2
40c: X = CH, R = OBn; Y = $^{+}NMe_3^{-}OTf$
40c': X = CH, R = OBn; Y = NO_2
40e: X = N, R = H; Y = Cl

[^{18}F]**34a:** X = CH; R = H
[^{18}F]**34b:** X = CH; R = OMe
[^{18}F]**34c:** X = CH; R = OBn
[^{18}F]**34e:** X = N; R = H

(c)

[^{18}F]**33a:** X = CH; R = H
[^{18}F]**33b:** X = CH; R = OMe
[^{18}F]**33c:** X = CH; R = OBn
[^{18}F]**33d:** X = CH; R = OH
[^{18}F]**33e:** X = N; R = H

Figure 5.9: Radiosynthesis of [^{18}F]**33a-c** and [^{18}F]**33e** by a two-step, one-pot reaction.
Reaction conditions: (a) [^{18}F]F^{-}, K⊂2.2.2, K_2CO_3, DMSO, 110 °C; (b) **30**, $NaBH_3CN$, DMSO, 110 °C; (c) Pd(black), $HCOONH_4$, MeOH, 60 °C, 10 min

For the reductive aminations performed here the addition of methanol to the reaction mixture was found unnecessary in contrast to acetic acid which is an essential reagent for the rapid formation of the immonium ion.

Furthermore, less radioactive side products were found by using DMSO instead of methanol. In DMSO a nearly quantitative conversion of the ^{18}F-labelled aldehyde to the tertiary amine could be observed by radio-HPLC analysis. Performing the one-pot reaction with DMF, which is also a suitable solvent for radiofluorination of aldehydes, or using lower temperatures, however, led to an extreme loss of the radiochemical yield. A general disadvantage of the one-pot synthesis, however, is the accumulation of inactive reactants and unidentified side products in the final reaction solution. Therefore, HPLC purification can severely be obstructed depending on the respective product.

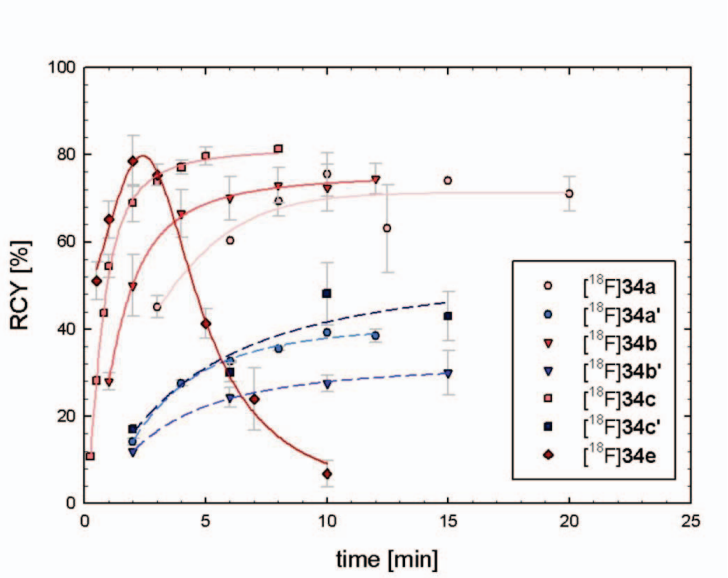

Figure 5.10: Time dependence of radiochemical yield of ^{18}F-labelling of benzaldehyde derivatives. For comparison nitro precursors (**34a'-c'**) are displayed in blue and with dashed lines while benzaldehyde trimethylammonium triflates are shown in red. 6-[^{18}F]Fluoropyridinealdehyde (**34e**), also displayed in red, shows the highest yields at short time but followed by rapid degradation.

Reaction conditions: n.c.a. [^{18}F]F$^-$, [**34a-e**] = 20-60 mmol/L, [K ⊂ 2.2.2] = 40 mmol/L, [K_2CO_3] = 20 mmol/L, DMSO = 0.5 mL, 110 °C

The unsubstituted and the methoxy compounds ([^{18}F]**33a**, [^{18}F]**33b**) could be generated as described above in radiochemical yields of about 60 % and with a molar activitiy of about 60 GBq/µmol, when starting with about 500-1000 MBq of [^{18}F]fluoride. By ^{18}F-fluorination of the extremely activated *ortho*-position of 6-chloronicotinaldehyde **40e** defluorination of [^{18}F]**34e** occurred after a very short reaction time after about 2 min depending on the precursor concentration. A higher amount of precursor acted as a pseudo carrier and diminished the rate of decomposition to some extend. The influence of both activating systems (aldehyde and pyridine) seems to polarize C-F binding that strong that even weaker nucleophiles (every halide, hydride or hydroxy) in low concentrations can displace [^{18}F]fluoride. Despite these findings no comparable observation is described in the literature for similar compounds like 6-chloronicotinic acid dietylamide during its ^{18}F-fluorination[76]. Back reaction with chloride as nucleophile, which is also conceivable would lead to an equilibrium which is not observed during the fluorination procedure (Fig. 5.13 A). Nevertheless, after reductive amination (Fig. 5.13 B) the chloro derivative **33e'** is observed as a main inactive side product. The unsubstituted derivative **33f** was also determined after reductive amination and confirmed the hypothesis of a defluorination (Fig. 5.11).

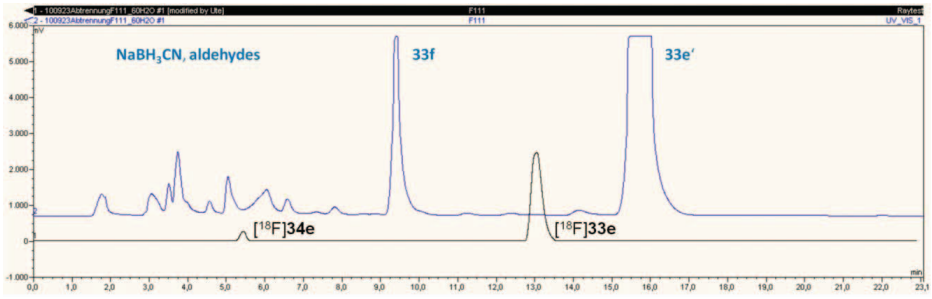

Figure 5.11: Chromatogram of semi-preparative HPLC-purification of the pyridine analogue [^{18}F]**33e**. The black line shows the output from the γ-counter while the blue line describes the UV-absorption. Main inactive side products are the chloro analogue 33e' as well as the unsubstituted derivative 33f. In the front inactive side products are supposed to consist of reactands, aldehydes and decomposition products but were not all identified.

HPLC-column: Gemini 5 µm C18 110Å, 250×10 mm, Phenomenex. Eluent: 40/60/0.1 MeCN/H_2O/TEA (v/v/v); 4 mL/min

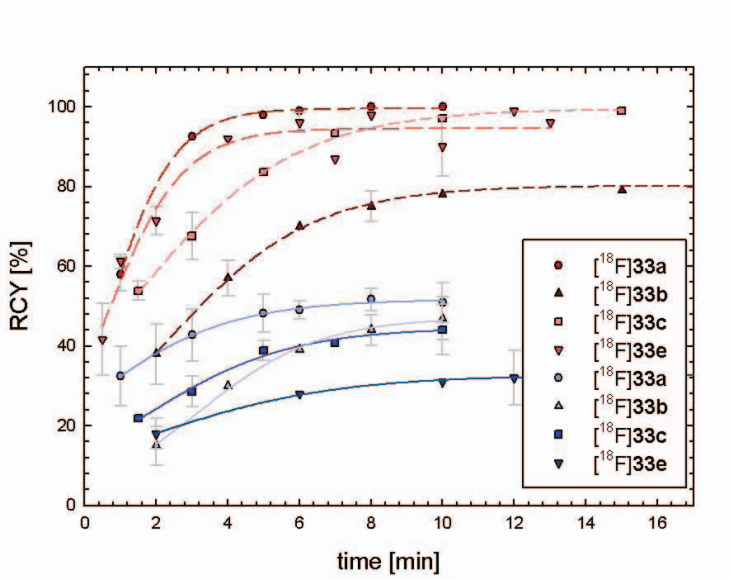

Figure 5.12: Time dependence of the total radiochemical yield of the amination reaction related to [^{18}F]F$^-$ (blue) as well as the radiochemical yield of the products ([^{18}F]**33a,b,c,e**) related to the intermediate aldehyde compounds ([^{18}F]**34a,b,c,e**) (red).
Reaction conditions: [**30**] = 46 mmol/L, $NaBH_3CN$ = 64 µmol, DMSO = 0.6 mL, AcOH = 40 µL, 110 °C

Defluorination was also the critical side reaction when the reductive amination reaction on [^{18}F]**34e** was performed. Any change of reaction parameters, however, such as reaction time, lowering the amine concentration or reaction temperature or using weaker reduction systems resulted in very poor radiochemical yields.

For pre-purification of [^{18}F]**33c** SepPac C18 cartridge were used. Problems with large amounts of persisting inactive lipophilic impurities which overly the product peak in HPLC could be removed by using the weaker, more hydrophilic eluent ethanol/water instead of acetonitrile, but the higher purity was only attained on the account of total yield.

For the production of the ^{18}F-labelled hydroxy derivative [^{18}F]**33d** ^{18}F-fluorination and amination with the benzyl protected aldehyde compound [^{18}F]**33c** were performed as described above. This intermediate product was easier separated from the reaction solution by adsorption on an EN cartridge since the benzyl group led to a considerable higher lipophilicity. Thus, the above described problems with final HPLC purification are not valid for the hydroxy derivative. Despite that, the obtained radiochemical yield after

semi-preparative radio HPLC separation was lower than for all others.

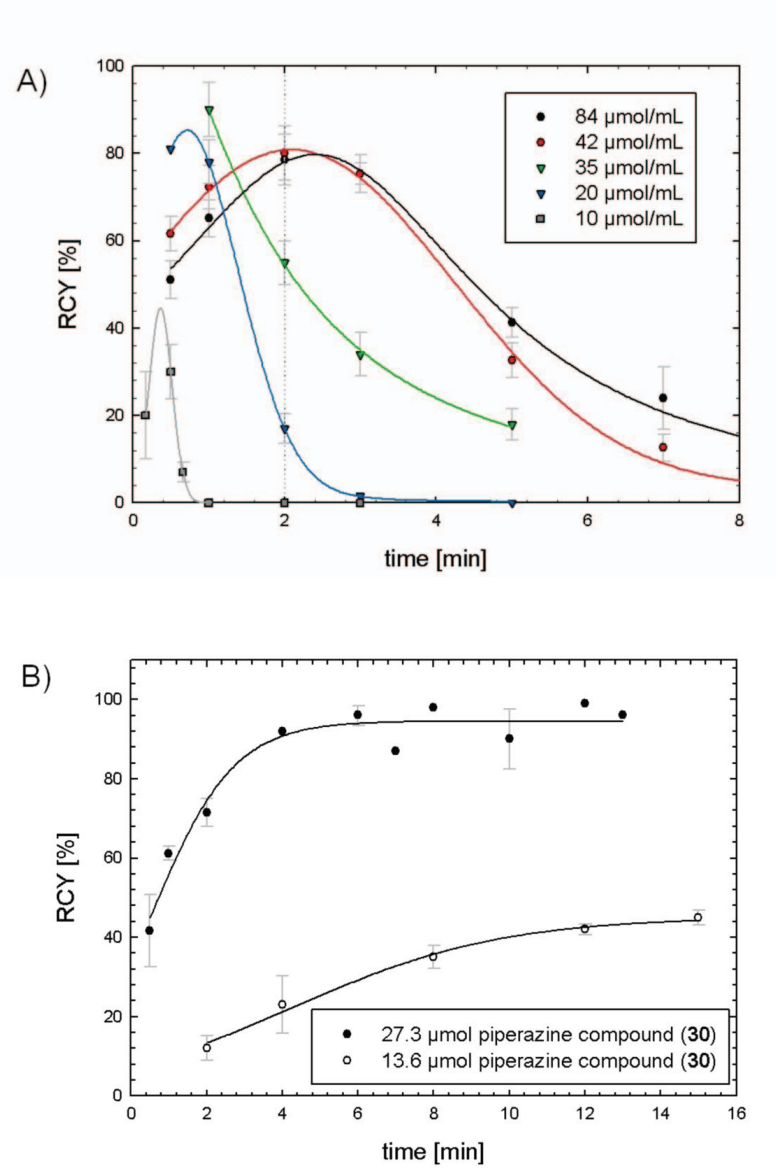

Figure 5.13: Time dependence of RCY of [^{18}F]**34e** (A) and of subsequent amination to [^{18}F]**33e** related to [^{18}F]**34e** (B) according to precursor and amine concentration, respectively. In both cases a lower concentration leads to a rapid degradation of [^{18}F]**34e**.

Losses during the synthesis of [^{18}F]**33d** can occur due to the additional reaction (cleavage) and therefore extraction step and adsorption processes during this cleaving step. The cleavage of the benzyl protection group was succeeded in methanol with ammonium formate and palladium black at 60 °C under inert conditions. Previously a complete drying of the benzyl-intermediate by a stream of argon and elution through an AluminaN® cartridge is necessary. An acid cleavage with strong acids like trifluoroacetic acid, which could possibly be performed without further separation, is not suitable because of a rapid degradation of the dioxine component and of enhancing more preferred side reactions. Similar degradations can be observed when cleavage of the methoxy substituent from [^{18}F]**33b** with BBr_3 is performed.

All radiosyntheses result in molar activities (A_M) of about 30-60 GBq/μmol (cf. Tab. 5.3) which are high enough to guarantee the possibility of a specific accumulation of every radioligand far from levels of saturation.

5.3.3 Comparison of ^{18}F-labelling methods for benzodioxine derivatives

While direct labelling is normally the method of choice and build-up synthesis is normally reserved for cases when the former fails, in direct comparison of both methods, here the latter lead to better results. In both cases of direct labelling only a radiochemical yield of about 1-5 % as achieved at the end of synthesis while the build-up syntheses lead to radiochemical yields of 9-35 %. The required reaction time of 120 min in case of [^{18}F]**33a**, exemplarily for [^{18}F]**33b** and [^{18}F]**33c** as well, could not keep up with the two-step amination reaction. This is due to the high ^{18}F-labelling yields with the trimethylammonium triflate benzaldehydes and the fact that the applicable one-pot operation demonstrates the advantage of a single step with respect to effort, product loss, and synthesis time. Further reasons include the insensitivity and therefore reproducability of the reductive amination reaction and its high conversion rates which make this reaction type remarkable appropriate for n.c.a. ^{18}F-chemistry.

An exception displays the pyridine derivative because generating the ^{18}F-labelled product [^{18}F]**33e** could be done in a single step. However, ^{18}F-fluorination of the 6-chloronicotinic aldehyde led to many inactive side products which complicate product separation processes and gave lower yields. On the other hand, the extremely poor yield obtained from direct labelling of the chloropyridine-methylpiperazine **33e'** compound

was surprising when compared to the normally good results of nucleophilic substitution at the *ortho*- or *para*-position of pyridines. Therefore, it seems worthwhile for further experiments to examine other leaving groups with this compound like the nitro substituent. Using microwave irradiation as it is described in many ^{18}F-labelling procedures of pyridines before would be another reasonable option for possible improvement.

Table 5.3: Radiochemical yields of radiofluorination and amination steps to yield [^{18}F]**33a-b** and [^{18}F]**33d-e** in a one-pot reaction according to figure 5.9.

precursor	***time (min)***	***[^{18}F]fluoro-aldehyde***	***RCY (%)***	***total time (min)***	***final product***	***RCY at EOS (%)***	***A_M (GBq/µmol)***
40a	10	[^{18}F]**34a**	75 ± 5	~90	[^{18}F]**33a**	35 ± 5	60
40a'	12		38 ± 1.5				
40b	10	[^{18}F]**34b**	72 ± 5	~90	[^{18}F]**33b**	20 ± 5	50
40b'	15		30 ± 5				
40c	5	[^{18}F]**34c**	80 ± 2	~120	[^{18}F]**33d**	9 ± 4	27
40c'	10		48 ± 7				
40e	2	[^{18}F]**34e**	80 ± 6	~80	[^{18}F]**33e**	15 ± 5	40

EOS = end of synthesis.

Table 5.4: Radiochemical yields of [^{18}F]**33a** and [^{18}F]**33e** by direct labelling in DMSO at 160 °C.

precursor	***final product***	***total synth. time (min)***	***RCY at EOS (%)***
32b	[^{18}F]**33a**	120	5 ± 2
33e'	[^{18}F]**33e**	50	1 ± 0.5

EOS = end of synthesis.

5.4 Pharmacological evaluation of ^{18}F-labelled benzodioxine derivatives as D_4 ligands

5.4.1 Lipophilicity

As an adequate estimation of this physicochemical property the MarvinSketch 5.1.4 software[239] and the ALOGPS 2.1 software[240] were used to calculate Log *P* values of compounds **33a-b** and **33d-e** which were estimated between 2.3 and 3.4 (Tab. 5.5). The two different algorithms showed very similar results. However, experimental lipophilicity values (Log P and Log D), ranging from 1.7 to 2.7, were again rather close to each other but clearly lower than the theoretical ones. Experimental values were obtained by two different methods at pH 7.4, i.e. shake flask and HPLC method, according to the OECD guidelines for the testing of chemicals[241]. As explained in chapter 2.5 the values obtained by the shake flask method include all species in solution (Log $D_{7.4}$) and is more real to the situation at biomembranes. Otherwise this method was not trusted at higher lipophilicity due to the easy contamination of the two phases. The obtained Log *P* and Log *D* values were determined to be between 1.7 to 2.4, a range that is proposed for ligands to penetrate the blood brain barrier, suggesting sufficient brain uptake of the corresponding radioligands.

Table 5.5: Calculated and experimental log $P_{7.4}$ values of the derivatives **33a**-**33e**

Ligand	***33a***	***33b***	***33d***	***33e***
cLog *P* (Marvin)	3.35	3.09	2.87	2.49
cLog *P* (ALOGPS)	3.23 ± 0.27	3.11 ± 0.45	2.81 ± 0.37	2.26 ± 0.32
Log $P_{7.4}$	2.71 ± 0.03	2.44 ± 0.07	1.70 ± 0.15	2.02 ± 0.17
Log $D_{7.4}$	n.d.	2.33 ± 0.09	1.78 ± 0.01	1.81 ± 0.05

Differences between calculated and experimental lipophilicity values of ΔLog *P* values of about 0.6 and 0.7, respectively, are very similar for the unsubstituted compound **33a** and its methoxy derivative **33b**. The highest difference with ΔLog *P* of about 1.1 is shown by the hydroxyl derivative **33d**. A possible reason can lay in the nature of the OH group which can form hydrogen bonds both as donor and acceptor and therefore lead to an unclear protonated state, 3D structure and solvent interaction of this molecule, which is

not comprised by the algorithms of the used programmes. The fact that differences in results within both experimental methods are small let presume that despite this, nearly only one species exists at pH 7.4. With ΔLog *P* of about 0.45 the difference between calculated and experimental values of the pyridine derivative **33e** is the smallest but lays in the range of **33a**/**b**. For the more hydrophilic compounds the trend observed with experimental values is reversely to that of the calculated ones. It is estimated that this observation is more due to the hydroxyl derivative which is assured by the linear slope (cp. Fig. 5.14). It is regarded that in case of plotting the lipophilicity against the non-specific binding, calculated cLog *P* values show the more definite trend.

5.4.2 Autoradiography

In vitro and *ex vivo* autoradiography as well as biodistribution and metabolization studies were performed in close cooperation with the radiopharmacology group of the INM-5.

As explained in detail in chapter 2.5, non-specific binding, the binding which remains after an addition of an access of inactive specific ligands, often leads to a disqualification of selective radioligands. In the majority this is related to lipophilic structures. Lesser known is, that the assumption non-specific binding would be totally unsaturable is wrong[184]. Therefore, the non-specific binding of two structures with a different pharmacological profile is not comparable and does not necessarily depend on their lipophilicity.

After determination of suitable affinity and subtype selectivity of all tested substances to the D_4 receptor, *in vitro* autoradiography studies on horizontal rat brain slices were performed with those ligands labelled with fluorine-18 in order to compare the non-specific binding pattern and the lipophilicity. For this, ^{18}F-labelled compounds were competed with an excess of the inactive standards **33a-33b** and **33d-33e**. No differences in competition behaviour could be found between competition with the original identical standard compound or with another ligand. Thereby a confirmation of the postulated relationship[185,192,242] between non-specific binding and lipophilicity (Fig. 5.14) was found.

The more lipophilic radioligands [^{18}F]**33a** and [^{18}F]**33b** showed inacceptable high non-specific binding of 96 % and 79 %, respectively, and seem therefore unsuitable as potential radiotracers. In contrast, non-specific binding of [^{18}F]**33d** was only 33 %, and

[^{18}F]**33e** showed even a lower non-specific binding of only 7 %. Although [^{18}F]**33e** exhibited a lower D_4 affinity than the other ligands, it therefor lends itself for further *ex vivo* studies due to its high selectivity and low non-specific binding.

In vitro autoradiography studies of the more hydrophilic compounds [^{18}F]**33d** and [^{18}F]**33e** showed generally a specific binding within the whole rat brain. Both compounds displayed a distinct high accumulation in the colliculus and in the medial nuclei of the cerebellum. As presented in Figure 5.15 there is no marked higher accumulation in hippocampus, frontal cortex and striatum.

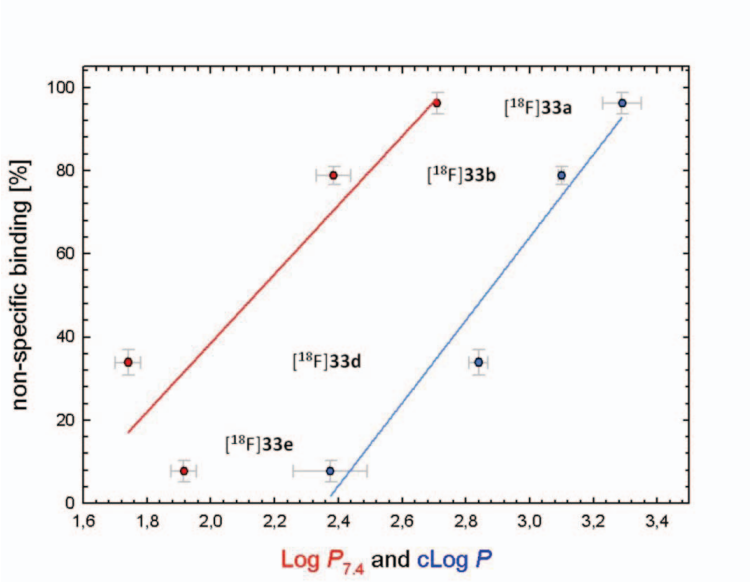

Figure 5.14: Relation of experimentaly determined Log $P_{7.4}$ values (red) and calculated cLog *P* values (blue) of the derivatives **33a, 33b** and **33d, 33e** and of non-specific binding of the ^{18}F-labelled compounds received by competition studies with reference compounds on Wistar rat brain slices *in vitro*.

By contrast, in *ex vivo* autoradiography studies with NMRI mice high binding was observed in the cortex and hippocampus. In comparison with the cresyl violet stained image of the same slice the good contrast allows differentiating between the outer layers of cortex with high binding and lower binding in middle layers of cortex. In the hippocampus high binding uptake was observed in dentate gyrus (GD) and cornu ammonis 3 (CA3). This is in agreement with findings of Prante et al.[243] who described a

significant higher uptake in the gyrus dentate of rat brain slices with a ^{18}F-labelled pyrazolo[1,5-α]pyridine D_4 ligand but not in the other regions of hippocampus. High uptake *in vitro* and *ex vivo* was observed in regions of the colliculus. This brain region, responsible for sorting out of optical and acoustical information, was described as a part of brain, where D_4 receptors should be found[130], but which often is not mentioned as region of interest. Otherwise the high accumulation of the radioligand in the cerebellum is controversial to the estimated D_4 distribution in brain, although there is information in the literature on D_4R expressing genes which are also found in this tissue[130]. However, no uptake in striatum was observed which is in accordance to the literature[130,131,133-135].

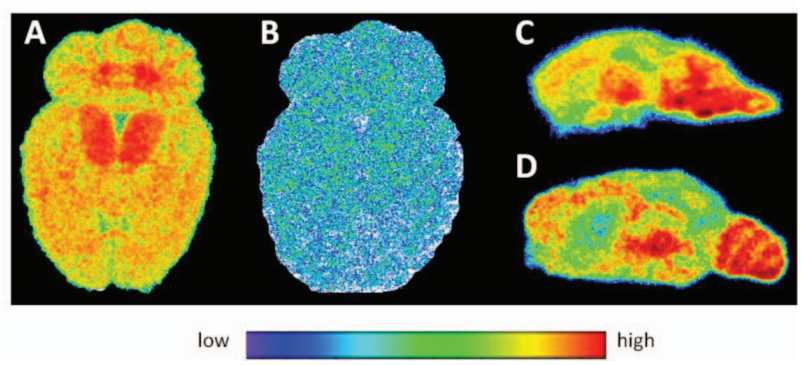

Figure 5.15: *In vitro* autoradiography of a rat brain (A) with 5 nmol/L [^{18}F]**33e** and after blocking with 10 µM **33e** (B) to show low non-specific binding. Sagittal slices of *in vitro* (C) and *ex vivo* (D) autoradiography studies of mouse brain with [^{18}F]**33e** are displayed for comparison.

In order to exclude that different binding *in vitro* and *in vivo* might be due to differences of species, *in vitro* autoradiography of NMRI mouse brain slices was also performed. Even though a slightly higher binding in cortex was recognized here, the contrast of radioligand accumulation was worse in comparison to the *ex vivo* autoradiograms. Possible reasons for that finding could be a metabolisation by a unforeseen significance of enzymes *in vitro* or by the used incubation buffer; however, both explanations were falsified by experiment. Thus, it was assumed, that a notable binding in intracellular compounds which are only accessibly *in vitro* may result in a higher non-specific background. For a comparison with an autoradiography of the rare

literature showing results with D_4 ligands, sagittal mouse brain slices were chosen and the *ex vivo* binding distribution compared with rat brain slices of the ^{131}I-labelled ligand FAUC113 (K_i = 2.6 nM)[244]. In both studies similar binding was found in cortex and thalamus, which affirms binding in the limbic system. Also cerebellar binding was in accordance with the previous work.

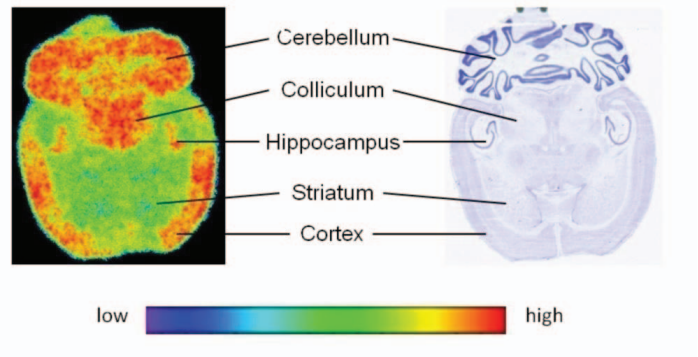

Figure 5.16: *Ex vivo* autoradiography (left) of horizontal planes of a mouse brain 15 min after injection of [^{18}F]**33e** and the corresponding histological image stained with cresyl violet (right).

5.4.3 Biodistribution and *in vivo* stability

For preliminary biodistribution studies of [^{18}F]**33e** each three NMRI mice were sacrificed at 5, 10, 15 and 30 min p.i.. Due to the low lipophilicity of the ligand there was a rapid accumulation in the kidney. As expected the hepatic uptake was lower. A high penetration of the blood brain barrier was observed in spite of the rather low log *P* of 1.8 with a brain uptake of about 5 % ID/g tissue after 5 min. After 30 min there was still more than 1 % ID/g in the brain. The data show a continuous decrease (Fig. 5.17) thus no compartment-trapping seems to be responsible for the high uptake.

In vivo stability of the radioligand [^{18}F]**33e** was checked by thin layer chromatography (TLC) on aluminium oxid layers. For thos, the whole blood activity and plasma activity as well as plasma activity and activity of plasma extracts was compared to ensure that all potential metabolites are analyzed.

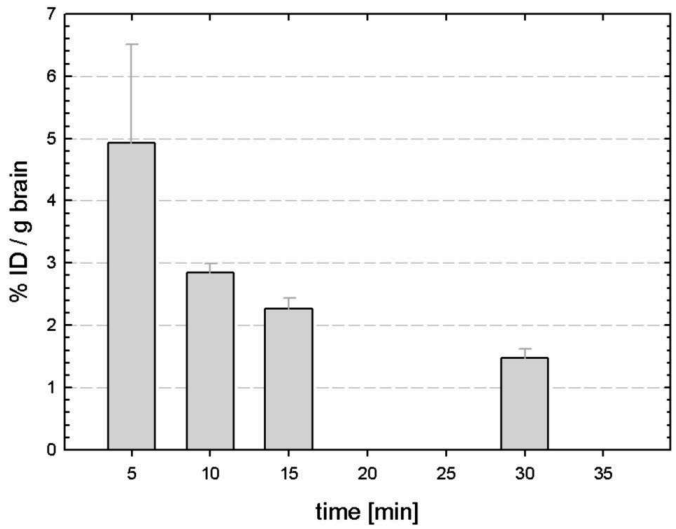

Figure 5.17: Time dependence of uptake of [^{18}F]**33e** as %ID/g in the brain of NMRI mice.

There was a loss of about 27 % of radioactivity in the plasma after centrifugation of the blood. This was lower than the hematocrit of mouse (35 - 49 %) why it is assumed that all losses were due to adsorbtion and that no binding to blood cells occurred. Similarly, there was no significant loss of radioactivity after deproteination of the plasma (< 2 %), so that all generated metabolites are analyzed. All observed metabolites did not move on the silica gel plates with the chosen solvent (ethyl acetate/methanol/diethyl amine 96:2:2), thus they were all hydrophilic. Furthermore, it is suggested, that defluorination did not take place to a considerable extend because of the very low bone uptake (< 2.7 %ID/g tissue) at all p.i. time points (Tab. 5.6). An increasing defluorination would lead to a rise of [^{18}F]fluoride accumulating bones, which is not observed. The half life of *in vivo* stability in blood of 38-39 °C (NMRI mouse) was about 5 min indicating fast metabolisation according to the fast metabolism of mice.

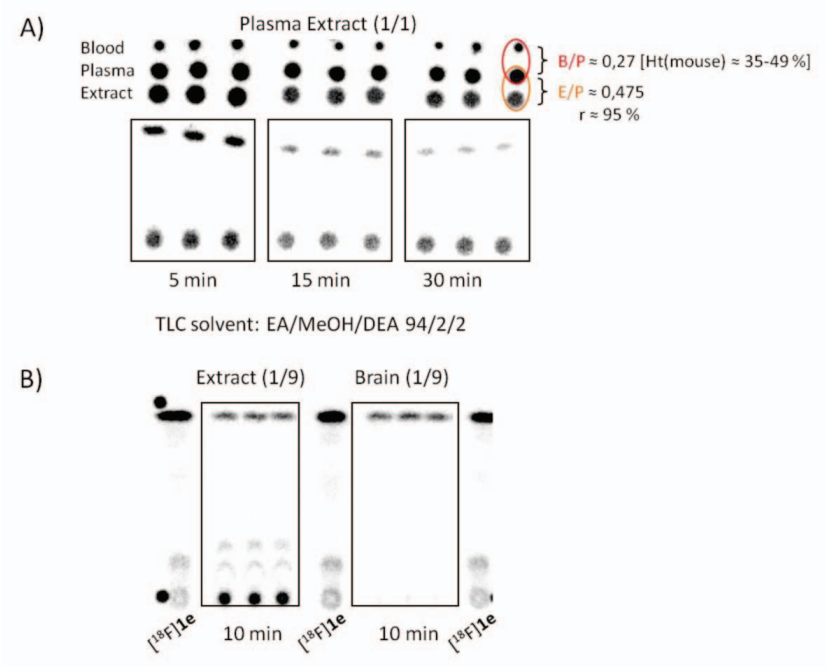

Figure 5.18: *In vivo* stability of [^{18}F]**33e** in NMRI mice determined by radio-TLC. In the plasma ectract (A) beside the ligand a single spot at the base line can be observed over the whole time which can be due to metabolites or "artifacts" or both.
To ensure that all active products are captured, recovery (r) of blood, plasma and plasma extract is determined. *In vivo* stability in plasma extract at a higher dilution with buffer and acetonitrile is compared to that in the brain (B). In the brain nearly no metabolites can be observed. B = blood; P = plasma; E = plasma extract; Ht = hematocrit; r = recovery; TLC = thin layer chromatography; EA = ethylacetate; DEA = diethylamine

Tests for metabolization in the brain were performed after 10 min in the same way but using a higher dilution during the extraction steps feasible by using higher amounts of radioactivity. There was only found an extremely slight sign of metabolization after 10 min in the mouse brain. Analysing the blood plasma of the same animals and also using a high dilution during extraction led to comparable findings of rapid metabolisation to those before.

Table 5.6: Biodistribution data of [^{18}F]**33e** in NMRI mice (n = 3)

	% ID / g tissue			
	5 min	***10 min***	***15 min***	***30 min***
Brain	4.93 ± 1.58	2.85 ± 0.14	2.27 ± 0.17	1.47 ± 0.15
Heart	1.80 ± 1.00	0.52 ± 0.04	0.58 ± 0.31	1.13 ± 0.35
Lung	12.99 ± 2.53	4.84 ± 1.21	4.79 ± 0.68	2.68 ± 0.80
Liver	4.13 ± 1.76	6.78 ± 0.28	5.67 ± 0.30	7.79 ± 0.39
Kidney	8.23 ± 2.85	5.86 ± 0.62	4.67 ± 0.40	6.03 ± 0.61
Spleen	4.42 ± 1.62	3.60 ± 0.15	3.19 ± 0.20	3.13 ± 0.18
Intestine	2.16 ± 0.70	2.68 ± 0.19	2.51 ± 0.39	4.47 ± 0.20
Pancreas	8.36 ± 3.55	11.10 ± 0.37	6.88 ± 1.44	7.43 ± 0.56
Bone	2.03 ± 0.51	2.54 ± 0.33	2.70 ± 0.89	0.93 ± 1.05
Blood final	1.62 ± 0.14	1.29 ± 0.16	1.23 ± 0.33	0.53 ± 0.21

Therefore, it is expected that the obtained *in vivo* stability curve of [^{18}F]**33e** (Fig. 5.19) does only contain a small amount of "pseudo-metabolites" (artifacts) which may occur by retaining of the radioligand by remaining dried proteins.

It can be assumed that the different metabolization rate indicated were due to a degeneration of the ligand on thin layer plates, which only occurs under n.c.a. conditions and which is rapid on silica but moderate on alox plates.

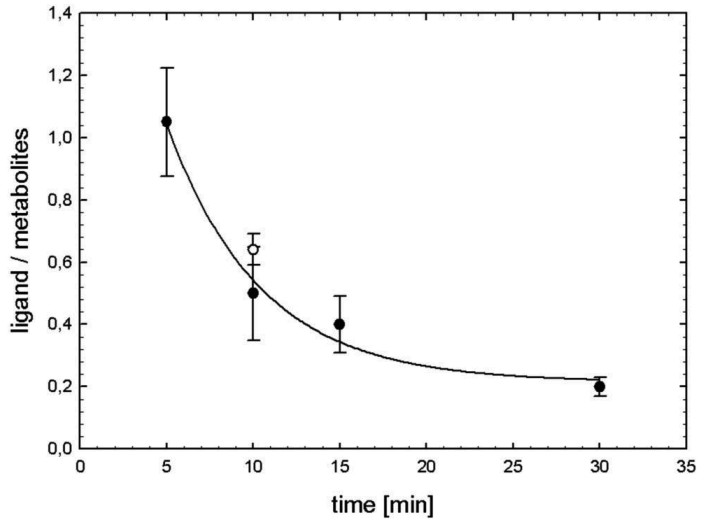

Figure 5.19: *In vivo* stability of [^{18}F]**33e** in blood plasma of NMRI mice measured by radio-TLC. The open circle point shows the result of the experiment with a higher dilution of analysed plasma extract from which was known that all measured activity except from the radioligand-spot were true metabolites and no artifacts.

5.5 Interim summary

The reductive amination reaction for the coupling of ^{18}F-labelled aldehydes with secondary amines proved very useful in radiochemistry also in this study here. Since this reaction tolerates water and requires relatively mild reaction conditions like 60-110 °C, a weak acid and mild reduction agents, the reproducibility of this method is high also with n.c.a. radiochemistry. Furthermore, the toleration of a lot of different solvents offers the possibility of performing a two step synthesis without interim separation. From all four examined derivatives here, only the fluoronicotine aldehyde [^{18}F]**34e** appeared a little

problematic due to its rapid decomposition during the first labelling step.

The alternative labelling concept by a direct nucleophilic substitution of phenyl-piperazinebenzodioxine precursors was possible but resulted in lower radiochemical yields for all derivatives tested. With the pyridine derivative [^{18}F]**33e** a direct labelling of corresponding precursors with other leaving groups (*e.g.* the nitro group) appears suitable offering the radiosynthesis by a single step reaction.

When plotting the non-specific binding on rat brain slices of all derivatives against its lipophilicity, an almost linear relation is recognized. The original ligand [^{18}F]**33a**, with a calculated lipophilicity similar to that of [^{18}F]FAUC 316, shows also a very high non-specific binding. The influence and binding behaviour to lipid membranes is therefore estimated as similar (cp. 2.4). In contrast, the two less lipophilic derivatives [^{18}F]**33d** and [^{18}F]**33e** with less non-specific binding appear suitable for *in vivo* imaging methods. Especially [^{18}F]**33e** which shows a good affinity and selectivity and a non-specific binding of only 7 %, appears as excellent candidate for D_4 receptor imaging. Its high brain uptake, adequate metabolisation (almost no metabolites in brain) and high-contrast brain distribution in the mouse model underline this assumption and encourage further preclinical examination.

6. Experimental

6.1 Materials, chromatographic and spectrometric procedures

All reagents and anhydrous solvents were purchased from Aldrich (Steinheim, Germany) or Fluka (Buchs, Switzerland) and used without further purification. Other compounds were synthesized according to literature methods.

Sep-Pak C-18 plus-cartridges were purchased from Waters (Eschborn, Germany), EN cartridges and Li-Chrolut glass columns (65 x 10 mm) from Merck (Darmstadt, Germany). Thin layer chromatography (TLC) was run on precoated plates of silica gel 60F254 (Merck) or Alumina N (Macherey-Nagel). The compounds were detected at 256 nm. HPLC was performed on the following system from Dionex (Idstein, Germany): an Ultimate 3000 LPG-3400A HPLC pump, an Ultimate 3000 VWD-3100 UV/VIS-detector (272 nm), a UCI-50 chromatography interface, an injection valve P/N 8215. Reversed-phase HPLC was carried out using a Gemini 5 mm C18 110A column, for analytical separations with a dimension of 250mm × 4.6mm (flow 1 mL/min) and for semi-preparative applications 250mm × 10mm (flow 5 mL/min) from Phenomenex (Aschaffenburg, Germany). Radio TLC chromatograms were detected on a Packard Instant Imager. ^{1}H, ^{13}C and ^{19}F NMR spectra were recorded on a Bruker DPX Avance 200 spectrometer with samples dissolved in $CDCl_3$ or d_6-DMSO. All shifts are given in δ ppm using the signals of the appropriate solvent as a reference. Mass spectra were obtained from a Finnigan Automass Multi mass spectrometer with an electron beam energy of 70 eV. High resolution electron spray mass spectra were recorded on an LTQ FT Ultra (Thermo Fischer). Melting points are uncorrected and were determined on a Mettler FP-61 apparatus in open capillaries.

6.2 Synthesis of [^{18}F]FAUC 316

6.2.1 Syntheses of precursor and standard compounds

6.2.1.1 Indole syntheses by intramolecular coupling

4-Amino-3-iodobenzonitrile (2)

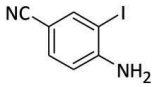

In a 1-L one-neck flask 16.05 g (63.3 mmol) of I_2 and 19.74 g (63.3 mmol) of silver sulphate were dissolved in 500 mL of absolute ethanol and 7.47 g (63.3 mmol) of 4-aminobenzo-nitrile was added. The flask was covered with aluminium foil and the solution was stirred for 20 h. The beige suspension was filtered from silver salts and the solution was evaporated to dryness in vacuo. The crude product was recrystallized from chloroform, washed twice with 100 mL of 5 % NaOH and once with 150 mL of water and dried over sodium sulphate. After evaporation the obtained slight red solid (9.69 g, 40 mmol, 63 %) could be used in the further reaction step without additional purification. Mp 109-110 °C (Lit.: 110-112 °C). TLC ($CHCl_3$): R_f = 0.4. ^{1}H NMR (200.13 MHz, DMSO-d_6): δ 4.67 (br, 2H), 6.73 (d, *J* = 8.4 Hz, 1H), 7.41 (dd, ^3J = 8.4 Hz, ^4J = 1.8 Hz, 1H), 7.91 (d, ^4J = 1.8 Hz 1H) ppm. FT-MS (ESI): *m/z* 244.81 $[M+H]^+$.

General procedure of Pd-catalysed indole synthesis (3, 4)

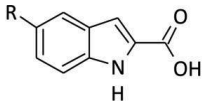

3: R = H
4: R = CN

In a well baked out flask with reflux condenser 4.4 g (40 mmol) of 1,4-diazabicyclo[2.2.2]octane, 1.32 g (15 mmol) of pyruvic acid and 10 mmol of the corresponding *ortho*-iodoaniline were dissolved under a stream of argon in 40 mL of dry DMF. The mixture was further degassed by the stream of argon through the solution by a hollow needle for 10 min and, after the addition of 115 mg (0.5 mmol, 5 mol%) of tris(dibenzylideneacetone)dipalladium(0), for another 15 min. The solution was heated for 2 h at 105 °C to complete the reaction and than cooled to room temperature. The mixture was concentrated to about 6 mL and 150 mL of ethyl acetate and 50 mL of 2 N HCl solution was added. The ethyl acetate phase was washed with another 50 mL of 2 N HCl solution, dried over sodium sulphate and 0.35 g of activated carbon (Darco G60) was

added for decolouring and then the suspension was stirred for 20 min. The mixture was filtered and concentrated to ~20 mL, 20 mL of *n*-heptane was added slowly obtaining a slurry. After filtration the crude product was dried in vacuo and purified by flash chromatography (chloroform/methanol 5:1).

***1H*-Indole-2-carboxylic acid (3)** was obtained from 2-iodoaniline (2.19 g, 10 mmol) as a slight yellow solid (1.0 g, 6 mmol, 60 %). TLC (chloroform/methanol 5:1): R_f = 0.62. ^{1}H NMR (200.13 MHz, $CDCL_3$) δ 7.07 (dd, *J* = 7.51 Hz, J = 8.0 Hz, 2H), 7.25 (t, *J* = 7.58 Hz, 1H), 7.47 (d, *J* = 7.58 Hz, 1H), 7.66 (d, *J* = 7.95 Hz, 1 H), 7.97 (s, 1H), 11.75 (s, 1H) ppm. ^{13}C NMR (50.33 MHz, $CDCL_3$) δ 107.96, 113.34, 120.76, 122.76, 125.02, 127.78, 129.69, 138.06, 163.51 ppm. FT-MS (ESI): 310.15 *m/z* (100) $[M+H]^+$.

5-Cyano-*1H*-indole-2-carboxylic acid (4) was obtained from 4-amino-3-iodobenzonitrile (**2**) (2.44 g, 10 mmol) as a beige solid (500 mg, 2.7 mmol, 27 %). Mp. 331 °C (degradation). TLC (chloroform/methanol 2:1): R_f = 0.30. ^{1}H NMR (200.13 MHz, $CDCL_3$) 7.23 (s, 1H), 7.59 (d, 2H), 8.25 (s, 1H), 12.37 (s, 1H), 13.73 (br, 1H) δ ppm. FT-MS (ESI): 186.85 *m/z* (100) $[M+H]^+$

2-((4-(4-Fluorophenyl)piperazine-1-yl)methyl)-*1H*-indole (29).

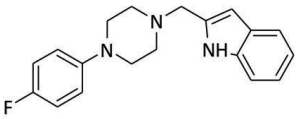

Method A: Under an atmosphere of argon 0.74 mmol of the corresponding amide was dissolved in 25 mL of dry THF and cooled at 0 °C. 0.74 mmol of lithium aluminium hydride (1 M in diethyl ether) was added dropwise and the reaction mixture was stirred for 4 h. After an addition of 40 mL of water the solution was extracted three times with 50 mL of chloroform, the organic phase was dried over sodium sulphate, evaporated in vacuo and purified by flash chromatography to obtain 117 mg (0.36 mmol, 50 %) of the product.

Method B: Under an atmosphere of argon 1 mmol of borane solution (1 M in THF) was cooled at 0 °C. 0.5 mmol of the corresponding amide was dissolved in dry THF and added all at once. The ice bath was removed and the solution was refluxed over night. After a second addition of 1 mmol of borane solution the mixture was stirred for a further night, then quenched with 10 mL of acetic acid and extracted with chloroform. The organic

phase was dried over sodium sulphate, evaporated in vacuo and purified by flash chromatography to obtain 63 mg (0.2 mmol, 41 %) of the product.

TLC (chloroform/methanol 20:1): R_f = 0.66. ^{1}H NMR (200.13 MHz, $CDCL_3$) δ 2.74 (m, 4H), 3.19 (m, 4H), 3.86 (s, 1H), 6.49 (s, 1H), 6.88 (m, 4H), 7.21-7.78 (m, 4H) ppm. FT-MS (ESI): 310.12 *m/z* (100) $[M+H]^+$.

6.2.1.2 Cyanoindole syntheses by intramolecular reductive amination

Ethyl 3-(5-cyano-2-nitrophenyl)-2-oxopropanoate or potassium (E)-1-(5-cyano-2-nitrophenyl)-3-ethoxy-3-oxoprop-1-en-2-olate (6)

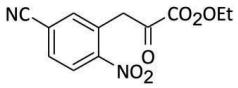

In a 250-mL two-neck flask with silicone septum 5 g (30.8 mmol) of 3-methyl-4-nitrobenzonitrile and 8 mL (8.64 g; 60 mmol) of diethyl oxalate were dissolved in 85 mL of dry ethanol, slightly cooled and 12.3 mL (30.9 mmol) of cooled (~ 4 °C) potassium ethanolate solution (24 wt% in ethanol) were added. After stirring for 20 min the solution was moderately heated to 40 °C and slowly stirred for 20 h. To quench the reaction and redissolve the red precipitate 150 mL of water and 100 mL of HCl solution (14 %) were added and the solution stored at 4 °C for crystallisation. The precipitate was filtrated, dissolved with chloroform, dried over sodium sulphate and evaporated to dryness. The crude product was purified by flash chromatography (n-hexane/ethyl acetate 2:1) to obtain 3.2 g (12.2 mmol, 40 %) of a sticky solid which is yellow in acid and red in base media. Mp. 98 °C. TLC (chloroform): R_f = 0.36. ^{1}H NMR (200.13 MHz, DMSO-d_6) δ 1.32 (td, *J* = 7.11 Hz, *J* = 1.81 Hz, 3H), 4.32 (qd, *J* = 7.12 Hz, *J* = 2.56 Hz, 2H), 4.66 (s, 2H), 7.95-8.33 (m, 3H) ppm. FT-MS (ESI): 263.03 *m/z* (30) $[M+H]^+$, 302.75 *m/z* (100) $[M+K]^+$ (poorly ionisable under ESI conditions).

Ethyl 5-cyano-1H-indole-2-carboxylate (5)

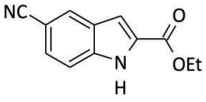

Under an atmosphere of argon 100 mg (0.38 mmol) of ethyl 3-(5-cyano-2-nitrophenyl)-2-oxopropanoate and 20 mg (0.19 mmol) of palladium on carbon were dissolved in 5 mL of dry methanol and 13.92 mg (0.114 mmol) of decaborane were added in portions. The reaction mixture was heated at 40 °C for 1.5 h until the starting material has disappeared completely. The reaction mixture was quenched with 50 mL of water, extracted with diethyl ether, washed with brine and dried over sodium sulphate. After evaporation in vacuo the crude product was purified by flash chromatography (n-hexane/ethyl acetate 2:1), and 57 mg (0.27 mmol, 70 %) of product was obtained as a with solid. TLC (chloroform/methanol 25:1): R_f = 0.66. ^{1}H NMR (200.13 MHz, DMSO-d_6) δ 1.36 (t, *J* = 7.11 Hz, 3H), 4.38 (q, *J* = 7.11 Hz, 2H), 7.27 (d, *J* = 2.0 Hz, 1H), 7.60 (s, 2H), 8.25 (s, 1H), 12.46 (s, 1H) ppm. ^{13}C NMR (50.32 MHz, DMSO-d_6) δ 15.06, 61.78, 103.35, 109.17, 114.80, 120.96, 127.38, 129.17, 130.68, 139.57, 161.63 ppm. FT-MS (ESI): 214.84 *m/z* (35) $[M+H]^+$, 429.27 *m/z* (100) $[2M+H]^+$ (poorly ionisable under ESI conditions).

2-(Hydroxymethyl)-1H-indole-5-carbonitrile (7)

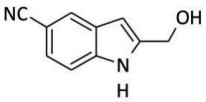

Under an atmosphere of argon a solution of 4.2 mL (4.2 mmol) of lithium aluminium hydride (1 M in THF) and 10 mL of dry diethyl ether were cooled to about -60 °C in a carbon dioxide / acetone bath. Subsequently 660 mg (3.1 mmol) of ethyl 5-cyano-1H-indole-2-carboxylate suspended in 30 mL of dry diethyl ether were added and the suspension was warmed to room temperature under stirring over night. The reaction was quenched with 10 mL of water, extracted twice with diethyl ether, washed with brine and dried over sodium sulphate. After evaporation in vacuo the crude product was purified by flash chromatography (n-hexane/ethyl acetate 2:1) to obtain 257 mg (1.5 mmol, 48 %) of a brownish crystalline product. TLC (chloroform/methanol 25:1): R_f = 0.66. ^{1}H NMR (200.13 MHz, DMSO-d_6) δ 2.06 (s, 2H), 6.08 (s, br, 1H), 6.68 (m, 1H), 7.32 (m, 1H), 7.47 (m, *J* = 4.96 Hz, 2H), 9.58 (s, 1H) ppm. FT-MS (ESI): 173.01 *m/z* (20) $[M+H]^+$, 194.90 *m/z* (30) $[M+Na]^+$, 345.18 *m/z* (20) $[2M+H]^+$, 367.18 *m/z* (100) $[2M+Na]^+$.

2-Formyl-1H-indole-5-carbonitrile (10)

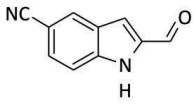

Method A: In a one-neck flask 230 mg (1.313 mmol) of 2-(hydroxymethyl)-1H-indole-5-carbonitrile (**7**) were dissolved in 5 mL of dry tetrahydrofurane and 656 mg (1.44 mmol, 1.1 eq) of Dess-Martin periodinane were added in portions. The suspension was stirred at room temperature for 45 min and quenched with 15 mL of a mixture of sodium thiosulphate solution and sodium bicarbonate solution (1:1). The solution was extracted with ethyl acetate, washed with brine and dried over sodium sulphate to obtain 220 mg (1.3 mmol, 99 %) of a slightly yellow product.

Method B: 0.43 mL (1.38 µmol) sodium bis(2-methoxyethoxy)aluminum hydride solution (65w% in toluol) in 0.3 mL of dry tetrahydrofurane was cooled at -10 °C and 122 µL (1.5 µmol) of pyrrolidine in 0.9 mL of dry tetrahydrofurane were added. The solution was warmed to room temperature, stirred for 1 h and 21.5 mg (0.2 mmol) of potasasium tert-butoxid were added. Under an atmosphere of argon the whole solution was added dropwise to 150 mg (0.7 mmol) of ethyl 5-cyano-1H-indole-2-carboxylate (**5**) dissolved in 0.8 mL of dry tetrahydrofurane. After stirring for 10 min 5 mL of 1 N HCl solution was added, the mixture was extracted with ethyl acetate, washed with brine, dried over sodium sulphate and evaporated in vacuo. The crude product was purified by flash chromatography (n-hexane/ethyl acetate 2:1) to obtain 30 mg (25 %) of product.

Mp. 220 °C (decomposition). TLC (dichloromethane/methanol 95:5): R_f = 0.73. ^{1}H NMR (200.13 MHz, $CDCL_3$-d_6) δ 7.46-7.80 (m, 3H), 8.38 (s, 1H), 19.20 (s, 1H), 12.53 (s, br, 1H) ppm. ^{13}C NMR (50.32 MHz, $CDCL_3$) δ 103.25, 114.75, 114.78, 120.43, 126.85, 126.90, 128.51, 129.88, 138.52, 184.11 ppm. FT-MS (ESI): no ionisation with ESI possible.

2-((4-(4-Fluorophenyl)piperazine-1-yl)methyl)-1H-indole-5-carbonitrile, FAUC 316 (1)

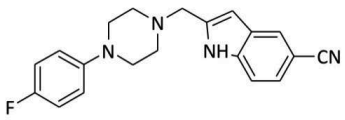

Method A: Under an atmosphere of argon 0.5 mL (0.5 mmol) of lithium aluminium hydride (1 M in THF) were added to 91 mg (0.5 mmol) of 1-(4-fluorophenyl)piperazine in 10 mL of dry tetrahydrofurane and stirred at 60 °C for

30 min. Subsequently 171 mg (0.8 mml) of ethyl 5-cyano-1H-indole-2-carboxylate (**5**) in 4 mL of dry tetrahydrofurane were added dropwise over a period of about 20 min. The solution was stirred for 20 min and quenched with saturated sodium bicarbonate solution. After extracted with dichloromethane and washed with brine the organic phases were dried over sodium sulphate, evaporated in vacuo and purified via flash chromatography (chloroform/methanol 20:1) to obtain 18 mg (53.9 µmol, 10 %) of **1**.

Method B: 200 mg (1.18 mmol) of 2-formyl-1H-indole-5-carbonitrile (**10**), 318 mg (1.76 mmol) of 1-(4-fluorophenyl)piperazine, 1 g (4.72 mmol) of sodium cyanoborohydride and 280 µL (4.72 mmol) of acetic acid were dissolved in 12 mL of methanol and heated at 60 °C for 20 h. After cooling to room temperature the solution was extracted with ethyl acetate, washed with brine and dried over sodium sulphate. Upon evaporation in vacuo the product was purified by flash chromatography (n-hexane/ethyl acetate 2:1) to obtain 190 mg (0.57 mmol, 49 %) of **1**.

Mp. 200 °C (decomposition). TLC (dichloromethane/methanol 95:5): R_f = 0.73. ^{1}H NMR (200.13 MHz, DMSO-d_6) δ 2.58 (t, br, *J* = 4.16 Hz, *J* = 5.1 Hz, 4H), 3.12 (t, br, *J* = 5.22 Hz, *J* = 4.12 Hz, 4H), 3.73 (s, 2H), 6.50 (s, 1H), 6.95-7.05 (m, 4H), 7.40 (dd, *J* = 8.42, *J* = 1.56, 1H), 7.51 (d, *J* = 8.46, 1H), 8.01 (s, 1H), 11.67 (s, 1H) ppm. ^{13}C NMR (50.32 MHz, DMSO-d_6) δ 49.42, 53.09, 55.25, 60.22, 101.25, 102.10, 112.73, 115.48, 115.91, 117.49, 117.64, 121.32, 123.96, 125.50, 128.14, 138.64, 139.38, 148.37, 170.78 ppm. ^{19}F NMR (188.28 MHz, DMSO-d_6) δ -125.61 ppm. FT-MS (ESI): 335.11 *m/z* (100) $[M+H]^+$.

1-Benzyl-2-formyl-1H-indole-5-carbonitrile (11)

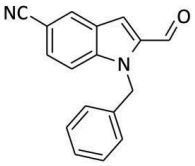

Under an atmosphere of argon 330 mg (1.94 mmol) of 2-formyl-1H-indole-5-carbonitrile (**5**) was suspended in 12 mL of anhydrous tetrahydrofuran (THF) and 400 mg (2.91 mmol, 1.5 eq) of anhydrous potassium carbonate was added. After addition of 0.46 mL (660 mg, 3.88 mmol) of benzylbromide the orange reaction mixture was refluxed and stirred over night. Upon cooling the reaction solution was quenched with 40 mL of water and the solution was extracted with ethyl acetate, washed with water and saturated sodium chloride solution and dried over sodium sulphate. After evaporation of

the solvent in vacuo the residue was purified by flash chromatography (n-hexan/ethyl acetat 2:1) to obtain 360 mg (1.4 mmol, 72 %) of **11** as a slight yellow solid. TLC (n-hexane/ethyl acetate 2:1): R_f = 0.57. ^{1}H NMR (200.13 MHz, DMSO-d_6) δ 5.91 (s, 2H), 7.10 (dd, *J* = 7.2 Hz, *J* = 1.54 Hz, 2H), 7.3 (m, 3H), 7.73 (s, 1H), 7.74 (dd, *J* = 8.6 Hz, *J* = 1.58 Hz, 1H), 7.87 (d, *J* = 8.8 Hz, 1H), 8.45 (s, 1H), 10.04 (s, 1H) ppm. FT-MS (ESI): 260.71 *m/z* (100) $[M+H]^+$.

General preparation of indolealdehydes by reductive amination (12, 13)

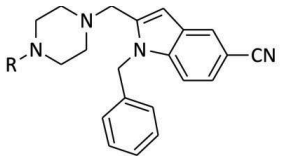

12: R = 4-fluorobenzene
13: R = Boc

The reductive amination of the indolealdehydes **11** was conducted under the same conditions as described for **1** (Method B). 1 equivalent of the indolealdehyde, 1.5 equivalents of 1-(4-fluorophenyl)piperazine or tert-butyl piperazine-1-carboxylate, 4 equivalents of sodium cyanoborohydride and 250 µL (4.2 mmol) of acetic acid were suspended in 10-12 mL of methanol and heated at 60 °C for 3-4 h. The solution was extracted with ethyl acetate, washed with brine and dried over sodium sulphate. After evaporation in vacuo the product was purified via flash chromatography (n-hexane/ethyl acetate 2:1).

1-Benzyl-2-((4-(4-fluorophenyl)piperazin-1-yl)methyl)-1H-indole-5-carbonitrile (12) was obtained from 1-benzyl-2-formyl-*1H*-indole-5-carbonitrile (**11**, 150 mg, 0.577 mmol) as a white, crystalline solid (150 mg, 0.35 mmol, 61 %). Mp. 111 °C. TLC (n-hexane/ethyl acetate 2:1): R_f = 0.61. ^{1}H NMR (200.13 MHz, $CDCL_3$-d_6) δ 2.52 (br, 2H), 2.94 (br, 4H), 3.69 (s, 2H), 5.64 (s, 2H), 6.67 (s, 1H), 6.86-6.93 (m, 2H), 6.99-7.08 (m, 4H), 7.22-7.26 (m, 3H), 7.45 (dd, *J* = 8.55, *J* = 1.54, 1H), 7.55 (d, *J* = 8.58, 1H), 8.10 (s, 1H) ppm. ^{13}C NMR (50.32 MHz, DMSO-d_6) δ 47.11, 49.32, 52.95, 54.26, 101.90, 104.06, 111.80, 115.48, 115.92, 117.50, 117.65, 121.05, 124.55, 125.97, 126.70, 127.37, 127.56, 129.00, 139.63, 139.91, 148.29, 148.34 ppm. ^{19}F NMR (188.28 MHz, DMSO-d_6) δ -125.63 ppm. FT-MS (ESI): 425.66 *m/z* (100) $[M+H]^+$.

Tert-butyl 4-((1-benzyl-5-cyano-1H-indol-2-yl)methyl)piperazine-1-carboxylate (13) was obtained from 1-benzyl-2-formyl-1H-indole-5-carbonitrile (231 mg, 0.89 mmol) as a white, crystalline solid (230 mg, 0.35 mmol, 60 %). Mp. 109 °C TLC (n-hexane/ethyl

acetate 2:1): R_f = 0.43. ^{1}H NMR (200.13 MHz, DMSO-d_6) δ 1.39 (s, 9H), 2.35 (t, br, *J* = 2.0 Hz, 4H), 3.18 (t, br, *J* = 1.85 Hz, 4H), 3.63 (s, 2H), 5.62 (s, 2H), 6.64 (s, 1H), 7.01 (dd, *J* = 7.77 Hz, *J* = 1.84 Hz, 2H), 7.30 (m, 3H), 7.45 (dd, *J* = 8.57 Hz, *J* = 1.61 Hz, 1H), 7.56 (d, *J* = 8.58 Hz, 1H), 8.09 (d, *J* = 1.5 Hz, 1H) ppm. FT-MS (ESI): 431.29 *m/z* (100) $[M+H]^+$.

General procedure of selective Boc-group cleavage (14a, 14)

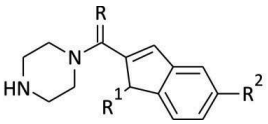

14a: R = O; R^1 = H; R^2 = H
14: R = H2; R^1 = Bn; R^2 = CN

With a hollow needle 30 mL of anhydrous ethyl acetate were treated under a constant stream of HCl gas for 30 min. From the ethyl acetate / HCl solution 15 mL were added under ice bath cooling to 0.5 mmol of the corresponding Boc-protected piperazine derivative and stirred at room temperature for 10 h. Afterwards the solution was extracted twice with 50 mL of water and the combined aqueous phase neutralized with a 1 M potassium hydroxide solution to about pH 8. The aqueous phase was extracted with chloroform and after drying over sodium sulphate evaporated in vacuo. If necessary the product can be recrystalized with ethyl acetate.

(1H-Indol-2-yl)(piperazin-1-yl)methanone (14a) was obtained from tert-butyl 4-(1H-indole-2-carbonyl)piperazine-1-carboxylate (320 mg, 0.97 mmol) as a yellow foam (220 mg, 0.96 mmol, 99 %). TLC (n-hexane/ethyl acetate 2:1): R_f = 0.22. ^{1}H NMR (200.13 MHz, DMSO-d_6) δ 2.76 (br, 4H), 3.69 (br, 4H), 6.77 (d, *J* = 1.45 Hz, 1H), 7.05 (td, *J* = 7.1 Hz, *J* = 0.92 Hz, 1H), 7.19 (td, *J* = 7.6 Hz, *J* = 1.22 Hz, 1H), 7.43 (d, *J* = 7.3 Hz, 1H), 7.61 (d, *J* = 7.62 Hz, 1H), 11.57 (s, 1H) ppm. FT-MS (ESI): 319.98 *m/z* (100) $[M+H]^+$.

1-Benzyl-2-(piperazin-1-ylmethyl)-1H-indole-5-carbonitrile (14) was obtained from tert-butyl 4-((1-benzyl-5-cyano-1H-indol-2-yl)methyl)piperazine-1-carboxylate (230 mg, 0.53 mmol) as a silver, crystaline solid (170 mg, 0.52 mmol, 99 %). Mp. 264 °C (decomposition). TLC (n-hexane/ethyl acetate 2:1): R_f = 0.22. ^{1}H NMR (200.13 MHz, DMSO-d_6) δ 2.53 (m, br, 4H), 2.82 (m, br, 4H), 3.67 (s, 2H), 5.62 (s, 2H), 6.69 (s, 1H), 7.0 (d, *J* = 6.94 Hz, 2H), 7.25-7.35 (m, 3H), 7.46 (dd, *J* = 8.58 Hz, *J* = 1.53 Hz, 1H), 7.58 (d, *J* = 8.58 Hz, 1H), 8.11 (s, 1H) ppm. FT-MS (ESI): 331.26 *m/z* (100) $[M+H]^+$.

6.2.1.3 Synthesis of 4-fluoroanilines

1-(4-Fluorophenyl)-4-methylpiperazine (24)

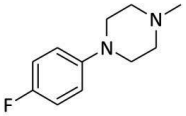

Under an argon atmosphere 0.1 mL (1.6 mmol) of methyliodide were added cautiously to 300 mg (1.6 mmol) of 1-(4-fluorophenyl)piperazine dissolved in 9 mL of dry tetrahydrofuran and 63 mg (1.6 mmol) of sodium hydride (60 % dispersion on mineral oil). The solution was stirred over night at room temperature. 10 mL of water were added, the solution was extracted twice with 30 mL of dichloromethane, washed with water and dried over sodium sulphate. After evaporation in vacuo the crude product was purified by flash chromatography to obtain 162 mg (0.83 mmol, 52 %) of the product as a high viscous oil. ^{1}H NMR (200.13 MHz, $CDCL_3$) δ 2.66 (s, 3H), 3.04 (m, 4H), 3.40 (m, 4H), 6.85-7.05 (m, 4H) ppm. ^{19}F-NMR (188 MHz, $CDCl_3$): δ -122.79 (1F, s). ^{13}C NMR (50.32 MHz, $CDCL_3$-d_6) δ 44.96, 48.92, 54.54, 115.58, 116.03, 118.65, 118.80, 146.91, 146.96, 155.40, 160.17 ppm. FT-MS (ESI): 195.57 *m/z* (100) $[M+H]^+$.

Tert-butyl 4-(4-fluorophenyl)piperazine-1-carboxylate (27)

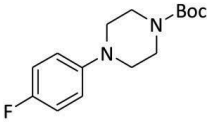

To 300 mg (1.66 mmol) 4-fluorophenylpiperazine suspended in 4 mL of water and 1.5 mL of tetrahydrofurane 405 mg (2 mmol) of di-*tert.*-butyl dicarbonate and 350 mg (3.3 mmol) of sodium carbonate were added and the suspension was stirred at 100 °C for 2 h. 15 mL of water were added and the solution was extracted three times with ethyl acetate, the combined organic layers were washed with brine and dried over sodium sulphate. After evaporation in vacuo the product was recrystallized from n-hexane/ethylacetate to obtain 460 mg (1.65 mmol, 99 %) of **27**.

^{1}H-NMR (200.13 MHz, $CDCl_3$): δ 1.36 (s, 9H), 3.03 (m, 4H), 3.37 (m, 4H), 7.21 (m, 4H) ppm. FT-MS (ESI): 180.43 *m/z* (100) $[M+H]^+$.

1-(4-Fluorophenyl)piperidine (23)

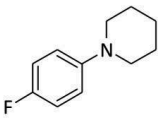

Under an atmosphere of argon 100 mg (0.25 mmol) of 2-dicyclohexylphosphino-2'-(*N*,*N*-dimethylamino)biphenyl (DavePhos), 230 mg (0.25 mmol) of $Pd_2(dba)_3$ and 575 mg (6 mmol) of sodium *tert*.-butoxide were dissolved in 25 mL of shortly heated dry toluene and 1.1 g (5 mmol) of 1-fluoro-4-iodobenzene and 635 mg (7.5 mmol) of piperidine were added. The reaction mixture was heated at 100 °C for 2 h and after cooling to room temperature washed with water. The solution was extracted 5 times with 20 mL of 2N HCl solution and the aquaous phase adjusted to pH 8 with sodium hydroxide subsequently. The solution was extracted with chloroform, dried over sodium sulphate and evaporated in vacuo. The crude product was purified by flash chromatography (n-hexane/ethyl acetate 5:1) to obtain 573 mg (3.2 mmol, 64 %) of crystalline product.

^{1}H-NMR (200.13 MHz, $CDCl_3$): δ 1.61 (m, 2H), 1.79 (m, 4H), 3.11 (t, 4H), 7.0 (d, 4H) ppm. ^{19}F-NMR (188 MHz, $CDCl_3$): δ -125.03 (1F, s)

6.2.1.4 Syntheses of iodonium precursors

1-Bromo-4-acetoxyiodobenzene (15)

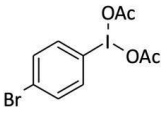

In a 250 mL flask 90 mL of glacial acetic acid were warmed to 40 °C, 2.83 g (10 mmol) of 1-bromo-4-iodobenzene were added and the flask was covered with aluminium foil. Afterwards over a period of 30 min 16.92 g (110 mmol) of sodium borate tetrahydrate were added and the solution was stirred for 23 h. In a rotary evaporator about half of the solvent was evaporated under about 35 mbar. 150 ml of water were added to the suspension and extracted once with 70 mL and twice with 50 mL of chloroform The organic phase was washed with water, dried over sodium sulphate and evaporated in vacuo. The product was recrystalysed with a small amount of acetic acid and methanol to obtain 3.155 mg (7.9 mmol, 79 %) of **15** as white crystals. TLC

(chloroform/methanol 4:1): R_f = 0.71. Mp. 159-161 °C. FT-MS (ESI): 340.78 *m/z* (100) $[M+H]^+$.

Bis(4-bromophenyl)iodonium trifluoromethanesulfonate (16)

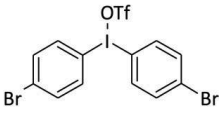

Under an atmosphere of argon 3.07 mg (7.65 mmol) of 1-bromo-4-acetoxyiodobenzene dissolved in 35 mL of dry dichloromethane was cooled to -15 °C and 1.34 mL (15.15 mmol) of trifluoromethanesulfonic acid were added dropwise. After stirring for 1 h the dark solution turned to clear orange, 1.29 mg (8.21 mmol) of bromobenzene were cautiously added and the yellow suspension was stirred at 0 °C for an additional 3 h. The solvent was concentrated in vacuo and diethylether was added. Under cooling at 4 °C the desired product was obtained as slight yellow precipitate (2.8 g, 4.76 mmol, 63 %). FT-MS (ESI): 438.95 *m/z* (100) $[M+H]^+$.

2-Diacetoxyiodotoluene (17)

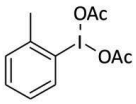

Under an atmosphere of argon and cooling in an ice bath 4.36 g (20 mmol) of 4-iodotoluene was treated with 9.12 g (48 mmol) of peracetic acid (w = 40 %) and stirred at 0 °C for 1.5 h. After removing of the ice bath the solution was cooled in a refrigerator over night. The obtained precipitate was removed, washed with water and dried under vacuo to obtain 6.39 g (19 mmol, 95 %) of crystalline product.

Mp. 147 °C. ^{1}H-NMR (200.13 MHz, DMSO-d_6): δ 1.92 (s, 6H), 2.66 (s, 3H), 7.34 (m, 1H), 7.63 (m, 2H), 8.33 (d, 1H) ppm. FT-MS (ESI): 235.16 *m/z* (100) $[M -2OAc +OH]^+$

2-(Hydroxy[tosyloxy])iodotoluene (18)

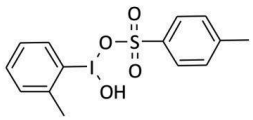

5.8 g (17.2 mmol) of 2-diacetoxyiodotoluene dissolved in 7 ml of hot acetonitrile and treated with 3.6 g (18.9 mmol) of *p*-toluenesulfonic acid dissolved in 3 ml of hot acetonitrile. The yellow reaction mixture was refluxed for 0.5 h and cooled

to -20 °C over night. The yellow precipitate was filtered and dried in vacuo to obtain 4.63 g (11.4 mmol, 66 %) of **18**. Mp.: 138-141 °C. ^{1}H-NMR (200.13 MHz, $CDCl_3$): 2.36 (s, 3H), 2.65 (s, 3H), 6.04 (br, 1H), 7.13 (m, J = 7.82 Hz, 3H), 7.30 (m, J = 7.62 Hz, J = 6.42 Hz, 2H), 7.57 (d, J = 8.1 Hz, 2H), 8.24 (d, J = 8.36 Hz, 1H) ppm. FT-MS (ESI): 235.18 *m/z* (100) $[M - OTs]^+$

1-Iodo-4-(hydroxy[tosyloxy])iodotoluene (19)

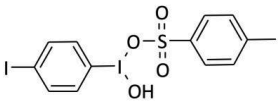

5.47 g (14 mmol) 2-(Hydroxy([tosyloxy])iodotoluene and 4.618 g (14 mmol) 1,4-diiodobenzene were dissolved in 35 ml of dichloromethane and stirred at room temperature. The precipitated product was separated from the solution by filtration several times. The precipitate was washed with dichlorometane and recrystallized from acetonitrile/methanol 80:20 (v/v) to obtain 3.27 g (6.3 mmol, 45 %) of **19**.

Mp. 141 °C. ^{1}H-NMR (200.13 MHz, DMSO-d_6): δ 2.31 (s, 3H), 7.23 (d, 2H), 7.49 (d, 2H), 7.98 (m, 4H) ppm. FT-MS (ESI): 346.98 *m/z* (100) $[M\text{-}OTs]^+$.

Bis(4-iodophenyl)iodonium trifluoromethanesulfonate (20)

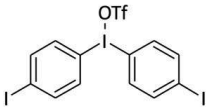

1.04 g (2 mmol) of 1-Iodo-4-(hydroxy[tosyloxy])iodotoluene and 0.408 g (2 mmol) of iodobenzene dissolved in 20 ml of dichloromethane were cooled at -78 °C and treated with 3 g (20 mmol) of trifluoromethanesulfonic acid. The reaction mixture was stirred until the solution reached room temperature and subsequently the solvent was evaporated in vacuo. After an addition of water the solution was extracted with chloroform and the organic phase was treated with diethylether. The obtained white precipitate of **20** (651 mg, 1 mmol, 50 %) was filtered and washed with diethylether.

Mp. 202 °C. FT-MS (ESI): 532.86 *m/z* (100) $[M+H]^+$

6.2.2 Radiosyntheses

Drying of n.c.a [^{18}F]fluoride

N.c.a. [^{18}F]fluoride was produced via the ^{18}O(p,n)^{18}F nuclear reaction by bombardment of an isotopically enriched [^{18}O]water in an Ti-target[245] with 17 MeV protons at the JSW cyclotron BC 1710 (INM-5, Research Center Jülich). The aqueous [^{18}F]fluoride solution (10 – 50 µL, 75 – 375 MBq) was filled into a 5 mL conical vial (Reactivial) containing 1 mL of acetonitrile, 10 mg of Kryptofix 2.2.2, 13 µl of an aqueous 1 M potassium carbonate solution [52]. The solvent was evaporated under a stream of argon at 80 °C and 600 mbar. This azeotropic drying was repeated twice using each time 1 mL of dry acetonitrile, followed by evaporation at 8-15 mbar for 5 min.

General preparation of 4-[^{18}F]fluorobromobenzene ([^{18}F]21) and 4-[^{18}F]fluoroiodobenzene ([^{18}F]22)

A solution of bis(4-bromophenyl)iodonium triflate (**16**, 17 mg, 30 µmol) or bis(4-iodophenyl)iodonium triflate (**20**, 20 mg, 30 µmol) dissolved in 0.5 mL of anhydrous DMF was added to the vial containing the dried [^{18}F]fluoride at 130 °C. Monitoring of the reaction progress was determined by radio HPLC of about 30 - 50 µL taken at regular time intervals aliquots (Gemini 5 µ RP18 A110, 250 · 4.6 mm, 1 mL/min, isocratic 75:25:0.5 v/v/v CH_3CN/H_2O/TEA) for the determination of radiochemical yields and the optimal reaction time.

In case of [^{18}F]**21** for further reaction steps after 15 min the solution was diluted with 20 mL of water and passed through a Sep Pak C18 cartridge, previously conditioned with 8 mL of ethanol and 8 mL of water. The cartridge was dried in a stream of argon and eluted through an unconditioned Alumina N cartridge with 2 mL of anhydrous toluene in a second reaction vial.

In case of [^{18}F]**22** after 10 min reaction time 100 mg of Celite 503 suspended in 20 mL of water was added to the reaction mixture and the total solid was removed by a Lichrolut cartridge (Merck) with a 10 µm PTFE strainer. After washing with 1 mL of water the nearly clear solution was passed through a Sep Pak C18 cartridge, conditioned with 8 mL of ethanol and 8 mL of water, previously washed with 5 mL of water dried for 5 min in a stream of argon. Subsequently the product was eluted through an unconditioned

Alumina N cartridge with 2 mL of anhydrous toluene in a second reaction vial.

General procedure of *N*-arylation *via* Hartwig-Buchwald cross-coupling

Large reaction batch: 5.5 µmol of the palladium catalyst ($Pd_2(dba)_3$ or Palladium(π-cinnamyl) chloride dimmer or $PdOAc_2$), 11 µmol of the biaryl phosphine ligand (2-dicyclohexylphosphino-2'-(*N*,*N*-dimethylamino)biphenyl (DavePhos), 2-(dicyclohexyl-phosphino)3,6-dimethoxy-2',4',6'-triisopropyl-1,1'-biphenyl (BrettPhos) or 2-dicyclohexyl-phosphino-2',6'-diisopropoxybiphenyl (RuPhos) or 2-(dicyclohexylphosphino)3,6-dimethoxy-2',4',6'-triisopropyl-1,1'-biphenyl (BrettPhos)), 100 µmol of the base (NaO*t*Bu or K_2CO_3 or K_3PO_4) and 50 µmol of the amine compound were exposed under argon in a reaction vial. Thereafter, 4-[^{18}F]fluoroiodobenzene ([^{18}F]**22**) was added in 2 mL of toluene or 1,4-dioxane from the reaction step before directly by elution from the cartridge into the vial, and the reaction mixture was heated at 100 °C. When the reaction was conducted in DMF the previous separation step was omitted. Reaction progress was mainly monitored by radio-HPLC (Gemini 5 µ RP18 A110, 250 × 4.6 mm, 1 mL/min, isocratic 75:25:0.5 v/v/v CH_3CN/H_2O/TEA) from aliquots of about 30-50 µL diluted ten fold with the elution solvent and typically containing of about 37 kBq of activity were injected.

Prepurification of 4-[^{18}F]fluorophenylpiperazine ([^{18}F]28)

Method A: Liquid-liquid extraction of 4-[^{18}F]fluorophenylpiperazine ([^{18}F]**28**). The reaction mixture was extracted twice with 2 mL of hydrochloric acid (2 M) and the aqueous phases were treated with 4 mL of a sodium hydroxide solution (2 M). The solution was afterwards passed through a Sep Pak C18 cartridge, conditioned with 8 mL of ethanol and 8 mL of water, and dried for 2 min in a stream of argon. The product was then eluted with 1-2 mL of anhydrous DMSO or acetonitrile.

Method B: Solid-liquid extraction of 4-[^{18}F]fluorophenylpiperazine ([^{18}F]**28**). The reaction mixture was diluted with 5 mL of methanol and passed through a Strata-X-CW weak cation exchanger cartridge, conditioned with 10 mL of methanol and 10 mL of water. The cartridge was washed with 5 mL of an ammonium acetate buffer (pH 6.3) and 5 mL of methanol. The product was eluted with formic acid (2 %) in 1-2 mL of a mixture of acetonitrile and methanol 80:20 (v/v) or DMSO.

General preparation of reductive amination reaction ([^{18}F]1, [^{18}F]29)

Sodium cyanoborohydride (4 mg, 64 µmol) in 50 µL of DMSO and 5.8 mg (40 µmol) of *1H*-indole-2-carbaldehyde or 6.8 mg (40 µmol) of 2-formyl-1*H*-indole-5-carbonitrile (**10**) in 50 µL of DMSO and 40 µL of acetic acid were added to the reaction vial containing the eluted 4-[^{18}F]fluorophenylpiperazine ([^{18}F]**28**) in DMSO. For determination of reaction progress the aliquots were analysed by radio HPLC using different systems: (A) Phenomenex Luna 5 µm C18(2) 100 Å 250×4 mm, 1 mL/min, isocratic 60:40:0.03 v/v/v CH_3CN/H_2O/TEA pH 9, (B) Phenomenex Gemini 5 µm C18 100 Å 250×4.6 mm, 1 mL/min, isocratic 60:40:0.03 v/v/v CH_3CN/H_2O/TEA pH 9, (C) Phenomenex Luna 5 µm PFP(2) 100 Å 250×4.6 mm, 1 mL/min, isocratic 50:50:0.01 v/v/v CH_3CN/H_2O/TEA pH 7.8. After addition of 20 mL of water the solution was passed through a Sep Pak C18 cartridge followed by washing with 5 mL water and drying with air. Then the cartridge was eluted with 1 mL of acetonitrile and the eluate injected on a semi-preparative HPLC system (Phenomenex Luna 5 µm PFP(2) 100 Å 250×10 mm, 4 mL/min, isocratic 50:50:0.01 v/v/v CH_3CN/H_2O/TEA pH 7.8.). The collected fraction was diluted with 15 mL of water, passed through a SepPak C18 cartridge, which was then washed with water (5 mL) and dried in a stream of argon. The cartridge was eluted with 4 mL of diethylether, the solvent was evaporated in vacuo (800 up to 330 mbar) and the product was redissolved in 100-300 µL of ethanol.

6.3 Synthesis of benzodioxine derivatives

6.3.1 Syntheses of precursor- and standard compounds

1-(1,4-Benzodioxine-6-yl)piperazine (30)

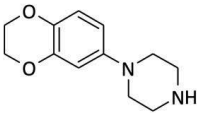

Under an atmosphere of dry argon a mixture of 1.27 g (8.4 mmol) of 6-amino-1,4-benzodioxine and 1.5 g (8.4 mmol) of bis(2-chloroethyl)amine hydrochloride in 3 mL of dry ethylene glycol was heated at 150 °C over night. After cooling to room temperature methanol was added to the mixture to precipitate a white crystalline solid. This was treated with saturated sodium carbonate solution and extracted with ethyl acetate. The combined organic layers were washed with brine, dried over sodium sulphate and concentrated in vacuo to give a pure white solid. The mother liquor was concentrated in vacuo to get rid of methanol and extracted with saturated sodium carbonate solution as described above. The product **30** was purified by column chromatography ($CHCl_3$/methanol 5:1) to obtain a slight beige solid (1.17 g, 5.3 mmol, 63 %). Mp 169-171 °C. TLC ($CHCl_3$/methanol, 5:1): R_f = 0.18. ^{1}H NMR (200.13 MHz, DMSO-d_6): δ 2.78 – 2.92 (m, 8H), 4.17 (m, 4H), 6.43 (m, 2H), 6.70 (d, 1H) ppm. FT-MS (ESI): *m/z* 221.21 $[M+H]^+$.

1-(2,3-Dihydrobenzo[*b*][1,4]dioxin-6-yl)-4-(4-fluorobenzyl)piperazine (33a)

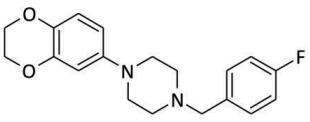

A mixture of 350 mg of **1** (1.6 mmol), 394 mg of 4-fluorobenzylbromid (2.08 mmol), 443 mg of K_2CO_3 (3.2 mmol) and 345 mg of potassium iodide (2.08 mmol) was suspended in 20 mL of dry acetonitrile and heated at 85 °C for 18 h. After cooling to room temperature the mixture was treated with 50 mL of water and extracted with ethyl acetate. The combined organic layers were washed with brine, dried over sodium sulphate and concentrated in vacuo. The product was purified by column chromatography (n-hexane/ethyl acetate 1:2) to obtain **33a** as a white solid (240 mg, 0.73 mmol, 46 %). Mp 120 °C. TLC (n-hexane/ethylacetat, 1:2): R_f = 0.7. ^{1}H NMR ($CHCl_3$, 400 MHz) δ 2.56 (t, *J* = 4.8 Hz, 4H), 3.06 (t, *J* = 4.8 Hz, 4H), 3.50 (s, 2H), 4.19 (m, *J* = 4.5 Hz,

2H), 4.21 (m, *J* = 4.6 Hz, 2H), 6.43 (m, 2H), 6.75 (m, 1H), 6.98 (m, 1H), 7.29 (m, 2H) ppm. FT-MS (ESI): *m/z* 329.166 $[M+H]^+$.

4-Fluoro-3-hydroxybenzaldehyde (34d)

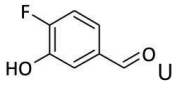

Under an atmosphere of argon 4-fluoro-3-methoxybenzaldehyde (1 g, 6.49 mmol) dissolved in 25 mL of dry dichloromethane was cooled in a dry ice/acetone bath at -78 °C. A solution of 1 M BBr_3 in dichloromethane (19 ml, 19 mmol) was cautiously added dropwise, afterwards the reaction mixture was warmed to room temperature and stirred for 18 h. At the end of the reaction 40 - 50 mL of ice cooled water were added while cooling the reaction mixture in an ice bath. The organic phase was separated, washed with 50 mL of a solution of saturated $NaHCO_3$ and extracted twice with a solution of 2 N NaOH. The brown aqueous NaOH solution was cooled in an ice bath and concentrated HCL was cautiously added until pH 1 - 3 was reached. Afterwards the solution was extracted 3 - 4 times with dichloromethane. The organic phase was washed with brine, dried over sodium sulphate and evaporated to dryness. The obtained light yellow solid of **34d** (563 mg, 4.02 mmol, 62 %) could be used in followed reaction steps without further purification. Mp. 101-103 °C. TLC (n-hexan/ethyl acetate 2:1): R_f = 0.42. ^{1}H NMR (DMSO-d_6, 400 MHz) δ 7.35-7.49 (br, 3H); 9.89 (s,1H); 10.5 (s, 1H)) ppm. FT-MS (ESI): *m/z* 140.91 (100) $[M+H]^+$.

General preparation of benzylated phenolaldehydes (34c, 40c')

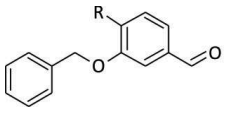

34c: R = F
40c': R = NO_2

Under an atmosphere of argon the corresponding hydroxyaldehyde (1.63 mmol) was dissolved in 4 mL of anhydrous *N,N*-dimethylformamid (DMF) and anhydrous potassium carbonate (243 mg, 1.76 mmol) was added. After addition of benzylbromide (0.34 mL, 0.49 g, 2.86 mmol) the reaction mixture was heated at 110 °C and stirred over night. After cooling the reaction solution was quenched with 40 mL of water and the solution was extracted with dichloromethane, washed with water and saturated sodium chloride solution and dried over sodium sulphate. After evaporation of the solvent in vacuo the residue was purified by flash chromatography

(n-hexan/ethyl acetat 4:1).

3-Benzyloxy-4-fluorobenzaldehyde (34c) was obtained from 4-fluoro-3-hydroxybenzaldehyde (**2d**) (200 mg, 1.4 mmol) as a white solid (126 mg, 0.55 mmol, 50 %). TLC (n-hexane/ethyl acetat 4:1): R_f = 0.56. (200.13 MHz, $CDCL_3$-d_6) δ 5.24 (s, 2H); 7.28-7.62 (br, 8H); 9.93 (s, 1H) ppm. FT-MS (ESI): *m/z* 231.09 (100) $[M+H]^+$.

3-Benzyloxy-4-nitrobenzaldehyde (40c') was obtained from 3-hydroxy-4-nitrobenzaldehyde (265 mg, 1.63 mmol) as yellow solid (212 mg, 0.92 mmol, 57 %). Mp 92 °C. TLC (n-hexane/ethyl acetat 4:1): R_f = 0.44. (200.13 MHz, DMSO-d_6) δ 5.42 (s, 2H); 7.35-7.48 (br, 5H); 7.71 (dd, *J* = 8.3 / 1.4 Hz, 1H); 7.92 (d, *J* = 1.4 Hz, 1H); 8.03 (d, *J* = 8.3 Hz, 1H); 10.8 (s, 1H) ppm.

4-Formyl-2-benzyloxy-*N,N*-dimethylaniline (9)

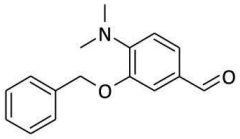

Under an atmosphere of argon 4-bromo-2-benzyloxy-*N,N*-dimethylaniline (500 mg, 1.65 mmol) was dissolved in 6 mL of anhydrous diethylether and cooled in an carbon dioxide/acetone bath at -78 °C. Carefully 1.75 mL of sec.-BuLi (2.45 mmol, 1.4 M in cyclohexane) was added and the reaction was stirred for 45 min at -78 °C. Subsequently DMF (200 µL, 2.6 mmol) was added all at once and the reaction mixture was stirred for 1 h at room temperature. For quenching the solution was diluted with 15 mL of water and 15 mL of saturated aqueous ammonium chloride and extracted with diethylether. After washing with a saturated sodium chloride solution the organic phase was dried over sodium sulphate, filtered and evaporated in vacuo to dryness. The crude product **9** was purified by flash chromatography on silica gel (n-hexane/ethyl acetate: 4:1) and obtained as a clear, light yellow liquid (240 mg, 0.95 mmol, 57 %). TLC (n-hexane/ethyl acetate: 4:1): R_f = 0.44. ^{1}H NMR (d6-DMSO, 200 MHz) δ 2.91 (s, 6H); 5.18 (s, 2H); 6.97 (d, 1H); 7.46 (m, 7H); 9.79 (s, 1H) ppm. MS (ESI): *m/z* 256.21 $[M+H]^+$.

General preparation of ammonium trifluoromethanesulfonates (40a, 40b, 40c)

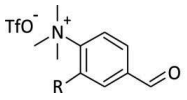

40a: R = H
40b: R = OMe
40c: R = OBn

The corresponding fluoroanalogue (24 mmol) was dissolved in 130 mL of DMSO and 40 mL of water. After further addition of potassium carbonate (60 mmol, 2.5 eq) and dimethylamine hydrochloride (36 mmol, 1.5 eq) the mixture was heated at 100 °C over night. Upon complete cooling of the reaction (!) the solution, it was extracted three times with diethylether to obtain the crude 4-(dimethylamino)benzaldehyde derivative which was further used without purification.

Under an atmosphere of argon the 4-(dimethylamino)benzaldehyde derivative was dissolved in 60 mL of dry methylene chloride. At rt 1 eq of methyl trifluoromethane-sulphonate was added and stirred for about 7 h. 40 mL of n-hexane were added subsequently and the solution cooled at 4 °C. The precipitate was filtered, washed with cold n-hexane and recrystalyzed from methylene chloride.

4-(Trimethylammonium)benzaldehyde trifluoromethanesulfonate (40a) was obtained from 3 g (24 mmol) 4-fluorobenzaldehyde as a white solid (6.4 g, 20.4 mmol, 85 %). (200.13 MHz, DMSO-d_6) 3.67 (s, 9H), 8.19 (m, 4H), 10.13 (s, 1H) δ ppm. FT-MS (ESI): 209.67 *m/z* (100) $[M+H]^+$.

4-(Trimethylammonium)-3-methoxybenzaldehyde trifluoromethanesulfonate (40b) was obtained from 3 g (19.46 mmol) 4-fluoro-3-methoxybenzaldehyde as a white solid (5.9 mg, 17.2 mmol, 88.4 %). (200.13 MHz, DMSO-d_6) δ 3.69 (s, 9H), 3.73 (s, 3H), 7.77-7.82 (m, 3H), 10.09 (s, 1H) ppm. FT-MS (ESI): 195.33 *m/z* (100) $[M+H]^+$.

4-(Trimethylammonium)-3-benzyloxybenzaldehyde trifluoromethanesulfonate (40c) was obtained from 100 mg (0.4 mmol) of 4-formyl-2-benzyloxy-*N,N*-dimethylaniline (**9**) as a white solid (154 mg, 0,37 mmol, 92 %). (200.13 MHz, DMSO-d_6) δ 3.70 (s, 9H), 5.51 (s, 2H), 7.43-7.64 (m, 5H), 7.49 (dd, *J* = 8.52 Hz, *J* = 1.72 Hz, 1H), 7.99 (d, *J* = 1.70 Hz, 1H), 8.19 (d, *J* = 8.56 Hz, 1H), 10.11 (s, 1H) ppm. FT-MS (ESI): 270.09 *m/z* (50) $[M+H]^+$.

6-Fluoronicotinealdehyd (34e)

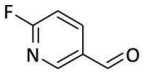

Method A: To 2-fluoro-5-methylpyridine (9.758 g, 88.15 mmol) suspended in 350 mL of distilled water, $KMnO_4$ (16.3 g, 103 mmol) was added and the reaction mixture was heated at 100 °C over night. Thereafter manganese dioxide was removed by using a filter paper circle (blue ribbon) and washed with water. After adding 20 mL of concentrated HCl to the clear solution the product crystallized at 4 °C and was separated by filtration to obtain 6-fluoronicotinic acid.

Under an atmosphere of argon to 6-fluoronicotinic acid (500 mg, 3.55 mmol) dissolved in 20 mL of dichloromethane (DCM) and one drop of *N,N*-dimethylformamid (DMF) oxalylchloride (450 µL, 5.25 mmol) was added and the reaction mixture stirred at 50 °C until evolution of CO_2 stopped (ca. 2 h). After evaporation of DCM in vacuo to dryness sodium borohydride (455 mg, 12.03 mmol) was added in portions at 0 °C to the acid chloride dissolved in 7.5 mL of dry tetrahydrofurane under an atmosphere of argon and the reaction mixture was stirred for 1 h at 0 °C and then 1 h at room temperature. After adding 60 mL of brine the solution was extracted three times with 50 mL of diethylether, the combined organic phase was dried over sodium sulfate and the solvent evaporated in vacuo.

To the crude product 6-fluoropyridine-3-yl-methanol (230 mg, 1.81 mmol) dissolved in 5 mL of dry tetrahydrofurane freshly produced Dess-Martin periodinane (908 mg, 2.14 mmol) was added in portions and the suspension was stirred for 1 h at room temperature. Thereafter 20 mL of a mixture of saturated sodium thiosulfate and saturated sodium bicarbonate (1:1) was added to the suspension and the obtained solution was extracted with ethyl acetate. The crude product was recrystallized from n-hexane/methanol or purified by flash chromatography (n-hexane/ethyl acetate 4:1) to obtain 6-fluoronicotinaldehyd as a white solid (220 mg, 1.76 mmol, 38.5 % related to 2-fluoro-5-methylpyridine).

Method B: A well baked out flask was evaporated and refilled with argon three times. After charging with 5-bromo-2-fluoropyridine (342 mg, 1.94 mmol) dissolved in 2 mL of absolute tetrahydrofurane (THF) isopropylmagnesium chloride (1 mL, 2 M in THF) was added drop wise. After stirring for 1 h at room temperature dry DMF was added all at once. The reaction mixture was stirred over night, quenched with 30 mL of water and

chloroform and extracted with chloroform. The organic phase was dried over sodium sulfate and evaporated in vacuo. The red oil was cooled and dried in vacuo until formation of crystals. The crude product was cautiously recrystallized from n-hexane/methanol to obtain light yellow crystals (24 mg, 0.19 mmol, 10 %) of **34e**.

Mp 65-67 °C. TLC (ethyl acetate/methanol/diethyl amine 96:2:2): R_f = 0.71. (200.13 MHz, DMSO-d_6) δ 6.76 (d, J = 9.07 Hz, 1H); 7.87 (d, J = 9.01 Hz, 1H); 8.59 (s, 1H); 9.74 (s, 1H) ppm.

General preparation of amides (32a, 32b, 32c)

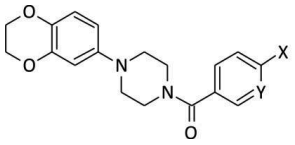

32a: X = NO_2, Y = CH
32b: X = F, Y = CH
32c: X = F, Y = N

The corresponding aromatic carboxylic acid (3.54 mmol) was dissolved in 20 mL of anhydrous DCM followed by a small amount of DMF (20 µL) and oxalylchloride (5.3 mmol, 1.5 equiv). The mixture was stirred at room temperature until evaporation of gas had stopped (2 - 3 h) and then the solvent was evaporated in vacuo to get the corresponding acid chloride.

Under an argon atmosphere 1-(1,4-benzodioxine-6-yl)piperazine **(30)** was dissolved in DCM and triethylamine (2.2 mmol, 0.6 equiv) was added. The solution was cooled in an ice bath at 0 °C and the respective acid chloride redissolved in 5 mL of DCM was added dropwise. The reaction mixture was warmed to room temperature and stirred over night for at least 10 h. To quench the reaction 20 mL of saturated sodium bicarbonate solution was added. The solution was extracted with DCM, washed with water and saturated sodium chloride solution and dried over sodium sulphate. After evaporation of the solvent in vacuo the residue was purified by flash chromatography.

(4-(2,3-Dihydrobenzo[b][1,4]dioxin-6-yl)piperazin-1-yl)(4-fluorophenyl)methanone (32a) was obtained from 4-fluorobenzoic acid (286 mg, 2.04 mmol) as white foamous solid (460 mg, 1.34 mmol, 66 %). TLC (n-hexane/ethyl acetat 1:2): R_f = 0.56. ^{1}H NMR ($CHCl_3$, 400 MHz) δ 3.04 (b, 4H, $4CH_2$); 3.7 (b, 4H, $4CH_2$); 4.19 (m, 2H, $2CH_2$); 4.22 (m, 2H, $2CH_2$); 6.44-6.45 (m, 2H, Ar-CH); 6.77 (m, 1H, Ar-CH); 7.08 (m, 2H, Ar-CH); 7.42 (m, 2H, Ar-CH) ppm. FT-MS (ESI): *m/z* 343.19 (100) $[M+H]^+$.

(4-(2,3-dihydrobenzo[b][1,4]dioxin-6-yl)piperazin-1-yl)(4-nitrophenyl)methanone (32b) was obtained from 4-nitrobenzoic acid (267 mg, 1.6 mmol) as a yellow solid (520 mg, 1.41 mmol, 88 %). TLC (n-hexane/ethyl acetat 1:2): R_f = 0.49. ^{1}H NMR ($CHCl_3$, 400 MHz) δ 2.92 (b, 2H); 2.97 (b, 2H); 3.13 (b, 2H); 3.45 (b, 2H); 4.19 (m, 2H); 4.22 (m, 2H) 6.44-6.45 (m, 2H); 6.77 (d, 1H); 7.58 (dt, *J* = 8,7 Hz; 2H); 8.28 (dd, *J* = 8,3 Hz, 2H) ppm. FT-MS (ESI): *m/z* 370.14 (90) $[M+H]^+$.

(4-(2,3-dihydrobenzo[b][1,4]dioxin-6-yl)piperazin-1-yl)(6-fluoropyridin-3-yl)-methanone (32c) was obtained from 2-fluoronicotinic acid (450 mg, 3.2 mmol) as a white solid (680 mg, 2 mmol, 62 %). TLC (n-hexane/ethyl acetat, 1:3): R_f = 0.48. ^{1}H NMR ($CHCl_3$, 400 MHz) δ 3.06 (br, 2H); 3.12 (br, 2H); 3.52 (br, 2H); 3.80 (br, 2H); 4.21 (m, 2H); 4.25 (m, 2H); 6.52 (s, 1H); 6.53 (dd, *J* = 2.8 Hz / 8.6 Hz, 1H); 6.79 (d, *J* = 9.2 Hz, 1H); 7.36 (dd, *J* = 2.5 Hz / 8.4 Hz, 1H); 8.15 (ddd, *J* = 2.5 Hz / 8.2 Hz / 8.2 Hz, 1H); 8.42 (d, *J* = 2.0 Hz, 1H) ppm. FT-MS (ESI): *m/z* 344.14030 (100) $[M+H]^+$.

General preparation of 3-substituted 6-(4-benzylpiperazine-1-yl)benzodioxine derivatives (33b, 33c, 3d, 33e, 33e', 33f) by reductive amination

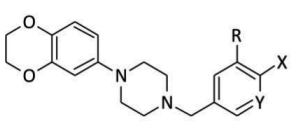

32b: R = OMe, X = F, Y = CH
32c: R = OBn, X = F, Y = CH
32d: R = OH, X = F, Y = CH
32e: R = H, X = F, Y = N
32e': R = H, X = Cl, Y = N
32f: R = H, X = H, Y = N

In a 100-ml two-neck flask 1-(1,4-benzodioxine-6-yl)piperazine (**30**) (1.816 mmol, 1 equiv) and the corresponding benzaldehyde (**34b-f**, 2.724 mmol, 1.5 equiv) were dissolved in 20 ml of dry methanol. After an addition of acetic acid (96 %, 5.45 mmol, 3 equiv) sodium cyanoborohydride (2.724 mmol, 1.5 equiv) was added in small portions and rinsed with methanol. The reaction was heated for 12-24 h at 60 °C. After cooling the reaction was quenched by addition of 50 ml of saturated sodium bicarbonate solution, extracted three times with chloroform and washed with brine. The organic layer was dried over sodium sulphate and evaporated to dryness after filtration. The residue was purified by chromatography over a silica gel column (n-hexane/ethyl acetate 1:2).

1-(2,3-Dihydrobenzo[*b*][1,4]dioxin-6-yl)-4-(4-fluoro-3-methoxybenzyl)piperazine (33b). The methoxy derivative was obtained from the commercially available 4-fluoro-3-methoxybenzaldehyde (**34b**) (420 mg, 2.724 mmol) as a pale yellow crystalline solid (551 mg, 1.54 mmol, 85 %). Mp 100 °C. TLC (n-hexane/ethylacetat, 1:2): R_f = 0.44. ^{1}H NMR ($CHCl_3$, 400 MHz) δ 2.56 (t, *J* = 4.8 Hz, 4H), 3.06 (t, *J* = 4.8 Hz, 4H), 3.48 (s, 2H), 3.88 (s, 3H), 4.18 (m, *J* = 1.6 Hz, 2H), 4.20 (m, *J* = 1.6 Hz, 2H), 6.44 (m, 1H), 6.45 (m, 1H), 6.75 (m, 1H), 6.82 (m, 1H), 6.98 (m, 2H) ppm. FT-MS (ESI): *m/z* 359.176 $[M+H]^+$.

1-(3-(Benzyloxy)-4-fluorobenzyl)-4-(2,3-dihydrobenzo[*b*][1,4]dioxin-6-yl)piperazine (33c) was obtained from 3-benzyloxy-4-fluoro-benzaldehyde (**34c**) (160 mg, 0.7 mmol) as a white crystalline solid (175 mg, 0.41 mmol, 58 %). Mp 94 °C. TLC (n-hexane/ethylacetat, 1:2): R_f = 0.74. ^{1}H NMR ($CHCl_3$, 400 MHz) δ 2.40 (m, 4H); 2.92 (m, 4H); 3.41 (s, 2H); 4.11 (m, 2H); 4.14 (m, 2H); 5.14 (s, 2H); 6.36 (d, J = 2.7 Hz, 1H); 6.38 (dd, J = 2.9 Hz / 8.6 Hz; 1H); 6.66 (d, J = 8.7 Hz, d); 6.84 (m,1H); 7.14 (m, 2H); 7.31-7.42 (m, 5H) ppm. FT-MS (ESI): *m/z* 345.20758 $[M+H]^+$.

5-((4-(2,3-Dihydrobenzo[*b*][1,4]dioxin-6-yl)piperazin-1-yl)methyl)-2-fluorophenol (33d). The hydroxyl derivative was obtained from 4-fluoro-3-hydroxybenzaldehyd (**34d**) (70 mg, 0.5 mmol) as a white crystalline solid (112 mg, 0.35 mmol, 66 %). Mp 186-187 °C. TLC (n-hexane/ethylacetat, 1:2): R_f = 0.35. ^{1}H NMR ($CHCl_3$, 400 MHz) δ 2.57 (m, 4H); 3.06 (m, 4H); 3.45 (s, 2H); 4.18 (m, 2H); 4.20 (m, 2H); 6.44 (m, 2H); 6.74 (m, 1H); 6.79 (m, 1H); 6.98 (m, 2H); 9.84 (br, 1H) ppm. FT-MS (ESI): *m/z* 345.19 (100) $[M+H]^+$.

1-(2,3-Dihydrobenzo[*b*][1,4]dioxin-6-yl)-4-((6-fluoropyridin-3-yl)methyl)piperazine (33e). Method A: Obtained from 6-fluoronicotinaldehyde (**34e**) (100 mg, 0.8 mmol) as a white crystalline solid (35 mg, 0.11 mmol, 13.7 %).

Method B: A 25 mL flask with a silicone septum was twice heated under vacuo after filled with argone. After cooling 1 mL of borane (1 M in THF) was filled into the flask and 150 mg of **5c** (0.44 mmol) dissolved in 4 mL of dry THF were added afterwards. The reaction mixture was heated to 65 °C for 7 h and a second portion of borane (0.7 mL, 1 M in THF) was added. After another 22 h the reaction was quenched by addition of small amounts of ice, extracted three times with chloroform and washed with brine. The

organic layer was dried over sodium sulphate and evaporated to dryness after filtration. The residue was purified over a silica gel column (chloroform/methanol 8:1) to obtain a white solid (43 mg, 0.132 mmol, 30 %). Mp 94 °C. TLC (chloroform/methanol 8:1): R_f = 0.63; (ethyl acetate/methanol/diethyl amine 96:2:2): R_f = 0.78 . ^{1}H NMR ($CHCl_3$, 400 MHz) δ 2.52 (br, 4H); 3.00 (br, 4H); 3.47 (s, 2H); 4.14 (m, 2H); 4.16 (m, 2H); 6.38 (m, 2H); 6.71 (m, 1H); 6.84 (dd, *J* = 2.8 Hz / 8.4 Hz, 1H); 7.74 (ddd, *J* = 2.3 Hz / 8.0 Hz / 8.1 Hz, 1H); 8.09 (d, *J* = 1.9 Hz, 1H) ppm. FT-MS (ESI): *m/z* 330.16 $[M+H]^+$.

1-((6-Chloropyridin-3-yl)methyl)-4-(2,3-dihydrobenzo[*b*][1,4]dioxin-6-yl)piperazine (33e'). It was also obtained by the general amination procedure from the commercially available 6-chloronicotinaldehyd (**34e'**) (380 mg, 2.68 mmol) as a white crystalline solid (445 mg, 1.29 mmol, 71 %). Mp 94 °C. TLC (n-hexane/ethylacetat, 1:2): R_f = 0.53. ^{1}H NMR ($CHCl_3$, 400 MHz) δ 2.45 (m, 4H); 2.94 (m, 4H); 3.51 (s, 2H); 4.10 (m, 2H); 4.14 (m, 2H); 6.36 (d, *J* = 2.5 Hz, 1H); 6.38 (dd, *J* = 2.7 Hz / 8.6 Hz, 1H); 6.66 (d, *J* = 8.6 Hz, 1H); 7.46 (d, *J* = 8.2 Hz, 1H); 7.77 (dd, *J* = 2.3 Hz / 8.1 Hz, 1H); 8.31 (d, *J* = 2.2 Hz, 1H) ppm. FT-MS (ESI): *m/z* 346.13150 $[M+H]^+$.

1-((Pyridin-3-yl)methyl)-4-(2,3-dihydrobenzo[*b*][1,4]dioxin-6-yl)piperazine (33f) was also obtained by the general amination procedure from the commercially available nicotinaldehyd (**34f**) (234 mg, 2 mmol, 1.1 eq) as a white crystalline solid (260 mg, 0.84 mmol, 46 %). TLC (n-hexane/ethylacetat, 1:2): R_f =0.49. ^{1}H NMR ($CHCl_3$, 200.13 MHz) δ 2.57 (tr, br, 4H), 3.12 (tr, br, 4H), 4.22 (m, 4H), 6.49 (m, 2H), 6.80 (d, 1H), 7.32 (m, 1H), 7.77 (d, 1H), 8.57 (m, 2H) ppm. ^{13}C NMR (50.32 MHz, $CDCL_3$-d_6) δ 50.14, 53.07, 60.12, 62.62, 64.27, 64.65, 105.77, 110.48, 117.40, 123.44, 123.51, 136.95, 137.52, 143.66, 146.32, 148.75, 148.94, 150.49 ppm.

6.3.2 Radiosyntheses

N.c.a. [^{18}F]fluoride was produced via the ^{18}O(p,n)^{18}F nuclear reaction by bombardment of isotopically enriched [^{18}O]water in a titanium target[245] with 17 MeV protons at the JSW cyclotron BC 1710 (INM-5, Research Center Jülich). The aqueous [^{18}F]fluoride solution (10 – 50 µL, 75 – 375 MBq) was filled into a 5 mL conical vial (Reactivial) containing 1 mL of acetonitrile, 10 mg of Kryptofix 2.2.2, 13 µl of an aquaous 1 M potassium carbonate solution [52]. The solvent was evaporated under a stream of argon at 80 °C and 600 mbar. This azeotropic drying was repeated twice using 1 mL of dry acetonitrile, followed by evaporation at 8-15 mbar for 5 min.

6-(4-[4-[^{18}F]Fluorobenzyl]piperazin-1-yl)benzodioxine ([^{18}F]33a). Method A: A solution of precursor **32a** (8 mg, 22 µmol) in 0.5 mL of anhydrous DMSO was added to the vial containing the dried [^{18}F]fluoride at 160 °C. Monitoring of the reaction progress was determined by radio HPLC from aliquots of about 30 - 50 µL (Gemini 5 µ RP18 A110, 250 × 4.6 mm, 1 mL/min, isocratic 60:40:0.1 v/v/v CH_3CN/H_2O/TEA) and by radio TLC (1:2 n-hexane/ethyl acetate) determining the reaction time for optimal radiochemical yields. For reduction of the intermediate compound the reaction mixture was diluted with 20 mL of water, passed through a Sep Pak C18 cartridge, washed with water (5 mL) and dried with air. The cartridge was eluted through a drying cartridge charged with 4 Å molecular sieve and 270 mg dry sodium sulphate using 5 mL absolute dichloromethane. After removal of the solvent in vacuo (800 up to 300 mbar) at room temperature 0.2 mL of BH_3THF (1M, 0.2 mmol) solution and 0.7 mL of dry THF were added and the solution was stirred for 10 min at 65 °C. The reaction mixture was cooled in an ice bath, carefully quenched with 20 mL of water and passed through a second Sep Pak C18 cartridge. After washing with water, drying in air and eluting with 1 mL of acetonitrile the solution was injected on a semi-preparative HPLC system (Gemini 5µ RP18 A110, 250 × 10 mm, 4 mL/min, isocratic 30:70:0.1 v/v/v CH_3CN/H_2O/TFA).

Method B: A solution of **40a** (8 mg, 25.5 µmol) in 0.5 mL of anhydrous DMSO was added to a reaction vial at 110 °C and the reaction was monitored via radio HPLC (Gemini 5 µ RP18 A110, 250 × 4.6 mm, 1 mL/min, isocratic 60:40:0.1 v/v/v CH_3CN/H_2O/TEA). A solution of **30** (8.7 mg, 40 µmol) in 40 µL acetic acid and 50 µL DMSO and a solution of

sodium cyanoborohydride (4 mg, 64 µmol) in 50 µL DMSO were added successively. The reaction mixture was stirred for 15 min, diluted with water and passed through a SepPak C18 cartridge, washed with water (5 mL) and dried with air. The cartridge was eluted with 1 mL of acetonitrile and injected on a semi-preparative HPLC system (Gemini 5µ RP18 A110, 250 × 10 mm, 4 mL/min, isocratic 30:70:0.1 v/v/v CH_3CN/H_2O/TFA). The separated fraction was diluted with 15 mL of water and passed through a second SepPak C18 cartridge. After washing with water and drying in an argon stream the cartridge was eluted with 5 mL of diethylether which was then evaporated in vacuo (800 up to 330 mbar). For *in vitro* studies [^{18}F]**3a** was formulated in 300 µL ethanol/saline (5:1).

1-(2,3-Dihydrobenzo[*b*][1,4]dioxin-6-yl)-4-(4-[^{18}F]fluoro-3-methoxybenzyl)piper-azine ([^{18}F]33b). Analoguous to method B of the radiosynthesis of [^{18}F]**33a** a solution of **40b** (7 mg, 20 µmol) in 0.5 mL of anhydrous DMSO was added to the reaction vial containing the dried [^{18}F]fluoride at 110 °C and the reaction progress was monitored as described above via radio HPLC (Gemini 5 µ RP18 A110, 250 × 4.6 mm, 1 mL/min, isocratic 60:40:0.1 v/v/v CH_3CN/H_2O/TEA). Without further separation a solution of **30** (8.7 mg, 40 µmol) in 40 µL of acetic acid and 50 µL of DMSO and a solution of sodium cyanoborohydride (4 mg, 64 µmol) in 50 µL of DMSO were rapidly added to the reaction vial at the same temperature. The reaction was stirred for 15 min, diluted with water and passed through a SepPak C18 cartridge, washed with water (5 mL) and dried with air. The cartridge was eluted with 1 mL of acetonitrile and injected on a semi-preparative HPLC system (Gemini 5µ RP18 A110, 250 × 10 mm, 4 mL/min, isocratic 30:70:0.1 v/v/v CH_3CN/H_2O/TFA). The collected fraction was diluted with 15 mL of water, passed through a SepPak C18 cartridge again, washed with water (5 mL) and dried in a stream of argon. The cartridge was eluted with 4 mL of diethylether and the solvent was evaporated in vacuo (800 up to 330 mbar). For further experimental use in *in vitro* autoradiography studies [^{18}F]**33b** was formulated in 300 µL ethanol/saline (5:1).

6-(4-[4-[^{18}F]Fluoro-3-hydroxybenzyl]piperazine-1-yl)benzodioxine ([^{18}F]33d). The benzyl-protected precursor **39** (3 mg, 7 µmol) dissolved in 0.5 mL of anhydrous DMSO added to the dried [^{18}F]fluoride containing vial was heated at 110 °C and the reaction progress was determined by radio HPLC (Gemini 5 µ RP18 A110, 250 × 4.6 mm, 1 mL/min,

isocratic 80:20 v/v CH_3CN/H_2O). A solution of **30** (6.5 mg, 30 µmol) in 40 µL acetic acid and 50 µL DMSO and a solution of sodium cyanoborohydride (4 mg, 64 µmol) in 50 µL DMSO were immediately added to the reaction vial and stirred for 7 min at 110 °C. Subsequently the solution was diluted with water (20 mL) and passed through an EN cartridge. After washing with water (5 mL) and drying in a stream of argon for 8 min the cartridge eluted through an unconditioned Alumina N cartridge with 5 mL of anhydrous diethylether in a second reaction vial. The ether was evaporated in vacuo and the residue was diluted with 1 mL of anhydrous methanol. Radio HPLC analysis showed a nearly quantitative conversion of [^{18}F]**34c** to [^{18}F]**33c**. 20 mg of Pd(black) and 250 mg of ammonium formate were added to the solution and the resulting suspension was stirred for 8 min at 60 °C. The start of the reaction could be observed by a strong evolution of gas. The mixture was cooled in an ice bath, filtered through a small glass column with two frits (Merck: pore size 4) and washed with a small amount of methanol. After solvent evaporation in vacuo the residue was diluted with 1 mL of methanol/phosphate buffer and injected on a semi-preparative HPLC system (Gemini 5µ RP18 A110, 250 × 10 mm, 4 mL/min, isocratic 60:40 v/v MeOH/phosphate buffer pH 8.5). The separated fraction was diluted with 15 mL of water, passed through a SepPak C18 cartridge, washed with water (5 mL) and dried in a stream of argon. The cartridge was eluted with 4 mL of diethylether and the solvent was evaporated in vacuo (800 up to 330 mbar). For further experimental use in *in vitro* autoradiography studies [^{18}F]**33d** was formulated in 300 µL of ethanol/saline (5:1).

1-(2,3-Dihydrobenzo[*b*][1,4]dioxin-6-yl)-4-((6-[^{18}F]fluoropyridine-3-yl)methyl)-piperazine ([^{18}F]33e). Method A: The precursor for direct labelling **33e'** (13.8 mg, 40 µmol) dissolved in 0.5 mL of anhydrous DMSO was added to the vial containing the [^{18}F]fluoride complex and the solution was stirred at 160 °C for 20 min. Progress of the reaction was monitored via radio HPLC (Gemini 5 µ RP18 A110, 250 × 4.6 mm, 1 mL/min, isocratic 50:50:0.1 v/v/v CH_3CN/H_2O/TEA). Water was added to the solution and it was passed through a Sep Pak C18 cartridge, washed with water and dried with air. The cartridge was eluted with acetonitrile (2 mL) and the solvent was evaporated in vacuo. The residue was diluted with 1 mL acetonitrile/water (50/50) and injected on a semi-preparative HOLC system (Gemini 5µ RP18 A110, 250 × 10 mm, 4 mL/min, isocratic 40:60:0.1 v/v/v CH_3CN/H_2O/TEA).

Method B: The radiochemical synthesis of [^{18}F]**33e** by reductive amination was performed in an identical manner as described for [^{18}F]**33a**, [^{18}F]**33b** and [^{18}F]**33c**, starting from 6-pyridinealdehyde (**40e**,5 mg, 35.5 µmol) solved in 0.5 mL of anhydrous DMSO and stirred for 2 min at 110 °C. The radiochemical yield of [^{18}F]**34e** was measured by radio HPLC (Gemini 5 µ RP18 A110, 250 × 4.6 mm, 1 mL/min, isocratic 60:40:0.1 v/v/v CH_3CN/H_2O/TEA). After reaching the optimal yield at 2 min, immediately a solution of **30** (6.5 mg, 30 µmol) in 40 µL of acetic acid and 50 µL of DMSO and a solution of sodium cyanoborohydride (4 mg, 64 µmol) in 50 µL of DMSO were added and the reaction mixture was further stirred for 8 min. After addition of 20 mL of water the solution was passed through a Sep Pak C18 cartridge followed by washing with 5 mL water and drying with air. The cartridge was eluted with 1 mL of ethanol/water (80/20) and injected on a semi-preparative HPLC system (Gemini 5µ RP18 A110, 250 × 10 mm, 4 mL/min, isocratic 40:60:0.1 v/v/v CH_3CN/H_2O/TEA). The collected fraction was diluted with 15 mL of water, passed through a SepPak C18 cartridge, washed with water (5 mL) and dried in a stream of argon. The cartridge was eluted with 4 mL of diethylether and the solvent was evaporated in vacuo (800 up to 330 mbar). For further experimental use [^{18}F]**33e** was formulated in 300 µL of saline containing 1% tween 80.

6.3.3 Radioanalytical methods

For identification of the labelled products and determination of their radiochemical yields (RCY) and purity both radio high performance liquid chromatography (radio-HPLC) and radio thin layer chromatography (radio-TLC) were used. All ^{18}F-labelled compounds were identified by their non-radioactive standard compounds by comparison of the UV-signals with the radioactive signals. The determination of volatile compounds like [^{18}F]**21** and [^{18}F]**22** as well as products directly obtained from these was of course not suitable by radio-TLC. Therefore these compounds were only analyzed by radio-HPLC.

6.3.3.1 Radio thin layer chromatography

Analytical radio thin layer chromatography was carried out in order to verify that no radioactive species especially very polar and non-polar ones other than those detected by radio-HPLC were present. As an alternative chromatography method on normal silica phases radio-TLC was further used to exclude a casually identic retention of product and a

given reference compounds. Radio-TLC was performed on precoated Merck silica plates (F_{254}) with different solvent systems. 1.5-3 µL of the radioactive sample solution was given on the TLC plates and developed in the appropriate solvent (Tab. 6.1).

Table 6.1. R_f-values of the standard compounds for chromatographic identification by radio-TLC on silica plates.

Compound	***R_f***
1-(4-Fluorophenyl)piperidine (**23**)	0.57 (A)
1-(4-Fluorophenyl)piperazine (**28**)	0.52 (B)
2-((4-(4-Fluorophenyl)piperazine-1-yl)methyl)-1H-indole-5-carbonitrile, FAUC316 (**1**)	0.73 (C)
2-((4-(4-Fluorophenyl)piperazine-1-yl)methyl)-1H-indole (**29**)	0.66 (D)
4-Fluorobenzaldehyde (**34a**)	0.61 (E)
4-Fluoro-3-methoxybenzaldehyde (**34b**)	0.89 (F)
4-Fluoro-3-benzyloxybenzaldehyde (**34c**)	0.56 (A)
1-(2,3-Dihydrobenzo[*b*][1,4]dioxin-6-yl)-4-(4-fluorobenzyl)piperazine (**33a**)	0.70 (F)
1-(2,3-Dihydrobenzo[*b*][1,4]dioxin-6-yl)-4-(4-fluoro-3-methoxybenzyl)piperazine (**33b**)	0.44 (F)
1-(3-(Benzyloxy)-4-fluorobenzyl)-4-(2,3-dihydrobenzo[*b*][1,4]dioxin-6-yl)piperazine (**33c**)	0.74 (F)
5-((4-(2,3-Dihydrobenzo[*b*][1,4]dioxin-6-yl)piperazin-1-yl)methyl)-2-fluorophenol (**33d**)	0.35 (F)
1-(2,3-Dihydrobenzo[*b*][1,4]dioxin-6-yl)-4-((6-fluoropyridin-3-yl)methyl)piperazine (**33e**)	0.63 (G); 0.78 (H)
(4-(2,3-Dihydrobenzo[b][1,4]dioxin-6-yl)piperazin-1-yl)(4-fluorophenyl)methanone (**32a**)	0.49 (F)

(A) n-hexane/ethyl acetate 4:1; (B) butanol/H_2O/acetic acid 4:1:1; (C) dichloromethane/methanol 95:5; (D) chloroform/methanol 20:1; (E) n‑hexane/ethyl acetat 2:1; (F) n‑hexane/ethyl acetat 1:2; (G) chloroform/methanol 8:1; (H) ethyl acetate/methanol/diethyl amine 96:2:2

The developed TL-chromatograms were measured for radioactivity on an Instant Imager™ (Packard, Canberra). Retardation factors (R_f-values) of individual standards are also listed in Table 6.1.

6.3.3.2 Radio high performance liquid chromatography

Analytical and semipreparative high performance liquid chromatography was performed using an Ultimate 3000 pump and variable wave length UV/Vis detector from Dionex. For measurement of radioactivity the outlet of the UV/Vis detector is connected to a Na(Tl) scintillation detector (Gabi star, raytest). The aliquots of the labelled compounds were analysed by different reverse phase (RP) columns as stationary phase and various acetonitrile/water systems with and without buffer as mobile phase. All measurements were performed at room temperature with a flow rate of 1 mL/min for analytical and 4 mL/min for semipreparative chromatography. Individual capacity factors (k') of the standard compounds are given in Table 6.2. k'-values are determined by equation (6.1) from individual retention times (t_R) and dead time (t_0) of the HPLC system.

$$k' = \frac{t_R - t_0}{t_0} \tag{6.1}$$

In practice for analytical radio-HPLC, samples were diluted with the eluent and about 40 kBq were injected *via* a Rheodyne injection valve and a 200 µL loop. Subsequent to the completed chromatographic sequence, equal volume samples were injected three times directly in front of the detectors *via* a second injection valve bypassing the column. For determination of the RCY in % the radioactivity of separated compounds (100 %) were related to the total radioactivity of the aliquots. In case of a previously performed separation (*e.g.* solid phase extraction) aliquots can not be related to the short activity of [^{18}F]fluoride and RCY are therefore related to the total radioactivity of the actual reaction step instead. For semipreparative radio-HPLC samples of an acetonitrile or ethanol solution were injected *via* a 1000 µL loop. The obtaind RCY at the end of synthesis (EOS) is not the product of all intermediate RCY but lower due to losses during extraction and purification.

Table 6.2. k'-values of the standard compounds for chromatographic identification by radio-HPLC.

Compound	***k'***
4-Fluorobromebenzene (**21**)	14.74 (C)
4-Fluoroiodobenzene (**22**)	7.41 (E)
1-(4-Fluorophenyl)piperidine (**23**)	2.04 (C)
1-(4-Fluorophenyl)-4-methylpiperazine (**24**)	2.97 (C)
Tert-butyl 4-(4-fluorophenyl)piperazine-1-carboxylate (**27**)	2.23 (C)
1-(4-Fluorophenyl)piperazine (**28**)	1.17 (C); 4.89 (G)
2-((4-(4-Fluorophenyl)piperazine-1-yl)methyl)-1H-indole-5-carbonitrile, FAUC316 (**1**)	8.7 (H)
2-((4-(4-Fluorophenyl)piperazine-1-yl)methyl)-1H-indole (**29**)	7.56 (D)
4-Fluorobenzaldehyde (**34a**)	1.88 (D)
4-Fluoro-3-methoxybenzaldehyde (**34b**)	1.65 (D)
4-Fluoro-3-benzyloxybenzaldehyde (**34c**)	4.35 (F)
6-Fluoronicotinaldehyd (**34e**)	1.28 (D); 2.06 (B)
1-(2,3-Dihydrobenzo[*b*][1,4]dioxin-6-yl)-4-(4-fluorobenzyl)piperazine (**33a**)	6.04 (D); 11.72 (C)
1-(2,3-Dihydrobenzo[*b*][1,4]dioxin-6-yl)-4-(4-fluoro-3-methoxybenzyl)piperazine (**33b**)	5.11 (D); 7.11 (A)
1-(3-(Benzyloxy)-4-fluorobenzyl)-4-(2,3-dihydrobenzo[*b*][1,4]dioxin-6-yl)piperazine (**33c**)	5.53 (F)
5-((4-(2,3-Dihydrobenzo[*b*][1,4]dioxin-6-yl)piperazin-1-yl)methyl)-2-fluorophenol (**33d**)	6.85 (A)
1-(2,3-Dihydrobenzo[*b*][1,4]dioxin-6-yl)-4-((6-fluoropyridin-3-yl)methyl)piperazine (**33e**)	4.19 (D); 5.87 (B)
1-((6-Chloropyridin-3-yl)methyl)-4-(2,3-dihydrobenzo[*b*][1,4]dioxin-6-yl)piperazine (**33e'**)	7.37 (B)
1-((Pyridin-3-yl)methyl)-4-(2,3-dihydrobenzo[*b*][1,4]dioxin-6-yl)piperazine (**33f**)	4.02 (B)

Table 6.2 continued

(4-(2,3-Dihydrobenzo[b][1,4]dioxin-6-yl)piperazin-1-yl)(4-fluorophenyl)methanone (**32b**)	2.97 (C); 2.28 (D)
1-(1,4-Benzodioxine-6-yl)piperazine (**30**)	0.62 (D)

Gemini 5 µ RP18 A110: (A) isocratic 30:70:0.03 v/v/v CH_3CN/H_2O/TEA pH 9; (B) isocratic 40:60:0.03 v/v/v CH_3CN/H_2O/TEA pH 9; (C) isocratic 50:50:0.03 v/v/v CH_3CN/H_2O/TEA pH 9; (D) isocratic 60:40:0.03 v/v/v CH_3CN/H_2O/TEA pH 9; (E) isocratic 75:25 v/v CH_3CN/H_2O; (F) isocratic 80:20:0.03 v/v/v CH_3CN/H_2O/TEA pH 9;

Phenomenex Luna 5 µm PFP(2) 100 Å: (G) isocratic 50:50:0.01 v/v/v CH_3CN/H_2O/TEA pH 7.8; (H) isocratic 70:30:0.01 v/v/v CH_3CN/H_2O/TEA pH 7.8

6.3.3.3 Determination of molar activities

For all pharmacological applications the molar activity of the labelled tracers has to be determined previously by measuring its amount of carrier. The analysis of the molar activity of [^{18}F]**1**, [^{18}F]**33a**, [^{18}F]**33b**, [^{18}F]**33d** and [^{18}F]**33e** was carried out by HPLC. The applied mass of the non-radioactive standard compounds is proportional to the integral of the UV-signal obtained by HPLC. Thus the measured peak areas were fitted as a function of varying masses of **1**, **33a**, **33b**, **33d**, and **33e**, respectively. The dependences between UV adsorbtion and the amount of substance is displayed for all fife labelled ligands in Figures 6.1-6.5. With this calibrations measured radioactivities of the γ-peak can be related to the mass or molarity of each ligand, respectively.

For 2-((4-(4-[^{18}F]fluorophenyl)piperazine-1-yl)methyl)-1H-indole-5-carbonitrile, FAUC 316 ([^{18}F]**1**) highest molar activity of 90 GBq/µmol was achieved. For the benzodioxine derivatives [^{18}F]**33a**, [^{18}F]**33b**, [^{18}F]**33d**, and [^{18}F]**33e** molar activities of about 60 GBq/µmol, 50 GBq/µmol, 25 GBq/µmol, and 40 GBq/µmol were achieved, respectively.

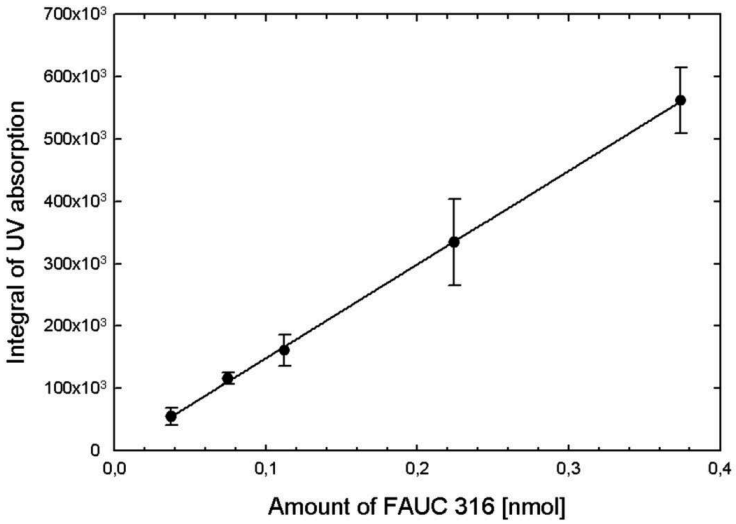

Figure 6.1: Dependence of the integral UV absorption (328 nm) on the amount of FAUC 316 (**1**) in HPLC chromatography.

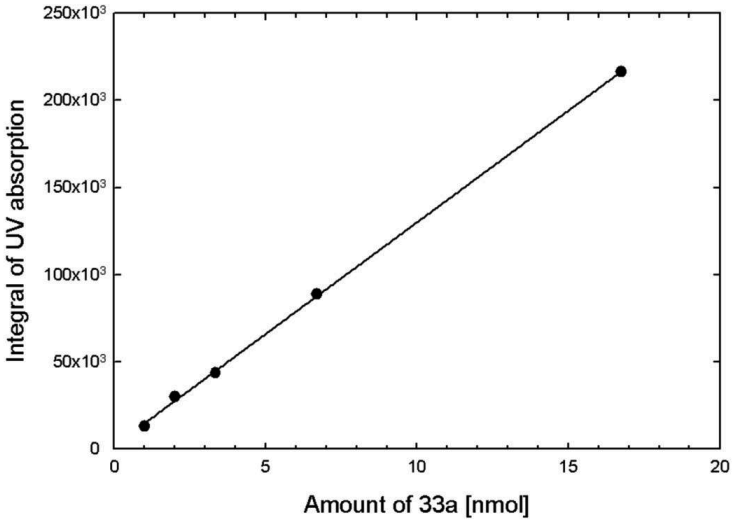

Figure 6.2: Dependence of the integral UV absorption (220 nm) on the amount of 1-(2,3-dihydrobenzo[*b*][1,4]dioxin-6-yl)-4-(4-fluorobenzyl)piperazine (**33a**) in HPLC chromatography.

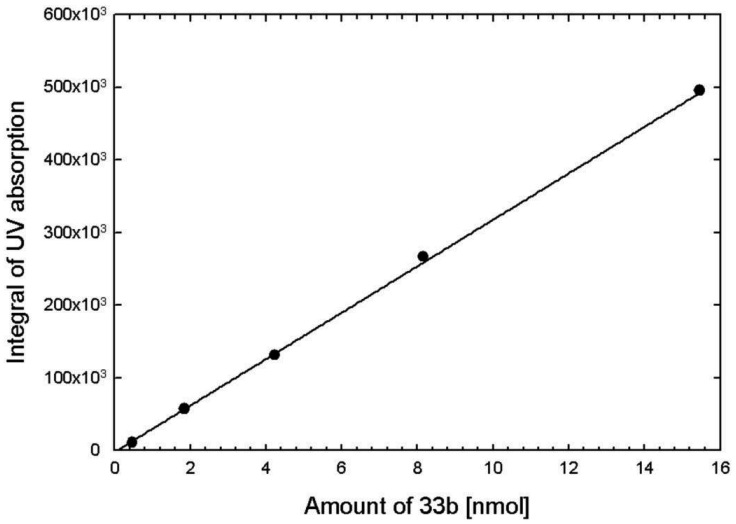

Figure 6.3: Dependence of the integral UV absorption (220 nm) on the amount of 1-(2,3-dihydrobenzo[*b*][1,4]dioxin-6-yl)-4-(4-fluoro-3-methoxybenzyl)piperazine (**33b**) in HPLC chromatography.

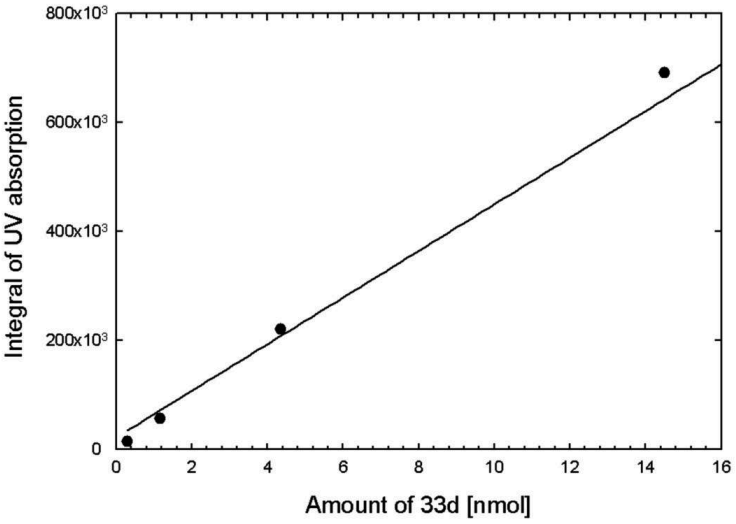

Figure 6.4: Dependence of the integral UV absorption (220 nm) on the amount of 5-((4-(2,3-dihydrobenzo[*b*][1,4]dioxin-6-yl)piperazin-1-yl)methyl)-2-fluorophenol (**33d**) in HPLC chromatography.

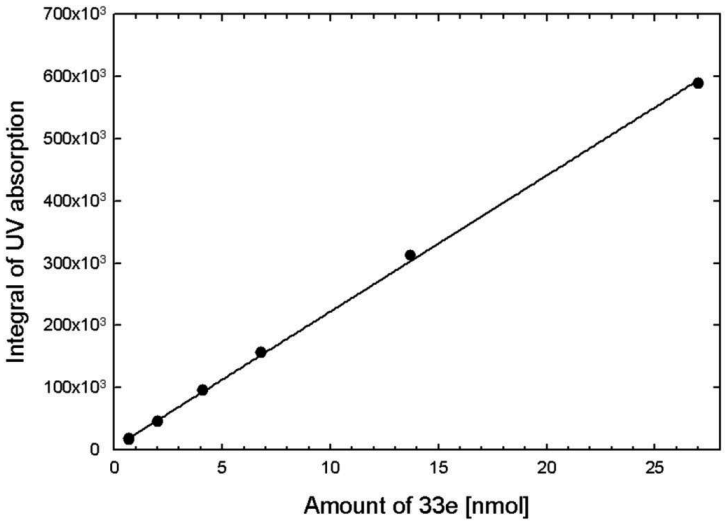

Figure 6.5: Dependence of the integral UV absorption (220 nm) on the amount of 1-(2,3-Dihydrobenzo[*b*][1,4]dioxin-6-yl)-4-((6-fluoropyridin-3-yl)methyl)piperazine (**33e**) in HPLC chromatography.

6.4 Pharmacology

6.4.1 Determination of partition coefficients

Using the HPLC method corresponding to the OECD guideline for the testing of chemicals[241], the lipophilicity of compounds was determined using a LiChrospher 100 RP-8 (5 mm) column (Merck). Soerensen buffer was used as eluent (methanol/phosphate buffer 75:25 (v/v) at a pH of 7.4). The retention time of a number of reference compounds (ascorbic acid, benzaldehyde, anisole, toluene, 4-bromoanisole, 4-iodoanisole) with known log *P* values (ranging from -1.67 to 3.24) were determined and the capacity factors k´ calculated. Plotting log k´ against log *P* gave the reference curve used to determine the log *P* values of **3a-e** *via* their respective retention time.

Using the shake flask method corresponding to the OECD guideline for the testing of chemicals[241], the lipophilicity of ligands was determined by analyzing the partitioning of the ^{18}F-labelled products between a phosphate-buffer (pH 7.4) and an n-octanol phase. The pure n.c.a. ^{18}F-labelled substance in 4.5 µL of absolute ethanol was added to a mixture of 1.5 mL of phosphate buffer and 150 µL of n-octanol. The system was shaken for 3 min and afterwards centrifuged for 5 min at 13000 r/min. On a silica TLC plate 2.5 µL of the organic phase and 5 µL of the buffer phase were stippled four times, respectively. Partitioning of radioactivity in both phases was determined by an Instant Imager.

6.4.2 Animals

4-6 month old Wistar rats (230–250 g body weight) and 2-6 month old female NMRI mice of 18-22 g were purchased from Charles River laboratories (Wilmington, Massachusetts). All animals were kept under a natural light/dark cycle and had access to water and food ad libitum. The local government approved all procedures according to the German Law on the Protection of Animals (§§7-9 TierSchG). Animal experiments were also approved by the Animal Research Committee of the Scientific and Technical Advisory Board of the Research Center Jülich. For conducting *ex vivo* experiments with living animals the number of approval was AZ 9.93.2.10.35.07.244.

6.4.3 *In vitro* autoradiography of rat and mouse brain slices

After anesthetising and decapitation of the animals whole brains were rapidly removed and immediately frozen at -80 °C until use. Rat brain sections were prepared in a cryostat microtome (CM 3050; Leica; section thickness 20 µm) at -20 °C, thaw-mounted onto silica-coated object slides dried on silicagel overnight at 4 °C and stored at -80 °C until use.

Incubation conditions for *in vitro* autoradiography of all tested substances were similar to those previously described by Zhang et al.[246]. All incubations were performed at 22°C in Tris-HCl buffer (50 mmol/L, pH 7.4). After preincubation in buffer for 10 min rat brain slices were incubated in 5 nmol/L of [^{18}F]**33a** or [^{18}F]**33b** or [^{18}F]**33e** or 10 nmol/L of [^{18}F]**33d** and mouse brain slices in 20 nmol/L of [^{18}F]**33e** for 30 min either with 10 µmol/L competitor (spiperone or cold standard) or with the same amount of DMSO, respectively. They were washed twice for 5 min in ice-cold Tris-HCl buffer, rapidly rinsed with ice-cold distilled water, and placed under a stream of dry air for rapid drying. Object slides were exposed to a γ-sensitive film for 15-30 min and then laser scanned by a phosphor imager BAS 5000 (Fuji). The evaluation of receptor autoradiography was processed according to standard image analysis software (AIDA 2.31; Raytest Isotopenmeßgeräte, Germany). Nonspecific binding was defined as the residual activity in the presence of cold standard. Specific binding was calculated as the difference between total and nonspecific binding.

6.4.4 *Ex vivo* biodistribution in mouse model

1.1-2.6 MBq of [^{18}F]**33e** in 50 µL of saline (containing 1 % tween 80) was injected to the tail vain of female NMRI mice. Animals were killed by cervical dislocation and organs were removed immediately. All organs and blood were weighted and the radioactivity measured in a gamma-counter (Auto-Gamma® MINAXI 5000 Packard). Brains were rapidly frozen at -80 °C and cut into horizontal or sagittal sections (thickness, 40 µm) at -20 °C.

6.4.5 *In vivo* stability of [^{18}F]33e

In order to determine the stability of [^{18}F]**33e** in mouse serum, removed blood (n = 3) was centrifuged for separation of the plasma which was deproteinated with two volumes of acetonitrile. Samples of 2.5 µL were taken from the extract and analyzed by radio-TLC

using ethyl acetate/methanol/diethyl amine (96:2:2). In order to estimate the recovery of [^{18}F]**33e** in the extracted solution and to exclude loss of original radioligand or possible labelled metabolites, samples of 2.5 µL of origin blood and plasma were submitted to TLC analysis.

For the determination of possible brain metabolites, mouse brains (n = 3) were homogenized with a Potter Elvehjem homogenizer with two volumes of Tris HCl buffer (0.1 M pH 7.4) and treated like above described with two volumes of acetonitrile.

6.4.6 Staining of brain slices by cresyl violet

After total decay of the fluorine-18 in the brain sections, cresyl violet staining of cell nuclei of these sections was performed to identify the different brain regions. After fixation with neutral buffered formalin for 30 min at 4°C the sections were rinsed twice with water and thereafter incubated in cresyl violet solution (40 mM natrium acetate in 10% glacial acetic acid) for 30 min at 60 °C. After a short water rinse the sections were dehydrated by 70%, 80%, 90% and 100% of ethanol followed by a xylol bath, each step for 5 min. The staining was sealed with DPX Mountant for histology (Fluka).

7. Summary and Outlook

Dopamine is a multifunctional neurotransmitter in the human brain which influences modulation of behaviour and cognition, voluntary movement, motivation, punishment and reward, sleep, mood, attention and learning. These effects are mediated through the interaction of only 5 different receptor molecules from which few are reasonably understood. For the D_4 type of dopamine receptors, impact on sexual behaviour, substance abuse, attention and personality traits are postulated. However, the extremely low density of this receptor subtype in the brain leads to demanding requirements for radioligands. Therefore to a lack of appropriate ones exists for functional *in vivo* imaging which prevents from a systematic examination of this receptor type in man until now. Otherwise, lead structures of putative D_4 ligands are known from studies of structure-activity relationship. Mostly they are derivatives of a 1-phenyl-4-benzylpiperazine backbone. In this work the ^{18}F-labelling of a couple of such putative ligands was developed and their preliminary pharmacological evaluation performed.

The radiosynthesis of [^{18}F]FAUC 316 ([^{18}F]**1**), a ligand of high affinity, was not described before due to the requirement of a multistep and complex implementation of no-carrier-added (n.c.a.) [^{18}F]fluoride in the aromatic phenyl moiety. Fluoride was obtained by a ^{18}O(p,n)^{18}F nuclear reaction on a [^{18}O]H_2O water target at a cyclotron. Radiosynthesis of [^{18}F]**1** as authentic tracer is expedient, since it exhibits extremely high values of affinity and selectivity which are not conserved when analogue labelling like ^{18}F-fluoroalkylation is performed. Furthermore, aromatic C-F bonds are rather stable under *in vivo* conditions.

In the first steps of radiosynthesis of [^{18}F]FAUC 316 ([^{18}F]**1**) the known iodonium salts bis(4-bromophenyl)iodonium triflate (**16**) and bis(4-iodophenyl)iodonium triflate (**20**) were labelled by nucleophilic substitution with n.c.a. [^{18}F]fluoride to obtain radiochemical yields (RCY) of up to 60 % of 4-[^{18}F]fluorobromobenzene ([^{18}F]**21**) and 4-[^{18}F]fluoroiodobenzene ([^{18}F]**22**). Subsequently, they were cross-coupled by a Hartwig-

Buchwald reaction (HBC) with piperazine to yield 4-[^{18}F]fluorophenylpiperazine ([^{18}F]**28**) with a RCY of up to 70 %. Thereby **20** appeared as more favourable precursor with higher yields both with fluorination and coupling of [^{18}F]**22**. Due to decomposition during fluorination of both precursors and the formation of colloidal by-products with **20**, solid phase extraction for solvent exchange became rather complex and demanding. The HBC was primarily conducted with $Pd_2(dba)_3$ and the phosphine ligands DavePhos and RuPhos in toluene. The use of $Pd(OAc)_2$ was also possible obtaining similar yields. With other solvents, especially DMF, no or only poor yields were obtained.

The possibility of an acid extraction of the free amine [^{18}F]**28** resulted in a good pre-purification. A subsequent reductive amination reaction using $NaBH_3CN$ and acetic acid with 5-cyanoindole-2-carbaldehyde **10** led to [^{18}F]**1** in a high conversion rate of 80-90 % and an overall RCY (related to starting [^{18}F]F^-) at the end of synthesis (EOS) of about 10 % and a molar activity of about 90 GBq/µmol. In contrast, a direct HBC of [^{18}F]**22** with the benzyl protected 1-benzyl-2-(piperazin-1-ylmethyl)-*1H*-indole-5-carbonitrile (**14**) was not successful. However, this path would not offer advantages, neither in the number of synthetic steps nor in reaction time, but cause disadvantages of a more complex precursor synthesis and abolition of the pre-purification step and therefore was not further persecuted.

For its use in pharmacological evaluation radio high performance liquid chromatography (HPLC) purification of [^{18}F]**1** was developed using the modern pentafluorophenyl phase to separate from non-isotopic carrier. In addition, a prepurification by extraction was employed to minimise non-radioactive side products and to enable the subsequent radio HPLC purification, which finally resulted in a radiochemical purity of about 99 %.

With [^{18}F]**28** a new “small labelling compound” was developed, which proved convenient for the preparation of ^{18}F-labelled 1-(4-fluorophenyl)-4-phenalkylpiperazines which are not only a chemical lead structure of nearly all D_4 selective ligands but, known so far, also of many D_3, D_2 and even 5-hydroxytryptamine (5-HT) ligands.

In the specific case of [^{18}F]FAUC 316 it was shown by *in vitro* autoradiography of animal brain tissue that an extremely high amount of non-specific binding of about 90 % prevents this radioligand from an *in vivo* imaging with positron emission tomography (PET).

Therefore 6-(4-benzylpiperazine-1-yl)benzodioxine was selected as new lead structure where now the benzyl moiety is the fluorine-carrying side. This situation enabled a direct labelling procedure of the corresponding amide. In order to challange the problem of non-specific binding, in this case the basic structure was derivatized systematically towards more hydrophilic compounds. This proved possible without falling below the lower threshold of lipophilicity for penetration of the blood-brain-barrier, which is assumed at a Log *P*/*D* of about 1.5 to 2. Thus, beside the unsubstituted 6-(4-[4-fluorobenzyl]piperazine-1-yl)benzodioxine (**33a**) with a Log $P_{7.4}$ of 2.7, the derivatives 6-(4-[4-fluoro-(3-methoxybenzyl)]piperazine-1-yl)benzodioxine (**33b**) with a Log $P_{7.4}$ of 2.4, 6-(4-[4-fluoro-(3-hydroxybenzyl)]piperazine-1-yl)benzodioxine (**33d**) with a Log $P_{7.4}$ of 1.7 and 6-(4-[6-fluoropyridin-3-yl]piperazine-1-yl)benzodioxine (**33e**) with a Log $P_{7.4}$ of 1.9 were successfully prepared. Direct labelling of the analoguously synthesized precursor 4-(2,3-dihydrobenzo[*b*][1,4]dioxin-6-yl)piperazin-1-yl)(4-nitrophenyl)methanone (**32b**) resulted in a radiochemical yield of 50 % of and subsequent reproducible reduction of the amide to the amine ([^{18}F]**33a**) resulted in a RCY of about 40 %. Nevertheless, the overall RCY after HPLC separation at the end of synthesis was only about 5 %.

In contrast the 2-step build up reaction starting from the labelled aldehydes 4-[^{18}F]fluorobenzaldehyde ([^{18}F]**34a**), 4-[^{18}F]fluoro-3-methoxybenzaldehyde ([^{18}F]**34b**), 4-[^{18}F]fluoro-3-benzyloxybenzaldehyde ([^{18}F]**34c**), 6-[^{18}F]fluoronicotinaldehyde ([^{18}F]**34e**) resulted in significant higher yields. For the ^{18}F-fluorination of the aldehydes the excellent leaving group trimethylammonium triflate could be employed, what was not possible for the direct labelling of **32b**. Using this leaving group for S_NAr of the aldehydes, RCY of 70-80 % were achieved which were on average 50 % higher than with the nitro leaving group.

For the subsequent coupling of the aldehydes to the pierazine **30** the above described reductive amination using $NaBH_3CN$ and acetic acid was used. Both reaction steps, fluorination and reductive amination, could be performed in DMSO without interim separation. Thereby RCY at the end of synthesis and HPLC-purification of 35 %, 20 %, and 15 % were obtained with [^{18}F]**33a**, [^{18}F]**33b**, and [^{18}F]**33e**, respectively, and with molar activities of 30-60 GBq/µmol. In this case the build-up synthesis exceeds the normally desired direct labelling in yield and reaction time. [^{18}F]**33d** required the additional cleavage of the benzyl protection group of the intermediate [^{18}F]**33c** using Pd and

ammonium formate in methanol, which was almost quantitative with a total RCY of 9 %. Fixation of [^{18}F]**33c** on a lipophilic EN cartridge led to a good pre-purification. Nevertheless, the RCY of [^{18}F]**33d** was the lowest due to the additional purification and reaction step.

Results confirm that the reductive amination reaction with $NaBH_3CN$ is an excellent method in radiofluoro-chemistry leading to high yields in short reaction times with high reproducibility. Especially the latter is decisive and not general with n.c.a. syntheses. Since dimethylsulfoxid (DMSO) is an excellently suited solvent for fluorination and reductive amination the whole procedure is simplified distinctly, since interim isolation is obsolete.

In vitro autoradiographic competing binding studies on rat brain slices of [^{18}F]**33a**, [^{18}F]**33b**, [^{18}F]**33d** and [^{18}F]**33e** with the unlabelled standard compounds and spiperone confirmed the dependence of non-specific binding on lipophilicity. While [^{18}F]**33a** and [^{18}F]**33b**, as well as [^{18}F]FAUC 316 before, were not suitable for further applications due to a high non-specific binding of 96 % and 79 %, respectively, the less lipophilic ligands [^{18}F]**33d** and [^{18}F]**33e** with a non-specific binding fraction of 33 % and 7 %, respectively, showed excellent qualifications.

The pyridine derivative [^{18}F]**33e** got preference over [^{18}F]**33d** and was selected for further pharmacological evaluation due to its better selectivity and its lowest non-specific binding as well as shorter radiosynthesis. The time dependence of organ uptake and metabolism as well as *ex vivo* distribution in brain was determined with Naval Medical Research Institute (NMRI) mice. The brain uptake of [^{18}F]**33e** amounted with 5 %ID/g after 5 min and still 1 %ID/g after 30 min exceedingly high. All observed peripheral metabolites were hydrophilic and did not penetrate the blood brain barrier. Defluorination was excluded due to a low bone uptake, and no significant metabolites were observed in brain. *Ex vivo* autoradiography showed an accumulation of [^{18}F]**33e** in parts of the limbic system, especially the hippocampus, as well as the frontal cortex. These are regions where occurrence of the D_4 receptor is postulated. Only the high accumulation in cerebellum could not be concretely explained but is not necessarily negative.

In conclusion, with [^{18}F]**33e** a radioligand was developed which holds great promise as tracer for the *in vivo* visualization of the D_4 receptor system. The results encourage

continued evaluation in preclinical studies using small animal PET. In case of a confirmation of the pharmacological parameters determined and the density distribution pattern with *in vivo* experiments, the whole radiosynthesis has to be adapted to a procedure suitable for an automated synthesis device. Since one-pot syntheses require few reaction and separation steps the automation of the radiosynthesis appears feasible.

8. Literature

[1] Gerrison, F.H. *History of Medicine* **1966**, Philadelphia: W.B. Saunders Company.

[2] Kuhar, M.J.; Murrin, L.C.; Malouf, A.T.; Klemm, N. Dopamine receptor binding in vivo: the feasibility of autoradiographic studies. *Life Sci.* **1977**, *22*, 203-210.

[3] Korenman, S.G.; Sherman, B.M. Radioligand assay in reproductive biology. *Sem. Nucl. Med.* **1975**, *5*, 263-272.

[4] Sandler, M.P.; Coleman, R.E.; Patton, J.A.; Wackers, F.J.Th.; Gottschalk, A. *Diagnostic nuclear medicine.* [4]**2002**, Philadelphia: Lippincott Williams & Wilkins.

[5] Wong, D.F.; Pomper, M.G. Predicting the success of a Radiopharmaceutical for In Vivo Imaging of Central Nervous System Neuroreceptor System. *Molecular Imaging and Biology.* **2003**, *5*, 350-362.

[6] Wagner, H.N.; Jr.; Burns, H.D.; et al. Imaging dopamine receptors in human brain by positron tomography. *Science.* **1983**, *221*, 1264-1266.

[7] Maziere M., Berger G. and Comar D. ^{11}C-Clomipramine: synthesis and analysis. *J. Radioanalyt. Chem.* **1978**, *45*, 453.

[8] Coenen, H.H. personal communication, **SS2010**, lecture: *Radionuclides in life science.*

[9] Mazière, B.; Coenen, H.H.; Halldin, C.; Någren, K.; Pike, V.W. PET Radioligands for dopamine receptors and re-uptake sites: Chemistry and biochemistry. *Nucl. Med. Biol.* **1992**, *19*, 497-512.

[10] Olivier, B.; van Wijngaarden, I.; Soudijn, W. *Serotonin Receptors and their ligands*. **1997**, Elesvier.

[11] Parsey, R.V. Serotonin Receptor Imaging: Clinically Useful? *J. Nucl. Med.* **2010**, *51*, 1495-1498.

[12] Ritz, M.C.; Cone, E.J.; Kuhar, M.J. Cocaine inhibition of ligand binding at dopamine, norepinephrine and serotonin transporters: A structure-activity study. *Life sciences* **1990**, *46*, 635-645.

[13] Pirker, W.; Asenbaum, S.; Hauk, M. Imaging Serotonin and Dopamine Transporters

with ^{123}I-β-CIT SPECT: Binding Kinetics and Effects of Normal Aging. *J. Nucl. Med.* **2000**, *41*, 36-44.

[14] Drewes, B.; Sihver, W.; Willbold, S.; Olsson, R.A.; Coenen, H.H. New 2α-tropane amides as potential PET ligands for the dopamine transporter. *Nucl. Med. Biol.* **2007**, *34*, 531-539.

[15] Ermert, J.; Hamacher, K.; Coenen, H.H. N.C.A. ^{18}F-labelled norephedrine derivatives via α-aminopropiophenones. *J. Label. Compd. Radiopharm.* **2000**, *43*, 1345-1363.

[16] Horti, A.G.; Gao, Y.; Kuwabara, H.; Dannals, R.F. Development of radioligands with optimized imaging properties for quantification of nicotinic acetylcholine receptors by positron emission tomography. *Life sciences* **2010**, *86*, 575-584.

[17] Eckelman, W.C. Curr. Imaging of muscarinic receptors in the central nervous system. *Pharm. Design* **2006**, *12*, 3901-3913.

[18] Bartenstein, P. PET in Neuroscience. Dopaminergic, GABA/benzodiazepine, and opiate system. *Nuklearmedizin* **2004**, *43*, 33-42.

[19] Boy, C.; Holschbach, M.; Herzog, H.; Bauer, A.; Coenen, H.H.; Zilles, K. Preoperative studies in epilepsy surgery: Analysis of GABA and adenosine receptors in pharmacoresistant focal temporal epilepsy via positron emission tomography (PET). *Klinische Neurophysiologie* **2002**, *32*, 147-155.

[20] Windhorst, A.D.; Albert, D.; Leurs, R.; Menge, W.M.P.B.; Timmerman, H.; Herscheid, J.D.M. Synthesis of radioligands for the histamine H3 receptor. *Pharmacochemistry Library* **1998**, *30*, 159-174.

[21] Mishina, M. Positron emission tomography for brain research. *J. Nipp. Med. School* **2008**, *2*, 259-270.

[22] Cohen, R.M. The Application of Positron-Emitting Molecular Imaging Tracers in Alzheimer's Disease. *Mol. Imaging Biol.* **2007**, *9*, 204-216.

[23] Nordberg, A. PET imaging of amyloid in Alzheimer's disease. *Lancet. Neurol.* **2004**, *3*, 519.

[24] Cai, L.S.; Innis, R.B.; Pike, V.W. Radioligand Development for PET Imaging of β-Amyloid (Aβ)-Current Status. *Curr. Med. Chem.* **2007**, *14*, 19-52.

[25] Frankle, W.G.; Slifstein, M.; Talbot, P.S.; Laruelle, M. Neuroreceptor imaging in psychiatry: theory and applications. *Internat. Rev. Neurobiol.* **2005**, *67*, 385-440.

[26] Frankle, W.G.; Laruelle, M. Neuroreceptor imaging in psychiatric disorders. *Annals*

Nucl. Med. **2002**, *16*, 437-446.

[27] Larisch, R.; Klimke, A.; Hamacher, K.; Henning, U.; Estaji, S.; Hohlfeld, T.; Vosberg, H.; Tosch, M.; Gaebel, G.; Coenen, H.H.; Muller-Gartner, H.W. Influence of synaptic serotonin level on [18F]altanserin binding to 5HT2 receptors in man. *Behav. Brain. Res.* **2003**, *139*, 21-29.

[28] Weber, W.A. Positron Emission Tomography As an Imaging Biomarker. *J. Clin. Oncol.* **2006**, *24*, 3282-3292.

[29] Langen, K.J.; Hamacher, K.; Weckesser, M.; Floeth, F.; Stoffels, G.; Bauer, D.; Coenen, H.H.; Pauleit, D. O-(2-[^{18}F]fluoroethyl)-l-tyrosine: uptake mechanisms and clinical applications. *Nucl. Med. Biol.* **2006**, *33*, 287-294.

[30] Laven, D.L.; Bednarczyk, E.M. CNS Assessment Using Functional Neuro-PET Imaging. *J. Pharmacy Practice* **2001**, 14, 308-331.

[31] Schelbert, H.R.; Schwaiger, M. PET studies of the heart. In: Phelps, M.; Mazziotta, J.; Schelbert, H. (eds.): *Positron Emission Tomography and Autoradiography*: Principles and Applications for the Brain and Heart. **1986**, Raven, New York, 581-661.

[32] Schwaiger, M.; Ziegler, S.; Nekolla, S.G. PET/CT: Challenge for Nuclear Cardiology. *J. Nucl. Med.* **2005**, *46*, 1664-1678.

[33] Dekemp, R.A.; Yoshinaga, K.; Beanlands, R.S.B. Will 3-dimensional PET-CT enable the routine quantification of myocardial blood flow? *J. Nucl. Cardiol.* **2007**, *14*, 380-397.

[34] Pissarek, M.; Ermert, J.; Oesterreich, G.; Bier. D.; Coenen, H.H. Relative Uptake, Metabolism, and β-Receptor Binding of (1R,2S)-4-^{18}F-Fluorometaraminol and ^{123}I-MIBG in Normotensive and Spontaneously Hypertensive Rats. *J. Nucl. Med*. **2002**, *43*, 366-373.

[35] Loveland, W.D.; Morrisey, D.J.; Seaborg, G.T. "*Modern Nuclear Chemistry*", Wiley Interscience, Hoboken, **2006**.

[36] Phelps, M.E. Positron emission tomography provides molecular imaging of biological processes. *PNAS* **2000**, *16*, 9226-9233.

[37] Phelps, M.E.; Mazziotta, J.; Schelbert, H.; *Positron Emission Tomography and Autoradiography.* Raven Press, New York **1986**.

[38] Herzog, H. In vivo functional imaging with SPECT and PET. *Radiochim. Acta* **2001**, *89*, 203-214.

[39] Boellaard, R. Standards for PET image acquisition and quantification data analysis. *J*

Nucl. Med. **2009**, *50*, S11-S20.

[40] Steinbach, J. Opening speech of the 17th annual meeting of the german work group in radiochemistry and radiopharmacy. Schellerhau, **2009**.

[41] Coenen, H.H.; Elsinga, P.H.; Iwata, R.; Kilbourn, M.R.; Pillai, M.R.A.; Rajan, M.G.R.; Wagner Jr. H.N.; Zaknun, J.J. Fluorine-18 radiopharmaceuticals beyond [18F]FDG for use in oncology and neurosciences. *J. Nucl. Med. Biol.* **2010**, *37*, 727-740.

[42] Qaim, S.M.; Coenen, H.H. Produktion pharmazeutisch relevanter Radionuklide. *Pharmazie in unserer Zeit.* **2005**, *34*, 460-466.

[43] Coenen, H.H. Radiopharmazeutische Chemie: Grundlagen zur in vivo Untersuchung molekularer Vorgänge mit PET. *Der Nuklearmediziner.* **1994**, *17*, 203.

[44] Stöcklin, G.; Quaim, S.M.; Rösch, F. The Impact of Radioactivity on Medicine. *Radiochimica Acta.* **1995**, *70/71*, 249.

[45] Stöcklin, G.; Pike. V.W. (eds.) *Radiopharmaceuticals for Positron Emission Tomography.* Methodical Aspects. Kluwer Academic Publishers, Dordrecht, Boston, London, **1993**.

[46] http://www.erigal.co.uk

[47] Hess, E.; Blessing, G.; Coenen, H.H.; Qaim, S.M. Improved target system for production of high purity [^{18}F]fluorine via the ^{18}O(p,n)^{18}F reaction. *Appl. Radiat. Isot.* **2000**, *52*, 1431-1440.

[48] Lieser, K.H. *Einführung in die Kernchemie.* Verlag Chemie, Weinheim, **1980**.

[49] Quaim, S.M.; Stöcklin, G. Production of some medically important short-lived neutron deficient radioisotopes of halogens. *Eur. J. Nucl.Med.* **1994**, *21*, 1151-1165.

[50] Coenen, H.H.; Franken, K.; Kling, P.; Stöcklin, G. Direct electrophilic radiofluorination of phenylalanine, tyrosine and DOPA. *Appl. Radiat. Isot.* **1988**, *39*, 1243-1250.

[51] Firnau, G.; Chirakal, R.; Sood, S.; Garnett, S. Aromatic fluorination with xenon difluoride: L-3,4-dihydroxy-6-fluoro-phenylalanine. *Can. J. Chem.* **1980**, *58*, 1449-1450.

[52] Coenen, H.H.; Franken, K.; Kling, P.; Stöcklin, G. Direct electrophilic radiofluorination of phenylalanine, tyrosine and dopa. *Int. J. Radiat. Appl. Instrum.* Part A. **1988**, *39*, 1243-1250.

[53] Fowler, J.S.; Shiue, C.Y.; Wolf, A.P.; Salvadori, P.A.; MacGregor, R.R. Synthesis of ^{18}F-labeled acetyl hypofluorite for radiotracer synthesis. *J. Label. Compd. Radiopharm.*

1982, *19*, 1634-1636

[54] Chirakal, R.; Firnau, G; Schrobilgen, G.J.; mcKey, J.; Garnett, E.S. The synthesis of [^{18}F]fluoride gas. *Appl. Radiat. Isot.* **1984**, *35*, 401-404.

[55] Tressaud, A.; Haufe, G. in: *Fluorine and Health: Molecular imaging, Biomedical materials and Pharmaceuticals.* **2008**, Elsevier Science

[56] Coenen, H.H. in: *PET chemistry: the driving force in molecular imaging.* Schubiger, P.A.; Lehmann, L.; Friebe, M. (eds.) **2007**, Chap. 2, 20.

[57] Taylor, S.D.; Kotoris, C.C.; Hum, G. Recent advances in electrophilic fluorination. *Tetrahedron* **1999**, *55*, 12431-12477.

[58] Coenen, H.H.; Klatte, B.; Knöchel, A.; Schüller, M.; Stöcklin, G. Preperation of n.c.a. 17-[^{18}F]fluoroheptadecanoic acid in high yields via aminopolyether supported nucleophilic fluorination. *J. Label. Compd. Radiopharm.* **1986**, *23*, 455-467.

[59] Block, D.; Klatte, B.; Knöchel, A.; Beckmann, R.; Holm, U. N.c.a. ^{18}F-labelling of aliphatic compounds in high yields via aminopolyether supported nucleophilic substitution. *J. Label. Compd. Radiopharm.* **1986**, *23*, 468-477.

[60] Coenen, H.H. No-carrier-added ^{18}F-chemistry of radiopharmaceuticals. In: *Synthesis and application of isotopically labeled compounds.* Baillie, T.A.; Jones, J.R. (eds.), Elsevier Science Publishers, Amsterdam **1989**, 443-448.

[61] Stöcklin G.; Handbuch der medizinischen Radiologie, Band 15/1B, Emissions-Computertomographie mit kurzlebigen Zyclotron-produzierten Radionukliden, **1989**, Springer, Berlin.

[62] Hammett, Louis P. The Effect of Structure upon the Reactions of Organic Compounds. Benzene Derivatives. *J. Am. Chem. Soc.* **1937**, 59**,** 96-103.

[63] Hamacher, K.; Coenen, H.H.; Stöcklin, G. Efficient stereospecific synthesis of no-carrier-added 2-[^{18}F]fluoro-2-deoxy-D-glucose using aminopolyether supported nucleophilic substitution. *J. Nucl. Med.* **1986**, *27*, 235-238.

[64] Ermert, J.; Gail, R.; Coenen, H.H. *J. Label. Compd. Radiopharm.* **1995**, *37*, 581-583.

[65] Sun, H.; DiMagno, S.G. Competetive demethylation and substitution in N,N,N-trimethylanilinium fluoride. *J. Fluor. Chem*. **2007**, *128*, 806-812.

[66] Karramkam, M.; Hinnen. F.; Berrehouma, M.; Hlavacek, C.; Vaufrey, F.; Halldin, C.; McCarron, J.A.; Pike, V.W.; Dollé, F. Synthesis of a [6-pyridinyl-18F]-labelled fluoro derivative of WAY-100635 as a candidate radioligand for brain 5-HT1*A* receptor

imaging with PET. *Bioorg. Med. Chem.* **2003**, *11*, 2769–2782.

[67] Ludwig, T.; Ermert, J.; Coenen, H.H. 4-[^{18}F]fluoroarylalkylethers via an improved synthesis of n.c.a. 4-[^{18}F]fluorophenol. Nucl. Med. Biol. 2002, 29,255-262.

[68] Kilbourn, M.R.; Dence, C.S.; Welch, M.J.; Mathias, C.J.; Fluorine-18 labeling of proteins. *J. Nucl.Med.* **1987**, *28*, 462-470.

[69] Ding, Y.S.; Fowler, J.S.; Dewey, S.L.; Wolf, A.P.; Logan, J.; Gatley, S.J.; Volkow, N.D.; Shea, C.; Taylor, D.P. Synthesis and PET studies of fluorine-18-BMY 14802: a potential antipsychotic drug. *J. Nucl. Med.* **1993**, *34*, 246-254.

[70] Shiue, C.Y,; Fowler, J.S.; Wolf, A.P.; McPherson, D.W.; Arnett, C.D.; Zecca, L. No-carrier-added fluorine-18-labeled N-methylspiroperidol: synthesis and biodistribution an mice. *J. Nucl. Med.* **1986**, *27*, 226-234.

[71] Lemaire, C.; Guillaume, M.; Christiaens, L.; Palmer, A.J.; Cantineau, R.A.; A new route for the synthesis of [^{18}F]fluoroaromatic substituted amino acids: no carrier added L-p-[^{18}F]fluorophenylalanine. *Appl. Radiat. Isot.* **1987**, *38*, 1033-1038.

[72] Ding, Y.S.; Shiue, C.Y.; Fowler, J.S.; Wolf, A.P.; Plenevaux, A. No-carrier-added (NCA) aryl [^{18}F]fluorides via the nucleophilic aromatic substitution of electron-rich aromatic rings. *J. Fluorine Chem.* **1990**, *48*, 189-205.

[73] Forngren, T.; Anderson, Y.; Lamm, B.; Langstrom, B. Synthesis of 4-[^{18}F]-1-bromo-4-fluorobenzene and ist use in palladium-promoted cross-coupling reactions with organostannanes. *Acta Chimica. Skandinavia.* **1998**, *52*, 475-479.

[74] Shiue, G.G.; Schirrmacher, R.; Shiue, C.Y.; Alave, A.A.; Synthesis of fluorine-18 labeled sulfonureas as β-cell imaging agents. *J. Label. Compd. Radiopharm.* **2001**, *44*, 127-139.

[75] Parent, E.E.; Dence, C.S.; Jenks, C.; Sharp, T.L.; Welsh, M.J.; Katzenellenbogen, J.A. Synthesis and biological evaluation of [^{18}F]bicalutamide, 4-[^{76}Br]bromobicalutamide and 4-[^{76}Br]bromothiobicalutamide as non-steroidal androgens for prostate cancerimaging. *J. Med. Chem.* **2007**, *50*, 1028-1040.

[76] Knust, E.J.; Machulla, H.J.; Molls, M. ^{18}F-Production in a water target with high yields for ^{18}F-labelling of organic compounds: Synthesis of 6-[^{18}F]-nicotinic acid diethylamid. *J. Label. Compd. Radiopharm.* **1982**, *19*, 1643-1644.

[77] Dolci, L. Dolle, F.; Jubeau, S.; Vaufrey, F.; Crouzel, C. 2-[^{18}F]Fluoropyridines by no-carrier-added nucleophilic aromatic substitution with [^{18}F]FK-K_{222}-a comparative

study. *J. Label. Compd. Radiopharm.* **1999**, *42*, 975-985.

[78] Shiue, C.Y.; Watanabe, M.; Wolf, A.P.; Fowler, J.S.; Salvadori, P. Application of nucleophilic substitution reaction to synthesis of no-carrier-added [^{18}F]fluorobenzene and other ^{18}F-labeled aryl fluorides. *J. Label. Compd. Radiopharm.* **1984**, *21*, 533-547.

[79] Predeep, K.G.; Sudha, G.; Zalutsky, M.R. Fluorine-18 labelling of monoclonal antibodies and fragments with preservation of immunoreactivity. *Bioconj. Chem.* **1991**, *2*, 44-49.

[80] Vaidyanathan, G.; Affleck, D. J.; M.R.; Zalutsky, M.R. (4-[^{18}F]Fluoro-3-iodobenzyl)guanine, a potential MIBG analogue for positron emission tomography. *J. Med. Chem.* **1994**, *37*, 3655-3662.

[81] Block, D.; Coenen, H.H.; Stöcklin, G. The N.C.A. nucleophilic ^{18}F-fluorination of 1,N-disubstituted alkanes as fluoroalkylation agents *J. Label. Compd. Radiopharm.* **1987**, *24*, 1029-1042.

[82] Coenen, H.H.; Colosimo, M.; Schüller, M.; Stöcklin, G. Preparation of N.C.A. [^{18}F]-CH_2BrF via aminopolyether supported nucleophilic substitution. *J. Label. Compd. Radiopharm.* **1986**, *23*, 587-595.

[83] Coenen, H.H.; Ermert, J. Direct nucleophilic 18F-fluorination of electron-rich arenes: Present limits of no-carrier-added reactions. *Curr. Radiopharm. Chem.* **2010**, *3*, 163-173.

[84] Ermert, J.; Coenen, H.H. No-carrier-added [^{18}F]fluorobenzene derivatives as intermediates for built-up radiosyntheses. *Curr. Radiopharm. Chem.* **2010**, *3*, 127-160.

[85] Pike, V.W.; Aigbirhio, F.I. Reactions of cyclotron-produced [^{18}F]fluoride with diaryliodonium salts—a novel single-step route to no-carrier-added [^{18}F]fluoroarenes *J. Chem. Soc. Chem. Commun.* **1995**, 2215-2216.

[86] Olah, G.A.; Sakakibara, T.; Asensio, G. Onium ions. 17. Improved preparation, carbon-13 nuclear magnetic resonance structural study, and nucleophilic nitrolysis (nitrative cleavage) of diarylhalonium ions. *J. Org. Chem.* **1978**, *43*, 463-468.

[87] Lancer, K.M.; Wiegand, G.H. The ortho effect in the pyrolysis of iodonium halides. A case for a sterically controlled nucleophilic aromatic (SN) substitution reaction. *J. Org. Chem.* **1976**, *41*, 3360-3364.

[88] Yamada, Y.; Okawara, M. Steric Effect in the Nucleophilic Attack of Bromide Anion on

Diaryl- and Aryl-2-thienyliodonium Ions. *Bull. Chem. Soc. Jpn.* **1972**, *45*, 1860-1863.

[89] Hoffman, R.; Howell, J.M.; Muetterties, E.L. Molecular orbital theory of pentacoordinate phosphorus. *J. Am. Chem. Soc.* **1972**, *94*, 3047-3058.

[90] Reich, H.J.; Cooperman, C.S. Structure and stereolability of triaryliodine (III) compounds. Degenerate isomerization of 5-phenyl-5H-dibenziodole. *J. Am. Chem. Soc.* **1973**, *95*, 5077-5078.

[91] Grushin, V.V.; Demkina, I.I.; Tolstaya, T.P. Unified Mechanistic Analysis of Polar Reactions of Diaryliodonium Salts. *J. Chem. Soc. Perkin. Trans.* **1992**, *2*, 505-511.

[92] Wadsworth, H.J.; Widdowson, D.A.; Wilson, E.; Carroll, M.A.; *PCT Int. Appl.* **2005**, WO 2005061415, 1-32.

[93] Carrol, M.A.; Nairne, J.; Smith, G.; Widdowson, D.A. *J. Fluor. Chem.* **2007**, *128*, 127-132.

[94] Ross, T.L.; Ermert, J.; Hocke, C.; Coenen, H.H. Nucleophilic ^{18}F-Fluorination of Heteroaromatic Iodonium Salts with No-Carrier-Added [^{18}F]Fluoride. *J. Am. Chem. Soc.* **2007**, *129*, 8018–8025

[95] Ermert, J.; Hocke, C.; Ludwig, T.; Gail, R.; Coenen, H.H. Comparison of pathways to the versatile synthon of no-carrier-added 1-bromo-4-[^{18}F]fluorobenzene. *J. Label. Compds. Radiopharm.* **2004**, *47*, 429-441.

[96] Gail, R.; Hocke, C.; Coenen, H.H. Direct n.c.a. ^{18}F-fluorination of halo- and alkylarenes via corresponding diphenyliodonium salts. *J. Label. Compds. Radiopharm.* **1997**, 40, 50-52.

[97] Walter, W.; Francke, W. *Beyer Walter – Lehrbuch der Organischen Chemie*, ^{23}**2003**, Hirzel Verlag Stuttgard.

[98] Zhang, M.-R.; Kumata, K.; Suzuki, K. A practical route for synthesizing a PET ligand containing [^{18}F]fluorobenzene using reaction of diphenyliodonium salt with [^{18}F]F^{-}. *Tetrahedron Lett.* **2007**, 48, 8632-8635.

[99] Huisgen, R. 1,3-Dipolar Cycloadditions. *Proceed. Chem. Soc. Lon.* **1961**, 357-396.

[100] Kolb, H.C.; Finn, M.G.; Sharpless, B. Click chemistry: diverse chemical function from a few good reactions. *Angewandte Chemie Int. Edit.* **2001**, *40*, 2004-2021.

[101] Moses, J.E.; Moorhouse, A.D. The growing applications of click chemistry. *Chem. Soc. Rev.* **2007**, *36*, 1249-1262.

[102] Ross, T.L. The click-chemistry approach applied zo fluorine-18. *Curr. Radiophar.* **2010**,

3, 202-223.

[103] Tykwinski, R.R. Evolution in the palladium-catalyzed cross-coupling of sp- and sp(2)-hybridized carbon atoms. *Angew. Chemie Intern. Edit.* **2003**, *42*, 1566-1568.

[104] Negishi, E. Transition metal-catalyzed organometallic reactions that have revolutionized organic synthesis. *Bull. Chem. Soc. Jap.* **2007**, *80*, 233-257.

[105] Gail, R.; Coenen, H.H. *Appl. Radiat. Isot.* **1994**, *45*, 105-111.

[106] Forngren T, Andersson Y, Lamm B, Långström B. Synthesis of 4-[^{18}F]-1-Bromo-4-fluorobenzene and its Use in Palladium-Promoted Cross-Coupling Reactions with Organostannanes. *Acta Chem. Scand.* **1998**, *52*, 475–479.

[107] Allain-Barbier L, Lasne M-C, Perrio-Huard C, Moreau B, Barr!e L. Synthesis of 4-[^{18}F]fluorophenyl-alkines and arenes via Palladium catalyzed coupling of 4-[^{18}F]fluoroiodobenzene with vinyl and aryl tin reagents. *Acta Chem. Scand.* **1998**, *52*, 480–489.

[108] Marriere E, Rouden J, Tadino V, Lasne M.-C. Synthesis of Analogues of (-)-Cytisine for in Vivo Studies of Nicotinic Receptors Using Positron Emission Tomography. *Organic. Lett.* **2000**, *2*, 1121-1124

[109] Wüst, F.R.; Kniess, T. No-carrier added synthesis of ^{18}F-labelled nucleosides using Stille cross-coupling reactions with 4-[^{18}F]fluoroiodobenzene. *J. Label. Compd. Radiopharm.* **2004**, *47*, 457-468.

[110] Wüst, F.R.; Kniess, T. Synthesis of 4-[^{18}F]fluoroiodobenzene and its application in sonogashira cross-coupling reactions. *J. Label. Compd. Radiopharm.* **2003**, *46*, 699-713.

[111] Marriére, E.; Chazalviel, L.; Dhilly, M.; Toutain, J.; Perrio, C.; Dauphin, F.; Lasne, M.C. *J. Label. Compd. Radiopharm.* **1999**, *42*, S69-S71.

[112] Wüst, F.R.; Kniess, T. *N*-Arylation of indoles with 4-[^{18}F]fluoroiodobenzene: synthesis of ^{18}F-labelled σ_2 receptor ligands for positron emission tpmography (PET). *J. Label. Compd. Radiopharm.* **2005**, 4831-43.

[113] Steiniger, B.; Wüst, F. Synthesis of ^{18}F-labelled biphenyls via SUZUKI cross-coupling with 4-[^{18}F]fluoroiodobenzene. *J. Label. Compd. Radiopharm.* **2006**, *49*, 817–827.

[114] Paul, F.; Patt, J.; Hartwig, J.F. Palladium-catalyzed formation of carbon-nitrogen bonds. Reaction intermediates and catalyst improvements in the hetero cross-coupling of aryl halides and tin amides. *J. Am. Chem. Soc.* **1994**, *116*, 5969-5970.

[115] Guram, A.S.; Buchwald, S.L. Palladium-Catalyzed Aromatic Aminations with in situ Generated Aminostannanes. *J. Am. Chem. Soc.* **1994**, *116*, 7901-7902.

[116] Cheng, Y.-C., Prusoff, W.H. Relationship between the inhibition constant (Ki) and the concentration of inhibitor which causes 50 per cent inhibition (I_{50}) of an enzymatic reaction. *Biochem. Pharmacol.* **1973**, *22*, 3099-3108.

[117] Kebabian, J.W.; Petzold, G.L.; Greengard, P. Dopamne-sensitive adenylate cyclase in caudate nucleus of rat brain, and its similarities to the "dopamine receptor". *Proc. Natl. Acad. Sci. USA* **1972**, *69*, 2145-2149.

[118] Kebabian, J.W.; Calne, D.B. Multiple receptors for dopamine. *Nature* **1979**, *277*, 93-96.

[119] Seeman, P.; Van Tol, H.H.M. Dopamine receptor pharmacology. *Trends. Pharmacol. Sci.* **1994**, *15*, 264-270.

[120] Sunahara RK, Guan HC, O´Dowd BF, Seeman P, Laurier LG, George SR, Torchia J, Van Tol HH, Niznik HB. Cloning of the gene for a human dopamine D5 receptor with higher affinity for dopamine than D1. *Nature* **1991**, *350*, 614- 619.

[121] Sokoloff P, Giros B, Martres MP, Barthenet ML, Schwartz JC. Molecular cloning and characterisation of a novel dopamine receptor (D3) as a target for neuroleptics. *Nature* **1990**, *347*, 146-151.

[122] Van Tol HH, Bunzow JR, Guan HC, Sunahara RK, Seeman P, Niznik HB, Civelli O. Cloning of the gene for a human dopamine D4 receptor with high affinity for the antipsychotic clozapine. *Nature* **1991**, *350*, 610-614.

[123] Jose PA, Raymond JR, Bates MD, Aperia A, Felder RA, Carey RM. The renal dopamine receptors. *J. Am. Soc. Nephrol.* **1992**, *2*, 1265-1278.

[124] Civelli, O.; Bunzow, J.R.; Grandy, D.K. Molecular diversity oft he dopamine receptors. *Annu. Rev. Pharmacol. Toxicol.* **1993**, *33*, 281-307.

[125] Jackson, D.M.; Westlind-Danielsson, A. Dopamine receptors: molecular biology, biochemistry and behavioural aspects. *Pharmacol. Ther.* **1994**, *64*, 291-370.

[126] Seeman, P.; Van Tol, H.H. Dopamine receptor pharmacology. *Trends. Pharmacol. Sci.* **1994**, *15*, 264-270.

[127] Neve, K.A.; Seamans, J.K.; Trantham-Davidson, H. Dopamine receptor signaling. *J. Recept. Signal Transduct. Res.* **2004**, *24*, 165–205.

[128] Lahti, R.A.; Roberts, R.C.; Cochrane, E.V. Direct determination of dopamine D_4

receptors in normal and schizophrenic postmortem brain tissue: a [3H]NGD-94–1 study. *Mol. Psychiatry.* **1998**, *3*, 528–533.

[129] Primus, R.J.; Thurkauf, A.; Xu, J. Localization and characterization of dopamine D4 binding sites in rat and human brain by use of the novel, D4 receptor- selective ligand 3H-NGD 94–1. *J. Pharmacol. Exp. Ther.* **1997**, *282*, 1020–1027.

[130] Noaín, D.; Avale, M.E.; Wedemeyer, C.; Calvo, D.; Peper, M.; Rubinstein, M. Identification of brain neurons expressing the dopamine D_4 receptor gene using BAC transgenic mice. *Eur. J. Neurosci.* **2006**, *24*, 2429-2438.

[131] Oak, J.N.; Oldenhof, J.; Van Tol, H.H. The dopamine D(4) receptor: one decade of research. *Eur. J. Pharmacol.* **2000**, *405*, 303-27.

[132] Van Tol, H.H.; Bunzow, J.R.; Guan, H.-C.; Sunahara, R.K.; Seeman, P.; Niznik, H.B.; Civelli, O. Cloning of the gene for a human D_4 receptor with high affinity for the antipsychotic clozapine. *Nature* **1991**, *350*, 610–614.

[133] Matsumotu, M.; Hidaka, K.; Tada, S.; Tasaki, Y.; Yamaguchi, T. Full-length cDNA cloning and distribution of human dopamine D4 receptor. *Molecular Brain Research* **1995**, *29*, 157-162.

[134] Lidow, M.S.; Wang, F.; Cao, Y.; Goldman-Rakic, P.S. Layer V neurons bear the majority of mRNAs encoding the five distinct dopamine receptor subtypes in the primate prefrontal cortex. *Synapse* **1998**, *28*, 10-20.

[135] Ariano, M.A.; Wang, J.; Noblett, K.L.; Larson, E.R.; Sibley, D.R. Cellular distribution of the rat D4 dopamine receptor protein in the CNS using anti-receptor antisera. *Brain Res.* **1997**, *752*, 26-34.

[136] Helmeste, D.M.; Tang, S.W.; Bunney, W.E. Decrease in sigma but no increase in striatal dopamine D4 sites in schizophrenic brains. Eur J Pharmacol 1996; 314: R3-5.

[137] Reynolds, G.P.; Mason, S.L. Absence of detectable striatal dopamine D4 receptors in drug-treated schizophrenia. *Eur. J. Pharmacol.* **1995**, *281*, R5-R6.

[138] Swanson, J., Oosterlaan, J., Murias, M., Schuck, S., Flodman, P., Spence, M.A., Wasdell, M., Ding, Y., Chi, H.C., Smith, M., Mann, M., Carlson, C., Kennedy, J.L., Sergeant, J.A., Leung, P., Zhang,Y.P., Sadeh, A., Chen, C., Whalen, C.K., Babb, K.A., Moyzis, R. & Posner, M.I. Attention deficit ⁄ hyperactivity disorder children with a 7-repeat allele of the dopamine receptor D4 gene have extreme behavior but normal performance on critical neuropsychological tests of attention. *Proc. Natl Acad. Sci.*

USA **2000**, *97*, 4754–4759.

[139] Faraone, S.V., Doyle, A.E., Mick, E. & Biederman, J. Meta–analysis of the association between the 7-repeat allele of the dopamine D(4) receptor gene and attention deficit hyperactivity disorder. *Am. J. Psychiatry*. **2001**, *158*, 1052–1057.

[140] Ebstein, R.P.; Novick, O.; Umansky, R.; Priel, B.; Osher, Y.; Blaine, D. Dopamine D4 receptor (DRD4) exon III polymorphism associated with the human personality trait of novelty seeking. *Nature. Genet.* **1996**, *12*, 78-80.

[141] Gelernter, J.; Kranzler, H.; Coccaro, E.; Siever, L.; New, A.; Mulgrew, C. L. D4 dopamine-receptor (DRD4) alleles and novelty seeking in substance-dependent, personality-disorder, and control subjects. Am J Hum Genet. **1997**, *61*, 1144–1152.

[142] Ebstein; R:P. Saga of an adventure gene: novelty seeking, substance abuse and the dopamine D4 receptor exon III repeat polymorphism. *Mol. Psychiatry.* **1997**, *2*, 381-384.

[143] Elsinger, P.H.; Hatano, K.; Ishiwata, K. *Curr. Med. Chem.* **2003**, 10, 2139-2153.

[144] Enguehard-Gueiffier, C.; Gueiffier, A. Recent progress in medicinal chemistry of D4 agonists. *Curr. Med. Chem.* **2006**, 13, 2981-2993.

[145] Ehrlich, K.; Gotz, A.; Bollinger, S.; Tschammer, N.; Bettinetti, L.; Harterich, S.; Hübner, H.; Lanig, H.; Gmeiner, P. Dopamine D2, D3, and D4 Selective Phenylpiperazines as Molecular Probes To Explore the Origins of Subtype Specific Receptor Binding. *J. Med. Chem.* **2009**, 52, 4923-4935.

[146] Glase, S.A.; Akunne, H.C.; Georgic, L.M.; Heffner, T.G.; MacKenzie, R.G.; Manley, P.J.; Pugsley, T.A.; Wise, L.D. Substituted [(4-phenylpiperazinyl)-methyl]benzamides: selective dopamine D4 agonists. *J Med Chem.* 1997, *40*, 1771-1772.

[147] Nakane, M.; Cowart, M.D.; Hsieh, G.C.; Miller, L.; Uchic, M.E.; Chang, R.; Terranova, M.A.; Donnelly-Roberts, D.L.; Namovic, M.T.; Miller, T.R.; Wetter, J.M.; Marsh, K.; Stewart, A.O.; Brioni, J.D.; Moreland, R.B. 2-[4-(3,4-Dimethylphenyl)piperazin-1-ylmethyl]-1H benzoimidazole (A-381393), a selective dopamine D_4 receptor antagonist. *Neuropharmacology* **2005**, 49, 112-121.

[148] Simpson, M.M.; Ballesteros, J.A.; Chiappa, V.; Chen, J.; Suehiro, M.; Hartman, D.S.; Godel, T.; Snyder, L.A.; Sakmar, T.P.; Javitch, J.A. Dopamine D4/D2 receptor selectivity is determined by a divergent aromatic microdomain contained within the second, third, and seventh membrane-spanning segments. *Mol. Pharmacol.* **1999**, 56,

1116-1126.

[149] Boström, J.; Bohm, M.; Gundertofte, K.; Klebe, G. A 3D QSAR Study on a Set of Dopamine D_4 Receptor Antagonists. *J. Chem. Comput. Sci.* **2003**, 43, 1020-1027.

[150] Boström, J.; Gundertofte, K; Liljefjors, T. A pharmacophore model for dopamine D4 receptor antagonists. *J. Comput. Aided. Mol. Des.* **2000**, 14, 769-786.

[151] Lanig, H.; Utz, W.; Gmeiner, P. Comparative Molecular Field Analysis of Dopamine D4 Receptor Antagonists Including 3-[4-(4-Chlorophenyl)piperazin-1-ylmethyl]pyrazolo[1,5-a]pyridine (FAUC 113), 3-[4-(4-Chlorophenyl)piperazin-1-ylmethyl]-1H-pyrrolo[2,3-b]pyridine (L-745,870), and Clozapine. *J. Med. Chem.* **2001**, *44*, 1151-1157.

[152] Thurkauf, A.; Chen, X. PCT Int. Appl. WO 9833784.

[153] Kulagowski, J.J.; Broughton, H.B.; Curtis, N.R.; Mawer, I.M.; Ridgill, M.P.; Baker, R.; Emms, F.; Freedman, S.B.; Marwood, R.; Patel, S.; Patel, S; Ragan, C.I.; Leeson, P.D. 3-[[4-(4-Chlorophenyl)piperazin-1-l]-methyl]-1*H*-pyrrolo[2,3-*b*]pyridine: An antagonist with high affinity and selectivity for the human dopamine D_4 receptor. *J. Med. Chem.* **1996**, *39*, 1941-1942.

[154] Löber, S.; Hübner, H.; Utz, W.; Gmeiner, P. Rationally based efficiacy tuning of selective dopamine D_4 receptor ligands leading to the complete antagonist 2-[4-(4-chlorophenyl)piperazine-1-ylmethyl]pyrazolo[1,5-a]pyridine (FAUC 213). *J. Med. Chem.* **2001**, *44*, 2691-2694.

[155] Steward, A.O.; Cowart, M.D.; Moreland, R.B.; Latshaw, S.P.; Matulenko, M.A.; Bhatia, P.A.; Wang, X.; Daanen, J.F.; Nelson, S.L.; Terranova, M.A.; Namovic, M.T.; Donnelly-Roberts, D.L.; Miller, L.N.; Nakane, M.; Sullivan, J.P.; Brioni, J.D. Dopamine D_4 ligands and models of receptor activation: 2-(4-pyridin-2-ylpiperazin-1-ylmethyl)-1H-benzimidazole and related heteroarylmethylarylpiperazines exhibit a substituent effect responsible for additional efficiacy tuning. *J. Med. Chem.* **2004**, *47*, 2348-2355.

[156] Prante, O.; Tietze, R.; Hocke, C.; Löber, S.; Hübner, H.; Kuwert, T.; Gmeiner, P. Synthesis, radiofluorination, and in vitro evaluation of pyrazolo[1,5-a]pyridine-based dopamine D_4 receptor ligands: discovery of an inverse agonist radioligand for PET. *J. Med. Chem.* **2008**, *51*, 1800-1810.

[157] Hübner, H.; Kraxner, J.; Gmeiner, P. Cyanoindole derivatives as highly selective dopamine D_4 receptor partial agonists: solid-phase synthesis, binding assays, and

functional experiments. *J. Med. Chem.* **2000**, *43*, 4563-4569.

158 Hodgetts, K.J.; Kieltyka, A.; Brodbeck, R.; Tran, J.N.; Wasley, J.W.F.; Thurkauf, A. 6-(4-Benzylpiperazine-1-yl)benzodioxines as selective ligands at cloned primate dopamine D_4 receptors. *Bio. Med. Chem.* **2001**, *9*, 3207-3213.

159 Jolliet Riant, P.; Tillement, J.P. Drug transfer across the blood-brain barrier and improvement of brain delivery. *Fundam. Clin. Pharmacol.* **1999**, *13*, 16-26.

160 Jolliet Riant, P.; Tillement, J.P. Mechanisms of nutrient and drug transfer through the blood-brain barrier and their pharmacological changes. *Encephale* **1999**, *25*, 135-145.

161 Rogers, R.D.; Willauer, H.D.; Griffin, S.T.; Huddleston, J.G. J. Chromatogr. *B. Analyt. Technol. Biomed. Sci.* **1998**, *711*, 255-263.

162 Jozan, M.; Takacsne Novak, K.; Szasz, G. Equilibrium solubility of new potential drugs in water, 1-octanol and cyclohexane. *Acta Pharm. Hung.* **1996**, *66*, 141–146.

163 Gulyaeva, N.; Zaslavsky, A.; Lechner, P.; Chait, A.; Zaslavsky, B. Relative hydrophobicity of organic compounds measured by partitioning in aqueous two-phase systems. *J. Chromatogr. B. Analyt. Technol. Biomed. Sci.* **2000**, *743*, 187–194.

164 Payne, M.P.; Kenny, L.C. Comparison of models for the estimation of biological partition coefficients. *J. Toxicol. Environ. Health A.* **2002**, *65*, 897–931.

165 O`Stergaard, J.; Hansen, S.H.; Larsen, C.; Schou, C.; Heegaard, N.H. Determination of octanol-water partition coefficients for carbonate esters and other small organic molecules by microemulsion electrokinetic chromatography. *Electrophoresis* **2003**, *24*, 1038–1046.

166 Van de Waterbeemd, H.; Smith, D.A.; Jones, B.C. Lipophilicity in PK design: methyl, ethyl, futile. *J. Comput. Aided Mol. Des.* **2001**, *15*, 273–286.

167 Greenblatt, D.J.; Arendt, R.M.; Abernethy, D.R.; Giles, H.G.; Sellers, E.M.; Shader, R.I. In vitro quantitation of benzodiazepine lipophilicity: relation to in vivo distribution. *Br. J. Anaesth.* **1983**, *55*, 985–989.

168 Altomare, C.; Tsai, R.S.; el Tayar, N.; et al. Determination of lipophilicity and hydrogen-bond donor acidity of bioactive sulphonyl-containing compounds by reversedphase HPLC and centrifugal partition chromatography and their application to structure-activity relations. *J. Pharm. Pharmacol.* **1991**, *43*, 191–197.

169 Caron, J.C.; Shroot, B. Determination of partition coefficients of glucocorticosteroids by high-performance liquid chromatography. *J. Pharm. Sci.* **1984**, *73*, 1703–1706.

[170] Aktories, K.; Förstermann, U.; Hofmann, F.B.; Starke, K. (eds.) *Allgemeine und spezielle Pharmakologie und Toxikologie.* [9]**2005**, Elsevier, Urban & Fischer, München.

[171] Laznicek, M.; Laznickova, A. The effect of lipophilicity on the protein binding and blood cell uptake of some acidic drugs. *J. Pharm. Biomed. Analy.* **1995**, *13*, 823–828.

[172] Kosa, T.; Maruyama, T.; Otagiri, M. Species differences of serum albumins: I. Drug binding sites. *Pharm. Res.* **1997**, *14*, 1607–1612.

[173] Van Bree, J.B.; De Boer, A.G.; Danhof, M.; Breimer, D.D. Drug transport across the blood–brain barrier. I. Anatomical and physiological aspects. *Pharm. Weekbl. Sci.* **1992**, *14*, 305–310.

[174] Wolburg, H.; Lippoldt, A. Tight junctions of the bloodbrain barrier: development, composition and regulation. *Vascul Pharmacol.* **2002**, *38*, 323–337.

[175] Kilberg, M.S.; Stevens, B.R.; Novak, D.A. Recent advances in mammalian amino acid transport. *Annu. Rev. Nutr.* **1993**, *13*, 137–165.

[176] Kanner, B.I. Glutamate transporters from brain. A novel neurotransmitter transporter family. *Febs Lett.* **1993**, *325*, 95– 99.

[177] Bendayan, R.; Lee, G.; Bendayan, M. Functional expression and localization of P-glycoprotein at the blood brain barrier. *Microsc. Res. Tech.* **2002**, *57*, 365–380.

[178] Doan, K.M.; Humphreys, J.E.; Webster, L.O.; et al. Passive permeability and P-glycoprotein-mediated efflux differentiate central nervous system (CNS) and non-CNS marketed drugs. *J. Pharmacol. Exp. Ther.* **2002**, *303*, 1029–1037.

[179] Poulin, P.; Theil, F.P. Prediction of pharmacokinetics prior to in vivo studies. II. Generic physiologically based pharmacokinetic models of drug disposition. *J. Pharm. Sci.* **2002**, *91*, 1358–1370.

[180] Lin, T.H.; Lin, J.H. Effects of protein binding and experimental disease states on brain uptake of benzodiazepines in rats. *J. Pharmacol. Exp. Ther.* **1990**, *253*, 45–50.

[181] Lewis, D.F.; Dickins, M. Baseline lipophilicity relationships in human cytochromes P450 associated with drug metabolism. *Drug Metab. Rev.* **2003**, *35*, 1–18.

[182] Jones, D.R.; Hall, S.D.; Jackson, E.K.; Branch, R.A.; Wilkinson, G.R. Brain uptake of benzodiazepines: effects of lipophilicity and plasma protein binding. *J. Pharmacol. Exp. Ther.* **1988**, *245*, 816–822.

[183] Arnold, J. Determinants of pharmacologic effects and toxicity of benzodiazepine hypnotics: role of lipophilicity and plasma elimination rates. *J. Clin. Psych.* **1991**, *52*,

S11–S14.

[184] Drayer, D.E. Lipophilicity, hydrophilicity, and the central nervous system side effects of beta blockers. *Pharmacother.* **1987**, *7*, 87–91.

[185] Wilson, A.; Garcia, A.; Chestakova, A.; Houle, S. How good is the correlation between lipophilicity/phospholipophilicity and non-specific binding. *NeuroImage* **2004**, *22*, Suppl. 2, T165.

[186] Mendel, C.M.; Mendel, D.B. 'Non-specific' binding. The problem, and a solution. *Biochem. J.* **1985**, *228*, 269-272.

[187] Cuatrecesas, P.; Hollenberg, M.D. Binding of insuling and other hormones to non-receptor materials: Saturability, specificity and apparent “negative cooperativity”. *Biochem. Biophys. Res. Commun.* **1977**, *62*, 31-41.

[188] Phillips, J.L. “Specific” binding of radioiodinated transferrin to polypropylene culture tubes. *Biochem. Biophys. Res. Commun.* **1976**, *71*, 726-732.

[189] Dana, S.E.; Brown, M.S.; Goldstein, J.L. Specific, saturable, and high affinity binding of 125I-low density lipoprotein to glass beads. *Biochem. Biophys. Res. Commun.* **1977**, *75*, 1369-1376.

[190] Mendel, C.M.; Almon, R.R. Associations of [^{3}H]dihydroalprenolol with biological membranes. *Gen. Pharmacol.* **1979**, *10*, 31-40.

[191] Munck, A. in Pasqualini, J.R. (eds) *Receptors and Mechanism of Action of Steroid Hormones*, part I, Marcel Dekker, New York, pp. 1-40.

[192] Sebai, S.; Baciu, M.; Ces, O.; Clarke, J.; Cunningham, V.; Gunn, R.; Law, R.; Mulet, X.; Parker, C.; Plisson, C.; Templer, R.; Gee, A. To lipophilicity and beyond—towards a deeper understanding of radioligand non-specific binding. *NeuroImage* **2006**, *31*, T56.

[193] Plenevaux, A; Lemaire, C.; Palmer, A.J.; Damhaut, P.; Comar, D. Synthesis of Non-activated ^{18}F-Fluorinated Aromatic Compounds Through Nucleophilic Substitution and Decarboxylation Reactions. *Appl. Radiat. Isot.* **1992**, *43*, 1035-1040.

[194] Chakraborty, P.K.; Kilbourn, M.R. [^{18}F]Fluorination/Decarbonylation: New Route to Aryl [^{18}F]Fluorides. *Appl. Radiat. Isot.* **1991**, *42*, 1209-1213.

[195] Angelini, G.; Speranza, M.; Wolf, A.P.; Shiue, C.-Y. Synthesis of N-(α,α,α-tri[^{18}F]fluoro-m-tolyl)piperazine. A potent serotonine antagonist. *J. Lab. Compd. Radiopharm.* **1990**, *28*, 1441-1448.

[196] Gribble, G.W. Recent developments in indole ring synthesis—methodology and

applications. *J. Chem. Soc., Perk. Trans.* I **2000**, 1045-1075.

[197] Chen, C.; Lieberman, D.R.; Larson, R.D.; Verhoeven, T.R.; Reider, P.J. Syntheses of indoles via a palladium-catalyzed annulation between iodoanilines and ketones. *J. Org. Chem*. **1997**, *62*, 2676-2677.

[198] Larock, R.C.; Yum, E.K. Synthesis of indoles via palladium-catalyzed heteroannulation of internal alkynes. *J. Am. Chem. Soc.* **1991**, *113*, 6689.

[199] Ferri, D.; Bürgi, T.; Borszeky, K.; Mallat, T.; Baiker, A. Enhanced Enantioselectivity in Ethyl Pyruvate Hydrogenation Due to Competing Enantioselective Aldol Reaction Catalyzed by Cinchonidine. *Journal of catalysis.* **2000**, *193*, 139-144.

[200] Reissert, A. *Ber.* Einwirkung von Oxalester und Natriumäthylat auf Nitrotoluole. Synthese nitrirter Phenylbrenztraubensäuren. **1897**, *30*, 1030-1053.

[201] Cavelier, F.; Enjalbal, C. Studies of selective Boc removal in the presence of silyl ethers. *Tetrahedron Lett.* **1996**, *37*, 5131-5134.

[202] McKillop, A.; Kemp, D. Further functional group oxidations using sodium perborate Tetrahedron. **1989**, *45*, 3299-3306.

[203] Koser, G.F. [Hydroxy(tosyloxy)iodo]benzene and closely related iodanes: the second stage of development. *Aldrichimica Acta* **2001**, *34*, 89-102.

[204] Surry, D.S.; Buchwald, S.L. Dialkylbiaryl phosphines in Pd-catalyzed amination: a user´s guide. *Chem. Sci.*, **2010**, DOI: 10.1039/c0sc00331.

[205] Wüst, F.R.; Kniess, T. N-Arylation of indoles with 4-[^{18}F]fluoroiodobenzene: synthesis of ^{18}F-labelled σ_2 receptor ligands for positron emission tomography (PET). *J. Label. Compd. Radiopharm.* **2005**, *48*, 31-43.

[206] Hartwig, J.F. Palladium-catalyzed amination of aryl halides and sulfonates. in: Didier, A. *Modern Arene Chemistry* **2002**, 107-168.

[207] Yang, B.H.; Buchwald, S.L. Palladium-catalyzed amination of aryl halides and sulfonates. *J. Organomet. Chem.* **1999**, *576*, 125-146.

[208] Wolfe, J.P.; Buchwald, S.L. Room Temperature Catalytic Amination of Aryl Iodides. *J. Org. Chem.* **1997**, *62*, 6066.

[209] Georg, J.; Sastry, N.V. Densities, Excess Molar Volumes at T = (298.15 to 313.15) K, Speeds of Sound, Excess Isentropic Compressibilities, Relative Permittivities, and Deviations in Molar Polarizations at T = (298.15 and 308.15) K for Methyl Methacrylate + 2-Butoxyethanol or Dibutyl Ether + Benzene, Toluene, or p-Xylene. *J.*

Chem. Eng. Data **2004**, *49*, 1116-1126.

[210] Christensen, H.; Kiil, S.; Dam-Johansen, K. Effekt of solvents on the product distribution and reaction rate of a Buchwald-Hartwig amination reaction. *Org. Proc. Res. Develop.* **2006**, *10*, 762-769.

[211] Beletskaya, I.P.; Bessmertnykh, A.G.; Guilard, R. Palladium-catalyzed amination of aryl dibromides with secondary amines: synthetic and mechanistic aspects *Tetrahedron Lett.* **1999**, *40*, 6393-6397.

[212] Stauffer, S.R.; Steinbeiser, M.A. Pd-catalyzed amination in a polar medium: rate enhancement, convenient product isolation, and tandem Suzuki cross-coupling. *Tetrahedron Lett.* **2005**, *46*, 2571-2575.

[213] Pitts, W.J.; Vaccaro, W.; Huynh, T.; Leftheris, K.; Roberge, J.Y.; Barbosa, J.; Guo, J.Q.; Brown, B.; Watson, A.; Donaldson, K.; Starling, G.C.; Kiener, P.A.; Poss, M.A.; Dodd, J.H.; Barrish, J.C. *Bioorg. Med. Chem. Lett.* **2004**, *14*, 2955-2958.

[214] Ohshita, K.; Ishiyama, H.; Oyanagi, K.; Nakata, H.; Kobayashi, J. Synthesis of hybrid molecules of caffeine and eudistomin D and its effects on adenosine receptors. *J. Bioorg. Med. Chem.* **2007**, *15*, 3235-3240.

[215] Barluenga, J.; Moriel, P.; Aznar, F.; Valdes, C. Palladium-Catalyzed Cross-Coupling between Vinyl Halides and tert-Butyl Carbazate: First General Synthesis of the Unusual N-Boc-N-alkenylhydrazines. *Org. Lett.* **2007**, *9*, 275-278.

[216] Cornils, B.; Hermmann, W.A. (eds.) Aqueous-phase *Organometallic Catalysis*, **2004**, Wiley-VCH, Weinhem.

[217] Leadbeater, N.E. Fast, easy, clean chemistry by using water as a solvent and microwave heating: the Suzuki coupling as an illustration. *Chem. Commun.* **2005**, *23*, 2881-2902.

[218] Scherman, D.; Hamon, M.; Gozlan, H.; Henry, J.P.; Lesage, A.; Mosson, M.; Rumigny, J.F. *Prog. Neuropsychopharmacol. Biol.* **1988**, *12*, 989-1001.

[219] Tabellen für das Labor, without year specification, Merck, Darmstadt.

[220] Prelog, V.; Driza, G.J. Sur la N-phénylpipérazine. *Collect. Czech. Chem. Commun.* **1933**, *5*, 497.

[221] Prelog, V.; Blazek, Z. Sur les pipérazines N-monoarylées et leurs dérivés. *Collect. Czech. Chem. Commun.* **1934**, *6*, 211.

[222] Liu, K.G.; Robichaud A. J. A general and convenient synthesis of *N*-aryl piperazines.

Tetrahedron Letters **2005**, *46*, 7921-7922.

[223] Wilson, A.A.; Dannals, R.F.; Ravert, H.T.; Wagner Jr., H.N.; Reductive amination of [^{18}F]fluorobenzaldehydes: Radiosyntheses of [2-^{18}F]- and [4-^{18}F]fluorodexetimides. *J. Label. Compd. Radiopharm.* **1990,** *8*, 1189-1199.

[224] Haka, M.S.; Kilbourn, M.R.; Watkins, G.L. Toorongian, S.A. Aryltrimethylammonium trifluoromethanesulfonates as precursors to aryl [^{18}F]fluorides: Improved synthesis of [^{18}F]GBR-13119. *J. Label. Compd. Radiopharm.* **1989**, 27(7), 823-833.

[225] Langer, O.; Dollé, F.; Valette, H.; Halldin, C.; Vaufrey, F.; Fuseau, C.; Coulon, C.; Ottaviani, M.; Någren, K.; Bottlaender, M.; Maziére, B.; Crouzel, C. *Bioorg. Med. Chem.* **2001**, 9, 677-694.

[226] Hayes, G.; Biden, T. J.; Selbie, L. A.; Shine, J. Structural subtypes of the dopamine D2 receptor are functionally distinct: expression of the cloned D2A and D2B subtypes in a heterologous cell line. *Mol. Endocrinol.* **1992**, *6*, 920–926.

[227] Sokoloff, P.; Giros, B.; Martres, M. P.; Bouthenet, M. L.; Schwartz, J. C. Molecular cloning and characterization of a novel dopamine receptor (D3) as a target for neuroleptics. *Nature* **1990**, *347*, 146–151.

[228] Asghari, V.; Sanyal, S.; Buchwaldt, S.; Paterson, A.; Jovanovic, V.; Vantol, H. H. M. Modulation of intracellular cyclic-Amp levels by different human dopamine D4 receptor variants. *J. Neurochem.* **1995**, *65*, 1157–1165.

[229] Hübner, H.; Haubmann, C.; Utz, W.; Gmeiner, P. Conjugated enynes as nonaromatic catechol bioisosteres: Synthesis, binding experiments, and computational studies of novel dopamine receptor agonists recognizing preferentially the D3 subtype. *J. Med. Chem.* **2000**, *43*, 756–762.

[230] Schlotter, K.; Boeckler, F.; Hübner, H.; Gmeiner, P. Fancy Bioisosteres: Metallocene-Derived G-Protein-Coupled Receptor Ligands with Subnanomolar Binding Affinity and Novel Selectivity Profiles. *J. Med. Chem.* **2005**, *48*, 3696-3699.

[231] Hübner, H.; Kraxner, J.; Gmeiner, P. Cyanoindole derivatives as highly selective dopamine D4 receptor partial agonists: solid-phase synthesis, binding assays, and functional experiments. *J. Med. Chem.* **2000,** *43*, 4563-4569.

[232] Chio, C. L.; Lajiness, M. E.; Huff, R. M. Activation of heterologously expressed D3 dopamine receptors: comparison with D_2 dopamine receptors. *Mol. Pharmacol.* **1994**, *45*, 51–60.

[233] Hübner, H.; Kraxner, J.; Gmeiner, P. Cyanoindole derivatives as highly selective dopamine D_4 receptor partial agonists: solid-phase synthesis, binding assays, and functional experiments. *J. Med. Chem.* **2000,** *43*, 4563-4569.

[234] Lemaire, C; Damhaut, P.H.; Plenevaux, A.; Cantineau, R.; Christiaens, L.; Guillaume, M. Synthesis of fluorine-18 substituted aromatic aldehydes and benzyl bromides, new intermediates for n.c.a. [^{18}F]fluorination. *Appl. Radiat. Isot.* **43** (1992), pp. 485–494.

[235] Leuckart, R. Über eine neue Bildungsweise von Tribenzylamin *Ber.* **1885**, 18, 2341-2344.

[236] Wallach, O. Zur Kenntniss der Terpene und der ätherischen Oele. Zweiundzwanzigste Abhandlung. I. *Ann.* **1893**, *272*, 99-122.

[237] Hai-Bin, T.; Duan-Zhi, Y.; Jun-Ling, Li; Lan, Z.; Cun-Fu, Z.; Yong-Xian, W.; Wie, Z. Radiosynthesis of 3-{[4-(4-[^{18}F]fluorobenzyl)]piperazin-1-yl}methyl-1H-pyrrolo[2,3-b]pyridine: A potential dopamine D_4 receptor imaging agent *Radiochim. Acta* **2003**, 91, 241-245.

[238] Neve, K.A. (ed.) The dopamine receptors **2010**, Humana Press.

[239] *MarvinSketch Demo V5.1.4*, **2009**: Available from: http://www.chemaxon.com/marvin/sketch/index. jsp.

[240] *Virtual Computational Chemistry Laboratory ALOGPS 2.1 program,* **2009***,* www.vcclab.org/lab/ alogps/start.html

[241] *OECD Guideline for the Testing of Chemicals*, 2004.

[242] Wang, Y.; Mathis, C.A.; Huang, G.F.; Debnath, M.L.; Holt, D.P.; Shao, L.; Klunk, W.E. Effects of lipophilicity on the affinity and nonspecific binding of iodinated benzothiazole derivatives. *J. Mol. Neurosci.* **2003**, *20*, 255-260.

[243] Prante, O.; Tietze, R.; Hocke, C.; Löber, S.; Hübner, H.; Kuwert, T.; Gmeiner, P. Synthesis, radiofluorination, and in vitro evaluation of pyrazolo[1,5-a]pyridine-based dopamine D4 receptor ligands: discovery of an inverse agonist radioligand for PET. *J Med Chem.* 2008; 51(6):1800-10.

[244] Prante, O.; Hocke, C.; Löber, S.; Hübner, H.; Gmeiner, P.; Kuwert. T. Tissue distribution of radioiodinated FAUC113. *Nuklearmedizin* 45 (2006) 41-8.

[245] Qaim, S.M.; Stöcklin, G. Production of some medically important short-lived neutron deficient radioisotopes of halogenes. *Radiochimica Acta* **1983**, 34, 25.

[246] Zhang, K.; Weiss, N.T.; Tarazi, F.I.; Kula, N.S.; Baldessarini, R.J. Effects of alkylating agents on dopamine D3 receptors in rat brain: selective protection by dopamine. *Brain Res*. **1999**, 847, 32-37.

Ich versichere, dass ich die von mir vorgelegte Dissertation selbständig angefertigt, die benutzten Quellen und Hilfsmittel vollständig angegeben und die Stellen der Arbeit − einschließlich Tabellen, Karten und Abbildungen −, die anderen Werken im Wortlaut oder dem Sinn nach entnommen sind, in jedem Einzelfall als Entlehnung kenntlich gemacht habe; dass diese Dissertation noch keiner anderen Fakultät oder Universität zur Prüfung vorgelegen hat; dass sie − abgesehen von unten angegebenen Teilpublikationen − noch nicht veröffentlicht worden ist sowie, dass ich eine solche Veröffentlichung vor Abschluss des Promotionsverfahrens nicht vornehmen werde. Die Bestimmungen der Promotionsordnung sind mir bekannt. Die von mir vorgelegte Dissertation ist von Herrn Prof. Dr. H. H. Coenen betreut worden.

Köln, 31. Oktober 2010

1. **Methoden zur integrierten Analyse metabolischer Netzwerke unter stationären und instationären Bedingungen**
   von S. A. Wahl (2008), 245 Seiten
   ISBN: 978-3-89336-506-7

2. **Strukturelle Untersuchungen an membranassoziierten Proteinen: NMR-Strukturen des HIV-1 Virus Protein U (39-81) und des humanen CD4 (372-433)**
   von M. Wittlich (2008), XVIII, 185 Seiten
   ISBN: 978-3-89336-510-4

3. **Identifizierung von physiologischen und artifiziellen Liganden von GABARAP und Charakterisierung der resultierenden Interaktionen**
   von J. Mohrlüder (2008), V, 158 Seiten
   ISBN: 978-3-89336-511-1

4. **Struktur und Funktion von Transaminasen aus *Corynebacterium glutamicum***
   von J. Marienhagen (2008), VI, 154 Seiten
   ISBN: 978-3-89336-512-8

5. **Implementierung eines Funk-Protokolls (IEEE 802.15.4) und Entwicklung eines adaptiven Zeitsynchronisationsverfahrens für ein Netzwerk intelligenter und autarker Sensoren**
   von M. Schlösser (2008), 77 Seiten
   ISBN: 978-3-89336-519-7

6. **Etablierung und Optimierung der sekretorischen Gewinnung thermostabiler Lipasen in Gram-positiven Bakterien**
   von H. Brundiek (2008), VIII, 154 Seiten
   ISBN: 978-3-89336-520-3

7. **Visuospatial Attention:** Neural Correlates and Pharmacological Modulation in Healthy Subjects and Patients with Spatial Neglect
   by S. Vossel (2008), XIV, 176 pages
   ISBN: 978-3-89336-526-5

8. **Analyse des Substratspektrums der ClpCP-Protease aus *Corynebacterium glutamicum***
   von J.-E. Schweitzer (2008), V, 130 Seiten
   ISBN: 978-3-89336-528-9

9. **Adaptive Verfahren zur automatischen Bildverbesserung kernspintomographischer Bilddaten als Vorverarbeitung zur Segmentierung und Klassifikation individueller 3D-Regionen des Gehirns**
   von J. Castellanos (2008), VI, 100 Seiten
   ISBN: 978-3-89336-539-5

10. **Posttranslationale Regulation der 2-Oxoglutarat-Dehydrogenase in *Corynebacterium glutamicum***
von C. Schultz (2009), VII, 151 Seiten
ISBN: 978-3-89336-560-9

11. **MtrA, ein bifunktionaler Antwortregulator aus *Corynebacterium glutamicum***
von M. Brocker (2009), VI, 125 Seiten
ISBN: 978-3-89336-561-6

12. **Strukturelle Charakterisierung von GABRAP-Ligand-Interaktionen**
von Y. Thielmann (2009), 166 Seiten (getr. pag.)
ISBN: 978-3-89336-563-0

13. **Acceleration on an image reconstruction algorithm for Positron Emission Tomography using a Graphics Processing Unit**
by T. Felder (2009), 97 pages
ISBN: 978-3-89336-566-1

14. **NMR-Lösungsstruktur der Loopregion Tyr^{67} - Leu^{77} des visuellen Arrestins im Komplex mit photoaktiviertem Rhodopsin**
von S. Feuerstein (2009), XVI, 140 Seiten
ISBN: 978-3-89336-571-5

15. **Development of a Process for the Cleavage of a Mucin Fusion Protein by Enterokinase**
by T. Kubitzki (2009), IV, 133 pages
ISBN: 978-3-89336-575-3

16. **Children´s health and RF EMF exposure**
project coord. P. Wiedemann (2009), 49 pages
ISBN: 978-3-89336-594-4

17. **Entwicklung einer Signalerfassungselektronik für eine Halbleiter-Photomultiplier (SiPM) Matrix**
von C. Parl (2009), IV, 128 Seiten
ISBN: 978-3-89336-595-1

18. **Medienorientierung biomedizinischer Forscher im internationalen Vergleich**
Die Schnittstelle von Wissenschaft & Journalismus und ihre politische Relevanz
herausg. von H. P. Peters (2009), 364 Seiten
ISBN: 978-3-89336-597-5
URN: urn.nbn:de: 0001-00542

19. **Identifizierung von Interaktionspartnern für HIV-1 Nef und ihre potentielle Relevanz bei der Entwicklung der HIV-assoziierten Demenz**
von J. Mötter (2010), VI, 172 Seiten
ISBN: 978-3-89336-604-0

20. **Biotransformationen mit Cytochrom P450 Monooxygenasen**
von D. Zehentgruber (2010), XI, 147 Seiten
ISBN: 978-3-89336-605-7

21. **Studies on central carbon metabolism and respiration of *Gluconobacter oxydans* 621H**
by T. Hanke (2010), 120 pages
ISBN: 978-3-89336-607-1

22. **Prozessentwicklung zur Produktion von 2-Keto-L-Gulonsäure, einer Vitamin C- Vorstufe**
von B. Osterath (2010), XXI, 213 Seiten
ISBN: 978-3-89336-612-5

23. **Visuell evozierte Antworten der corticalen Areale V1/V2 und V5/MT nach Schachbrettmusterumkehrreizung – Magnetenzephalographische Untersuchungen in Kombination mit cytoarchitektonischen Wahrscheinlichkeitskarten**
von B. U. Barnikol (2010), III, 138 Seiten
ISBN: 978-3-89336-615-6

24. **Biochemische und regulatorische Analyse des TCA-Zyklus und Glyoxylat-Shunts in Escherichia coli**
von M. Kunze (2010), 191 Seiten
ISBN: 978-3-89336-620-0

25. **Metabolomananalyse als Grundlage für ^{13}C-Stoffflussanalyse und dynamischer Modellierung am Beispiel der Lysinbiosynthese**
von M. G. Wellerdiek (2010), xvi, 182 Seiten
ISBN: 978-3-89336-621-7

26. **Neue Thiamindiphosphat-abhängige Enzyme für die Synthese enantiokomplementärer 2-Hydroxyketone**
von G. Kolter (2010), IX, 168 Seiten
ISBN: 978-3-89336-626-2

27. **Genetische Analyse von Substrat-Translokase-Wechselwirkungen bei der Tat-abhängigen Proteintranslokation in *Escherichia coli***
von F. Lausberg (2010), 174 Seiten
ISBN: 978-3-89336-628-6

28. **Silicium Nanodrähte für die extrazelluläre Ableitung elektrischer Aktivität**
von J. F. Eschermann (2010), xii, 191 Seiten
ISBN: 978-3-89336-639-2

29. **Causality measures between neural signals from invasively and non-invasively obtained local field potentials in humans**
by E. Florin (2010), xxix, 220 pages
ISBN: 978-3-89336-646-0

30. **Regulatory and metabolic aspects of the phosphate starvation response of *Corynebacterium glutamicum***
by H. M. Woo (2010), III, 111 pages
ISBN: 978-3-89336-664-4

31. **Ligand interaction analysis of membrane-anchored proteins**
by J. Glück (2010) VIII, 87 pages (getr. pag.)
ISBN: 978-3-89336-683-5

32. **Novel insights into characteristics, relevance, and regulation of corynebacterial aconitase**
by M. Baumgart (2010), V, 147 pages
ISBN: 978-3-89336-682-8

33. **Investigation of GABARAP complexes with apoptosis-related proteins and structural characterization of GABARAP lipidation**
by P. Ma (2011), VI, 139 pages (getr. pag.)
ISBN: 978-3-89336-699-6

34. **GABARAP-artige Proteine, Nix und Bcl-2: Strukturelle Basis molekularer Interaktionen an der Schnittstelle zwischen Autophagie und Apoptose**
von M. Schwarten (2011), VIII, 164 Seiten (getr. pag.)
ISBN: 978-3-89336-700-9

35. **Einflussfaktoren auf die Stabilität und Aktivität der Benzaldehydlyase aus *Pseudomonas fluorescens* in Carboligasereaktionen mit aromatischen Aldehyden**
von M. Schwarz (2011), XI, 176 Seiten
ISBN: 978-3-89336-701-6

36. **Untersuchungen zur Bildung von D-Aminosäuren mit *Corynebacterium glutamicum***
von N. C. Stäbler (2011), VIII, 104 Seiten
ISBN: 978-3-89336-702-3

37. **Charakterisierung von Wirkstoffen für die Diagnose und Therapie von Morbus Alzheimer**
von D. Bartnik (2011), XII, 105 Seiten
ISBN: 978-3-89336-703-0

38. **Identifizierung und Charakterisierung von Regulatoren der Acyl-CoA Carboxylasen in *Corynebacterium glutamicum***
von J. Nickel (2011), IV, 127 Seiten
ISBN: 978-3-89336-712-2

39. **Metabolische 13C-Stoffflussanalyse vom isotopisch stationären zum instationären Fall**
von K. Grönke (2011), getr. pag.
ISBN: 978-3-89336-713-9

40. **Enzyme supported crystallization of chiral amino acids**
by K. Würges (2011), XI, getr. pag.
ISBN: 978-3-89336-715-3

41. **Systemische Analyse des Citratzyklus in *Corynebacterium glutamicum***
von J. van Ooyen (2011), 116 Seiten
ISBN: 978-3-89336-731-3

42. **Einfluss intrazellulärer Nukleotid-Cofaktoren auf Redoxreaktionen in rekombinanten Ganzzellsystemen**
von D. Minör (2011), XII, 138 Seiten
ISBN: 978-3-89336-737-5

43. **Development of ^{18}F-labelled radioligands for molecular imaging of the dopamine D_4 receptor**
by F. Kügler (2011), xiv, 161 pages
ISBN: 978-3-89336-738-2

Gesundheit / Health
Band / Volume 43
ISBN 978-3-89336-738-2

JÜLICH
FORSCHUNGSZENTRUM